

DISSERTATION

submitted to the

COMBINED FACULTY OF MATHEMATICS,
ENGINEERING AND NATURAL SCIENCES

of

HEIDELBERG UNIVERSITY, GERMANY

for the degree of

DOCTOR OF NATURAL SCIENCES

Put forward by

ANDREAS PATRICE BEATRIJS BALLY

Born in Edegem, Belgium

Oral examination: 15 November 2023

NEW APPROACHES TO NATURALNESS IN THE LHC ERA:

From a

RADIATIVE TOP YUKAWA

to a

LIGHT COMPOSITE HIGGS

Referees:

DR. FLORIAN GOERTZ

PROF. DR. TILMAN PLEHN

Abstract

The puzzling lightness of the Higgs boson, when one considers the Standard Model as an effective field theory to be completed, has driven much of the particle physics research over the last decades. Two paradigms have emerged as solutions to this puzzle: supersymmetry and compositeness. The absence of signals at the LHC pushes these solutions into regions of evermore fine-tuning. We present three novel approaches aimed at explaining the absence of these signatures. The first one, exploiting the large contribution of the top Yukawa to the Higgs mass, proposes a non-symmetry-based solution in which the top Yukawa only obtains its sizeable value in the IR and we discuss its new phenomenological signatures. Secondly, we present a minimal model of 5D warped gauge-Higgs grand unification, study its compelling flavor structure and analyse the resulting constraints. Although these constraints push the model to high scales, additional scalars that reside below the Kaluza-Klein states may provide accessible experimental signatures. Finally, we provide a novel model of composite Higgs generating the Higgs potential at subleading order using a remarkable property of group representations. The model is analysed and can evade existing bounds with little tuning. New light particles are predicted with unusual decays in which naturalness at the LHC may be hidden.

Zusammenfassung

Die rätselhafte Leichtigkeit des Higgs-Bosons, wenn man das Standardmodell als eine zu vervollständigende effektive Feldtheorie betrachtet, hat einen Großteil der Teilchenphysikforschung in den letzten Jahrzehnten angetrieben. Zwei Paradigmen haben sich als Lösungen für dieses Rätsel etabliert: Supersymmetrie und Kompositivität. Das Fehlen von Signalen am LHC drängt diese Lösungen in Regionen mit immer mehr Tuning. Wir stellen drei neue Ansätze vor, die das Fehlen dieser Signaturen erklären sollen. Der erste Ansatz, der den großen Beitrag des Top-Yukawa zur Higgs-Masse ausnutzt, schlägt eine nicht-symmetrische Lösung vor, bei der das Top-Yukawa seinen großen Wert nur im IR erhält, und wir diskutieren seine neuen phänomenologischen Signaturen. Zweitens stellen wir ein minimales Modell der 5D Warped Gauge-Higgs Grand Unification vor, untersuchen dessen überzeugende Flavor-Struktur und analysieren die sich daraus ergebenden Einschränkungen. Diese zwingen das Modell auf hohe Skalen, dennoch können zusätzliche Skalare, die sich unterhalb der Kaluza-Klein-Teilchen befinden, zugängliche experimentelle Signaturen liefern. Schließlich stellen wir ein neuartiges Modell für ein Komposit-Higgs vor, das das Higgs-Potential bei untergeordneter Ordnung erzeugt, wobei eine bemerkenswerte Eigenschaft von Gruppendarstellungen genutzt wird. Das Modell wird analysiert und kann bestehende Grenzen mit geringem Tuning ausweichen. Es werden neue leichte Teilchen mit ungewöhnlichen Zerfällen vorhergesagt, in denen die Natürlichkeit des Higgs-Bosons am LHC verborgen sein könnte.

Contents

Publications	vii
1 Introduction	1
1.1 The Standard Model	1
1.2 Shortcomings and Unification	3
1.3 Naturalness and the Hierarchy Problem	4
1.4 Supersymmetry and Compositeness	6
1.5 Outline	8
2 A Radiative Top Yukawa	9
2.1 Twin Higgs	10
2.2 Mitigating the Top Loop	12
2.3 Running Top Yukawa	16
2.3.1 Simple Perturbative Extensions	17
2.3.2 Beyond the Perturbative Bound	19
2.4 A Radiative Top Yukawa	22
2.4.1 A Simplified Scalar Model	23
2.4.2 Top Yukawa Coupling from a Loop	25
2.4.3 Radiative Top Mass Generation	26
2.4.4 Exact Expressions and QCD Effects	27
2.4.5 Analysis of the Fine-Tuning	28
2.4.6 Bottom Sector and Custodial Symmetry	29
2.5 Phenomenology	30
2.5.1 Running Top Mass	30
2.5.2 Top Yukawa Coupling Measurement	30
2.5.3 Form Factors	32
2.5.4 Four Tops Cross Section	32
2.5.5 Flavor Constraints	34
2.5.6 Electroweak Precision Tests	35
2.5.7 Zbb Coupling	36
2.5.8 Direct Searches	37
2.6 Summary	37

3	Minimal Gauge-Higgs Grand Unification	39
3.1	Gauge-Higgs Unification	40
3.1.1	Electroweak Gauge-Higgs Unification	44
3.2	Extra Dimensions	45
3.2.1	Flat Extra Dimensions	45
3.2.2	A Warped Extra Dimension	47
3.3	Minimal Gauge-Higgs Grand Unification	51
3.3.1	The Model	53
3.3.2	Zero Mode Approximation	55
3.3.3	The Flavor Puzzle	58
3.4	Phenomenology	62
3.4.1	Meson Mixing	63
3.4.2	Tree-level Lepton Flavor Violation	64
3.4.3	Loop-level Lepton Flavor Violation	66
3.4.4	Results	68
3.5	The Scalar Potential	70
3.5.1	Generation of the Leptoquark Mass	72
3.5.2	Generation of the Singlet Mass	73
3.6	Summary	75
4	A Natural Composite Higgs	77
4.1	Composite Higgs	78
4.1.1	Technicolor	78
4.1.2	Composite Higgs	80
4.1.3	CCWZ-construction	82
4.1.4	Generating the pNGB Potential	85
4.1.5	UV Completions of Composite Higgs	87
4.2	The Minimal Composite Higgs	89
4.3	A Natural Composite Higgs	93
4.3.1	Mirror Fermions	94
4.3.2	A Model	99
4.3.3	Naive Dimensional Analysis	101
4.3.4	Numerical Results	102
4.3.5	Phenomenology of the Exotic	103
4.3.6	The Holographic 5D Dual	105
4.4	Summary	106
5	Conclusion	109
	Acknowledgments	115

A	A NJL UV completion	117
A.1	A New Global Symmetry	117
A.2	An NJL Model	118
A.3	Connecting Elementary with Strong Sector	120
B	Warped Gauge and Fermion Fields	123
B.1	Gauge Fields	123
B.2	Fermion Fields	126
B.3	Zero Mode Approximation	128
C	A Three-Site Model	131
	Bibliography	133

Publications

The content of this thesis is heavily based on the following published and unpublished work completed during the author's PhD studies from October 2019 to June 2023 in collaboration with others. Figures, equations and ideas have been freely taken from these works without additional reference.

Chapter 2 is based on the following published work:

- [I] A. Bally, Y. Chung and F. Goertz, *The Hierarchy Problem and the Top Yukawa: An Alternative to Top Partner Solutions*, *Phys. Rev. D.* **108** (2023) 055008 [arXiv:2211.17254].

Chapter 3 is based on the following published works:

- [II] A. Angelescu, A. Bally, S. Blasi and F. Goertz, *Minimal $SU(6)$ gauge-Higgs grand unification*, *Phys. Rev. D.* **105** (2022) 035026 [arXiv:2104.07366].
- [III] A. Angelescu, A. Bally, F. Goertz and S. Weber, *$SU(6)$ gauge-Higgs grand unification: minimal viable models and flavor*, *JHEP* **04** (2023) 012 [arXiv:2208.13782].

Chapter 4 is based on, as of yet, unpublished work:

- [IV] A. Angelescu, A. Bally, F. Goertz and M. Hager, *Restoring Naturalness via Conjugate Fermions*, [arXiv:2309.05698]

The following publications have also been completed as part of the author's PhD studies but are not included in this thesis:

- [V] A. Bally, S. Jana and A. Trautner, *Neutrino self-interactions and XENON1T electron recoil excess*, *Phys. Rev. Lett.* **125** (2020) 161802 [arXiv:2006.11919].
- [VI] G. Arcadi, A. Bally, F. Goertz, K. Tame-Narvaez, V. Tenorth and S. Vogl, *EFT interpretation of XENON1T electron recoil excess: Neutrinos and dark matter*, *Phys. Rev. D.* **103** (2021) 023024 [arXiv:2007.08500].

All these publications can be also be found in the bibliography under [1–6] See also [7, 8] for related conference proceedings.

Chapter 1

Introduction

1.1 The Standard Model

The discovery of the positron [9], with the associated notion of pair-production and particle non-conservation, steadfastly marked the replacement of particle wave-functions with fields in relativistic quantum mechanics. With fields spanning space-time as the fundamental objects, particles are considered as excitations of the fields and are created at will provided energy-momentum is conserved. The application of this formalism to the theory of Quantum Electrodynamics (QED) took twenty years to be fully understood with the calculation of the electron anomalous magnetic moment [10] as its culmination. As new forces and particles were discovered, this led to a systematic construction of Quantum Field Theories (QFT) which are built by specifying the gauge symmetry of the underlying theory, the matter sector consisting of fermions, and a scalar sector whose ground state may spontaneously break (or more accurately, hide in a non-linear fashion) some of the gauge symmetries. The most general Lagrangian of the QFT is then constructed by combining all fields respecting space-time and gauge symmetries into a renormalizable theory.

The Standard Model (SM) of particle physics is no exception and contains all three of these elements. The gauge symmetries of the SM consists of the non-abelian color charge, $SU(3)_c$, the left-handed charge, $SU(2)_L$, and the abelian hypercharge, $U(1)_Y$. These internal symmetries give rise to the forces colloquially known as the strong force, the weak force and electromagnetism. Next, the matter content is specified consisting of five fermion fields in three generations: the left-handed quark doublet Q_L , two right-handed quark singlets u_R and d_R , the lepton doublet L_L and the right-handed electron singlet e_R . These fields transform under representations of the gauge symmetries shown in Table 1.1.

Importantly this charge assignment is chiral, meaning that the left- and right-handed components of a single massive Dirac field are charged differently. It poses the basic question of how one can combine left- and right-handed fields

	$SU(3)_c$	$SU(2)_L$	$U(1)_Y$
Q_L	3	2	1/6
u_R	3	1	2/3
d_R	3	1	-1/3
L_L	1	2	-1/2
e_R	1	1	-1

Table 1.1: The fermion content of the SM and their charges.

into a gauge invariant mass term. This is where the third sector of the SM comes into play: a charged $SU(2)_L$ scalar, H , the Higgs. Such a scalar allows us to write down gauge-invariant Yukawa terms combining the left- and right-handed fields:

$$\mathcal{L}_{\text{yuk}} = -y_u \bar{Q}_L H u_R - y_d \bar{Q}_L \tilde{H} d_R - y_e \bar{L}_L \tilde{H} e_R + \text{h.c.} . \quad (1.1)$$

If the scalar has a potential with a non-zero Vacuum Expectation Value (VEV), it would lead to masses for the SM fermions. The simplest parametrization of such a potential involves a mass term $-\mu^2$ and a quartic λ :

$$-\mathcal{L}_H \supset -\mu^2 H^\dagger H + \lambda (H^\dagger H)^2 . \quad (1.2)$$

This *Mexican hat* potential, although completely $SU(2)_L$ symmetric from far away, exhibits the feature that from the ground state, or minimum, of the potential, things are not so clearly $SU(2)$ symmetric anymore. A potential, exhibiting the spontaneous breakdown of continuous symmetries, was realized to give rise to massless spinless particles [11–13]. These particles are called Nambu-Goldstone (NG) bosons.

When the said continuous symmetries are gauged, as in the case of $SU(2)_L$, the spontaneous breaking does not lead to massless spinless bosons in the spectrum. Instead the gauge bosons related to the broken symmetries acquire a mass (or in other words the Nambu-Goldstone boson associated to the broken generator provides the longitudinal component of the now massive spin 1 particle). This mechanism, known as the Brout–Englert–Higgs mechanism, worked out in the 1960’s [14–16] features prominently in the SM as the source for the mass of the W and Z boson, and of all the SM fermions as described in [17, 18].

The elucidation of the zoo of particles called hadrons in terms of quarks and non-abelian Yang-Mills theory occurred a few years later with the discovery of asymptotic freedom [19, 20], the flip side of which is confinement and remains not understood, and largely completed the understanding of the SM as we know it. Experimentally the SM was completed in 2012 with the discovery of the Higgs boson [21, 22]. Despite extraordinary confirmation of the SM in a wide variety of experiments going from the low-energy realm to the high-energy frontier, the model must be completed in order to account for some of the deepest mysteries of nature.

1.2 Shortcomings and Unification

Most of the shortcomings of the SM become clear from looking at cosmology. The evolution of the Universe since the big bang is nowadays very well described by the Standard Model of cosmology (Λ CDM) whose parameters are very well measured by the Planck telescope [23]. There are however great mysteries behind the vast success of this model: the vast majority of our current energy budget is made up of unknown quantities which were dubbed dark energy and dark matter. We can measure the impact of these forms of energy on the cosmological evolution of our Universe since they interact gravitationally as any type of energy does. Dark matter is believed to be a particle however no suitable candidate exists in the SM [24]. Moreover the SM would predict an empty Universe as matter annihilates with anti-matter. At a minimum, the SM needs to be extended to provide a dark matter candidate and a mechanism to account for the observed baryons. These experimental facts are hard mismatches between theory and observation. It is therefore now well accepted that the SM is merely an Effective Field Theory (EFT) that needs completion at some unknown UV scale Λ_{UV} .

These experimental challenges lead us to think about what kind of possible theories could UV complete the SM and whether such theories can explain these experimental challenges. Moreover we are led to the question whether such UV completions could unify different phenomena of the SM and provide more insight into its structure. After all, the history of physics is one long tale of unification and the SM, with its 19 different parameters, could certainly use some unification.

A beautiful example of such a UV theory which unifies the structure of the SM is a Grand Unified Theory (GUT). It was remarked that the three gauge groups of the SM can fit neatly into a simple Lie group such as $SU(5)$ and $SO(10)$ [25–27] while the fermion representations fit equally neatly in larger fermion representations of the unified group. Fitting the three different gauge couplings into a single gauge coupling is impossible at the classical level. However, with the advent of quantum loops and the techniques of renormalization, it was realized that all parameters of the Lagrangian, including the gauge couplings, receive contributions from all scales and thus *run* according to the scale. In the case of gauge couplings, they scale logarithmically and the value of the gauge couplings seem to unify quite well at the high scale of $M_{GUT} = 10^{16}$ GeV indicating that the unification of the SM into a GUT may very well happen.

The example of GUTs provides us with a good lesson: UV completions of the SM may very well only happen at very high scales and a good understanding of the evolution of the SM parameters may give us hints about these scales. This automatically brings us to the next section which asks about the natural values of these parameters.

1.3 Naturalness and the Hierarchy Problem

Dirac was the first to posit about the origin of numbers in physics and the associated notion of Dirac Naturalness [28] is named after him. In an EFT formulation this notion becomes particularly transparent in which the coefficient of every operator must be $\mathcal{O}(1)$ up to appropriate powers of the scale of the theory. This is not merely a statement of dimensional analysis, but it is also in fact supported by the nature of quantum corrections. If not, that operator generically receives large loop contributions and it begs the question why that operator appears so small at long distances.

As 't Hooft remarked, this notion is too general if the operator in question breaks a symmetry [29]. In that case, radiative corrections to the operator, as the UV theory is evolved down to long distances, are proportional to the value of the operator. Therefore technically natural coefficients, once set small in the UV, remain radiatively stable and small in the IR. Its smallness is therefore not necessarily a mystery and could be explained in the UV theory. An illustrating example of which are the fermion masses. Fermion masses are technically natural as they break chiral symmetry. Once set in the UV, they remain set over many energy scales. This does not eliminate the mystery surrounding their small value. Indeed, one of the most intriguing question is how the fermion mass hierarchies, spanning over twelve orders of magnitude from the neutrinos to the top quark, arise. However the UV theory could provide an explanation to how these small values arise from Dirac natural ones. In contrast, if the operator in question is not technically natural, the question surrounding its smallness in the IR cannot be postponed to the UV theory as radiative correction would spoil any UV resolution.

This brings us to the hierarchy problem which comes from applying the above principles to the SM. In the SM there is one such dimensionful parameter which does not obey technical naturalness: the Higgs mass $-\mu^2(H^\dagger H)$ from the Higgs potential Eq. (1.2). Unlike fermion masses protected by chiral symmetry and gauge masses protected by gauge symmetry, no symmetry gets restored in the limit of $\mu \rightarrow 0$. If we do not wish to embed the SM in a UV theory, its smallness is of no concern since there is no associated cutoff – it is simply an input. But as we now know, the SM is an EFT and we eventually expect the Higgs mass to be an output of the UV theory. Let us understand this a bit more quantitatively. We will follow the approach from [30]. Suppose such a fundamental theory predicts a Higgs mass of $-\mu_{\text{UV}}^2$ in the UV. At scales below Λ_{UV} , the SM degrees of freedom will induce radiative corrections to the Higgs mass, the most important of which are the top, gauge and Higgs self-coupling diagrams from Fig. 1.1. The Higgs mass we measure in the IR theory is therefore perfectly predictable and consists of the sum of these two types of contributions:

$$-(88\text{GeV})^2 = -\mu_{\text{UV}}^2 + \frac{\Lambda_{\text{UV}}^2}{16\pi^2} \left(-6y_t^2 + \frac{9}{4}g^2 + \frac{3}{4}g'^2 + 6\lambda \right). \quad (1.3)$$

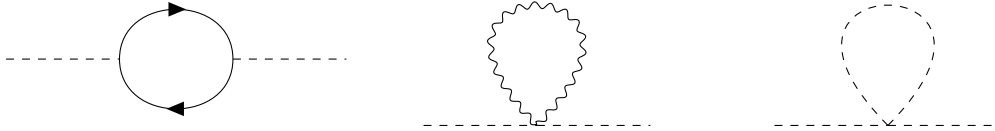


Figure 1.1: Quadratically sensitive radiative contributions from the top quark, the electroweak gauge bosons and the Higgs to the Higgs mass in the SM effective field theory.

Now we can start to see the nature of what is called the hierarchy problem. If the cutoff of the SM is high, the SM radiative corrections will be equally high and must cancel with an unrelated UV term to obtain a light Higgs. Instead, if the Higgs mass was a technically natural quantity we may have expected the radiative corrections to be proportional to the Higgs mass itself with a logarithmic sensitivity to Λ_{UV} . In that case one could still expect that in the UV a small natural value for the Higgs mass is predicted (we know of mechanisms that predict small ratios such as dimensional transmutation or axion-type mechanisms). Although this would get rid of the hierarchy problem, it would also eliminate any reason to expect the UV completion of the SM to be close to the electroweak scale. Indeed if we require the SM UV completion to be *natural*, or in other words not fine-tuned, it puts a stringent constraint on the maximum Λ_{UV} scale. Requiring a maximum of 10% fine-tuning for the UV completion and only taking the top radiative contribution which is the largest, we find the following constraint¹

$$\Delta \equiv \frac{-\frac{3}{8\pi^2}y_t^2\Lambda_{\text{UV}}^2}{(-88\text{GeV})^2} \lesssim 10 \implies \Lambda_{\text{UV}} \lesssim 1500 \text{ GeV}, \quad (1.4)$$

implying a UV completion of the SM should be right around the corner at the TeV scale! Moreover such a UV completion cannot just be any UV completion, it must be very special as we know there are higher scales in nature that also require a UV completion. If we want these higher scales to not spoil the naturalness of the Higgs, our TeV UV completion should be of particular structure. It should make sure that any potential higher scale of nature does not induce new contributions to the Higgs. An example of a higher scale in nature that is expected to give large corrections to the Higgs mass is the Planck scale at which quantum effects of gravity become important. And even omitting gravity, something, such as for example a GUT, must happen before the Landau pole of hypercharge, the ultimate cutoff of the SM at 10^{41} GeV, is reached.

¹The following is an underestimate, as there could also be tuning within μ_{UV}^2 , which would imply the UV completion to appear at an even lower scale.

1.4 Supersymmetry and Compositeness

There are two traditional frameworks that stabilise the Higgs mass: supersymmetry (SUSY) and composite Higgs. Unsurprisingly from the discussion of technical naturalness both frameworks involve the appearance of a new symmetry. Before moving to the latter framework, to which a large part of this thesis will be devoted, we start with SUSY.

SUSY exploits a loophole in the Coleman-Mandula theorem by also considering anti-commutating fermionic generators as part of the symmetry group of the Lagrangian [31]. These fermionic generators Q turn a boson into a fermion and vice-versa. Therefore the basic particle fields are not of a definite spin anymore but become superfields which includes at least one fermion and one boson. Since the fermionic operator commutes with $P_\mu P^\mu$ and the internal symmetries, the fermion and boson of the superfield must have equal masses and charges. Of course, this is not phenomenologically viable and SUSY must be softly broken [32]. The minimal viable extension of the SM to include SUSY is the Minimal Supersymmetric Standard Model (MSSM). Together with the remarkable unification of gauge couplings [33,34], SUSY fits extremely well into the GUT paradigm. To understand how radiative corrections to the Higgs mass are tamed in SUSY, we have to consider the new particle content. There will now be a counterpart to each SM degree of freedom with its own contribution to the Higgs mass. Consider for example the top superpartner, more commonly known as the stop, \tilde{t} , which will contribute to the Higgs mass with the Feynman diagram of Fig. 1.2.

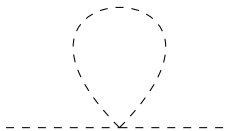


Figure 1.2: The main stop loop contribution to the Higgs mass.

Since SUSY enforces the quartic coupling from Fig. 1.2 above to be equal to y_t^2 and the degrees of freedom of the stops to be also equal to the degrees of freedom of the top, namely $N_c = 3$, the addition of this loop, with opposite sign, will tame the quadratic sensitivity of the top loop:

$$\Delta m_H^2|_{\text{top}} + \Delta m_H^2|_{\text{stop}} \sim -\frac{3}{8\pi^2} \left(m_t^2 \ln \left(\frac{\Lambda_{\text{UV}}^2}{m_t^2} \right) + \dots \right). \quad (1.5)$$

Indeed, the remaining sensitivity is merely logarithmic. The same cancellation holds for the other SM superpartners running in the loop. We see that SUSY is powerful enough to render the radiative corrections to the Higgs mass merely logarithmically sensitive to the UV scale. The only condition is that the stop masses must not be too much removed from the electroweak scale, in

other words SUSY must not be broken at too high scales and the degeneracy between partner and superpartners must be under control.

The second framework in which to address the hierarchy problem is that of composite Higgs. As the name suggests the Higgs is no longer an elementary scalar but a composite particle and the hierarchy problem only exists for elementary scalars. Indeed we know plenty of scalars in nature, more particularly in QCD, and we do not seem to worry about their mass generation. That is because a composite scalar has a finite localization $l \sim m_*$. Quantum corrections, such as those from Fig. 1.1, probe two different regimes. At smaller scales $E < m_*$, the finite extent of the composite scalar is not probed and these corrections will be quadratically sensitive. At higher scales $E > m_*$, the virtual quanta start probing the structure of the composite particle through form factors and the corrections quickly converge. In such a scenario it becomes important that the generation of the scale m_* itself does not generate another hierarchy problem. We know, thanks to QCD, that such a mechanism exists: dimensional transmutation. A small dimensionful quantity is generated through a dimensionless quantity. In QCD, the coupling constant, g_s , after including quantum effects, has a logarithmic dependency on the energy scale through the beta function:

$$\frac{\partial g_s}{\partial \log \mu} = \beta(g_s). \quad (1.6)$$

In non-Abelian Yang-Mills theories, β can be negative due to the anti-screening of the force carriers, and as such the coupling can become divergent in a perturbative calculation at a scale Λ_{QCD} which can be exponentially smaller with respect to higher scales such as the Planck scale. The divergence is just an indication of our lack of understanding and the breakdown of perturbation theory, but the coupling becomes large and forms bound colorless states of mass around Λ_{QCD} , a process known as confinement.

Both of these very elegant frameworks, which protect the Higgs mass from higher scales, come with many associated signatures (superpartners for SUSY and composite particles for composite Higgs scenarios). This led to high anticipation for the Large Hadron Collider (LHC) to discover not only the Higgs but a plethora of other particles. Although the Higgs mass was discovered in 2012, there has been no trace of any other particle. This has led to these theories becoming evermore fine-tuned in order to escape detection at the LHC.

Actually the null results of the LHC (of course, the Higgs discovery itself is a fantastic scientific success for mankind) is not such an unfamiliar situation. Already after the Large Electron-Positron collider (LEP) there were those who saw the writing on the wall [35]: a light Higgs in combination with a high cutoff for some higher dimensional operators that LEP very well constrained, meant traditional solutions were already generally fine-tuned. But after more than a decade after turning on the LHC the situation looks significantly worse. This has led to speculations that, just as the naturalness principle seem to fail for the Cosmological Constant and can be explained by anthropic principles in-

stead [36], a similar situation could be at play for the weak scale. Or new ideas, such as a dynamical cosmological evolution in the early Universe that drives the Higgs mass to a value much smaller than the cutoff [37], have emerged.

While these ideas are very exciting and need to be taken seriously, their phenomenological signatures are generically out of reach of TeV colliders and 21st century humans. Since observational signatures within the author's lifetime is a sincerely held bias of the author, this thesis focuses on exploring if the absence of signatures at the LHC could still be compatible with a natural Higgs and proposing new signatures which could be looked at.

1.5 Outline

In Chapter 2 we propose a new solution to the absence of top partners at the LHC. Instead of opting for a symmetry-based solution such as models of twin Higgs, where the quadratic sensitivity of the top loop is cancelled by uncolored top-partners, we investigate the possibility that the large top Yukawa only acquires its large value in the IR while at the multi-TeV scale it could be much smaller due to quantum effects or even completely vanish. In this case the expected scale at which the hierarchy problem should be addressed can be postponed to higher scales. However such strong changes in the top Yukawa would imply non-traditional phenomenological signatures which we study.

In Chapter 3 we present a minimal model of gauge-Higgs grand unification in a warped background. Using the power of the fifth dimension, we provide a compelling model of grand unification and of flavor. We study the stringent bounds from the flavor sector which, without imposing additional flavor symmetries, push the model into larger scales. Nevertheless, additional scalars due to the large unified structure may be accessible at colliders. We study the mass generation of these scalars.

We end in Chapter 4 with a novel model of composite Higgs which features little tuning. It shows how a natural model of composite Higgs could still be operating at the TeV scale while escaping detection. The mechanism relies on the cancellation of the top contribution to the composite Higgs potential with the introduction of mirror fermions that cancel the top contribution. In contrast to models of twin Higgs, it does not rely on a SM *twin sector* with an extra Z_2 symmetry. Instead it relies on a curious property of certain group representations. We discuss the very unique phenomenological signatures of the model.

Chapter 2

A Radiative Top Yukawa

As we discussed in the introduction, traditional solutions to the instability of the Higgs potential such as supersymmetry or compositeness do not suffice anymore to have a *natural Higgs*, that is to say a Higgs potential without any fine-tuning. The basic problems can be simply phrased as follows: if supersymmetry or compositeness indeed protects the Higgs potential from quadratically divergent corrections, these ideas should be realized at the electroweak scale. Herein lies the problem: after more than a decade of LHC, one has started to probe and understand scales up to the TeV quite well. In the case of supersymmetry, one should start to probe the supersymmetry and produce the superpartners of the SM such as the stops, while for compositeness one should start to probe the composite nature of the Higgs bosons and observe the composite partner of the top for instance. The higher the scale of supersymmetry or Higgs compositeness, Λ_{UV} , the more *residual* fine tuning is required to explain the hierarchy:

$$\Delta \sim \frac{\Lambda_{\text{UV}}^2}{m_H^2}. \quad (2.1)$$

Although there are specific solutions to reduce the residual fine tuning in both the SUSY or compositeness scenario (the last chapter of this thesis is devoted to such a solution for composite Higgs scenarios), the increasing bounds on the stops and the top partners have become worrisome for the naturalness paradigm. Indeed one can naively estimate the state of naturalness by considering how general top partners, with mass M_T , cancel the quadratic sensitivity of the Higgs mass to larger scales

$$\Delta m_H^2|_{\text{top}} + \Delta m_H^2|_{\text{top partner}} \sim -\frac{3}{8\pi^2} y_t^2 M_T^2 \log\left(\frac{\Lambda_{\text{UV}}^2}{M_T^2}\right), \quad (2.2)$$

where the logarithm and its dependence on the UV scale Λ_{UV} , indicates that a full calculation of the Higgs mass requires to specify the UV completion. Nevertheless, requiring radiative corrections from the top and its partner to be

comparable to the observed Higgs mass, we find

$$\Delta m_H^2 \sim \frac{-3}{8\pi^2} y_t^2 M_T^2 = -(88\text{GeV})^2 \left(\frac{M_T}{450\text{GeV}} \right)^2. \quad (2.3)$$

Therefore $M_T = 450$ GeV is the scale we expect for natural top partners. Years of searches by the ATLAS and CMS collaboration have pushed the bounds on colored top partners around 1500 GeV for both scalar partners [38, 39] and fermionic partners [40–44]. This naively implies a fine-tuning of $\Delta_{\text{FT}} = \Delta m_H^2 / m_H^2 \sim 10\%$. Although it must be noted that this estimate only accounts for the radiative top/stop corrections and in concrete computations within the MSSM, where a Higgs potential is already present at tree-level, the tuning is generally well below the percent-level (see for example [45]) while in composite Higgs frameworks (see Chapter 4 for example) it is at the few percent level.

Rather than completely abandoning naturalness (although this has become an interesting field alas without necessarily TeV scale signals), a new framework has emerged which has resulted in new and exciting ideas. Rather than stabilising the weak scale, composite Higgs or SUSY might only kick in at a larger scale $\Lambda_{\text{UV}} \sim 10$ TeV, explaining the absence of SUSY or composite states and deviations in EWPTs. Instead of simply accepting the residual tuning, another mechanism, producing different signatures, harder to observe, might be responsible for the residual hierarchy - a framework called *the little hierarchy*.

In this chapter we discuss such a mechanism, which stresses the importance of the large top Yukawa to the hierarchy problem. Indeed, if the top Yukawa would be smaller at larger scales due to large running effects, its general contribution to the Higgs mass would be reduced as the prefactor y_t^2 would become smaller at higher energies. Before presenting a general discussion of such a solution to the little hierarchy problem in Sec. 2.2, we briefly review a very popular, symmetry-based, solution to the little hierarchy problem in Sec 2.1. We then discuss two incarnations of our approach to the little hierarchy problem in Sec. 2.3 which relies on large Yukawa running and Sec. 2.4 which entirely generates the top Yukawa at the loop level. In Sec. 2.5 we discuss different signatures of the mechanism.

2.1 Twin Higgs

Twin Higgs [46] provides a model example of how the weak scale can be stabilised yet lack traditional naturalness signatures. The basic idea is based on a global $SU(4)$ symmetry that is linearly realized. The Higgs H_A is embedded with a twin Higgs H_B into a fundamental scalar of $SU(4)$, $H = (H_A, H_B)^T$. The $SU(4)$ -invariant potential is then

$$V = -m^2(H^\dagger H) + \lambda(H^\dagger H)^2, \quad (2.4)$$

whose negative quadratic will give a VEV to $\langle H \rangle = (m/\sqrt{2}\lambda) \equiv f$ and trigger the spontaneous breaking of $SU(4)$ to $SU(3)$ resulting in 7 Nambu-Goldstone bosons. The global group is explicitly broken by gauging the $SU(2)_A \times SU(2)_B$, with $H_{A/B}$ transforming respectively as a doublet under $SU(2)_{A/B}$ and $SU(2)_A$ identified with the SM weak charge $SU(2)_L$. Due to the gauging of the global symmetry, therefore introducing explicit breaking, the massless Nambu - Goldstone bosons become pseudo-Nambu-Goldstone bosons and pick up a mass. The leading gauge boson loop contribution to the potential goes as

$$\Delta V = \frac{9g_A^2\Lambda^2}{64\pi^2}(H_A^\dagger H_A) + \frac{9g_B^2\Lambda^2}{64\pi^2}(H_B^\dagger H_B) + \dots, \quad (2.5)$$

and we unsurprisingly obtain the usual quadratically sensitive contribution to the potential from gauge boson loops. Twin Higgs works by imposing an additional Z_2 symmetry, dubbed *twin parity*, which interchanges the A -states with those of the B -sector. Since this symmetry forces the gauge couplings of both sectors to be equal $g_A = g_B \equiv g$, we now find that the quadratically sensitive gauge contribution goes as

$$\Delta V = \frac{9g^2\Lambda^2}{64\pi^2}(H_A^\dagger H_A + H_B^\dagger H_B) + \dots = \frac{9g^2\Lambda^2}{64\pi^2}(H^\dagger H) + \dots, \quad (2.6)$$

and is $SU(4)$ invariant therefore not contributing to the potential for the scalars. Although the quadratic sensitivity is cancelled, there will still be a logarithmic contribution sensitive to the eventual UV completion at Λ_{UV} that is not $SU(4)$ symmetric of the form

$$\Delta V \sim \frac{3g^4}{16\pi^2} \log(\Lambda_{UV}/gf)(|H_A|^4 + |H_B|^4) + \dots \quad (2.7)$$

Importantly the Higgs sector can be made custodially symmetric by changing the global symmetry to $O(8)$. The twin parity symmetry and by construction this mechanism can be extended for all the other SM particles. In particular the quadratic nature of the top quark loop, which is the largest SM contribution, can be cancelled by including the color group $SU(3)_A$ and its twin $SU(3)_B$ into $SU(6)$. The total global symmetry of the model is therefore $SU(6) \times SU(4) \times U(1)^2$ with the SM gauge group and its twin sector being gauged. The top Yukawa interaction can be modeled respecting the global symmetry by introducing two chiral fermions under $SU(6) \times SU(4)$ that decompose under the SM gauge group and its twin as respectively

$$\begin{aligned} Q_L &= (\mathbf{6}, \bar{\mathbf{4}}) \\ &= (\mathbf{3}, \mathbf{2}; \mathbf{1}, \mathbf{1}) + (\mathbf{1}, \mathbf{1}; \mathbf{3}, \mathbf{2}) + (\mathbf{3}, \mathbf{1}; \mathbf{1}, \mathbf{2}) + (\mathbf{1}, \mathbf{2}; \mathbf{3}, \mathbf{1}) \\ &\equiv q_A + q_B + \tilde{q}_A + \tilde{q}_B \\ T_R &= (\bar{\mathbf{6}}, \mathbf{1}) \\ &= (\bar{\mathbf{3}}, \mathbf{1}; \mathbf{1}, \mathbf{1}) + (\mathbf{1}, \mathbf{1}; \bar{\mathbf{3}}, \mathbf{1}) \\ &\equiv t_A + t_B. \end{aligned} \quad (2.8)$$

An invariant Yukawa coupling can then be obtained as $yHQ_L T_R + \text{h.c.}$. Notice that the chiral *exotic* fermions \tilde{q}_A, \tilde{q}_B are massless but are made heavy by the introduction of vector-like masses and right-handed partners for them $M(\tilde{q}_A^c \tilde{q}_A + \tilde{q}_B^c \tilde{q}_B)$. Although this mass respects the twin parity symmetry, it only softly breaks $SU(4)$ and is the only source of its breaking in the fermion sector. The contribution to the potential from this term will therefore be finite. To obtain a phenomenologically viable potential it is also important to introduce a Z_2 -breaking term $\mu^2 H_A^\dagger H_A$. Six of the Goldstones are eaten by the two $SU(2)$ groups and the remaining scalar is identified with the Higgs boson. In order to be SM-like it should be dominantly composed of $h_A = (\text{Re}(H_A^0) - v_A)/\sqrt{2}$. The twin Higgs is protected from radiative corrections above the scale f . However the scale f , which impacts directly the Higgs mass when substituting $|H_B|^2 \approx f^2 - h^2$ into Eq. (2.7), is itself not stabilised. Indeed the fundamental scalar of $SU(4)$ from Eq. (2.4) will itself give rise to a hierarchy problem but can be further addressed by SUSY or compositeness. For example, twin Higgs can be embedded into a composite Higgs scenario and is known as composite Twin Higgs [47–49], while a UV completion of Twin Higgs can also be realised in a supersymmetric extra-dimensional model on an orbifold and is known as *folded supersymmetry* [50].

The main takeaway from this model is that the Higgs can be stabilized without the presence of new light particles charged under the SM gauge group, instead in twin Higgs setup the new particles are charged under the twin gauge groups that are neutral under the SM. The color factor $N_c = 3$ in Eq. 2.2, necessary to cancel the quadratic sensitivity of the Higgs mass to new scales, is just a counting factor and can come from any gauge group. Only a Z_2 symmetry is necessary to relate the Yukawa couplings of both sectors. In these scenarios, the collider constraints are very mild and challenge the conventional searches for naturalness at colliders. This more general paradigm of cancelling the top loop contribution to the Higgs by uncolored partners, now known as *neutral naturalness*, has grown into a rich literature over the last decades with various dark matter candidates, connections to cosmology, astrophysics, neutrinos and flavor (see [51] for a recent review).

2.2 Mitigating the Top Loop

We now proceed with our novel proposal to address the little hierarchy problem. As we have now repeatedly remarked, solving the (little) hierarchy problem usually involves cancelling the quadratic sensitivity of the Higgs boson mass to the cutoff scale by introducing a partner particle for each SM particle (be it a superpartner for SUSY, a composite resonance in the case of composite Higgs or even a neutral partner in neutral naturalness) whose quadratic sensitivity to the cutoff cancels the one from the SM particle. All these solutions heavily rely on a symmetry between a SM particle and its partner. Here we propose a more

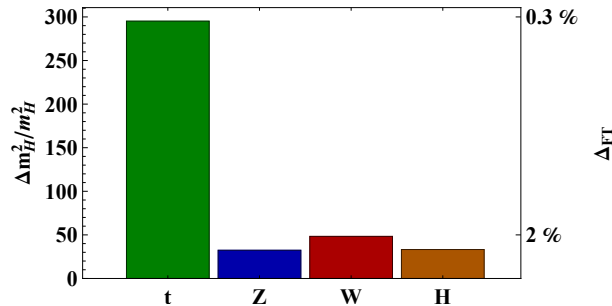


Figure 2.1: The various contributions to the Higgs mass squared for $\Lambda_{\text{NP}} = 10$ TeV.

bottom-up solution to the little hierarchy problem. Although all the massive SM particles talk to the Higgs and thus contribute to the hierarchy problem, the top quark due to its large mass, stands out. Indeed, let us assume the SM is embedded in a UV completion at a scale Λ_{NP} , the four largest radiative contributions from the new physics at that scale come from the top-, W-, Z-, and Higgs sectors (with $B = T, W, Z, H$ respectively)

$$(\Delta m_H^2)_B = \frac{3}{2} g_B^2 \frac{\Lambda_{\text{NP}}^2}{16\pi^2}, \quad (2.9)$$

with $g_T^2 = 4y_t^2$, $g_W^2 = g^2$, $g_Z^2 = (g^2 + g'^2)/2$, $g_H^2 = 4\lambda$. In Fig. 2.1 these contributions are normalised to the Higgs mass and expressed as a measure of fine-tuning $\Delta_{\text{FT}} = \Delta m_H^2 / m_H^2$, it becomes clear that the tuning due to the top is an order of magnitude worse than the next contribution coming from the W boson and is the driving force behind the little hierarchy problem. Requiring an acceptable fine-tuning of 5% leads to a generic bound on the new physics scale of $\Lambda_{\text{NP}} \sim 2.5$ TeV.

For a very large Λ_{NP} , all these loops become problematic giving large corrections to the Higgs mass, illustrating the necessity of a solution to the full hierarchy problem. However, when considering the little hierarchy problem, we are only considering a relatively low scale NP scale of $\Lambda_{\text{NP}} = 10$ TeV where only the top quark contribution becomes problematic. Therefore the issue of the little hierarchy problem is mainly one of the top-loop. A solution to the little hierarchy problem could therefore be exclusively secluded to the top-sector. In contrast to twin Higgs, which can be applied to all the SM particles contributing to the Higgs mass, the solution discussed further below only addresses the quadratic sensitivity of the top quark.

The idea is to make the top Yukawa coupling strongly dependent on the energy scale, $y_t = y_t(\mu^2)$, or even directly on the momentum running through the vertex, $y_t = y_t(k^2)$. Indeed, a careful calculation of the radiative contribution to the Higgs mass reveals that it is sensitive to all the energy scales until the Λ_{NP} , and in particular the top Yukawa coupling is probed at all these different

scales

$$\Delta m_H^2|_{\text{top}} = -2iN_c \int_{m_t}^{\Lambda_{\text{NP}}} \frac{d^4k}{(2\pi)^4} y_t^2(k^2) \frac{k^2 + m_t^2}{(k^2 - m_t^2)^2}, \quad (2.10)$$

which after a Wick rotation will probe the top Yukawa coupling at space-like momenta $y_t(-Q^2)$. Notice that even in the SM, at first order in perturbation theory, the top Yukawa is not a constant, but is a scale dependent quantity, mostly due to the gluon correction to the top Yukawa vertex. This is the same effect that makes the top mass run at the one-loop level, although it is not nearly enough in the SM to significantly impact the radiative correction of the Higgs mass.

In case the top Yukawa has a significant scale dependence due to new physics, the integral above gets tamed at high momenta due to the smaller vertex and the naive estimate becomes invalid. In the more exotic case in which non-trivial dynamics generate the top Yukawa at the loop level, the above integral can actually become finite and the fine-tuning associated to the top-loop can become bounded. Indeed, if the top Yukawa drops off around $k^2 \sim \Lambda_T^2$, the integration of Eq. (2.10) becomes finite

$$\Delta m_H^2|_{\text{top}} \sim -\frac{3}{8\pi^2} y_t^2 \Lambda_T^2, \quad (2.11)$$

and the contribution of the top quark to the fine tuning of the Higgs mass is bounded. The corresponding Feynman diagram is shown in Fig. 2.2 where the blob represents the scale dependence of the top Yukawa.

Such a behavior would imply a nontrivial origin for the large top Yukawa in the IR due to new degrees of freedom (but not top partners) significantly below the new physics scale where a SUSY or composite Higgs type model provides a UV completion for the full hierarchy problem. In the following we will discuss how these degrees of freedom should look like.

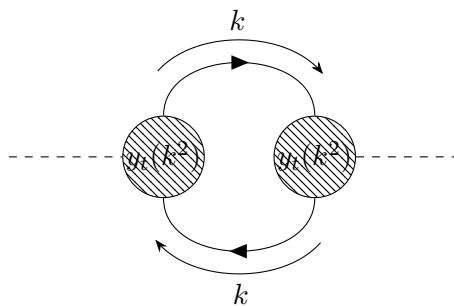


Figure 2.2: The top-loop contribution to the Higgs mass for a non-trivial top Yukawa $y_t(k^2)$.

Interestingly this mechanism relies on the fact that we have not measured the top Yukawa at high energies. While a strong reduction of the top Yukawa at electroweak scales would be in tension with Higgs (production and decay)

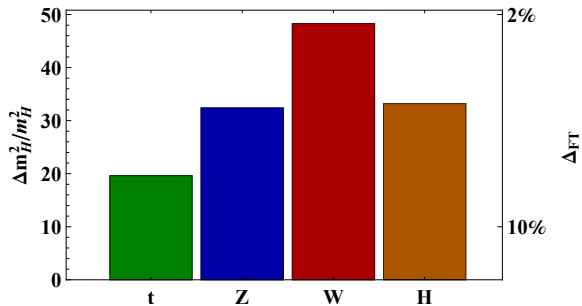


Figure 2.3: Various contributions to the Higgs mass squared for $\Lambda_{\text{NP}} = 10$ TeV in case $y_t(\Lambda_{\text{NP}}^2) \lesssim 0.2$ or equivalently $\Lambda_T \lesssim 1/5 \Lambda_{\text{NP}}$.

measurements at the LHC [52–54], at high scales, $\Lambda_{\text{NP}} \gg M_{\text{EW}}$, a large reduction remains phenomenologically viable [55–58]. In the UV, the top quark would behave rather as the other quarks and only obtain its large coupling to the Higgs in the IR, *i.e.* $y_t(M_{\text{EW}}^2) \approx y_t^{\text{SM}}(M_{\text{EW}}^2)$, but $y_t(\Lambda_{\text{NP}}^2) \ll y_t^{\text{SM}}(\Lambda_{\text{NP}}^2)$. Such a mechanism would also impact the running of the top mass which is especially made relevant by the fact that CMS has provided the first measurement of the running top mass up to the TeV scale [59]. Such measurements open up additional handles for testing the idea and we will confront model predictions with the corresponding limits.

Before going to specific implementations of the idea, let us see how the situation of Fig. 2.1 can change in the presence of either a strongly scale dependent top Yukawa, $y_t(\Lambda_{\text{NP}}^2) \lesssim 0.2 \ll y_t(M_{\text{EW}}^2)$ or due to cutting off the top loop at $\Lambda_T \lesssim 1/5 \Lambda_{\text{NP}}$.

In Fig. 2.3 we see a new picture emerging, there is no dominant top Yukawa contribution to the fine-tuning of the Higgs anymore, rather now the W boson loop is the dominant force in the little hierarchy problem with the fine-tuning reduced by an order of magnitude. This reduction translates into a threefold increase of the naive scale where we expect, due to the naturalness criterion, a solution to the full hierarchy problem.

Still, taming or even cutting off completely the top loop contribution is not enough and at the latest around $\Lambda_{\text{NP}} = 10$ TeV, a full UV completion - cancelling the contributions from the bosonic loops - should kick in. The scenario discussed here is therefore playing an assistant role, relieving the strong bounds on naturalness coming from the top partner searches. It is especially helpful in composite Higgs completions where an $\mathcal{O}(1)$ Yukawa coupling providing a large breaking of the Goldstone shift symmetry is problematic. The biggest tension of these models with LHC data, being the absence of light top partners [60–66], is in fact caused by this large Yukawa coupling.

In the rest of this chapter we will scrutinize such a scenario and hypothesize about the possible microscopic origin of the top Yukawa and its impact on the little hierarchy problem, potentially changing the vanilla picture. After all, the LHC is only probing energy scales just above the weak and it is crucial to

ponder whether an acceptable tuning of 5% implies $\Lambda_{\text{NP}} \sim 2.5$ TeV or could allow $\Lambda_{\text{NP}} \sim 10$ TeV. Besides unique signatures of new physics associated to the top Yukawa, the ultimate test of naturalness would then be postponed to a 100 TeV collider. While such a collider could explore in detail the potential origins of the top Yukawa, null findings would drive the new physics scales high enough such that the tuning associated to the gauge bosons and the Higgs becomes unnaturally large.

In Sec. 2.3 we will study scenarios in which a reduction of tuning is achieved by a modified renormalization group evolution (RGE) of the top Yukawa, providing possible realizations that could drive y_t significantly to lower values. Afterwards, in Sec. 2.4 we consider a strongly coupled model where the top Yukawa is fully generated at one loop. We discuss the phenomenological aspects of the model in Sec. 2.5.

2.3 Running Top Yukawa

In fact, it comes as no surprise that at the one-loop level, the top Yukawa is already evolving with the energy scale $t = \ln \mu$ in the SM according to

$$\frac{dy_t}{dt} = \frac{y_t}{16\pi^2} (9/2 y_t^2 - 8 g_3^2 - 9/4 g_2^2 - 17/12 g_Y^2), \quad (2.12)$$

with $g_{Y,2,3}$ being the $U(1)_Y, SU(2)_L, SU(3)_c$ gauge couplings. Since all SM gauge groups tend to screen the top Yukawa at higher scales, we expect that additional gauge interactions could lead to a further decrease of the top Yukawa increasing the modest decrease of the SM [67,68]. More precisely, adding a new abelian or non-abelian force to the SM with coupling strength \tilde{g}_N ¹ under which the left- and right-handed quarks are charged respectively with charges Y_L and Y_R for the abelian case, results in the following RGE [69–71] for the y_t

$$\frac{dy_t(t)}{dt} = \frac{y_t(t)}{16\pi^2} (9/2 y_t^2(t) - B(N) \tilde{g}_N^2), \quad (2.13)$$

with $B(1) \equiv 3(Y_L^2 + Y_R^2)$ for the abelian case and $B(N) \equiv 3(N^2 - 1)/N$ for $N > 1$.

As a benchmark for the potential effect of such an extra gauge group, we focus on an $U(1)$ extension and take $Y_L = Y_R = 2$, $\tilde{g}_1 = 2.5$ for a new gauge boson of mass $M = 2.5$ TeV. The modified RGE of the top Yukawa is depicted in Fig. 2.4 and we observe that $y_t(\mu=10 \text{ TeV}) \approx 0.2$ while $y_t(\mu=20 \text{ TeV}) \approx 0.1$. Such a drastic running allows for significant mitigation of the hierarchy problem due to new physics coupled to the top quark. One can now recalculate the fine-tuning in the Higgs mass with this extra force due to generic new physics at the scale $\Lambda_{\text{NP}} = 10$ TeV. This situation is the one of Fig. 2.3 with the top

¹We assume in our analysis that the running of the gauge coupling itself is negligible in the region of interest.

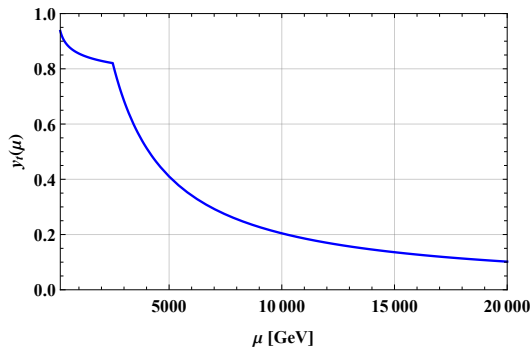


Figure 2.4: Running of the top Yukawa coupling in the simple $U(1)$ extension with $Y_L = Y_R = 2$, $\tilde{g}_1 = 2.5$, and a mass of the new gauge boson of $M = 2.5$ TeV.

contributions becoming subdominant and the fine tuning being driven by weak gauge bosons. Now requiring less than 5% tuning allows for a generic higher scale of

$$\Lambda_{\text{NP}} = 7.5 \text{ TeV}, \quad (2.14)$$

a three-fold increase in comparison to no change in the top Yukawa and beyond generic LHC reach.

2.3.1 Simple Perturbative Extensions

We now discuss a few realistic setups that can impact the running of the top Yukawa. The underlying assumption is that the new particles could be light, impacting the RGE running while not contributing large thresholds to the Higgs mass. A full solution to the hierarchy problem (like SUSY or composite Higgs scenarios) could appear at larger scales without creating a residual *little* hierarchy problem.

$U(1)$ extensions of the SM are constrained by the stringent requirement of anomaly cancellation [72]. Requiring flavor diagonal charge assignments or, less constraining, one set of charge assignments for some of the generations, one is left with the well-known SM hypercharge symmetry or that symmetry restricted to one or two generations. Extending the SM minimally with right-handed neutrinos, ν_R , $B - L$ is also anomaly free. For each of the scenarios below, we will consider a gauge boson mass of 2.5 TeV.

$(B - L)_3$ Scenario Gauging only the third generation of $(B - L)$ [73] avoids stringent constraints on a universal $B - L$ boson coming from LEP data which constrains the mass over coupling ratio to $M_X/g_X > 18$ TeV [74]. The vector boson X_μ couples in a vector like fashion to the third generation:

$$\mathcal{L} \supset g_X X_\mu \left(\bar{t} \gamma^\mu t + \bar{d} \gamma^\mu d - 3 \bar{\tau} \gamma^\mu \tau - 3 \bar{\nu}_\tau \gamma^\mu \nu_\tau \right). \quad (2.15)$$

To have maximum impact on the running, we wish to take the gauge coupling as large as possible, only bounded by the requirement of perturbativity. We will take the perturbative limit to be $\Gamma(X)/M_X \lesssim 50\%$. Due to the three times larger coupling of the gauge boson to leptons in comparison to quarks, the width is

$$\frac{\Gamma(X)}{M_X} = \frac{2}{\pi} g_X^2, \quad (2.16)$$

imposing a limit of $g_X < 0.89$ on the coupling. The top Yukawa is only reduced to a very modest 0.74 at 10 TeV for such a gauge boson versus 0.77 in the SM. This immediately shows the limitations of an anomaly free $U(1)$ extension for our goal.²

Purely Top-philic Setup The situation above could be addressed by avoiding unnecessary large couplings to leptons, by employing a purely top-philic boson:

$$\mathcal{L} \supset g_X X_\mu (\bar{t} \gamma^\mu t). \quad (2.17)$$

The anomaly cancelling UV completion would be more baroque but the width of the vector boson is reduced

$$\frac{\Gamma(X)}{M_X} = \frac{2}{8\pi} g_X^2, \quad (2.18)$$

making couplings of strength $g_X \lesssim 2.5$ possible. Such a gauge boson would allow for a reduction of the top Yukawa to $y_t = 0.55$ at 10 TeV, still only a modest reduction in total fine-tuning.

Third Generation non-Abelian Models We now turn to non-abelian scenarios which only couple to the third generation. A non-universal left-right model [75] in which only the third generation of right-handed fermions is charged under the new $SU(2)_R$ gauge group provides a first example. The Lagrangian for the Z'_μ reads:

$$\mathcal{L} \supset g_R/2 Z'_\mu (\bar{b}_R \gamma^\mu b_R - \bar{t}_R \gamma^\mu t_R + \bar{\tau}_R \gamma^\mu \tau_R - \bar{\nu}_R \gamma^\mu \nu_R). \quad (2.19)$$

There is also a W'_μ , although its production at the LHC is less problematic [75]. The corresponding width for both gauge bosons is given by

$$\frac{\Gamma(Z')}{M_{Z'}} = \frac{\Gamma(W')}{M_{W'}} = \frac{1}{12\pi} g_R^2, \quad (2.20)$$

which implies $g_R < 4.3$. The impact of such a model on the running of the top Yukawa can be studied by substituting $B(N) \tilde{g}_N^2 \rightarrow \frac{9}{4} g_R^2$ in Eq. (2.13), where the additional factor 1/2 takes into account the fact that only the right-handed top

²Gauging multiple $(B-L)_3$ symmetries cannot improve the situation due to perturbative unitarity bounds on scattering cross sections that would be enhanced by multiplicity factors.

couples to the new force. The decay of the Z' into tau pairs, drives the minimal mass to $m_{Z'} > 2.5$ TeV. The maximal reduction in the top Yukawa running at 10 TeV is merely $y_t = 0.52$. A desired running to $y_t = 0.2$ would imply a coupling as large as $g_R \sim 8.2$, well outside of the validity of perturbation theory.

A last perturbative example comes from a broken $SU(3)$ gauge symmetry, known as Topcolor [76], only affecting the third generation quarks with the following Lagrangian:

$$\mathcal{L} = g_3' G_\mu^A (\bar{q}_L \gamma^\mu T^A q_L + \bar{t}_R \gamma^\mu T^A t_R + \bar{b}_R \gamma^\mu T^A b_R). \quad (2.21)$$

To achieve the desired top Yukawa of $y_t \sim 0.2$ at 10 TeV, the coupling should be $g_3' \sim 4.5$, while the perturbative limit on the width of the heavy gauge boson, otherwise known as the *coloron*, is $g_3' < 4.3$ which could borderline be fulfilled. Therefore such a scenario could bring the corresponding contribution of the top quark to the fine tuning down to that of the electroweak and Higgs bosons. It is thus conceivable that the hierarchy problem is fully relieved within a perturbative region, although in the corners of parameter space. For a more stable solution, we have to enter the non-perturbative regime.

2.3.2 Beyond the Perturbative Bound

As we have seen in the last section, if we wish drastic changes to the top Yukawa running, the gauge coupling should be large, entering the domain of non-perturbative physics. A ubiquitous consequence of non-perturbative dynamics is the formation of bound states. We restrict our analysis to the minimal setup in which only q_L and t_R participate in the strong dynamics. The resulting bound state is a scalar field with the quantum numbers identical to that of the Higgs, known as top-Higgs H_t [77, 78]. The properties of this bound state can be elegantly described by the Nambu-Jona-Lasinio (NJL) model [79, 80]. This model was originally considered, before the advent of QCD and even the notion of quarks, to model the nucleons. It provides a physical picture of chiral symmetry breaking, or how the nucleons achieve their large dynamical mass, even though the tree-level Lagrangian respects chiral symmetry. The model consists of a fermion ψ , possibly transforming under some flavor symmetry, $SU(2)$ isospin in the case of the original NJL model, with the following chiral-symmetric Lagrangian

$$\begin{aligned} \mathcal{L}_{\text{NJL}} &= \bar{\psi}(i\cancel{\partial} - m)\psi + G/4 \left((\bar{\psi}\psi)^2 - (\bar{\psi}\gamma^5\psi)^2 \right) \\ &= \bar{\psi}(i\cancel{\partial} - m)\psi + (G)(\bar{\psi}_L\psi_R)(\bar{\psi}_R\psi_L), \end{aligned} \quad (2.22)$$

with $G = g_X^2/M_X^2$ a dimensionful constant. In the second line we clearly see that the four-fermion interaction is chiral-symmetric with the exception of a possible small bare mass m . Interestingly this interaction is contained, after a

Fierz rearrangement, in the exchange potential of a massive gluon with mass M_X . The above equation can thus be viewed as a rough approximation of QCD close to the QCD scale and indeed it provides a picture of spontaneous chiral symmetry breaking and the generation of a large dynamical mass for the fermion (either for ψ representing a nucleon or later, with the advent of QCD, ψ representing a quark). The theory is then solved at low energies by summing up fermion loops [81], i.e. the fermion bubble approximation. A convenient alternative is to rewrite the above with an auxiliary scalar field H (which will represent a bound scalar developing a possible VEV)

$$\mathcal{L}_{\text{NJL}} = \bar{\psi}(i\not{\partial} - m)\psi + (g_X \bar{\psi}_L \psi_R H + \text{h.c.}) - M_X^2 H^\dagger H, \quad (2.23)$$

evolving the above to lower scales $\mu < M_X$, we find the following effective Lagrangian for H (see [82])

$$\mathcal{L}_{\text{NJL},\mu} = |\partial H|^2 - \tilde{M}^2 |H|^2 - \tilde{\lambda} |H|^4 - \tilde{y}_t \bar{\psi}_L \psi_R H + \text{h.c.}, \quad (2.24)$$

with coefficients depending on the scale μ as

$$\begin{aligned} \tilde{M}(\mu)^2 &= \left(\frac{4\pi}{\sqrt{NC}} \frac{M_X}{g_X} \right)^2 \left(1 - \frac{g_X^2}{g_c^2} + \frac{g_X^2 \mu^2}{g_c^2 M_X^2} \right), \\ \tilde{\lambda}(\mu) &= \frac{16\pi^2}{NC}, \quad \tilde{y}_t(\mu) = \frac{4\pi}{\sqrt{NC}}, \end{aligned} \quad (2.25)$$

with N is the number of colors of the new gauge symmetry and $C \equiv \ln(M_X^2/\mu^2)$. The Yukawa \tilde{y}_t represents the interaction between the scalar bound state and its constituents. We observe that the low energy theory has an unbroken or broken phase characterised by a condensate of the bound state $\langle H \rangle \neq 0$, depending on the size of the gauge coupling g being larger or lower than the *critical* coupling $g_c \equiv \sqrt{8\pi^2/N}$.

In our case, we will be interested in changing the nature of the top Yukawa running and thus at the very least q_L and t_R will participate in the new interaction with the scalar bound state $H_t \sim (\bar{q}_L t_R)$ having Higgs-like quantum numbers.

The Unbroken Phase For a coupling g smaller than the critical coupling g_c we enter the non-perturbative regime but no condensate forms for the bound state H_t . Its mass will be M_X on the order of the other heavy bound states as we find:

$$M_{H_t} = \tilde{M}(\mu) \sim \frac{4\pi}{\sqrt{NC}} \frac{M_X}{g_X}. \quad (2.26)$$

Furthermore since $M_{H_t} \gg m_H$ mixing with the SM Higgs through the top is small as the top-Higgs decouples.

What is the effect on the running of the top Yukawa that we can achieve with such a setup? In the (non)-abelian case, taking $N = 1(3)$, we find a critical

coupling of $g_c = 9(5)$. The benchmark values calculated above $g_X = 5(g'_3 = 4.5)$ belong to this scenario, meaning an optimal reduction to $\mathcal{O}(0.2)$ at 10 TeV due to running is indeed achievable. The desired amount of running is thus inherently part of a non-perturbative gauge theory in the unbroken phase. In this case, the top loop contribution to the hierarchy problem is thus relieved at the price of new composite and broad resonances, including the gauge boson X_μ and the top-Higgs H_t .

The Broken Phase For a larger coupling $g_X > g_c$, we enter the broken phase and the setup changes drastically. Not only is EWSB triggered due to a non-zero vev $\langle H_t \rangle \neq 0$, but a large top mass is also simultaneously generated (fully analogous to how in the NJL model a large chiral symmetry breaking mass is generated for the quarks). This setup is known as top quark condensation [81, 83, 84]. This model aimed to explain, using fully the VEV of H_t , electroweak symmetry breaking but has since then been ruled out due to a too large top mass $m_t \sim 600$ GeV. Instead, here we would like the SM Higgs to be fully responsible for EWSB and the top mass and therefore we require a small VEV for H_t . Using the predictions of the NJL model we then find

$$\langle H_t \rangle \equiv v_t = \sqrt{\frac{-\tilde{M}^2}{2\tilde{\lambda}}} \sim \frac{M_X}{g_X} \sqrt{\frac{g_X^2}{g_c^2} - 1} . \quad (2.27)$$

The generic VEV v_t will thus be much too large and we need to tune g_X against g_c to obtain a sufficiently small v_t . Moreover the VEV will contribute to the top quark mass with the following contribution

$$\tilde{m}_t = \frac{1}{\sqrt{2}} \tilde{y}_t v_t . \quad (2.28)$$

If this mass is greater than that from the SM Higgs, the top is mostly generated from the dynamical symmetry breaking triggered by its own condensate. Such a scenario is known as Topcolor-Assisted Technicolor [85] and we will therefore focus on the small v_t case.

A crucial element of the broken phase scenario is that we expect the top-Higgs doublet H_t to decompose into a CP even neutral scalar h_t and top-pions. The latter are massless (fully analogous to the almost massless pions in QCD) and the former has according to the NJL model a mass of:

$$M_{h_t} = \sqrt{2\tilde{\lambda}_0} v_t = 2\tilde{m}_t < 350 \text{ GeV} . \quad (2.29)$$

A realistic model requires additional breaking terms to lift the massless top-pions. Nonetheless, these light states with strong coupling to the top quark are severely constrained and the broken phase scenario is thus disfavored.

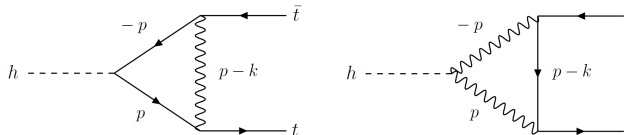


Figure 2.5: Two types of loop diagrams which can generate the top Yukawa coupling. The solid lines represent a fermion and the wavy line could be either a vector boson or a scalar boson.

Strong running from an extra dimension Lastly let us briefly comment on another possible source for large running: an extra dimension. It is well known that flat extra dimensions turn the usual logarithmic running into a power law running due to the Kaluza-Klein tower [86, 87]. Indeed the beta function for a Yukawa coupling, in an extra dimension of length R , obtains contributions from each kinematically accessible Kaluza-Klein (KK) mode below the energy scale E

$$\beta_y^{\text{UED}}(N_{\text{KK}}) = \beta_y^{\text{SM}} + (N_{\text{KK}} - 1)\beta_y^{(\text{KK})}, \quad (2.30)$$

with $N_{\text{KK}} = ER$ and $\beta_y^{(\text{KK})}$ being the (universal) contribution from a KK mode. For a benchmark value of $R' \approx 1$ TeV, a top Yukawa of 0.2 can be achieved at 20 TeV [88], with even stronger running achievable with more extra dimensions. The experimental extraction of the running top Yukawa at high scales as a probe of such power-law running would be very relevant for extra dimensions and has been discussed in [55].

2.4 A Radiative Top Yukawa

Having discussed scenarios in which the top Yukawa exists at high energy but with considerable running when moving to lower energies, we will now present a second option, where the top Yukawa is fully generated from quantum effects. Having an external elementary Higgs and external top quarks, there are two possibilities to have a loop diagram as shown in Fig. 2.5. We have already discussed extensively the left diagram which is the typical top Yukawa running due to a new force, but which presupposes the existence of a tree-level Yukawa term in the UV. The right diagram is a new scenario in which the top Yukawa is *generated* from a loop diagram. The two wavy lines can represent either both vector bosons or scalar bosons, and the solid line is a new vector-like fermion. The loop is UV convergent and has a $1/M^2$ suppression. We will take the diagram with scalar bosons as an example. Restoring the electroweak symmetry in Fig. 2.6, the $1/M^2$ suppression coming from the momentum integration should

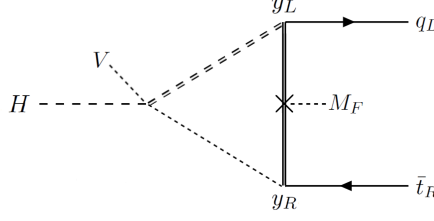


Figure 2.6: The loop diagram that can generate the top Yukawa coupling from a dimension-6 operator. The solid lines represent a fermion and the dashed lines correspond to scalar bosons.

be compensated by two mass scales. One comes from the mass of the vector-like fermion M_F , required to flip chirality, and one from the trilinear coupling, V .

The expected size of the resulting top Yukawa coupling can then be estimated as

$$y_t \sim \frac{1}{16\pi^2} y_L y_R \frac{V M_F}{M^2} \sim 1, \quad (2.31)$$

with M the mass of the heaviest particle in the loop. It becomes clear that to fully generate the large top Yukawa at the loop level, the couplings need to be large itself. This might seem borderline, especially in a perturbative calculation, however one should imagine that the vertices originate from a new strongly coupled UV theory. In a strongly coupled theory the expected top Yukawa is actually $\sim 4\pi$ and one needs additional suppression to bring it down to the measured 1. We will leave possible UV origins for Appendix A, focusing here on a simplified model.

2.4.1 A Simplified Scalar Model

To complete the loop from Fig. 2.6, three new couplings are required

$$\mathcal{L}_{\text{int}} = -V S_R S_L^\dagger H - y_L \bar{q}_L S_L F_R - y_R \bar{t}_R S_R F_L + \text{h.c.}, \quad (2.32)$$

with S_L a scalar doublet and S_R a scalar singlet and the vector-like singlet fermion F . The hypercharge of the new particles is not determined by the loop due to an accidental $U(1)$ symmetry. The hypercharge is allowed to be

$$Q(F) = Q_F, \quad Q(S_L) = \frac{1}{6} - Q_F, \quad Q(S_R) = \frac{2}{3} - Q_F, \quad (2.33)$$

but in the following analysis we will take $Q_F = 2/3$, meaning the vector-like fermion and the right-handed top quark carry the same charge. S_L has then the same quantum numbers as the Higgs doublet while S_R is a singlet under the SM. As we will discuss in Sec. 2.4.6, this will make it possible to extend

the model into a custodially protected model, necessary to evade electroweak precision constraints. In addition, we add masses for the new particles:

$$\mathcal{L}_{\text{mass}} = -M_L^2 |S_L|^2 - M_R^2 |S_R|^2 - M_F \bar{F}_L F_R + \text{h.c.} . \quad (2.34)$$

In order to understand the mechanism behind the generation of the top Yukawa, we focus on the neutral scalars and rotate to the mass eigenstates. The Lagrangian reads

$$\begin{aligned} \mathcal{L}_{\text{neutral}} &= |\partial S_L|^2 + |\partial S_R|^2 - M_L^2 |S_L|^2 - M_R^2 |S_R|^2 \\ &\quad - V S_R S_L^\dagger H + \text{h.c.} \end{aligned} \quad (2.35)$$

$$\begin{aligned} &= |\partial s_L|^2 + |\partial s_R|^2 - M_L^2 |s_L|^2 - M_R^2 |s_R|^2 \\ &\quad - M_{LR}^2 (s_L^* s_R + s_R^* s_L), \end{aligned} \quad (2.36)$$

with s_L and s_R the (complex) neutral components of S_L and S_R . The coefficient of the mass mixing term is $M_{LR}^2 \equiv V \langle H \rangle = V v / \sqrt{2}$. Therefore the trilinear coupling leads to mass mixing between s_L and s_R which upon rotation leads to the mass eigenstates s_h and s_l denoting respectively the heavy and light mass eigenstates

$$\begin{pmatrix} s_L \\ s_R \end{pmatrix} = \begin{pmatrix} c_\beta & -s_\beta \\ s_\beta & c_\beta \end{pmatrix} \begin{pmatrix} s_h \\ s_l \end{pmatrix}, \quad (2.37)$$

and with $c_\beta \equiv \cos \beta$, $s_\beta \equiv \sin \beta$. The angle satisfies

$$s_\beta c_\beta = M_{LR}^2 / \sqrt{4M_{LR}^4 + (M_L^2 - M_R^2)^2}. \quad (2.38)$$

The free Lagrangian in the mass basis reads

$$\mathcal{L}_{\text{neutral}} = |\partial s_h|^2 + |\partial s_l|^2 - M_s^2 |s_h|^2 - m_s^2 |s_l|^2, \quad (2.39)$$

with $M_s(m_s)$ the mass of the heavy (light) neutral scalar. Their values are given by:

$$M_s^2(m_s^2) = \frac{1}{2} (M_L^2 + M_R^2) \pm \sqrt{M_{LR}^4 + \frac{1}{4} (M_L^2 - M_R^2)^2}. \quad (2.40)$$

The interaction terms between the scalars and the Higgs boson becomes

$$\begin{aligned} \mathcal{L}_{\text{trilinear}} &= -\sqrt{2} V c_\beta s_\beta h |s_h|^2 + \sqrt{2} V c_\beta s_\beta h |s_l|^2 \\ &\quad - \frac{V(c_\beta^2 - s_\beta^2)}{\sqrt{2}} h s_h^* s_l + \text{h.c.}, \end{aligned} \quad (2.41)$$

while the interaction terms with the vector-like fermion read:

$$\begin{aligned} \mathcal{L}_{\text{fermion}} &= - (y_L c_\beta \bar{t}_L s_h F_R + y_R s_\beta \bar{t}_R s_h F_L) \\ &\quad - (-y_L s_\beta \bar{t}_L s_l F_R + y_R c_\beta \bar{t}_R s_l F_L) + \text{h.c.} . \end{aligned} \quad (2.42)$$

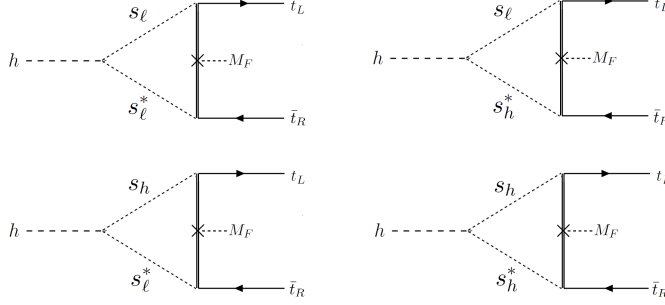


Figure 2.7: The four loop diagrams which contribute to the top Yukawa coupling: Loop 1 (upper left) with two light scalars, Loop 2 (upper right) and Loop 3 (lower left) with both heavy and light scalars, and Loop 4 (lower right) with only heavy scalars.

We will need these interaction terms at hand to calculate the top Yukawa and related quantities. These new interactions can also produce additional corrections to the Higgs at one-loop, namely the scalar loop will give a generic contribution of:

$$\Delta m_H^2|_{\text{scalar}} \sim \frac{1}{16\pi^2} V^2 \ln \left(\frac{\Lambda_{\text{NP}}^2}{M^2} \right). \quad (2.43)$$

The loop is not quadratically sensitive to Λ_{NP} and no additional hierarchy problem is reintroduced. However, as we will see for concrete benchmarks, V can be quite large in realistic models, and it will be important to consider this contribution.

2.4.2 Top Yukawa Coupling from a Loop

With the minimal new physics described in the last section, it is possible to dynamically generate the top Yukawa by integrating out the new heavy degrees of freedom. Below these heavy degrees of freedom, one will not only generate the top Yukawa but a whole series of higher dimensional operators reading

$$\mathcal{L}_{\text{top}} = c_6 (\bar{q}_L H t_R) + c_{6+4n} (H^\dagger H)^n (\bar{q}_L H t_R). \quad (2.44)$$

The first term in the expansion with coefficient c_6 corresponds to the SM-like top Yukawa, while the higher dimensional operators will result in deviations of the top and Higgs properties from the SM which we will study. By moving towards higher scales, the coefficients of the EFT will change, replacing the EFT description by form-factor couplings. It is this form factor behavior that will make the top Yukawa non-trivial and result in a finite contribution to the Higgs mass at the loop level.

To determine the form factors, a loop calculation is necessary. In the mass basis the two neutral scalars s_l and s_h contribute in four diagrams as shown in

Fig. 2.7 to the top Yukawa . The contributions coming from the four loop have the following form

$$\text{Loop 1: } 2 V y_{LYR} c_\beta^2 s_\beta^2 \int [s_\ell, s_\ell, F] \quad (2.45)$$

$$\text{Loop 2: } V y_{LYR} (c_\beta^2 - s_\beta^2) (-s_\beta^2) \int [s_\ell, s_h, F] \quad (2.46)$$

$$\text{Loop 3: } V y_{LYR} (c_\beta^2 - s_\beta^2) c_\beta^2 \int [s_h, s_\ell, F] \quad (2.47)$$

$$\text{Loop 4: } 2 V y_{LYR} c_\beta^2 s_\beta^2 \int [s_h, s_h, F], \quad (2.48)$$

where the square bracket is a symbolic representation of the triangle-loop integration with the various fields. Summing these contributions we find overall:

$$y_t = V y_{LYR} \left((c_\beta^2 - s_\beta^2)^2 \int [s_\ell, s_h, F] + 2 c_\beta^2 s_\beta^2 \int [s_\ell, s_\ell, F] + 2 c_\beta^2 s_\beta^2 \int [s_h, s_h, F] \right). \quad (2.49)$$

If M denotes the heaviest particle in the loop, we have roughly

$$y_t \sim V y_{LYR} \frac{1}{16\pi^2} \frac{M_F}{M^2}, \quad (2.50)$$

which corresponds to the estimate in Eq. (2.31). In Sec. 2.4.4 we will provide the exact expressions.

2.4.3 Radiative Top Mass Generation

The most direct consequence of the model is that now also the top quark mass is generated at the loop level through radiative effects. The generated top mass can be calculated from the two diagrams as shown in Fig. 2.8 and their contribution reads:

$$\text{Loop 1: } -y_{LYR} c_\beta s_\beta \int [s_\ell, F] \quad (2.51)$$

$$\text{Loop 2: } y_{LYR} c_\beta s_\beta \int [s_h, F]. \quad (2.52)$$

Summing up both diagrams we find the following radiative top mass:

$$m_t = y_{LYR} c_\beta s_\beta \left(\int [s_\ell, F] - \int [s_h, F] \right). \quad (2.53)$$

With M again representing the heaviest particle in the loop, we roughly obtain

$$m_t \sim y_{LYR} c_\beta s_\beta \frac{M_F}{16\pi^2} \left(\frac{M_s^2 - m_s^2}{M^2} \right) = \frac{y_{LYR} M_F V}{16\pi^2} \frac{v}{M^2 \sqrt{2}}, \quad (2.54)$$

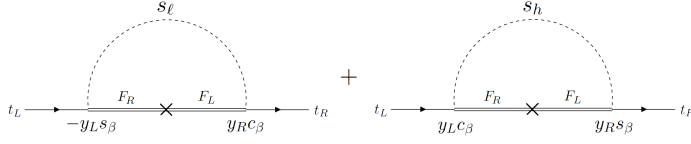


Figure 2.8: The two loop diagrams which contribute to the top mass. The first loop features the light scalar while the second loop the heavy scalar.

which matches our estimation of the top Yukawa coupling in Eq. (2.50). These were merely estimates and the Yukawa and mass will get contributions from all the terms in Eq. (2.44) in a different fashion. A key signature of the model will thus be a nontrivial $\kappa_t \equiv y_t/y_t^{\text{SM}}$ due to the higher dimensional operators. We now provide exact numerical calculations in order to obtain these crucial deviations in the SM behavior.

2.4.4 Exact Expressions and QCD Effects

In this section we will compute more general expressions for arbitrary mass hierarchies between s_h , s_l and F , which gives a momentum dependent mass:

$$m_t(p) = \frac{y_L y_R c_\beta s_\beta}{16\pi^2} M_F \times \int_0^1 dx \ln \left(\frac{p^2 x^2 - x p^2 + x M_F^2 + (1-x)m_s^2}{p^2 x^2 - x p^2 + x M_F^2 + (1-x)M_s^2} \right). \quad (2.55)$$

Similarly, the top Yukawa triangle loop with the light scalar and vector-like fermion for momenta p and p' of the top quarks is UV finite and reads

$$\int [s_\ell, s_\ell, F](p, p') = \frac{M_F}{32\pi^2} \int_0^1 dx \int_0^{1-x} dy \times \frac{2}{p^2 x(x-1) + p'^2 y(y-1) + M_F^2(1-x-y) + m_s^2(x+y)}, \quad (2.56)$$

to which one should add the fully analogous heavy scalar loop $m_s \rightarrow M_s$. In the maximal mixing scenario, with $s_\beta = c_\beta = 1/\sqrt{2}$, to which we will restrict our analysis, the mixed loops will vanish. It will be convenient to parameterise these expression according to their approximate momentum dependence along space-like momentum $p^2 = p'^2 = -Q^2$

$$m_t(Q^2) \sim \frac{m_t(Q^2=0)}{(1+Q^2/\Lambda_m^2)^n}, \quad y_t(Q^2) \sim \frac{y_t(Q^2=0)}{(1+Q^2/\Lambda_y^2)^n}, \quad (2.57)$$

where $n = 1$ shows the quadratic suppression with momentum and $\Lambda_m \sim \Lambda_y \sim M_F + M_s$. We take additional one-loop QCD effects into account which results in large corrections on the order of

$$m_{\text{QCD}}(p=0) = \frac{\alpha_s}{\pi} C_F m_t(p=0) \ln(\Lambda_m^2/m_t^2), \quad (2.58)$$

which are on the order of 25% and similar for the QCD corrections to the top Yukawa.

2.4.5 Analysis of the Fine-Tuning

In order to give a more detailed analysis of the resulting fine-tuning in this simplified model, we stick to two benchmarks: one rather conservative (BM1) and one with more striking effects (BM2)

$$\begin{aligned} M_F &= 1530 \text{ GeV}, m_s = 0.4M_F, M_s = 0.9M_F \text{ (BM1)} \\ M_F &= 865 \text{ GeV}, m_s = 0.5M_F, M_s = 1.5M_F \text{ (BM2)}. \end{aligned} \quad (2.59)$$

The effective scales of these benchmarks read:

$$\begin{aligned} \Lambda_m &= 3230 \text{ GeV}, \Lambda_y = 2980 \text{ GeV}, \text{ (BM1)} \\ \Lambda_m &= 2220 \text{ GeV}, \Lambda_y = 1840 \text{ GeV}, \text{ (BM2)}. \end{aligned} \quad (2.60)$$

A key difference between these benchmarks is the lower effective scale of BM2 which results in a larger deviation from the SM top Yukawa of $\kappa_t = 1.32$, while BM1 features an experimentally safe deviation of $\kappa_t = 1.1$.

These two benchmarks necessitate large Yukawa couplings $y_L = y_R = 7$ (taking QCD loop effects into account), demanding a strongly coupled origin which will be detailed in Appendix A. We now compute the level of fine-tuning associated to the top Yukawa loop. The (usually) divergent Higgs mass contribution coming from the top loop can be calculated from Eq. (2.10). Upon rotation to Euclidean space, the top-Yukawa is probed along space-like momentum where Eq. (2.57) is valid, leading to a strictly UV finite contribution of:

$$\Delta m_H^2 = -\frac{3y_t(p=0)^2\Lambda_y^2}{8\pi^2(2n-1)} \left[1 - (1 + (\Lambda_{\text{NP}}/\Lambda_y)^2)^{-(2n-1)} \right]. \quad (2.61)$$

If $n > 1$, the precise value of where the top-loop is cut off, Λ_{NP} , has a negligible impact on the expression in brackets and the fine-tuning is estimated as:

$$\Delta_{\text{FT},n>1} = \frac{3y_t(p=0)^2\Lambda_y^2}{8\pi^2(2n-1)(88 \text{ GeV})^2}. \quad (2.62)$$

In contrast for $n = 1$, the value of Λ_{NP} has a more considerable effect on the amount of fine-tuning. At worst, when there is no new physics that cuts off the top-loop ($\Lambda_{\text{NP}} \rightarrow \infty$), the total mass contribution is still finite and given by the above expression. When the top-loop is cut off at a lower scale of $\Lambda_{\text{NP}} \sim \Lambda_y$ the fine-tuning is halved

$$\Delta_{\text{FT},n=1} = \frac{3y_t(p=0)^2\Lambda_y^2}{16\pi^2(88 \text{ GeV})^2}, \quad (2.63)$$

resulting in a fine-tuning of $\Delta_{\text{FT},n=1}$ of $\sim 5\%$ for both benchmarks. Although BM2 is more aggressive, featuring a lower Λ_y , it gets compensated by a larger top Yukawa at zero momentum $y_t(p=0)$. In the more exotic case of the top quark being a composite made up of n constituent *preons*, the formula Eq. (2.57) for $n > 1$ would hold [89] and more extreme reductions in fine-tuning are expected.

To conclude this section, let us check whether the newly introduced interactions do not itself recreate large radiative contributions to the Higgs mass. In both of our benchmarks, both heavy and light scalar loops introduce the following mass corrections

$$\Delta m_H^2 = \frac{(V/\sqrt{2})^2}{16\pi^2} \left(\ln\left(\frac{\Lambda_{\text{UV}}^2}{m_s^2}\right) + \ln\left(\frac{\Lambda_{\text{UV}}^2}{M_s^2}\right) \right) \sim \frac{V^2}{16\pi^2}, \quad (2.64)$$

with Λ_{UV} the scale at which the scalar loop is cut off due to the emergence of the strongly coupled UV theory. If we assume a low-scale UV completion, the correction leads to an approximate $\sim 7\%$ tuning for both benchmarks, which is at the same order as the now reduced top quark tuning. The new interactions therefore do not worsen the reduced fine-tuning of the setup.

2.4.6 Bottom Sector and Custodial Symmetry

Before discussing the key phenomenological signatures of the model, we provide a simple extension of the simplified model to generate a bottom Yukawa coupling with

$$\Delta\mathcal{L} = -M'_F \bar{F}'_L F'_R - y'_L \bar{q}_L S_L F'_R - y'_R \bar{b}_R S_R F'_L + \text{h.c.}, \quad (2.65)$$

where the newly introduced vector-like fermion F' is uncharged under $SU(2)_L$ and carries hypercharge $Q(F') = Q_F - 1 = -1/3$. We set $M'_F = M_F$ and $y'_L = y_L$, while the y'_R coupling is taken much smaller than y_R to account for the smaller bottom quark mass.

With these additional interactions that provide the bottom mass, one can show violation in custodial symmetry is sequestered to a single parameter. To do so we rewrite the Lagrangian in terms of $SU(2)_L \times SU(2)_R$ representations. Both the Higgs and the scalar doublet S_L having identical quantum numbers can be written in matrix form Ω and Ω_L respectively as a $(2, 2)$ representation. An $SU(2)_R$ doublet q_R can be formed from combining t_R and b_R , while the two vector-like fermions F and F' can be similarly combined into a vector-like $SU(2)_R$ doublet $Q_{L/R} = (F_{L/R}, F'_{L/R})^T$. The whole Lagrangian is now given by

$$\begin{aligned} \Delta\mathcal{L} = & -V S_R \Omega_L^\dagger \Omega - \bar{q}_L Y_L \Omega_L Q_R - \bar{q}_R Y_R S_R Q_L \\ & - M_L^2 |\Omega_L|^2 - M_R^2 |S_R|^2 - M_F \bar{Q}_L Q_R + \text{h.c.}, \end{aligned} \quad (2.66)$$

where $Y_L = \text{diag}(y_L, y_L)$ and $Y_R = \text{diag}(y_R, y'_R)$ correspond to the 2×2 coupling matrices. The mass splitting between bottom and top is generated by the difference between the couplings y_R and y'_R and is also the unique source of custodial symmetry violation within the new physics sector. The related constraints coming from electroweak precision tests will be discussed in the next section.

2.5 Phenomenology

The scenario of a modified top Yukawa impacts several aspects of top physics. In this section we will both consider the running top scenario coming from a new strong gauge interaction and the more drastic scenario of a fully loop generated top Yukawa. Interestingly, for the latter scenario of a loop-level origin of the top Yukawa, the best tests come from indirect measurements.

2.5.1 Running Top Mass

A large running in the top Yukawa will generically result in a running of the top quark mass. Concerning the first scenario, the additional heavy gauge bosons will induce a shift in the SM running at the mass threshold of the gauge bosons. For the second scenario, the momentum dependence of the top mass originates from the same loops in Fig. 2.8 that determine its mass. The prospect of a large effect in the running of the top mass is made more relevant by the fact that the first measurement of such a running has been made by the CMS collaboration with run 2 data for an integrated luminosity of 35.9 fb^{-1} [59]. In Fig. 2.9 we compare the results for both benchmarks with the CMS measurement. One can see that BM2 is already slightly in tension with the measurement in the highest bin, showing the relevancy of this indirect measurement for testing these scenarios. The CMS measurement has been reinterpreted in [90], claiming the measurement is only sensitive up to half of the original scales. The measurement would then be only sensitive up to energy scales of 0.5 TeV. The bound on the running of the top mass would in this case become weaker and even lighter new physics with more drastic running would be allowed.

2.5.2 Top Yukawa Coupling Measurement

A second relevant constraint for these scenarios is the measurement of the top Yukawa coupling. In the scenario of a running of the top Yukawa, its EW scale value is not impacted as the idea only necessitates a running of the top Yukawa at larger scales. In contrast, for the second scenario where the top Yukawa is radiatively generated at leading order by the diagram of Fig. 2.6, a series of higher order diagrams will inevitably contribute. These subleading diagrams will shift $\kappa_t \equiv y_t/y_t^{\text{SM}}$ from its SM value of 1. These corrections are naively suppressed by $(V^2 v^2/M^4)^n$ (with M being the mass of the heaviest particle in

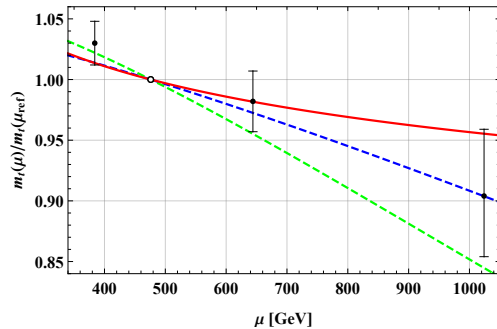


Figure 2.9: The top mass running in the SM (red) versus the running in our conservative BM1 (blue) and for BM2 (green) where the effects are larger, compared with the data points from CMS [59].

the loop). One can see that to relieve the hierarchy problem as much as possible – requiring the new degrees of freedom to be light – will impact κ_t significantly. The bound on κ_t translates therefore directly into how much big of a reduction in fine-tuning we can achieve.

At the LHC, κ_t is extracted by ATLAS and CMS from a combined analysis of the different Higgs boson productions and decays. The former measures $0.80 < \kappa_t < 1.04$ at 95% confidence [52] while the latter obtains $0.79 < \kappa_t < 1.23$ featuring a higher central value and larger error bars [53]. It is important to mention that both of these measurements are driven by gluon fusion which itself probes the top Yukawa through the loop at different scales. We therefore expect gluon fusion itself to be modified and in particular to be reduced in our model. More direct measurements have been performed in top-associated final states such as $t\bar{t}H$ and tH events. The resulting measurement reads $0.7 < \kappa_t < 1.1$ at 95% confidence level [54]. However, we again expect off-shell top quarks to reduce the bound.

We calculate κ_t from the ratio $y_t v/m_t$ using the exact expressions from Sec. 2.4.4 and taking into account the QCD effects. A large κ_t comes as a result of the breaking of the degeneracy of the two scalars (or V^2/m_S^2). BM1 has a safe $\kappa_t = 1.1$ while BM2 has a more optimistic $\kappa_t = 1.32$. It is interesting to observe that the model tends to drive up κ_t which itself worsens the amount of fine-tuning due to a larger electroweak scale top Yukawa. Although BM2 seems to be in conflict with experimental measurements, the top Yukawa is quickly driven down above the electroweak scale which, we remind, impacts the effective gluon fusion vertex. Assuming the form of Eq. (2.57), we expect a modification of the gluon fusion operator by $(1 - 2m_t^2/\Lambda_y^2 \ln(\Lambda_y^2/m_t^2))$ which would effectively transform the experimentally unviable $\kappa_t = 1.32$ into a $\kappa_t = 1.21$, safely within the CMS bound.

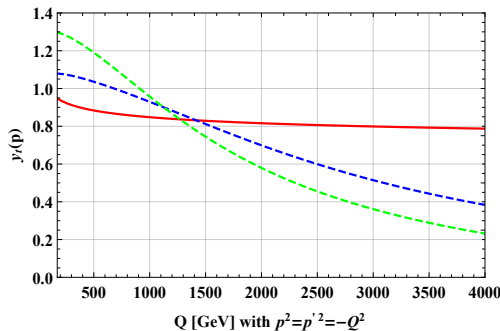


Figure 2.10: The top Yukawa form factor running in the SM (red) versus the running in our conservative BM1 (blue) and for BM2 (green) where the effects are larger.

2.5.3 Form Factors

Of course, the most direct way to test the idea would be to probe the top Yukawa above the electroweak scale. For this we have to derive the top-Higgs form factor, which describes the momentum dependence of y_t [55–58]. Fig. 2.10 shows the top Yukawa form factor in our two benchmarks together with the SM Yukawa running. The deviations are especially large when the off-shellness of the top becomes comparable to Λ_y and could be observed in the high energy tails of momentum distributions. For a process like $t\bar{t}h$ production, the top is probed along time-like momentum - and therefore the pole structure - leading to resonant enhancement of the cross section and especially again in differential distributions [58]. More quantitative statements on this subject would require a dedicated analysis which is outside the scope of this work.

2.5.4 Four Tops Cross Section

A common requirement for both scenarios in modifying the top Yukawa is the introduction of new strong interactions among the top quarks. As we will comment upon later, resonance searches are not very promising to look for these new interactions due to the large width of the new states. However the effect of these new interactions can be caught in a measurement of the four top quark cross section. Due to its small rate in the SM, this process mimics a precision test and large deviations would easily be discoverable. According to SM calculations, the cross section is estimated to be [91]:

$$\sigma_{t\bar{t}t\bar{t}}^{\text{SM}} = 12 \pm 2.4 \text{ fb.} \quad (2.67)$$

On the experimental side, searches using different final states have been performed by both the ATLAS [92, 93] and CMS [94, 95] collaboration using the full LHC run 2 data. Very recently, CMS has improved its analysis techniques to obtain enough significance to claim the observation of simultaneous four top

quark cross section [96]. The ATLAS measured cross section reads

$$\sigma_{t\bar{t}t\bar{t}}^{\text{ATLAS}} = 24_{-6}^{+7} \text{ fb}, \quad (2.68)$$

with a central value of about twice the SM prediction. The measurement of the CMS collaboration is more precise and closer to the SM prediction:

$$\sigma_{t\bar{t}t\bar{t}}^{\text{CMS}} = 17_{-5}^{+5} \text{ fb}. \quad (2.69)$$

One can derive upper bounds on the cross section at the 95% level to constrain BSM models with a modified top sector:

$$\sigma_{t\bar{t}t\bar{t}} < 38 \text{ (27) fb from ATLAS (CMS)}. \quad (2.70)$$

In recent years multiple analysis have been performed aimed at interpreting these results in terms of either simplified models or effective field theories [97–99]. Here we will follow the analysis of [97], constraining a top-philic vector singlet boson with coupling g_V and mass M_V

$$\frac{g_V}{M_V} < 2.1 \text{ (1.8) from ATLAS (CMS)}, \quad (2.71)$$

at the 95% confidence level. While a similar bound on a top-philic scalar singlet boson with coupling g_S and mass M_S reads

$$\frac{g_S}{M_S} < 3.0 \text{ (2.6) from ATLAS (CMS)}. \quad (2.72)$$

The vector constraint is relevant for the case of a strongly coupled $U(1)$ gauge interaction giving rise to a top-philic vector boson X_μ in the running top Yukawa scenario. Our considered benchmark from Sec. 2.3 is right around the 95% confidence level bound reading $g_X/M_X = 2$. For the top-Higgs H_t scenario described in section 2.3.2, the scalar bound will be important especially in the broken phase where the top-pions are generically light. For a new strong non-Abelian interaction such as heavy QCD, the top-philic vector boson - the coloron G' - is a color octet. For the benchmark case of a $M_{G'} = 2.5$, the bound from pair production reads

$$\frac{g'_3}{M_{G'}} < 2.9 \text{ (2.5) from ATLAS (CMS)}, \quad (2.73)$$

which means our benchmark with $g'_3/M_{G'} \sim 1.7$ lies safely within the current constraint.

Having considered the running top Yukawa scenarios, we can now move to the loop-generated top Yukawa model. The situation is complicated by the fact that multiple four-top operators are generated at the one-loop level both with scalar-like and vector-like operators:

$$a(\bar{t}t)(\bar{t}t), b(\bar{t}\gamma^\mu t)(\bar{t}\gamma_\mu t), c(\bar{t}\gamma^5 t)(\bar{t}\gamma^5 t), d(\bar{t}\gamma^\mu \gamma^5 t)(\bar{t}\gamma_\mu \gamma^5 t). \quad (2.74)$$

For our considered benchmarks, the coefficients of these operators read respectively

$$\begin{aligned} (a, b, c, d) &= \frac{1}{M_F^2} (1.81, -0.49, -1.40, -0.45), \\ (a, b, c, d) &= \frac{1}{M_F^2} (1.18, -0.37, -0.66, -0.31), \end{aligned} \quad (2.75)$$

where $M_F = 1530$ GeV (and $M_F = 865$ GeV) for BM1 (and BM2) respectively. To compare these results with experimental constraints we sum and recast the operators into a standard basis [97] as

$$(b + d)O_{QQ}^1 + (b + d)O_{tt}^1 + (c - a)/3 O_{Qt}^1 + 2(c - a)O_{Qt}^8, \quad (2.76)$$

where we omitted the operators with coefficient $(a + c)$ and $(b - d)$ due to an approximate cancellation. It turns out that in general (and in particular for our benchmarks) the first three coefficients are approximately equal which will allow us to combine them. Conveniently, the combination turns out to be the same as the generated operators in a top-philic singlet vector V with the following ratio

$$\frac{g_V}{M_V} \sim \sqrt{-2(b + d)}, \quad (2.77)$$

which for the considered benchmarks translates into the safe predictions of ~ 0.9 and ~ 1.4 for BM1 and BM2 respectively. One should caution these results with the remark that by modelling our simplified model with a top-philic vector singlet, the O_{Qt}^8 operator is neglected while the O_{tt}^1 operator is slightly underestimated. The former has a larger coefficient, however its contribution in four top production is suppressed when compared to the other operators as an EFT analysis has demonstrated [99]. Even with these caveats, the four top quark final state can only give a rather weak constraint on models with a loop-generated top Yukawa.

2.5.5 Flavor Constraints

The same four top quark operators that can modify the four top cross section have also an effect on flavor physics through mixing, producing dangerous FCNCs. If we take the mixing angles for the left-handed bottom quarks $\theta_{23} \gg \theta_{13}$, inspired by the CKM matrix, then the strongest constraint is expected to come from $B_s - \bar{B}_s$ mixing. The following operator parameterises the mixing:

$$\Delta\mathcal{L}_{B_s} = C_{sb}(\bar{s}_L\gamma_\mu b_L)(\bar{s}_L\gamma_\mu b_L). \quad (2.78)$$

Taking the calculation of [100] we can relate the operator to the deviation in the mass difference ΔM_s of the two neutral mass eigenstates as:

$$\frac{\Delta M_s}{\Delta M_s^{SM}} \approx 1 + \left(22\,304 \text{ TeV}^2\right) C_{sb}^2. \quad (2.79)$$

Comparing the SM prediction [101] with the measurement of the mixing parameter [102] leads to the following bound at 95% CL:

$$|C_{sb}| \leq \left(\frac{1}{274 \text{ TeV}} \right)^2. \quad (2.80)$$

For the case of a singlet top-philic vector boson V , the coefficient reads

$$C_{sb} \approx -\frac{1}{2} \frac{g_V^2}{M_V^2} \theta_{sb}^2 \implies \frac{g_V}{M_V} \theta_{sb} \leq \frac{1}{194 \text{ TeV}}, \quad (2.81)$$

with θ_{sb} the rotation angle between the second and third generations of down-type quarks in the mass basis. For the running top scenario with $g_X/M_X = 2$, the angle should be smaller than 0.003 while for the radiative top Yukawa the constraint is slightly weaker at $\theta_{sb} \lesssim 0.005$.

2.5.6 Electroweak Precision Tests

As discussed in Sec. 2.4.6, our simplified model is symmetric under $SU(2)_L \times SU(2)_R$ with the exception of the coupling to the right-handed top and bottom which is necessary to lift the degeneracy between top and bottom mass. This coupling will therefore be the leading contribution of our model to the T parameter [103, 104] as measured in electroweak precision tests. Recently many analysis have been performed on the oblique parameters [105–109] due to the recent new measurement of the M_W by the CDF collaboration [110] showing a significant deviation from the SM prediction and implying a new source of custodial symmetry violation. Following the analysis of [109] and omitting the CDF measurement one obtains $T \lesssim 0.25$ at 95% CL while using only the CDF measurement yields the 2σ region of $0.12 \lesssim T \lesssim 0.42$. We therefore take as a benchmark for the T parameter $\Delta T = 0.25$ which serves as both the central value of the CDF measurement and the upper bound without including the CDF measurement. The T parameter is related to the coefficient of the custodial symmetry breaking operator in the following way:

$$\mathcal{L}_T = c_T \left| H^\dagger D_\mu H \right|^2, \text{ where } \Delta T = -\frac{v^2}{2\alpha} c_T. \quad (2.82)$$

The requirement of $\Delta T = 0.25$ becomes:

$$|c_T| = 1/(3.95 \text{ TeV})^2. \quad (2.83)$$

In the case of the strongly running top Yukawa scenario, this operator is induced by the top loop with additional strong interactions inside which is a two loop diagram leading to

$$c_T \sim c_N \left(\frac{1}{16\pi^2} \right)^2 y_t^4 g_X^2 \frac{1}{M_X^2}, \quad (2.84)$$

where $c_1 = 3$ and $c_{N>1} = (N^2 - 1)/2$ for $SU(N)$ vector bosons. The two-loop nature suppresses the contribution well below the bound to $|c_T| \sim 1/(45 \text{ TeV})^2$ for both the abelian and non-abelian case.

Concerning the loop-generated top Yukawa scenario including the custodially symmetric setup from Sec. 2.4.6, the first violating operator, coming from a $F - t_R$ loop, only appears at the three-loop level and gives

$$c_T \sim \left(\frac{1}{16\pi^2} \right)^3 N_c V^4 y_R^4 \frac{1}{M_{S/F}^6}, \quad (2.85)$$

with $N_c = 3$ the color factor and $M_{S/F}$ corresponding to the mass of the heaviest particle in the loop. BM1 is well below the bound with $|c_T| \sim 1/(17 \text{ TeV})^2$, while the value for BM2 is right at the experimental constraint at $|c_T| \sim 1/(3.3 \text{ TeV})^2$.

2.5.7 Zbb Coupling

A complementary probe to the T parameter is the $Zb\bar{b}$ coupling which was well measured at LEP. Especially deviations in the left-handed coupling, δg_{b_L} , are constrained within 0.5% at 95% CL [111, 112] while the equivalent constraint on the right-handed coupling, δg_{b_R} , is only at 3%. If we take $|\delta g_{b_L}| \sim |\delta g_{b_R}|$, a negative δg_{b_L} with $|\delta g_{b_L}| < 3 \times 10^{-3}$ is preferred. Transforming this value into the coefficient of a higher-dimensional operator, we find

$$\mathcal{L}_{Zbb} = c_b \left(H^\dagger D_\mu H \right) (\bar{q}_L \gamma^\mu q_L), \quad \text{where } \delta g_{b_L} = -\frac{v^2}{2} c_b, \quad (2.86)$$

and the bound becomes

$$|c_b| < 1/(3.17 \text{ TeV})^2, \quad (2.87)$$

which is similar to the bound on the custodial violating parameter c_T .

Concerning the first scenario of a running top Yukawa, this operator is first generated at the loop level with the following naive size

$$c_b \sim \frac{c_N}{16\pi^2} y_t^2 g_X^2 \frac{1}{M_X^2}, \quad (2.88)$$

with $c_1 = 1$ and $c_{N>1} = (N^2 - 1)/2N$. We find again that the contribution is below experimental constraints, but larger than the c_T constraint discussed previously, at $|c_b| \sim 1/(5.4 \text{ TeV})^2$ for both the case of a new abelian and non-abelian gauge interaction.

In the second scenario in which the top Yukawa is generated at the loop level, this operator is first generated at the three-loop level with the following size:

$$c_b \sim \left(\frac{1}{16\pi^2} \right)^3 V^2 y_R^4 y_L^2 \frac{1}{M_{S/F}^4}. \quad (2.89)$$

Both BM1 and BM2 are safely under the experimental constraint with respective values of $|c_b| \sim 1/(12 \text{ TeV})^2$ and $|c_b| \sim 1/(4 \text{ TeV})^2$.

2.5.8 Direct Searches

We end the phenomenology with a discussion of direct searches for these new degrees of freedom. Usually direct searches provide the most straightforward way of testing models with TeV-scale new physics. However, due to the strongly coupled nature of the models discussed here, direct searches are not that promising.

In the case of the running top Yukawa scenario due to an additional strong (non)-abelian gauge interaction, the concerned gauge bosons have necessarily large widths, $\gtrsim 50\%$, including possible additional bound states coming from such a sector, which necessitates analysis that go beyond traditional narrow resonances searches. Furthermore, in the minimal case for which the gauge bosons purely couple to top quarks, the final state of the pair-produced gauge boson corresponds exactly to four top quarks, a signature which we have discussed in section 2.5.4.

For the second scenario of a top Yukawa generated at the one-loop level, we have to introduced new degrees of freedom: fermions and scalars running inside of the loop. In principle the hypercharge of these new particles is not fixed. If we wish to incorporate custodial symmetry in the new physics sector as done in Sec. 2.4.6, then the residual freedom becomes fixed and the new vector-like fermion must have the same hypercharge as the right-handed top quark. In this case, the production of a $F\bar{F}$ pair is expected to be the most promising signal with each $F(\bar{F})$ decaying to a $t(\bar{t})$ and the light scalar s_l . One can distinguish two scenarios in which the light scalar is either stable or unstable. In the first case the final state corresponds to $t\bar{t}$ with missing energy. Such a final state corresponds to searches for stop pair production in which the stops decay into a top and a stable neutralino [113–118]. Current results exclude stops up to masses of a 1200 GeV for a 600 GeV neutralino which is still safe for BM1 with $M_F = 1530$ GeV and $m_s = 612$ GeV. In contrast, BM2, with $M_F = 865$ GeV and $m_s = 433$ GeV, would be safely excluded. This bound can be avoided in case the light scalar is unstable, coupling to gluons through a new operator $s_l GG$. The final state then becomes $t\bar{t}$ and jets which has a much larger background. A similar search by CMS [119] can be reinterpreted to our model which constrains $M_F > 670$ GeV when $m_s = 100$ GeV which would allow BM2.

2.6 Summary

We have started this chapter with a summary of the little hierarchy problem: if the instability of the Higgs mass is addressed by supersymmetry or composite Higgs, where are its signs? In particular, the stops or the top partners, necessary to tame the large quadratic sensitivity of the Higgs mass due to the top loop contribution, should be light and accessible at the LHC in order to have a *natural* Higgs. This question has driven theorists over the last decades and we

have started this chapter with a discussion of a symmetry based solution: twin Higgs.

In this chapter we entertained a different idea: what if the top Yukawa has a strong scale dependency and becomes smaller at high scales? We have only just started to probe this parameter and only at the electroweak scale. This could have important implications for the current state of naturalness as the top-loop contribution to the Higgs mass could be significantly reduced. The idea is not even that far-fetched: we already know that in the SM the top Yukawa becomes smaller at higher scales due to QCD effects. What if an additional strongly coupled gauge force, broken in the low TeV scale, runs the top Yukawa down significantly in the UV?

We investigated this running top Yukawa scenario at the hand of a few perturbative models. We found that to have any significant effect on the hierarchy problem, the gauge coupling must be large, at the border of the perturbative regime. For larger coupling, supposing only the left-handed doublet and the right-handed top are charged under the new force, the bound state $H_t = \bar{t}_R q_L$ forms, which we described using the NJL model. The required gauge coupling falls within the unbroken phase where the bound state is heavy and decouples from the low-energy physics.

In a second stage, we considered a more speculative idea which would be to completely generate the top Yukawa at the loop level and therefore it would cease to exist beyond the mass threshold of the new degrees of freedom. Beyond this scale, the top quark contribution to the Higgs mass would dissolve and is strictly finite. We showed the promise of such a scenario using a simplified model, which necessitates a strongly coupled UV completion (see Appendix A), showing how the top-loop contribution to the Higgs mass tuning can be controlled to be at the 5% level.

We studied the phenomenology of such a mechanism which suggests looking at new observables in contrast to usual top partner scenarios. We found the precision measurement of the four-top cross section to be a promising signal of new top-philic interactions. In the case where the top Yukawa is generated at the loop level, important deviations in the $\kappa_t = y_t/y_{SM}$ are expected and current measurements by CMS and LHC are already constraining the scenario. Such a mechanism would also manifest itself in a running top mass which has been recently measured by CMS.

Chapter 3

Minimal Gauge-Higgs Grand Unification

A recurring theme of the preceding pages is the lack of a symmetry protecting the mass of elementary scalars. Unlike fermions or gauge bosons, that have chiral symmetry and gauge symmetry respectively ensuring that quantum corrections to their mass are proportional to that mass, elementary scalars do not possess such a symmetry. One can ask whether it is still possible to have such a symmetry by relaxing the requirement of an elementary *four-dimensional* scalar. Gauge-Higgs unification [120, 121] is a fascinating and beautiful answer to this question. It hypothesizes that the Higgs field is the fifth component of a five-dimensional gauge field. Indeed, a five-dimensional gauge field, once the fifth dimension is compactified in some way with length R , will split from the point of view of the low-energy observer, not probing the fifth dimension, into a four dimensional gauge field plus an extra scalar. In simple terms it is the consequence of the following decomposition:

$$\mathbf{5} = \mathbf{4} \oplus \mathbf{1}. \tag{3.1}$$

A crucial difference with respect to having just a four dimensional elementary scalar is that now there is a symmetry protecting the mass of the scalar from quantum corrections: the five-dimensional gauge symmetry. Indeed at high scales, $E \gg 1/R$, the fifth dimension is on equal footing as the other dimensions and one recovers full five-dimensional gauge symmetry protecting the scalar from mass contributions. Interestingly, at low energies, $E \ll 1/R$, one starts to probe the finite volume of the space and the five-dimensional gauge symmetry is badly broken resulting in a mass for the scalar at the loop level: the *Hosotani Mechanism* [122–124].

In Sec. 3.1, we introduce the basic concepts of gauge-Higgs unification. In Sec. 3.2 we give a short overview of different types of extra dimension which will lead us to the use of a warped extra dimension. In Sec. 3.3 we present our model of gauge-Higgs unification based on a $SU(6)$ bulk gauge group. The

particularity of this model is the inclusion of the full SM in the bulk gauge group, resulting in a model of gauge-Higgs *grand* unification. This model is the first phenomenologically viable of its kind. We show how unification of quarks and leptons leads to new insights into the flavor puzzle. In Sec. 3.4 we give a brief overview over the different flavor constraints on the model, while in Sec. 3.5 we analyse the scalar potential of the model.

3.1 Gauge-Higgs Unification

Before going into the details of gauge-Higgs unification we should begin with a word on the topology of the extra dimension. Originally gauge-Higgs unification was discussed in (compact) extra dimensions with no fixed points such as a circle, S^1 . These models are phenomenologically not very appealing as they cannot give chiral fermions. Instead orbifold constructions, originally discussed in a string theory context [125–127] are a more natural topological space in which to discuss an extra dimension as it allows chiral fermions: a necessary ingredient of any BSM theory. Orbifolds arise when points in an extra dimension are identified with each other, or *modded out*, such that a fixed point remains. A popular example is the S^1/Z_2 orbifold which comes from identifying points related by $y \rightarrow -y$ (a reflection symmetry around $y = 0$), on a circle $(-\pi R, \pi R]$. The fundamental domain is now reduced to a line segment with boundaries which can give rise to chiral fermions.

Indeed, requiring the fields to obey the Z_2 -orbifold symmetry places restrictions on its values at the fixed point $y = 0$. This results in a set of possible boundary conditions for fields. For fermion fields this leads to the introduction of chiral fermions while for gauge fields, it leads to the very interesting possibility of reducing the gauge symmetry by these boundary conditions. The application of this symmetry breaking to the breaking of a GUT theory was analysed in [128–131] (see [132] for a review).

However it was soon realized that the boundary conditions obtained from orbifolding are rather constraining. Indeed orbifolds cannot reduce the rank of the bulk symmetry [133]. It is therefore more convenient, from a bottom-up perspective, to work on a general interval of length L with two boundaries $y = 0, L$ with a general bulk gauge group G in the interior. The gauge symmetry G can be broken consistently on the boundaries with unitarity preserved as shown in [134]. This realization itself has given rise to models in which electroweak symmetry breaking is realized purely by boundary conditions without the need for a Higgs, so-called *Higgsless* theories. Since the discovery of the Higgs, these models have become out of fashion.

In this chapter we will follow the bottom-up approach of formulating our extra dimensional theory on an interval of length L . Furthermore we place two 3-branes at the end coordinates $y = 0$ and $y = L$ at which additional 4D fields can be localized. We will not preoccupy ourselves about the origin

of such a setup. We will merely mention that superstring theory, a leading candidate of a theory of quantum gravity, is only consistently defined in ten dimensions [135]. The compactification of the six extra superfluous dimensions can result in a vast number of ways. We thus merely assume that a 5D theory emerges somewhere between the string scale and the electroweak scale and study its phenomenological consequences.

For now we neglect the influence of gravity and simply assume a flat extra dimension

$$ds^2 = G_{MN}dx^M x^N = \eta_{\mu\nu}dx^\mu x^\nu - dy^2, \quad (3.2)$$

where $\eta_{\mu\nu}$ is the 4D Minkowski metric and y is the coordinate parameterizing the extra dimension between the two branes at $y = 0$ and $y = L$. As any discussion of gauge-Higgs unification must include a higher dimensional gauge field, we consider a general bulk gauge field G , with generators $\text{Tr}(T^a T^b) = \delta^{ab}/2$, with the usual Yang-Mills action:

$$\begin{aligned} S_{\text{YM}} &= \int_0^L d^4x dy \sqrt{G} \left(-\frac{1}{2} G^{MN} G^{AB} \text{Tr}(F_{MA} F_{NB}) \right) \\ &= \int_0^L d^4x dy \left(-\frac{1}{4} F_{\mu\nu}^a F^{\mu\nu,a} + \frac{1}{2} F_{\mu 5}^a F_5^{\mu,a} \right). \end{aligned} \quad (3.3)$$

We will solve the above action at the quadratic level finding the free equations of motion. The second term contains mixing terms between the A_μ and A_5 which is eliminated by the following gauge-fixing term:

$$S_{\text{GF}} = \int_0^L d^4x dy \left(-\frac{1}{2\xi} \left(\partial_\mu A^{\mu,a} - \xi \partial_5 A_5^a \right)^2 \right). \quad (3.4)$$

One can now derive the equations of motions for the gauge-fixed action, $S_{\text{YM}} + S_{\text{GF}}$, together with boundary terms resulting from integration by parts along the extra dimension, from which we can derive the following boundary conditions for the two boundaries:

$$\begin{aligned} (+) : A_5|_{y=0,L} &= 0, \quad \partial_5 A_\mu|_{y=0,L} = 0, \\ (-) : A_\mu|_{y=0,L} &= 0, \quad \partial_5 A_5|_{y=0,L} = 0, \end{aligned} \quad (3.5)$$

where we note that A_μ and A_5 have opposite boundary conditions. We denote symbolically by (+)/(-) Neumann/Dirichlet boundary condition for the vector component of the gauge field A_μ . One can apply different boundary conditions for each gauge/scalar field, A_μ^a, A_5^a , associated to a generator, T^a , of the bulk group G . In doing so, one can reduce the general gauge symmetry in the bulk G , to smaller residual gauge symmetries on the bulk. We will provide later an explicit example of this.

One can now solve the 5D equations of motions by a separation of variables or a Kaluza-Klein (KK) decomposition for the gauge- and scalar fields

$$A_\mu(x, y) = \sum_n f_{n,A}(y) A_{\mu,n}(x), \quad A_5(x, y) = \sum_n f_{n,5}(y) A_{5,n}(x), \quad (3.6)$$

where we find for the wavefunctions or bulk profiles of the KK modes the following:

$$-m_n^2 f_{n,A} = \partial_5^2 f_{n,A}, \quad -m_{5,n}^2 f_{n,5} = \xi \partial_5^2 f_{n,5}. \quad (3.7)$$

From the first equation we find unsurprisingly that a massless gauge boson has a flat constant profile, which implies $(+, +)$ boundary conditions. This is unsurprising as Neumann boundary conditions leave the gauge symmetry unbroken in contrast to Dirichlet boundary conditions. Concerning the second equation, the dependence on the ξ parameter indicates that something conspicuous is going on, after all physics cannot depend on the gauge fixing parameter. Moreover, we note that for a general massive gauge boson, $m_n > 0$, with a profile $f_{n,A}$, with certain boundary conditions, we find automatically a solution for a scalar mode with bulk profile $f_n^5 = \partial_5 f_{n,5}/m_n$ and with correct boundary conditions. Crucially the mass of the scalar mode depends on the gauge parameter, $m_{5,m} = \sqrt{\xi} m_n$. This mass exactly corresponds to the usual relation between a gauge field and its Goldstone that will provide the longitudinal polarization [136]. Therefore we can go to unitary gauge $\xi \rightarrow \infty$ and decouple all unphysical scalar modes. What happens is that at the level of each KK level, the gauge boson eats the corresponding scalar and becomes massive. There is however one exception, namely a massless scalar can exist with a flat profile. Indeed, the dependence on ξ in Eq. (3.7) vanishes for a massless scalar and therefore is a physical scalar. Moreover the flat profile indicates it must have Dirichlet boundary conditions for the corresponding gauge field A_μ and thus corresponds to a *broken* generator.

Therefore in general the resulting physical spectrum of a broken five dimensional Yang-Mills theory will consist of, massless (for $(+, +)$ boundary conditions) gauge bosons, a tower of massive gauge bosons and a massless scalar (for $(-, -)$ boundary conditions). Models of gauge-Higgs unification exploit this spectrum by embedding the Higgs within such a scalar mode. We will study how a potential for this scalar mode can be generated (and how it impacts the hierarchy problem), which can induce the formation of a VEV, triggering the spontaneous breaking of additional symmetries under which the scalar is charged:

$$\langle A^{5,\hat{a}}(x) \rangle = v^{\hat{a}}. \quad (3.8)$$

However at tree-level no potential for the scalar is generated. This is simply a consequence of the absence of non-derivative terms involving A_5 in the field strength $F_{MN} F^{MN}$ and thus of 5D gauge invariance. This does not mean no scalar potential can be generated at all, since even though at high scales the 5D gauge invariance may seem intact, it is broken by the finiteness of the fifth dimension. Therefore we should expect in general the presence of a potential at the loop level. Moreover a VEV for the scalar will certainly impact the spectrum for the gauge bosons and other fields present. Indeed the gauge bosons, depending on their quantum number, will get a bulk mass term from

this VEV from the non-abelian interaction term

$$\mathcal{L}_{\text{YM}} \supset -\frac{1}{4}g_5^2 f^{abe} f^{cde} A^{\mu,a} A_\mu^c \langle A^{5,b} \rangle \langle A_5^d \rangle, \quad (3.9)$$

while matter fields will talk to the scalar VEV via the 5D covariant derivative in a representation \mathbf{R} of G , $D_M^{\mathbf{R}}$ which now includes the fifth component of the gauge fields namely:

$$D_M^{\mathbf{R}} \supset \partial_M - ig_5 A_M^a T^{\mathbf{R},a}. \quad (3.10)$$

Indeed, these two interactions will be how the electroweak bosons and the SM fermions communicate to the Higgs and how they gain a mass in models of gauge-Higgs unification. However the above equations are difficult to solve in the 5D bulk, but there is a trick we can perform to remove the VEV $v^{\hat{a}}$ from the bulk. Indeed there is still residual gauge freedom in the gauge-fixing term Eq. (3.4). One can choose the following gauge-transformation, $\Omega(x, y)$ of G which acts on the gauge fields as [137, 138]

$$A_M \rightarrow \Omega A_M \Omega^\dagger - \frac{i}{g_5} \Omega \partial_M \Omega^\dagger, \quad \Omega(x, y) = \exp\left(ig_5 \int_0^y dy' f_5(y') v^{\hat{a}} T^{\hat{a}}\right), \quad (3.11)$$

with $f_5(y)$ the bulk profile of the scalar mode. This transformation leaves the gauge-fields invariant while it removes the VEV from the bulk:

$$A_5^{\hat{a}}(x, y) T^{\hat{a}} \rightarrow \Omega \left(A_5^{\hat{a}}(x, y) T^{\hat{a}} - f_5(y) v^{\hat{a}}(x) T^{\hat{a}} \right) \Omega^\dagger. \quad (3.12)$$

Moreover this transformation does not impact the gauge-fixing term Eq. (3.4) and is thus indeed a residual symmetry. As such, it would seem that a VEV is unphysical as it can simply be gauged away. However the gauge transformation has to be applied consistently, including on the two branes. On the UV brane, the gauge transformation is trivial, $\Omega(y=0) = 1$, but on the IR brane it reads

$$\Omega(y=L) = \exp\left(i\sqrt{L}g_5 v^{\hat{a}} T^{\hat{a}}\right). \quad (3.13)$$

The IR boundary conditions have to be consistently applied to the gauge transformed bulk fermion and gauge fields namely:

$$\begin{aligned} A_\mu(y=L) &\rightarrow \Omega(y=L) A_\mu(y=L) \Omega(y=L)^\dagger \\ \Psi(y=L) &\rightarrow \Omega(y=L) \Psi(y=L). \end{aligned} \quad (3.14)$$

Even though the VEV was removed from the bulk, the IR boundary conditions will depend on the VEV $v^{\hat{a}}$. The physical spectrum, determined by the IR boundary conditions, will therefore be impacted by a non-zero VEV. We can start to understand the generation of a physical VEV as a consequence of the compactness of the extra dimension. Indeed for an infinite extra dimension,

a VEV for $A_5^{\hat{a}}$ can always simply be gauged-away and is therefore unphysical. On the contrary, in a compact space, the VEV cannot be eliminated and is gauged onto the boundary conditions. The KK spectrum will encode this dependency and one can compute the one-loop scalar potential through the Coleman-Weinberg potential which explicit calculations show it to be finite.

The finiteness of the potential can also be seen to originate from the original 5D gauge invariance which forbids a potential in the bulk while the branes are protected from the generation of a potential by the gauge symmetry acting on the boundaries $A_5^{\hat{a}} \rightarrow A_5^{\hat{a}} + \partial_5 \xi^{\hat{a}}$ with ξ the gauge parameters [139, 140]. This means that the potential must be a non-local effect and thus finite since no local counterterms could possibly cancel such divergences. Instead the non-local origin of the Higgs potential can be understood to come from the Wilson line along the extra dimension $\mathcal{W} = \mathcal{P} \exp\left(i \int A_5^{\hat{a}} T^{\hat{a}}\right)$ which contains a potential for the scalar. By combining two of such lines, stretching across and back the extra dimension, one obtains a gauge-invariant quantity from which the non-local origin of the scalar potential originates [141].

3.1.1 Electroweak Gauge-Higgs Unification

After this short introduction to the ideas of gauge-Higgs unification one can now start with realistic model building and this has indeed been done over the years (see [142] for a review). We turn to an illustrative example using a bulk gauge group $SU(3)$ [143], which is broken to $SU(2)_L \times U(1)_Y$ on both branes and where we identify $U(1)_Y$ with the eight generator in $SU(3)$, T_8 that commutes with $SU(2)_L$ ¹. We will only be interested in the $W_\mu^{1,2}$ gauge bosons as an example. Since the generators are unbroken on the UV brane, their wavefunction is given by

$$f_{n,W}(y) = C_n \cos(m_n y), \quad (3.15)$$

with C_n a normalization constant. We identify the Higgs degrees of freedom with the four broken generators of $SU(3)_L$. Applying the boundary condition on the IR brane, after the gauge transformation from Eq. (3.13), we find that the tower of KK masses for the W boson depends unsurprisingly on the Higgs VEV

$$m_n(v) = \frac{g_5 v}{2\sqrt{L}} + \frac{\pi n}{L}, \quad (3.16)$$

for $n = 0, 1, 2, \dots$ and where we identify the lightest mode with the SM gauge boson. One can now, using the Coleman-Weinberg formula, calculate the full

¹This will give the wrong Weinberg angle $\sin^2 \theta_W = 3/4$, resulting in a Z boson mass twice the W boson mass. This can be solved by either adding an extra $U(1)_X$ in the bulk and identifying the hypercharge with a linear combination of $T_8 + T_X$ or using brane localized gauge kinetic terms [144].

one-loop potential namely

$$V_{\text{CW}}(v) = \frac{N}{2} \sum_n \int \frac{d^4k}{(2\pi)^4} \log(p^2 + m^2(v)), \quad (3.17)$$

where we sum over the whole KK tower and with N the number of degrees of freedom. By not including the full tower of KK modes, one would obtain the usual quadratically divergent potential characteristic of the hierarchy problem. However including the full tower of KK modes we arrive instead at the following finite potential [145–147]

$$V(\alpha) = -\frac{2 \times 3}{32\pi^2 L^4} \mathcal{F}(\alpha), \quad \mathcal{F}(\alpha) = \frac{3}{2} \sum_{n=1}^{\infty} \frac{\cos(2\pi\alpha n)}{n^5}, \quad (3.18)$$

with $\alpha = \frac{gvL}{2\pi}$. One can observe that the W boson brings stability to the potential and electroweak symmetry remains unbroken. The inclusion of fermions can offset the positive contribution and as a result electroweak symmetry gets broken. A tedious problem in these models is the generation of Yukawa couplings. Since Yukawa couplings are contained in the covariant derivative and its size is determined by the overlap between Higgs and fermions, it is a challenge to obtain a realistic mass spectrum and the naive size of the Yukawa couplings is on the order of the gauge coupling $y \sim g$. One can embed matter into bulk fermions and use the bulk mass to distort the fermion localization close to a brane [148] which exponentially reduces the Yukawa couplings. A different approach is to introduce the SM matter on the orbifold fixed points. Yukawa couplings are then generated by mixing the brane matter with bulk fields [134, 143]. We will not go into details on these models as eventually we will study gauge-Higgs unification in warped space where all these model building issues have elegant solutions. Nevertheless the main feature of gauge-Higgs unification is already clear, we have a finite radiative Higgs potential that is fully determined by the matter and gauge content of the model. Moreover, the scale of the potential is set by the compactification scale $\sim L$ so if we wish to avoid fine tuning the potential, the compactification scale should be set by the weak scale. Therefore even though the quantum gauge problem is solved (the radiative corrections to the Higgs are finite), the tree level problem of relating this low compactification scale with a larger UV scale in nature, such as the Planck scale, remains unsolved. Or formulated differently, it is unclear how to reproduce gravity in such a setup without reintroducing a tree-level fine tuning.

3.2 Extra Dimensions

3.2.1 Flat Extra Dimensions

No discussion of extra dimensions can be complete without including gravity. Indeed gravity is intrinsically linked to the space-time structure and we must

therefore understand the impact of the extra dimension on the resulting force of gravity. More precisely we have to make sure that we recover the usual Einstein-Hilbert (EH) action

$$S_{\text{EH}} = -2M_{\text{pl}}^2 \int d^4x \sqrt{g} R, \quad (3.19)$$

when integrating out the extra dimension. How do we embed gravity in a flat extra dimension? The propagating degrees of freedom of gravity are encoded in the fluctuations of the metric. For a single flat extra dimension of length L that was discussed in the previous section, the metric has the following form

$$ds^2 = (\eta_{\mu\nu} + h_{\mu\nu}) dx^\mu dx^\nu - dy^2, \quad (3.20)$$

with $\eta_{\mu\nu} = \text{diag}(1, -1, -1, -1)$ the mostly minus 4D Minkowski metric while $h_{\mu\nu}$ encode the fluctuations of 4D gravity. The five dimensional gravitational action is then simply given by the generalization of the Einstein-Hilbert action

$$S_{5D\text{-EH}} = -2M_5^3 \int d^4x dy \sqrt{g_5} R_5, \quad (3.21)$$

with g_5 the determinant of the five-dimensional metric tensor, R_5 the five-dimensional Ricci scalar and M_5 the five-dimensional Planck scale. If we now wish to understand how 4D gravity will appear to the low-energy observer we have to integrate out the fifth dimension and relate the five-dimensional quantities g_5, R_5 in terms of the analogous four-dimensional quantities g, R . This results in the following:

$$S_{5D\text{-EH}} = -2M_5^3 L \int d^4x \sqrt{g} R. \quad (3.22)$$

We then see that for gravity to appear with the usual Planck-scale strength and obey Newton's law of gravitation, the following equation has to be obeyed:

$$M_{\text{pl}}^2 = M_5^3 L. \quad (3.23)$$

In order for the Higgs potential to be of its natural scale, one should have $L \sim 1/10^3$ GeV which implies that the five dimensional gravitation constant is $M_5 \sim 10^{11}$ GeV. Although such a setup correctly reproduces four-dimensional gravity and contains an electroweak scale Higgs potential that is protected from UV scales, it is not clear how such an extra dimensional setup can be stabilized in a natural way. Indeed we have just traded the $v/M_{\text{pl}} \ll 1$ hierarchy for a new hierarchy of $M_5 L \gg 1$. Indeed we would expect that the stabilization of the brane at $y = L$ occurs in a natural way only when $M_5 L \sim 1$. Therefore gauge-Higgs unification in a flat extra dimension is not a fully satisfactory solution. We note that (3.23) suggests an alternative approach to the hierarchy problem: the addition of an extra dimension in which gravity propagates has rendered the fundamental scale of gravity lower than what it appears to be to the four

dimensional observer. This suggests the possibility that gravity is so much weaker than the other forces of nature simply because it is diluted in the other dimensions [149–151]. Generalizing (3.24) to more than one extra dimension $n \geq 1$ we find

$$M_{\text{pl}}^2 = M^{2+n} L^n, \quad (3.24)$$

where L^n represents the volume in which gravity is diluted. It is then tempting to hypothesize that the fundamental scale of gravity is actually of the same order as the electroweak scale, $M \sim v$, which results in the following scale of the extra dimensions

$$L \sim 10^{30/n-17} \text{ cm}. \quad (3.25)$$

The case of $n = 1$ is excluded as it would imply modifications of Newtonian gravity on the order of solar-system distances, but the option of $n > 1$ is still experimentally allowed. For example the case of $n = 2$ implies sub-millimeter scale extra dimension which is right at the edge of experimental constraints that are looking for modifications of Newton’s law of gravitation. For example using torsion pendulums [152] gravity is tested at the micrometer level and the case $n = 2$ already pushes $M > 4$ TeV at 95% CL. Of course the other forces of nature should be localized on a 3-brane since they are very well tested up to the weak scale. Again, this model is not fully satisfactory as it doesn’t explain the hierarchy between the now very large size of the extra dimensions L and the scale of the higher dimensional gravity M .

3.2.2 A Warped Extra Dimension

We now discuss a particularly elegant model of extra dimensions by Randall and Sundrum known as the RS model which can explain the hierarchy problem without introducing any new hidden hierarchies: indeed it will turn out that the hierarchy between the five-dimensional Planck scale and the compactification or length scale of the extra dimension is mild and can be naturally obtained by what is known as the Goldberger-Wise mechanism. This model of extra dimension will provide the gravitational background in which we will embed our model of gauge-Higgs unification.

The model is also known as a warped extra dimension, as the solution of the metric is given by

$$ds^2 = e^{-2kr_c\phi} \eta_{\mu\nu} dx^\mu dx^\nu - r_c^2 d\phi^2, \quad (3.26)$$

with ϕ an angular coordinate $\phi \in [0, \pi]$ parameterizing the extra dimension and r_c the compactification scale. We note that length scales of the usual 4D metric are rescaled exponentially as a function of the location along the extra dimension. The model is compactified on an orbifold S_1/Z_2 with two orbifold fixed points at $\phi = 0, \pi$ on which one places two 3-branes called respectively the UV- and IR brane or equivalently the Planck and TeV brane. Randall and

Sundrum showed [153, 154] that such a warped metric can be obtained from the following five dimensional configuration

$$S_{\text{RS}} = \int d^4x \int_0^\pi d\phi \sqrt{G} (-\Lambda - 2M^3 R_5) + \int d^4x \sqrt{-g_{\text{UV}}} (-V_{\text{UV}}) + \int d^4x \sqrt{-g_{\text{IR}}} (-V_{\text{IR}}), \quad (3.27)$$

where G_{MN} corresponds to the 5D metric tensor and $g_{\text{UV/IR},\mu\nu}$ is the induced metric on the UV respectively IR brane. Λ is a constant bulk cosmological constant, while $V_{\text{UV/IR}}$ are vacuum energies on the UV and IR brane respectively also known as *brane tensions*. As such, the RS model starts from nothing more than the investigation of the consequences of non-trivial vacuum energies for the branes and the bulk. Solving the Einstein's equation for the above action and inserting the ansatz metric (3.26) with exponential warp factor, $e^{-2\sigma(\phi)}$, left unspecified, the following non-trivial solution for $\sigma(\phi)$ is found for a negative 5D cosmological constant $\Lambda < 0$

$$\begin{aligned} \sigma(\phi) &= kr\phi, \\ k &\equiv \sqrt{\frac{-\Lambda}{24M^3}}, \end{aligned} \quad (3.28)$$

with k the curvature of the warped extra dimension. The above solution requires a tuning amongst the brane tensions:

$$V_{\text{UV}} = -V_{\text{IR}} = -\Lambda. \quad (3.29)$$

This relation ensures that the resulting effective 4D cosmological constant vanishes. The RS model therefore does not offer a solution to the cosmological constant problem and instead it is recast into the tuning amongst the two brane tensions. In total the RS model contains three free parameters M, k and r_c where we traded the bulk cosmological parameter, Λ , for the curvature, k . The remaining question that needs to be investigated is if one can have all three parameters with no large hierarchies amongst them while reproducing standard 4D gravity with the observed strength of M_{pl} . Moreover how does the hierarchy problem manifest itself in this warped background – is it possible to obtain naturally smaller scales in such a warped background? First of all, in order to understand the emergence of 4D gravity we have to consider the fluctuations around the background metric of (3.26) in terms of the graviton fluctuations, $g_{\mu\nu}$:

$$ds^2 = e^{-2k\phi T(x)} g_{\mu\nu} dx^\mu dx^\nu - T(x)^2 d\phi^2. \quad (3.30)$$

We also replaced the seemingly free parameter r_c , which determines the location of the IR brane with respect to the UV brane with a scalar field $T(x)$ whose expectation value sets the compactification length $\langle T(x) \rangle = r_c$. Indeed, until now the RS solution is valid for an arbitrary r_c . This means that there will be a

massless scalar field in the 4D effective theory corresponding to the fluctuations of the IR brane around r_c . Its masslessness is due to the arbitrariness of r_c in the original formulation of RS (indeed it can be seen as an integration constant) and therefore it has no potential nor mass. Such fields that determine the stabilization of extra dimensions are also known as modulus fields and need to acquire a potential and mass. Most importantly in order not to violate the equivalence principle [155] but also as we will see, the specific location of r_c is crucial in order to obtain a solution to the hierarchy problem.

Plugging in the above metric (3.30) with the massless modes $g_{\mu\nu}(x)$ and $T(x)$ into the 5D action (3.27) and integrating over the fifth dimension the following effective 4D Lagrangian is obtained [156]

$$S_{\text{RS-eff}} = \frac{2M^3}{k} \int d^4x \sqrt{-g} \left[(1 - (\varphi/h)^2) R + \frac{1}{2} \partial_\mu \varphi \partial^\mu \varphi \right], \quad (3.31)$$

where the radion was redefined as $\varphi(x) \equiv h \exp(-k\pi T(x))$ with $h \equiv \sqrt{24M^3/k}$ and R is the 4D Ricci scalar constructed from the metric $g_{\mu\nu}$. One can then derive the effective four dimensional Planck scale as:

$$M_{\text{pl}}^2 = \frac{M^3}{k} (1 - e^{-2\pi k r_c}). \quad (3.32)$$

No hierarchies are necessary between M_5 and k to account for the correct weakness of gravity. Interestingly, the equation above continues to hold in the limit of $r_c \rightarrow \infty$ challenging the conventional wisdom that Newton's law implies only four non-compact dimensions [154]. Note that implicit in the above solution is the assumption that $k < M$ such that the 5D curvature $R_5 = -20k^2$ is small compared to M_5 and the bulk metric solution can indeed be trusted. If not, higher order terms in the curvature would have to be considered in the action.

Having studied how 4D gravity is obtained in the RS model one can now investigate how the hierarchy problem or lack thereof manifests itself. We consider a Higgs field with a potential localized on the IR brane [153]

$$S_{\text{IR}} = \int d^4x \sqrt{-g_{\text{IR}}} (g_{\text{IR}}^{\mu\nu} (D_\mu H)^\dagger D_\nu H - \lambda (H^\dagger H - v_0^2)^2), \quad (3.33)$$

with $g_{\text{IR},\mu\nu} = e^{-2\pi k r_c} g_{\mu\nu}$ the induced metric on the IR brane. After substituting the induced metric one needs to canonically normalize the kinetic term with the following substitution $H \rightarrow e^{\pi k r_c} H$ and one obtains the following Lagrangian:

$$S_{\text{IR}} = \int d^4x \sqrt{-g} (g^{\mu\nu} (D_\mu H)^\dagger D_\nu H - \lambda (H^\dagger H - e^{-2\pi k r_c} v_0^2)^2). \quad (3.34)$$

As RS noted, a remarkable thing has happened. The Lagrangian parameter setting the VEV v_0 of the Higgs potential with natural scale on the order of

the $M \sim k$ UV scale, is effectively scaled down due to the warped metric and instead appears with scale:

$$v \equiv e^{-\pi k r_c} v_0. \quad (3.35)$$

Furthermore this result is completely general and continues to hold for any mass parameter on the IR brane. Therefore if $e^{-\pi k r_c}$ is of order 10^{-15} , requiring only a mild hierarchy between the curvature and the compactification length of $k r_c \approx 10$, one can obtain TeV scale mass parameters from a Planck scale of 10^{19} GeV. Therefore the question of the stabilization of the IR brane at $k r_c \approx 10$, or the generation of a potential for the radion $T(x)$, becomes crucial. Goldberger and Wise showed two months later the existence of an elegant mechanism [157] providing such a stabilization. The solution comes from considering a minimal matter sector consisting of bulk scalar field Φ with the following bulk action:

$$S_{\text{GW,bulk}} = \int d^4x d\phi \sqrt{G} \left(\frac{1}{2} G^{MN} \partial_M \Phi \partial_N \Phi - \frac{1}{2} m^2 \Phi^2 \right). \quad (3.36)$$

Furthermore brane potentials for the bulk field are added on both UV and IR branes:

$$S_{\text{GW,UV/IR}} = - \int d^4x \sqrt{-g_{\text{UV/IR}}} \lambda_{\text{UV/IR}} (\Phi^2 - v_{\text{UV/IR}}^2)^2. \quad (3.37)$$

For large $\lambda_{\text{UV/IR}}$, the boundary conditions for the bulk field Φ are fixed to the brane VEVs $v_{\text{UV/IR}}$. In consequence, a non trivial bulk VEV will be developed for the field

$$\Phi(x, \phi) = \Phi(\phi) + \sum_n f_n(\phi) \phi_n(x), \quad (3.38)$$

where the first term is the bulk VEV while the second term is the tower of massive KK modes. Inserting the bulk VEV solution $\Phi(\phi)$ into the action of Eq. (3.36) and integrating over the fifth dimension we obtain the following stabilized 4D potential for the radion or size of the extra dimension [156]:

$$V(\varphi) = \frac{k^3}{144M^6} \varphi^4 (v_{\text{IR}} - v_{\text{UV}}(\varphi/h)^\epsilon)^2. \quad (3.39)$$

The competing effects in the bulk between the derivative term preferring a flat VEV and thus a large fifth dimension and the mass term preferring a small extra dimension will yield the following size of the extra dimension:

$$k r_c = \frac{4k^2}{\pi m^2} \log \left(\frac{v_{\text{UV}}}{v_{\text{IR}}} \right). \quad (3.40)$$

A value of $k r_c \approx 11$ motivated by the hierarchy problem can thus be perfectly obtained with order one numbers and $\epsilon = m^2/4k^2 \ll 1$ while the mass of the radion is

$$m_\varphi^2 = \frac{\partial^2 V(\varphi)}{\partial \varphi^2} = \frac{k^2 v_{\text{IR}}^2}{3M^3} \epsilon^2 e^{-2\pi k r_c}, \quad (3.41)$$

which, due to the presence of the warped factor, appears as a TeV scale resonance. Note that due to the small ϵ suppression the radion will typically be the lightest new particle in RS scenarios. Once the radion is stabilized, it was shown that standard FRW cosmology is recovered at low temperatures [158]. In [159] the above results were improved taking into account the wavefunction of the radion and the backreaction of the bulk scalar field on the metric.

The RS model also features a tower of massive KK gravitons due to its compact nature with the lightest appearing at the scale of $3.83ke^{-\pi kr_c}$ [160]. In contrast to the massless graviton, these couple with TeV scale strength to the energy-momentum tensor and can therefore be produced at colliders.

3.3 Minimal Gauge-Higgs Grand Unification

Having introduced both the idea of gauge-Higgs unification and a warped extra dimensions, one can combine both ideas in models of gauge-Higgs unification in a warped background. By combining them, that is to say, considering a Higgs boson as the fifth component of a gauge field in a warped background, we not only provide a solution to the quadratic sensitivity of the Higgs boson mass, it is also possible to relate the large Planck scale to the electroweak scale.

We will work in a conformal coordinate system where the fifth coordinate, ϕ , is parameterized by

$$z \equiv \frac{e^{kr_c\phi}}{k}, \quad (3.42)$$

in which the resulting metric is given by

$$ds^2 = \left(\frac{R}{z}\right)^2 (\eta_{\mu\nu} dx^\mu dx^\nu - dz^2), \quad (3.43)$$

where we denote the location of the boundaries of the warped space with the new parameters $z = R \equiv 1/k$, for the UV brane, and $z = R' \equiv e^{kr_c\pi}/k$, for the IR brane.

For our study of gauge-Higgs unification in a warped background, we will need to understand how such 5D bulk gauge fields behave [161, 162]. Likewise, it will be beneficial for phenomenological reason to introduce the SM fermion into 5D bulk fermion fields [163, 164]. We refer to Appendix B for a review on the KK decomposition of bulk fermion and gauge fields in a warped extra dimension and provide the bulk wavefunctions.

Having an understanding of the behavior of fermion and gauge fields in 5D, one can now explore concrete models of gauge-Higgs unification. The first choice contains the gauge symmetry in the bulk, G . There are a few requirements on G . First of all, the bulk gauge fields must still contain the SM gauge group, G_{SM} . One can take two options at this point, either the $SU(3)_c$ gauge group is considered an external gauge group, such that the total bulk gauge field consists of a product group $G \times SU(3)_c$. The option consists of the original models

of electroweak gauge-Higgs unification (see [165] for the original warped gauge Higgs model based on $SU(3)$, while the later [166] is based on the custodial coset $SO(5)$). Since the Higgs is not charged under $SU(3)_c$, it is indeed sufficient to embed only the electroweak gauge group within G .

In this chapter we will pursue a different option of including the whole SM gauge group within a single simple Lie algebra, also known as models of gauge-Higgs *grand* unification:

$$SU(3)_c \times SU(2)_L \times U(1)_Y \subset G. \quad (3.44)$$

This option, although it increases the complexity of the model-building due to the inclusion of color, is motivated by the observed charge quantization of the SM to which GUTs [25–27] are an elegant elucidation. It provides a unified origin for the three different gauge groups and provides the SM fermions as simple representations of the unified group. Moreover the unification of gauge couplings has been studied in such setups and shown to improve with respect to the SM [167].

A second requirement on the gauge group choice for a successful gauge-Higgs unification, is that a Higgs doublet should be embedded within the bulk gauge field. Since a gauge field always transforms according to the adjoint representations, it places a strict requirement on the choice of the group G . As we have seen, only the broken generators with a Dirichlet boundary condition, $T^{\hat{a}}$, will give rise to a (massless) scalar degree of freedom. Therefore the resulting unbroken gauge symmetries on the UV and IR brane, respectively $H_0, H_1 \subset G$, will be crucial, and determine the scalar content:

$$A^{\hat{a}} T^{\hat{a}} = G / (H_0 \cup H_1). \quad (3.45)$$

Models of gauge-Higgs grand unification that obey both of the conditions in Eqs. (3.44), (3.45) are based on two main gauge groups: $SU(6)$ and $SO(11)$. The latter gauge group has the additional benefit of featuring a custodial symmetry (see next Chapter 4.2 for a discussion on custodial symmetry) and was studied in [168, 169] and later also in six dimensions [170, 171] to cure unwanted light exotics (see also [172–179]). We will study the gauge-Higgs grand unification based on an $SU(6)$ model, past studies include both supersymmetric [148, 180, 181] and non-supersymmetry [182] context. The constraining nature of the bulk gauge group, $SU(6)$, leads to light exotic fermions and massless down-type quarks and one is forced to localize the SM fermions on a brane and include extra bulk fermions [183–185].

In the rest of this chapter, we will present a gauge-Higgs grand unified $SU(6)$ model which manages to correctly produce the full SM spectrum from a minimal amount of 5D fields without putting matter on the brane. We will see how the unique combination of a warped 5D model in combination with a GUT gives a new perspective on the flavor hierarchies in nature. The constraints coming from flavor observables will be studied in detail and we analyse the mass generation of the extended scalar spectrum.

3.3.1 The Model

We begin by outlining the gauge structure of $SU(6)$. The bulk gauge symmetry, $SU(6)$, is broken to subgroups on the UV and IR via boundary conditions. The remnant of the bulk symmetry on the UV, H_0 and IR, H_1 is given by:

$$H_0 = SU(3)_c \times SU(2)_L \times U(1)_Y, \quad H_1 = SU(5). \quad (3.46)$$

The above can be visualized in terms of the boundary conditions for the different $SU(6)$ generators as:

$$A_\mu^a T^a = \left(\begin{array}{cc|ccc|c} (++) & (++) & (-+) & (-+) & (-+) & (--) \\ (++) & (++) & (-+) & (-+) & (-+) & (--) \\ \hline (-+) & (-+) & (++) & (++) & (++) & (--) \\ (-+) & (-+) & (++) & (++) & (++) & (--) \\ (-+) & (-+) & (++) & (++) & (++) & (--) \\ \hline (--) & (--) & (--) & (--) & (--) & (--) \end{array} \right), \quad (3.47)$$

where a broken symmetry corresponds to a Dirichlet BC $(-)$ for the corresponding gauge field. We see the unbroken subgroups $SU(2)_L$ and $SU(3)_c$ in the highlighted submatrices. The off-diagonal generators are both charged under color and the electroweak group and have the quantum numbers equal to the usual 4D X, Y gauge bosons, namely an $SU(3)_c$ triplet and $SU(2)_L$ doublet $(X^{4/3}, Y^{1/3}) \sim (\mathbf{3}^*, \mathbf{2})_{5/6}$. As discussed in Appendix B, $(-, +)$ boundary conditions give rise to a tower of massive gauge bosons with the lightest excitation at $(-, +) \sim 2.45/R'$. Furthermore, we find $(-, -)$ modes which will correspond to the totally broken generators and give rise to massless scalars. The massless scalars transform under the SM gauge group as :

$$G/(H_0 \cup H_1) = (\mathbf{1}, \mathbf{2})_{1/2} \oplus (\mathbf{3}, \mathbf{1})_{-1/3} \oplus (\mathbf{1}, \mathbf{1})_0. \quad (3.48)$$

We therefore find an extended scalar spectrum with besides a Higgs doublet, a scalar leptoquark and a scalar singlet.

Having discussed the gauge sector, we now turn to the matter sector in which we discuss the fermion embedding. Since the Higgs field is a bulk field, it is natural to also include the SM fermions as 5D bulk fermions. It is already well known that bulk fermions in warped space can be very successful in addressing the flavor hierarchies of the SM [163, 164, 186, 187]. Indeed, small Yukawa couplings can be obtained by localizing the fermions appropriately along the extra dimension such that the overlap with the bulk Higgs can result in vast range of magnitudes (this mechanism predates the RS model [188]). However if we wish SM fermions to be embedded within 5D bulk fermions, this implies that the Yukawa couplings come from the five dimensional covariant derivative. The minimal fermionic content that contains all the Yukawa couplings of the SM are a $\mathbf{20}$ and a $\mathbf{15}$ of $SU(6)$. Indeed the former contains an up-type quark Yukawa coupling while the latter contains both the down-type quark Yukawa

coupling and the charged lepton Yukawa coupling. In the following we will also include a $\mathbf{6}$ of $SU(6)$ which contains a Yukawa coupling for the neutrino. However we will see that this scenario would lead to too heavy neutrinos. This problem can be minimally solved by introducing an additional bulk singlet $\mathbf{1}$.

Another ingredient of the fermion sector is the introduction of mass mixing terms on the branes. Without these mixing terms, it would imply the existence of two distinct quark doublets, one embedded within the $\mathbf{20}$ for the up-type quark Yukawa and one within the $\mathbf{15}$ for the down-type Yukawa. In a similar fashion there would be two lepton doublets, one embedded within the $\mathbf{15}$ for the charged lepton Yukawa and one within the $\mathbf{6}$ for the neutrino Yukawa. With brane masses on the UV/IR boundaries the doublets mass mix and only one physical doublet survives while the other becomes heavy and decouples.

Therefore the full matter content of the model consists of the following 5D fermion fields where we show the decomposition into $SU(5)$ and the SM gauge group:

$$\begin{aligned}
\mathbf{20} \rightarrow \mathbf{10} &= q'(\mathbf{3}, \mathbf{2})_{1/6}^{+,-} \oplus E_R(\mathbf{3}^*, \mathbf{1})_{-2/3}^{-,-} \oplus e^c(\mathbf{1}, \mathbf{1})_1^{+,-} \\
\mathbf{10}^* &= (\mathbf{3}^*, \mathbf{2})_{-1/6}^{+,-} \oplus u(\mathbf{3}, \mathbf{1})_{2/3}^{-,-} \oplus (\mathbf{1}, \mathbf{1})_{-1}^{+,-}, \\
\mathbf{15} \rightarrow \mathbf{10} &= q(\mathbf{3}, \mathbf{2})_{1/6}^{+,+} \oplus E_L(\mathbf{3}^*, \mathbf{1})_{-2/3}^{+,+} \oplus e^c(\mathbf{1}, \mathbf{1})_1^{+,+} \\
\mathbf{5} &= d'(\mathbf{3}, \mathbf{1})_{-1/3}^{-,+} \oplus l^c(\mathbf{1}, \mathbf{2})_{1/2}^{-,+}, \\
\mathbf{6} \rightarrow \mathbf{5} &= d(\mathbf{3}, \mathbf{1})_{-1/3}^{-,-} \oplus l^c(\mathbf{1}, \mathbf{2})_{1/2}^{-,-} \oplus \nu^c(\mathbf{1}, \mathbf{1})_0^{+,+}, \\
\mathbf{1} &\rightarrow \nu^c(\mathbf{1}, \mathbf{1})_0^{+,-}.
\end{aligned} \tag{3.49}$$

The boundary conditions refer the ones of the left-handed fields (the right-handed fields have thus opposite boundary conditions, see Appendix B). The fashion in which the chiral SM fermions are embedded within the bulk fields are indicated by their usual symbols: q, u, d, l^c, e^c, ν^c , while the vector-like fermions with identical quantum numbers that mass mix with these chiral fermions after including boundary terms are indicated by the primed symbols: q', d', l^c, e^c, ν^c . The fermions in the $\mathbf{20}$ and $\mathbf{15}$ without any symbols are additional fermions that do not mix with SM fermions but are necessary to complete the bulk representation into complete $SU(6)$ representations. Although these *exotics* are not relevant for the flavor structure and constraints of the model, they do have an important role in the generation of the singlet scalar mass as we will discuss. In particular, the exotics dubbed E_L and E_R with electric charge $-2/3$ will be crucial for the mass generation of the singlet which we will discuss in the last section of this chapter. The brane masses on the IR consists of all the allowed $SU(5)$ invariant terms

$$S_{\text{IR}} = - \int d^4x \left(\frac{R'}{R} \right)^4 (M_{q/e} \bar{\Psi}_{R,10}^{\mathbf{20}} \Psi_{L,10}^{\mathbf{15}} + M_{d/l} \bar{\Psi}_{R,5}^{\mathbf{6}} \Psi_{L,5}^{\mathbf{15}} + M_\nu \bar{\Psi}_R^{\mathbf{1}} \Psi_{L,1}^{\mathbf{6}}) |_{z=R'}, \tag{3.50}$$

where we decompose a bulk field of representation \mathbf{R} of $SU(6)$ as $\Psi^{\mathbf{R}} = (\Psi_L^{\mathbf{R}}, \Psi_R^{\mathbf{R}})^T$ and denote subrepresentations with lower indices. These are the only non-vanishing IR brane masses and will result in mass mixing of the different bulk fermions. On the UV brane there is only one non-vanishing brane mass which connects up-type quarks from the bulk $\mathbf{20}$ and $\mathbf{15}$ in the exotic sector:

$$S_{\text{UV}} = - \int d^4x (M_{\bar{u}} \bar{\Psi}_{R,(3^*,1)}^{\mathbf{20}} \Psi_{L,(3^*,1)}^{\mathbf{15}} + \text{h.c.}). \quad (3.51)$$

Importantly we will not assume any particular form for these brane masses and will therefore be general order one 3×3 matrices with anarchic entries. Since these brane masses will be the source of flavor mixing in our model, it corresponds to not imposing any flavor symmetry in our model.

3.3.2 Zero Mode Approximation

In order to understand the implications of the above model, we will work within the zero mode approximation (ZMA). Concretely this approximation consists in ignoring all the fermion KK modes with the exception of the zero modes but including mixing. This will be an excellent model for understanding how the model performs in explaining the flavor hierarchies, or for the calculation of tree-level flavor constraints. For the calculation of loop-level constraints where the exchange of fermion KK modes becomes important, one needs to go beyond this approximation. As an illustration of the ZMA we take the up-type quark. We see that there is a single right-handed up-type singlet within the $\mathbf{20}$. Following the results from the Appendix B, we find for this fermion the following KK decomposition

$$\Psi_{u_R}(z, x) = \left(\frac{1}{\sqrt{R'}} \left(\frac{z}{R} \right)^2 \left(\frac{z}{R'} \right)^{c_{20}} f(-c_{20}) \right) u_{R,0}(x) + \sum_{n>0} f_n(z) u_{R,n}(x), \quad (3.52)$$

where we single out the zero mode and the prefactors ensure the kinetic term for $u_{R,0}(x)$ is canonically normalized and $f(c)$ is known as the *flavor function*

$$f(c) = \frac{\sqrt{1-2c}}{\sqrt{1-(R'/R)^{2c-1}}}, \quad (3.53)$$

which features an exponential sensitivity to the bulk 5D mass c . This is a straightforward example as the zero mode is entirely within the $\mathbf{20}$. The situation is more complicated for the left-handed quark doublet, q_L , where due to the IR boundary term of Eq (3.50) the q_L within the $\mathbf{15}$ mass mixes with the q'_L within the $\mathbf{20}$. The zero mode will thus be contained in both the $\mathbf{15}$ and

20. We therefore write the following two KK decompositions

$$\begin{aligned}\Psi_{q_L}(z, x) &= C_1 \left(\frac{1}{\sqrt{R'}} \left(\frac{z}{R} \right)^2 \left(\frac{z}{R'} \right)^{-c_{15}} f(c_{15}) \right) q_{L,0}(x) + \sum_{n>0} f_n(z) q_{L,n}(x) \\ \Psi_{q'_L}(z, x) &= C_2 \left(\frac{1}{\sqrt{R'}} \left(\frac{z}{R} \right)^2 \left(\frac{z}{R'} \right)^{-c_{20}} f(c_{20}) \right) q_{L,0}(x) + \sum_{n>0} f_n(z) q_{L,n}(x),\end{aligned}\quad (3.54)$$

where we have used the general bulk solution for a zero mode with unknown normalization constants C_1 and C_2 . One can eliminate one of them using the correct boundary condition that results from the IR mass mixing term (see for example [134]):

$$\Psi_{q'_L}(R') = M_{q/e} \Psi_{q_L}(R'), \quad (3.55)$$

which allows us to eliminate C_2 in favor of C_1 . The profiles of the zero modes are then

$$\begin{aligned}\Psi_{q_L}(z, x) &= C_1 \left(\frac{1}{\sqrt{R'}} \left(\frac{z}{R} \right)^2 \left(\frac{z}{R'} \right)^{-c_{15}} f(c_{15}) \right) q_{L,0}(x) + \dots \\ \Psi_{q'_L}(z, x) &= C_1 \left(\frac{1}{\sqrt{R'}} \left(\frac{z}{R} \right)^2 \left(\frac{z}{R'} \right)^{-c_{20}} f(c_{15}) \right) M_{q/e} q_{L,0}(x) + \dots,\end{aligned}\quad (3.56)$$

where the remaining C_1 can be found by imposing canonically normalized kinetic terms for $q_{L,0}(x)$. Indeed plugging these profiles into the bulk fermion Lagrangian and integrating out the fifth dimension we find the following kinetic term for $q_{L,0}(x)$:

$$\begin{aligned}S_{\text{bulk}} &\supset \int d^4x C_1^2 \left[1 + f(c_{15}) M_{q/e}^* f(c_{20})^{-2} M_{q/e} f(c_{15}) \right] \bar{q}_{L,0} \gamma^\mu \partial_\mu q_{L,0} \\ &\equiv \int d^4x C_1^2 K_q \bar{q}_{L,0} \gamma^\mu \partial_\mu q_{L,0},\end{aligned}\quad (3.57)$$

where we have named the uncanonical term in brackets as K_q . Therefore the inclusion of a brane mass has not only resulted in the left-handed doublet zero mode to be localized within two bulk field, the kinetic terms have become uncanonical. This can be fixed by the redefinition:

$$q_{L,0} \rightarrow C_1^{-1} K_q^{-1/2} q_{L,0}. \quad (3.58)$$

Now that we have derived the correct profiles for the zero modes $q_{L,0}$ and $u_{R,0}$, one can determine the resulting mass by determining the overlap with the Higgs. Remember that the 5D covariant derivative of the **20** contains the up-type Yukawa coupling

$$\begin{aligned}S_{\text{bulk}} &\supset \int d^4x dz \bar{\Psi}^{\mathbf{20}} \gamma^5 (\partial_5 - ig_5 A_5^{\hat{a}} T^{\hat{a}}) \Psi^{\mathbf{20}} \\ &\supset ig_5 \int d^4x dz \bar{\Psi}_L^{\mathbf{20}} (A_5^{\hat{a}} T^{\hat{a}}) \Psi_R^{\mathbf{20}} + \text{h.c.} \\ &\supset ig_5 \int d^4x dz \bar{\Psi}_{q'_L} (A_5^{\hat{a}} T^{\hat{a}}) \Psi_{u_R} + \text{h.c.}\end{aligned}\quad (3.59)$$

where we extract the interaction within the **20** between the q'_L and u_R . Once we identify the real component of the Higgs with a broken generator $T^{\hat{a}}$ and plug the zero mode profiles of Ψ_{u_R} and $\Psi_{q'_L}$ (see Eqs. (3.52) and (3.56)) and of the Higgs $A_5^{\hat{a}}$ (see Appendix B), one can integrate over the extra dimension and recover the following 4D mass for the up-type quark

$$\bar{q}_{L,0} M_u u_{R,0} = \bar{q}_{L,0} \frac{g_* v}{2\sqrt{2}} f(c_{15}) M_{q/e}^* f(-c_{20}) u_{R,0}, \quad (3.60)$$

where we define the dimensionless component of the 5D bulk coupling g_5 as g_* :

$$g_* \equiv g_5 / \sqrt{R}. \quad (3.61)$$

The bulk coupling g_5 is determined by reproducing the correct $SU(2)_L$ gauge coupling strength g .² This expression for the up-type quark mass is before canonical normalization and we therefore still need the transformation from Eq. (3.58) to have canonical kinetic terms, although in general the effects will be small.

The above expressions for the ZMA have straightforward generalization to the three generation case. The $M_{q/e}$ brane mass then becomes a 3×3 matrix and is the source of generational mixing, while the corresponding flavor functions becomes diagonal³ 3×3 matrices denoted by:

$$f_c = \text{diag}(f(c_1), f(c_2), f(c_3)). \quad (3.62)$$

In Appendix B we provide the bulk profiles of all the SM zero modes, the resulting mass matrices and the resulting uncanonical kinetic terms in the flavor basis.

We end this section with the interpretation of the UV brane mass, see Eq. (3.51). It will be a crucial ingredient in the mass generation of the scalar singlet as we will discuss in Sec. 3.5. The UV brane mass connects the two chiral exotic fermions within the **20** and **15** which we dub E_R and E_L . In the ZMA we use the zero mode profiles for the E_R and E_L and compute the resulting Dirac mass from these two zero modes. The profiles can be straightforwardly found:

$$\begin{aligned} \Psi_{E_R}(z, x) &= \left(\frac{1}{\sqrt{R'}} \left(\frac{z}{R} \right)^2 \left(\frac{z}{R'} \right)^{c_{20}} f(-c_{20}) \right) E_{R,0}(x) + \sum_{n>0} f_n(z) E_{R,n}(x), \\ \Psi_{E_L}(z, x) &= \left(\frac{1}{\sqrt{R'}} \left(\frac{z}{R} \right)^2 \left(\frac{z}{R'} \right)^{-c_{15}} f(c_{15}) \right) E_{L,0}(x) + \sum_{n>0} f_n(z) E_{L,n}(x). \end{aligned} \quad (3.63)$$

²In models of gauge-Higgs grand unification this creates the problem that the gluons and hypercharge bosons couple with identical strength as the weak bosons, although this can be easily solved by using brane-localized field strengths on the UV brane to lift the degeneracy.

³We work in a basis where the bulk is diagonal in flavor and the sole source of flavor mixing are the brane masses, see [189].

As appropriate for the zero mode approximation, we cut off the higher KK tower and plug these profiles into the UV brane mass of Eq. (3.51) finding

$$\begin{aligned}
S_{\text{UV}} &= - \int d^4x M_{\tilde{u}} \bar{\Psi}_{E_R}(z=R) \Psi_{E_L}(z=R) \\
&\supset - \int d^4x \frac{M_{\tilde{u}}}{R'} \left(\frac{R}{R'}\right)^{c_{20}-c_{15}} f(-c_{20}) f(c_{15}) \bar{E}_{R,0} E_{L,0} \\
&\equiv - \int d^4x m_E \bar{E}_{R,0} E_{L,0},
\end{aligned} \tag{3.64}$$

where we define the resulting 4D Dirac mass for the exotic as m_E . Unsurprisingly for both a UV localized Ψ_{E_R} and Ψ_{E_L} (thus $c_{20} < -0.5$ and $c_{15} > 0.5$), the overlap of the fermions with the UV brane is significant and thus the UV brane mass is large and the 4D Dirac mass for the exotic fermion has a UV brane value of $1/R$ and decouples from the low-energy phenomenology. In contrast, if both fermions are IR localized as in the case for the third generation in order to reproduce the large top mass, one gets an exponential suppression of the mass:

$$\begin{aligned}
m_E &\sim \frac{M_{\tilde{u}}}{R}, & c_{15} > 0.5, & \quad c_{20} < -0.5 \\
m_E &\sim \frac{M_{\tilde{u}}}{R'} \left(\frac{R}{R'}\right)^{c_{20}-c_{15}}, & c_{15} < 0.5, & \quad c_{20} > -0.5,
\end{aligned} \tag{3.65}$$

and Dirac mass significantly below the Planck scale are possible and in particular for $c_{15} \sim c_{20}$ one recovers IR scale masses.

3.3.3 The Flavor Puzzle

The flavor puzzle of the SM refers to the values observed in the Yukawa sector. First of all, the fermion masses range from $m_e \sim 0.5$ MeV for the electron to the heavy $m_t \sim 173$ GeV for the top: a discrepancy of almost six orders of magnitude in Yukawa couplings. The puzzle becomes even stranger when including the neutrinos, whose masses are at least another six orders of magnitudes below the electron mass. And although such very hierarchical Yukawa couplings are technically natural, it is still worthwhile to ask if a UV completion of the SM can shed light on these hierarchies.

Another part of the flavor puzzle comes when we consider flavor mixing in the quark sector as parameterized by the CKM matrix and in the lepton sector by the PMNS matrix. The absolute values of the entries of the CKM matrix are namely highly hierarchical [190]

$$V_{\text{CKM}} \sim \begin{pmatrix} |V_{ud}| & |V_{us}| & |V_{ub}| \\ |V_{cd}| & |V_{cs}| & |V_{cb}| \\ |V_{td}| & |V_{ts}| & |V_{tb}| \end{pmatrix} \sim \begin{pmatrix} 1 & \lambda & \lambda^3 \\ \lambda & 1 & \lambda^2 \\ \lambda^3 & \lambda^2 & 1 \end{pmatrix}, \tag{3.66}$$

with $\lambda \approx 0.23$ the Wolfenstein parameter. In contrast the PMNS matrix does not contain any remarkable hierarchies

$$V_{\text{PMNS}} \sim \begin{pmatrix} 0.82 & 0.55 & 0.15 \\ 0.37 & 0.58 & 0.71 \\ 0.40 & 0.59 & 0.69 \end{pmatrix}, \quad (3.67)$$

where we take the central values from [191].

It is well known that warped extra dimensions can shed a new light on the hierarchical Yukawa couplings. Indeed, the masses are exponentially sensitive to the localization of the fermions through the flavor function $f(c)$. Wildly different masses can thus be obtained by localizing the light generation in the UV, while the heavier third generation can be localized more in the IR. It is also known that a hierarchical CKM matrix can be accommodated in such a setup. After applying these mechanisms to our model, we will also consider whether the seemingly anarchic structure of the PMNS can be explained. This is a non-trivial question, because after specifying the quark sector, the lepton sector is almost fully determined, due to our unified model, and no more degrees of freedom are available for generating the PMNS matrix.

We therefore begin with the quark sector for which we find the following mass matrices in the ZMA:

$$\begin{aligned} \mathcal{M}_u &= \frac{g_* v}{2\sqrt{2}} f_{c_{15}} M_{q/e}^\dagger f^{-c_{20}}, \\ \mathcal{M}_d &= \frac{g_* v}{2\sqrt{2}} f_{c_{15}} M_{d/l}^\dagger f^{-c_6}. \end{aligned} \quad (3.68)$$

The generation of the CKM matrix comes from the mathematical observation that the bi-unitary diagonalization of the above mass matrices will feature rotation matrices with distinct hierarchies [186]. For the left-handed down sector for instance, we find the following hierarchies

$$U_{L,d} \sim \begin{pmatrix} 1 & \frac{f(c_{15,1})}{f(c_{15,2})} & \frac{f(c_{15,1})}{f(c_{15,3})} \\ \frac{f(c_{15,1})}{f(c_{15,2})} & 1 & \frac{f(c_{15,2})}{f(c_{15,3})} \\ \frac{f(c_{15,1})}{f(c_{15,3})} & \frac{f(c_{15,2})}{f(c_{15,3})} & 1 \end{pmatrix}, \quad (3.69)$$

with the rotation matrices in the left-handed up sector being analogous. Thus, by taking the bulk masses of the **15** such that the following conditions are fulfilled

$$f(c_{15,1})/f(c_{15,2}) \sim \lambda, \quad f(c_{15,2})/f(c_{15,3}) \sim \lambda^2, \quad f(c_{15,1})/f(c_{15,3}) \sim \lambda^3, \quad (3.70)$$

the left-handed rotation matrices in both the up and the down sector will feature similar hierarchies as the CKM matrix (see also [61, 189]). The CKM matrix, being the simple product of the left-handed rotation matrices $V_{\text{CKM}} = U_{L,u}^\dagger U_{L,d}$, will then naturally take over these hierarchies.

The generation of the SM mass hierarchies works by choosing different localizations, encoded in the 5D bulk masses, for the different bulk fermions. The large top mass leads us to choose an IR localization for both the **15** hosting the left-handed quark doublet of the third generation and the **20** hosting the right-handed top quark. The **15**'s hosting the lighter two generations will then naturally be UV localized by virtue of the above CKM conditions Eq. (3.70). The remaining localizations for the **20** and **6** are then fixed by matching the mass matrices (3.68) to the measured SM quark masses resulting in the following constraints on the localizations

$$\begin{aligned} \frac{m_c}{m_t} &\sim \lambda^2 \frac{f(-c_{20,2})}{f(-c_{20,3})}, & \frac{m_u}{m_t} &\sim \lambda^3 \frac{f(-c_{20,1})}{f(-c_{20,3})} \\ \frac{m_b}{m_t} &\sim \frac{f(-c_{6,3})}{f(-c_{20,3})}, & \frac{m_s}{m_t} &\sim \lambda^2 \frac{f(-c_{6,2})}{f(-c_{20,3})}, & \frac{m_d}{m_t} &\sim \lambda^3 \frac{f(-c_{6,1})}{f(-c_{20,3})}, \end{aligned} \quad (3.71)$$

We therefore see the attractiveness of warped 5D models in generating both the CKM matrix and the mass hierarchies that are observed in nature using 5D bulk mass of order 1. We now study the impact on the lepton sector and in particular the PMNS matrix. The mass matrix of the charged (conjugate) leptons in the flavor basis is given by

$$\mathcal{M}_{ec} = \frac{g_* v}{2\sqrt{2}} f_{-c_6} M_{d/l} f_{c_{15}}. \quad (3.72)$$

We note a degeneracy between the charged lepton and down-type quark matrices, identical to the usual $SU(5)$ 4D GUTs. However, the gauge symmetry on the UV brane is merely G_{SM} and thus can be used to lift the degeneracy by introducing $SU(5)$ -breaking effects. A minimal solution is introducing kinetic terms on the UV brane for the 5D fermion l_R^c embedded in the **6** with dimensionless coefficient κ :

$$S_{\text{kin},UV} = \int d^4x i\kappa R \bar{l}_R^c \bar{\sigma}^\mu \partial_\mu l_R^c|_{z=R}. \quad (3.73)$$

The above boundary term will shift the normalization of the kinetic term into

$$\begin{aligned} K_{l_R^c} &= 1 + f_{-c_6} M_{d/l} f_{-c_{15}}^{-2} M_{d/l}^\dagger f_{-c_6} \\ &\rightarrow 1 + \kappa R f_{l_R^c}^2(z=R) + f_{-c_6} M_{d/l} f_{-c_{15}}^{-2} M_{d/l}^\dagger f_{-c_6} \\ &\approx 1 + (-2c_{-6} - 1)\kappa + f_{-c_6} M_{d/l} f_{-c_{15}}^{-2} M_{d/l}^\dagger f_{-c_6}, \end{aligned} \quad (3.74)$$

where the approximation in the second line holds for UV-localized fermions with $c < -0.5^4$. By the following choice for κ , it becomes possible to break the degeneracy between the charged lepton and down-type quark and obtain

⁴For IR localized fermions, unsurprisingly, the effect of a UV kinetic term is negligible.

correct masses for the charged leptons:

$$\kappa = \begin{pmatrix} \frac{(m_d/m_e)^2-1}{-2c_{6,1}-1} & 0 & 0 \\ 0 & \frac{(m_s/m_\mu)^2-1}{-2c_{6,2}-1} & 0 \\ 0 & 0 & \frac{(m_b/m_\tau)^2-1}{-2c_{6,3}-1} \end{pmatrix}. \quad (3.75)$$

Before we can discuss the PMNS matrix, we need to comment on neutrino masses whose mass matrix in the flavor basis is given by:

$$\mathcal{M}_{\nu^c} = \frac{g_* v}{2\sqrt{2}} f_{-c_6} f_{c_6}. \quad (3.76)$$

Since the left-handed lepton doublet and right-handed neutrino singlet are both embedded in the bulk $\mathbf{6}$, it is unsurprising that the masses are depending on the localization of the $\mathbf{6}$. This creates the problem that the localization of the $\mathbf{6}$ already sets the masses of the down-type quarks and charged leptons, which will result in too heavy neutrino masses. The introduction of a bulk singlet $\mathbf{1}$ that mixes with the $\mathbf{6}$ on the IR brane is therefore crucial, since for very UV localized singlets, $c_1 > 0.5$, the neutrino mass eigenstate will mostly reside in the bulk singlet $\mathbf{1}$ with only a small admixture of the $\mathbf{6}$, resulting in the following neutrino masses (see [II] and [III] for a complete derivation):

$$\frac{m_{\nu_i}}{m_{\nu_j}} \simeq \frac{f(-c_{6,i})f(c_{1,i})}{f(-c_{6,j})f(c_{1,j})}. \quad (3.77)$$

Due to the exponential sensitivity of the flavor function, $f(c)$, to the localization parameter, only minor differences in the localization of the singlets, $c_{1,i}$, are necessary to produce a realistic neutrino mass spectrum. One can now discuss the PMNS matrix: it is equal to the product of the two left-handed lepton rotation matrices $V_{PMNS} = U_{L,\nu}^\dagger U_{L,e}$. In a similar reasoning that lead to Eq. (3.69), the left-handed rotation matrices are given by:

$$(U_{L,\nu})_{ij} \sim (U_{L,e})_{ij} \sim \frac{f(-c_{6,i})}{f(-c_{6,j})}, \quad i \leq j. \quad (3.78)$$

It turns out these hierarchies (or lack thereof) are ideal to explain V_{PMNS} . Indeed the $\mathbf{6}$ localizations were chosen to be almost degenerate (which was noted e.g. in [192] but with a different purpose of protecting the RH down sector from FCNCs) in order to reproduce the SM mass hierarchies. This was possible since there are no strong hierarchies remaining: the mass hierarchies in the down-type and charged lepton sector are almost fully determined by the localization of the bulk $\mathbf{15}$ (which itself was determined by the CKM matrix). Extracting the numerical values from Eq (3.71), we indeed find mild hierarchies:

$$\frac{f(-c_{6,2})}{f(-c_{6,1})} \sim 4, \quad \frac{f(-c_{6,3})}{f(-c_{6,2})} \sim 2. \quad (3.79)$$

These mild hierarchies will result in anarchic left-handed rotation matrices in the lepton sector and thus the PMNS matrix will remain anarchic as is observed in nature. We note that this result is not spoiled for different benchmarks for the neutrino masses since the left-handed rotation matrices depend on the **6** hierarchies as shown in Eq (3.79) while the neutrino mass hierarchies are dependent on the **1** hierarchies.

It is remarkable that three different observables in the flavor sector, namely the anarchic features of the PMNS matrix, the hierarchic features of the CKM matrix and the mass hierarchies, are in such a strict mathematical relation to each other in warped GUT models without the use of hierarchies. Indeed take any two combination of these three observables and the remaining observable comes out.

3.4 Phenomenology

Having found a minimal model with elegant features to account for the PMNS and CKM matrix, we now turn to the phenomenology of the model, in particular constraints coming from the flavor sector. Since all the localizations of the bulk fermions are essentially fixed by the requirement of reproducing the flavor hierarchies, the resulting flavor constraints are mostly fixed. We divide our observables in two broad categories: flavor violation in the quark sector due to meson mixing and flavor violation in the lepton sector in charged lepton violation. Typically, these observables provide very stringent constraints on the masses of the KK gauge bosons, mediating these FCNCs processes, pushing the IR scale, $1/R'$, up. In the past [61, 189, 193–208], flavor has been well studied in both the lepton and quark sector but usually independently from each other and often for a IR brane Higgs as in the original RS model. In a gauge-Higgs grand unification model, these effects can no longer be studied separately since quark and leptons are unified.

In warped extra dimensions, flavor violation is suppressed for UV localized fermions as their overlap with the KK gauge bosons is nearly universal, resulting in only small flavor violation in the extra dimension, a mechanism known as the RS-GIM mechanism [164, 186, 194, 209, 210] (which is analogous to the GIM mechanism [211] at work in the SM in suppressing FCNCs). Without such protection the bounds on the mass of the lightest KK gauge boson would be on the level of $\sim 10^4$ TeV. Nevertheless, the mechanism is not as effective as in the SM and strong bounds from flavor violation are still expected. We will see that these bounds push the IR scale, $1/R'$, in the far TeV region making it hard to obtain an un-tuned Higgs potential.

This ubiquitous feature of warped extra-dimensional models (and like-wise for many other SM UV completions), has resulted in using flavor symmetries to tame these bounds in the lepton sector [212–225] (see also [226, 227] for a recent review) and in the quark sector [192, 228–232]. We will not take a similar

approach in the following. First of all because of the quark-lepton unification inherent in our setup, none of the above flavor symmetries can be directly taken over. Secondly, although it is possible to implement additional flavor protection in our model and it would be an interesting question for follow-up work, we want to investigate how stringent the flavor bounds are in a fully anarchic model and what it implies for the amount of fine-tuning in the Higgs potential. This approach is similar in spirit to [233], accepting tuning in the Higgs potential but providing a compelling model of gauge-Higgs grand unification that evades the flavor constraints and explains the observed flavor hierarchies. Moreover, the extra new scalars provide potential experimental targets to test the model in the future.

3.4.1 Meson Mixing

We first discuss FCNCs in $\Delta F = 2$ flavor observables such as $B_s - \bar{B}_s$, $B_d - \bar{B}_d$, $D - \bar{D}$ and $K - \bar{K}$ mixing, with the latter generally being the most constraining. The large $SU(3)_c$ gauge coupling, ensures that the dominant contribution is from a tree-level exchange of the lightest KK gluon, although also the KK photon and the electroweak gauge bosons and their KK modes contribute sub-leadingly. The Lagrangian, with off-diagonal couplings to the first KK gluon in the mass basis, is given by

$$\mathcal{L} = (g_{L,q}^{ij} \bar{q}_L^{\alpha,i} \gamma_\mu q_{\beta,L}^j + g_{R,q}^{ij} \bar{q}_R^{\alpha,i} \gamma_\mu q_{\beta,R}^j) (T^a)_\alpha^\beta G_\mu^{a,1}, \quad (3.80)$$

where $q = u, d$ are flavor indices and i, j are generation indices. We provide here the full expressions for these couplings in the mass basis:

$$\begin{aligned} g_{L,u} &= g_s U_{L,u}^\dagger K_{qL}^{-\frac{1}{2}\dagger} \left(\lambda_{(+,+),c_{15}} + f_{c_{15}} M_{q/e}^\dagger f_{c_{20}}^{-1} \lambda_{(+,+),c_{20}} f_{c_{20}}^{-1} M_{q/e} f_{c_{15}} \right) K_{qL}^{-\frac{1}{2}} U_{L,u} \\ g_{R,u} &= g_s U_{R,u}^\dagger \lambda_{(+,+),c_{20}} U_{R,u} \\ g_{L,d} &= g_s U_{L,d}^\dagger K_{qL}^{-\frac{1}{2}\dagger} \left(\lambda_{(+,+),c_{15}} + f_{c_{15}} M_{q/e}^\dagger f_{c_{20}}^{-1} \lambda_{(+,+),c_{20}} f_{c_{20}}^{-1} M_{q/e} f_{c_{15}} \right) K_{qL}^{-\frac{1}{2}} U_{L,d} \\ g_{R,d} &= g_s U_{R,d}^\dagger K_{dR}^{-\frac{1}{2}\dagger} \left(\lambda_{(+,+),-c_6} \right. \\ &\quad \left. + f_{c_{-6}} M_{d/l} f_{-c_{15}}^{-1} \lambda_{(+,+),-c_{15}} f_{-c_{15}}^{-1} M_{d/l}^\dagger f_{-c_6} \right) K_{dR}^{-\frac{1}{2}} U_{R,d}. \end{aligned} \quad (3.81)$$

We denote with $\lambda_{(+,+),c}$ the generic coupling of a fermion zero mode with localization c to the first gauge boson KK mode of signature $(+, +)$ for which we refer to the more extensive paper [III]. We see in the above expression the effect of the zero modes being localized in two bulk fermions (with the exception of the u_R), which is responsible for the second term and the canonical normalization through the multiplication by the hermitian matrices K_ψ . Integrating out the lightest KK gluon with mass $m_{G_1} = 2.45/R'$, the following effective 4D

Hamiltonian (focusing on the down sector) is obtained

$$\begin{aligned} \mathcal{H} = & C_1^{ij}(m_{G_1})(\bar{d}_L^{\alpha,i}\gamma_\mu d_{L,\alpha}^j)(\bar{d}_L^{\beta,i}\gamma^\mu d_{L,\beta}^j) + \tilde{C}_1^{ij}(m_{G_1})(\bar{d}_R^{\alpha,i}\gamma_\mu d_{R,\alpha}^j)(\bar{d}_R^{\beta,i}\gamma^\mu d_{R,\beta}^j) \\ & + C_4^{ij}(m_{G_1})(\bar{d}_L^{\alpha,i}d_{R,\alpha}^j)(\bar{d}_R^{\beta,i}d_{L,\beta}^j) + C_5^{ij}(m_{G_1})(\bar{d}_L^{\alpha,i}d_{R,\beta}^j)(\bar{d}_R^{\beta,i}d_{L,\alpha}^j), \end{aligned} \quad (3.82)$$

with

$$\begin{aligned} C_1^{ij}(m_{G_1}) &= \frac{g_{L,d}^{ij}g_{L,d}^{ij}}{6m_{G_1}^2}, & \tilde{C}_1^{ij}(m_{G_1}) &= \frac{g_{R,d}^{ij}g_{R,d}^{ij}}{6m_{G_1}^2}, \\ C_4^{ij}(m_{G_1}) &= -\frac{g_{L,d}^{ij}g_{R,d}^{ij}}{m_{G_1}^2}, & C_5^{ij}(m_{G_1}) &= \frac{g_{L,d}^{ij}g_{R,d}^{ij}}{3m_{G_1}^2}. \end{aligned} \quad (3.83)$$

We take the strong bounds on the coefficients of these operators from [234]. Especially in the kaon sector these bounds are particularly strong: the imaginary component of $C_4^{21}(\Lambda)$ requires a new physics scale of $\sim 10^4$ TeV with order one couplings. The coefficients depend considerably on the renormalization scale and they should be translated to our new physics scale $\sim m_{G_1}$ (see [61]). Since the $C_4^{21}(\Lambda)$ coefficient only receives contributions from the KK gluon exchange (and not from photon or other electroweak gauge bosons), we are well motivated into only taking gluon exchange into account.

3.4.2 Tree-level Lepton Flavor Violation

We now turn to observables in the lepton sector from tree-level processes, namely $\mu^+ \rightarrow e^+e^-e^+$ decay and $\mu - e$ conversion in nuclei. The relevant Lagrangian mediating these processes consists of the couplings of the leptons to the Z boson (and its first KK mode):

$$\mathcal{L} = \frac{g}{c_W} \left(g_L^{ij} \bar{e}_L^i \gamma_\mu e_L^j + g_R^{ij} \bar{e}_R^i \gamma_\mu e_R^j \right) Z^{0,\mu} + \frac{g}{c_W} \left(g_L^{ij} \bar{e}_L^i \gamma_\mu e_L^j + g_R^{ij} \bar{e}_R^i \gamma_\mu e_R^j \right) Z^{1,\mu}. \quad (3.84)$$

The coefficients in the mass basis read:

$$\begin{aligned} g_L &= (-1/2 + s_W^2) \left(U_{L,e^c}^\dagger K_{l_R}^{\dagger,-1/2} \left(\lambda_{Z^0,-c_6} \right. \right. \\ &\quad \left. \left. + f_{-c_6} M_{d/l} f_{c_{15}}^{-1} \lambda_{Z^0,-c_{15}} f_{c_{15}}^{-1} M_{d/l}^\dagger f_{-c_6} \right) K_{l_R}^{-1/2} U_{L,e^c} \right) \\ g_R &= s_W^2 \left(U_{R,e^c}^\dagger K_{e_L}^{\dagger,-1/2} \left(\lambda_{Z^0,-c_6} \right. \right. \\ &\quad \left. \left. + f_{-c_6} M_{d/l} f_{c_{15}}^{-1} \lambda_{Z^0,-c_{15}} f_{c_{15}}^{-1} M_{d/l}^\dagger f_{-c_6} \right) K_{e_L}^{-1/2} U_{R,e^c} \right). \end{aligned} \quad (3.85)$$

$\lambda_{Z^0,c}$ denotes the coupling of a zero mode fermion with localization c to the Z boson. The equivalent couplings to the first KK Z boson are obtained by the substitution $\lambda_{Z^0,c} \rightarrow \lambda_{(+,+),c}$. We refer to the more extensive paper for these expressions [III].

- $\mu^+ \rightarrow e^+ e^- e^+$:

Flavor violation in $\mu \rightarrow 3e$ can be parameterized with the following effective Lagrangian [235, 236]:

$$\begin{aligned} \mathcal{L} = & -\frac{4G_F}{\sqrt{2}} \left(g_1(\bar{e}_R \mu_L)(\bar{e}_R e_L) + g_2(\bar{e}_L \mu_R)(\bar{e}_L e_R) + g_3(\bar{e}_R \gamma^\mu \mu_R)(\bar{e}_R \gamma_\mu e_R) \right. \\ & + g_4(\bar{e}_L \gamma^\mu \mu_L)(\bar{e}_L \gamma_\mu e_L) + g_5(\bar{e}_R \gamma^\mu \mu_R)(\bar{e}_L \gamma_\mu e_L) + g_6(\bar{e}_L \gamma^\mu \mu_L)(\bar{e}_R \gamma_\mu e_R) \\ & \left. + m_\mu A_R \bar{e}_R \sigma^{\mu\nu} \mu_L F_{\mu\nu} + m_\mu A_L \bar{e}_L \sigma^{\mu\nu} \mu_R F_{\mu\nu} + \text{h.c.} \right). \end{aligned} \quad (3.86)$$

We recognize in the above Lagrangian the loop-level dipole operators, which are subdominant with respect to the tree-level contact interactions. However these dipole operators do induce the striking $\mu \rightarrow e\gamma$ decay which we will discuss in the next section. Since the scalar contact interactions are absent ($g_1 = g_2 = 0$) in the model at hand, we find the branching ratio [235, 236]:

$$\text{Br}(\mu \rightarrow 3e) = 2(g_3^2 + g_4^2) + g_5^2 + g_6^2. \quad (3.87)$$

Dating from 1988, the current experimental bound on $\mu \rightarrow 3e$ still reads [237]:

$$\text{Br}(\mu \rightarrow 3e) < 10^{-12}. \quad (3.88)$$

The bound is expected to be improved by the upcoming Mu3e experiment: [238]

$$\text{Br}(\mu \rightarrow 3e) < 10^{-16}. \quad (3.89)$$

By integrating out the Z boson and its first KK mode, with mass $m_{Z_1} = 2.45/R'$, we obtain the following couplings contributing to the $\mu \rightarrow 3e$ process:

$$\begin{aligned} g_3 &= 2 \left(g_R^{12} g_R^{11} + g_R'^{12} g_R'^{11} \left(\frac{m_Z}{m_{Z_1}} \right)^2 \right), \\ g_4 &= 2 \left(g_L^{12} g_L^{11} + g_L'^{12} g_L'^{11} \left(\frac{m_Z}{m_{Z_1}} \right)^2 \right), \\ g_5 &= 2 \left(g_R^{12} g_L^{11} + g_R'^{12} g_L'^{11} \left(\frac{m_Z}{m_{Z_1}} \right)^2 \right), \\ g_6 &= 2 \left(g_L^{12} g_R^{11} + g_L'^{12} g_R'^{11} \left(\frac{m_Z}{m_{Z_1}} \right)^2 \right). \end{aligned} \quad (3.90)$$

- $\mu - e$ conversion:

We now turn to $\mu - e$ conversion in nuclei for which we need the following quark-lepton effective operators [235, 236]:

$$\begin{aligned} \mathcal{L} = & -\frac{2G_F}{\sqrt{2}} \left(\bar{e}(s - p\gamma^5)\mu \sum_q \bar{q}(s_q - p_q\gamma^5)q \right. \\ & \left. + \bar{e}\gamma^\alpha(v - a\gamma^5)\mu \sum_q \bar{q}\gamma_\alpha(v_q - a_q\gamma^5)q + \text{h.c.} \right). \end{aligned} \quad (3.91)$$

We omit tensor couplings as they lead to non-coherent transitions and are therefore suppressed by the number of nucleons: only the scalar and vector couplings are relevant for coherent conversion. These have to be converted from the quark level to the nucleon level, which then results in the conversion rate [235, 236]

$$\begin{aligned} \text{Br}(\mu \rightarrow e)_N = & \frac{G_F^2 F_p^2 m_\mu^5 \alpha^3 Z_{\text{eff}}^4}{2\pi^2 Z \Gamma_{\text{capt}}} \times \left(|4eA_L Z + (s-p)S_N + (v-a)Q_N|^2 \right. \\ & \left. + |4eA_R Z + (s+p)S_N + (v+a)Q_N|^2 \right), \end{aligned} \quad (3.92)$$

where Γ_{capt} denotes the total muon capture rate and Q_N, S_N are defined by:

$$\begin{aligned} S_N &= s_u(2Z + N) + s_d(2N + Z), \\ Q_N &= v_u(2Z + N) + v_d(2N + Z). \end{aligned} \quad (3.93)$$

The parameters for ${}^{48}_{22}\text{Ti}/{}^{27}_{13}\text{Al}/{}^{197}_{79}\text{Au}$ nuclei are $F_p \sim 0.55/0.66/0.16$, $Z_{\text{eff}} \sim 17.61/11.62/33.5$, and $\Gamma_{\text{capt}} \sim (2.6/0.71/13.07) \times 10^6 \text{ sec}^{-1}$ [239, 240]. The strongest experimental constraint come from ${}^{48}_{22}\text{Ti}$ and ${}^{197}_{79}\text{Au}$ and read [241, 242]:

$$\begin{aligned} \text{Br}(\mu \rightarrow e)_{\text{Ti}} &< 6.1 \times 10^{-13}, \\ \text{Br}(\mu \rightarrow e)_{\text{Au}} &< 9.1 \times 10^{-13}. \end{aligned} \quad (3.94)$$

The bounded conversion rate for the titanium atom is slightly smaller and as a result we will only show bounds for it. The upcoming experiments COMET and Mu2e [243] are expected to probe $\mu - e$ conversion in aluminium with a sensitivity of

$$\text{Br}(\mu \rightarrow e)_{\text{Al}} < 8 \times 10^{-17}, \quad (3.95)$$

at the 90% confidence level (CL). We will also use this upcoming experiment in our analysis.

The contributions from the Z boson and its first KK mode are obtained from Eq. (3.84) by integrating them out (and including the respective quark couplings) which can then be matched to Eq. (3.91), giving us the values for v and a :

$$\begin{aligned} v &= \left(g_L^{12} + g_L'^{12} \left(\frac{m_Z}{m_{(+,+)}} \right)^2 \right) + \left(g_R^{12} + g_R'^{12} \left(\frac{m_Z}{m_{(+,+)}} \right)^2 \right), \\ a &= \left(g_L^{12} + g_L'^{12} \left(\frac{m_Z}{m_{(+,+)}} \right)^2 \right) - \left(g_R^{12} + g_R'^{12} \left(\frac{m_Z}{m_{(+,+)}} \right)^2 \right). \end{aligned} \quad (3.96)$$

3.4.3 Loop-level Lepton Flavor Violation

We now turn to lepton flavor violation at the loop level, in the form of $\mu \rightarrow e\gamma$, which is mediated by penguin diagrams with different gauge and scalar mediators. These processes have been studied in a fully 5D framework in [203].

Here we will favor working in a KK picture as it makes the calculation more transparent, as was done in [201], where only the Higgs-mediated loop was considered. In addition we will also take into consideration the Z -loop and W -loop contribution and most relevant for our model of $SU(6)$ gauge-Higgs grand unification, the scalar leptoquark. These calculations necessitate the careful treatment of KK fermions for which we refer to [III].

The amplitude for a general process $\mu(p) \rightarrow e(p')\gamma(q)$ reads $\mathcal{A} = e \epsilon_\mu^*(q) M^\mu$ [244]. Gauge invariance constrains that the amplitude remains invariant under $\epsilon_\mu \rightarrow \epsilon_\mu + q_\mu$, leading to the general form

$$M^\mu = \bar{u}_{p'}(C_L \Sigma_L^\mu + C_R \Sigma_R^\mu)u_p/m_\mu, \quad (3.97)$$

with:

$$\begin{aligned} \Sigma_L^\mu &= (p^\mu + p'^\mu)P_L - \gamma^\mu(m_e P_L + m_\mu P_R), \\ \Sigma_R^\mu &= (p^\mu + p'^\mu)P_R - \gamma^\mu(m_e P_R + m_\mu P_L). \end{aligned} \quad (3.98)$$

$C_{L/R}$ are model dependent coefficients that are calculated in the appendix of [III]. For on-shell processes the above expression simplifies due to $q^2 = 0$ and $\epsilon_\mu^* q^\mu = 0$ resulting in:

$$M^\mu = \bar{u}_{p'} i \frac{\sigma^{\mu\nu} q_\nu}{m_\mu} (C_L P_L + C_R P_R) u_p. \quad (3.99)$$

From this amplitude the decay width for $\mu \rightarrow e\gamma$ is given by:

$$\Gamma(\mu \rightarrow e\gamma) = \frac{(m_\mu^2 - m_e^2)^3 (|C_L|^2 + |C_R|^2)}{16\pi m_\mu^5}. \quad (3.100)$$

After dividing by the dominating $\mu \rightarrow e\nu\bar{\nu}$ decay width of $\Gamma(\mu \rightarrow e\nu\bar{\nu}) = m_\mu^5 G_F^2 / 192\pi^3$, the branching ratio is:

$$\text{Br}(\mu \rightarrow e\gamma) = \frac{12\pi^2 (C_L^2 + C_R^2)}{(G_F m_\mu^2)^2}. \quad (3.101)$$

The branching ratio has been best constrained by the MEG experiment [245], reading

$$\text{Br}(\mu \rightarrow e\gamma) < 4.2 \times 10^{-13}, \quad (3.102)$$

at 90% CL. An update from MEG II [246] is expected in the upcoming years with a projected sensitivity of:

$$\text{Br}(\mu \rightarrow e\gamma) < 6 \times 10^{-14}. \quad (3.103)$$

The same diagrams that induce $\mu \rightarrow e\gamma$ also create an electric dipole moment (and an anomalous magnetic moment). Using the above formulas, the dipole (and magnetic) moment are $d_l = (C_L^l - C_R^l)/2m_l = \text{Im}(C_L^l)/m_l$ (and $a_l = (C_L^l + C_R^l)/e = 2\text{Re}(C_L^l)/e$) for the diagonal elements $C_R^{l*} = C_L^l \equiv (C_L)_l$. In particular, the very stringent bound on an electron electric dipole moment $d_e/e < 0.11 \times 10^{-28}$ cm at 90% will be used to constrain the model [247].

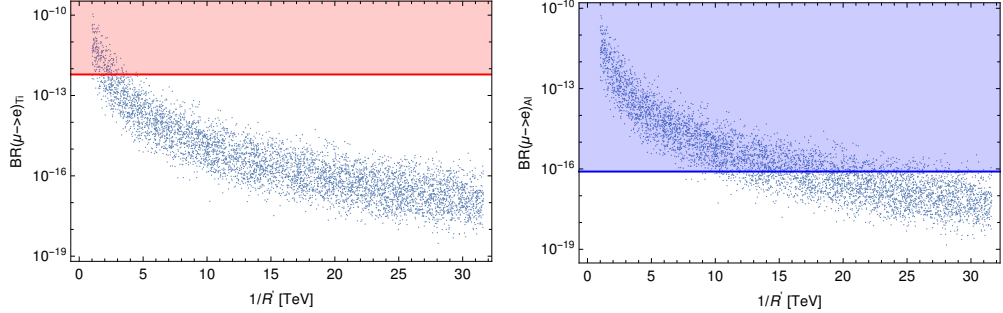


Figure 3.1: The current bound on $\mu - e$ conversion in titanium (left) and the future bound in aluminium (right), together with the results of our scan as a function of $1/R'$. The points in the red (blue) region are (expected to be) excluded.

3.4.4 Results

We now perform a scan of the model such that the SM mass hierarchies, the CKM matrix and the PMNS matrix are reproduced to within 20% accuracy. These datapoints are then used to evaluate the constraints from the flavor observables discussed above.

In Fig. 3.1, we illustrate the constraints coming from $\mu - e$ conversion. The current bound from titanium is rather weak for our model and can be neglected for $1/R' > 3$ TeV. However upcoming experiments in aluminium will exclude the model for scales of up to $1/R' < 10$ TeV. These results agree with previous studies of $\mu - e$ conversion in extra dimensional models [201], see also [226, 227, 248].

In Fig. 3.2 we display the current and upcoming bound on the $\mu \rightarrow 3e$ decay and the constraints from $K - \bar{K}$ meson mixing. The current bound on $\mu \rightarrow 3e$ is very weak but the upcoming constraint should exclude the model up to the 6 TeV region. In the quark sector, the constraint from $K - \bar{K}$ meson mixing is rather weak too. The bounds from $\mu - e$ conversion in titanium therefore provide the more reliable tree level constraint on the model. Our results agree relatively well with previous studies of $K - \bar{K}$ meson mixing [61, 198].

Finally we display the current and upcoming bounds on the loop level decay of $\mu \rightarrow e\gamma$ on the left panel of Fig. 3.3. This process excludes IR scales $1/R'$ lower than 20 TeV. It provides therefore the most stringent constraint on the IR scale of the model from flavor. The future improvement will probe the parameter space for $1/R' < 30$ TeV. On the right panel of Fig. 3.3, we display the breakdown of the $\text{Br}(\mu \rightarrow e\gamma)$ branching ratio in terms of the different loop contributions (under the assumption that only one mediator is present). The leptoquark contribution gives the strongest, with the Higgs boson and W/Z boson contributions being subleading. This allows us to understand the more constraining nature of our results in comparison to the literature [201] since

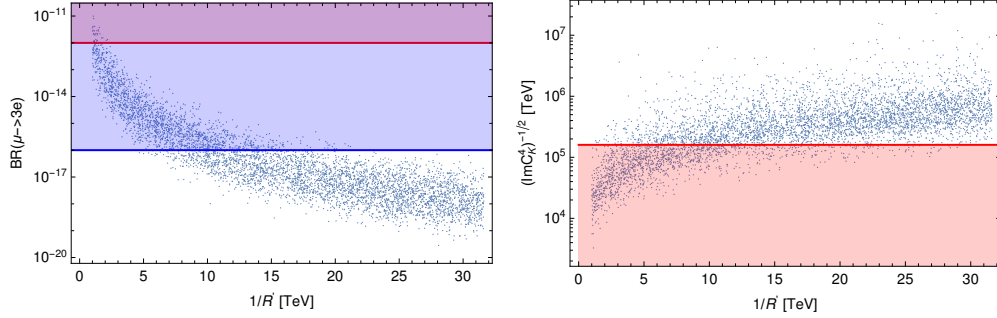


Figure 3.2: Current (red) and future (blue) constraints on the $\mu \rightarrow 3e$ decay (left) and on the $(\text{Im}C_K^4)^{-1/2}$ operator (right), together with the results of our scan as a function of $1/R'$.

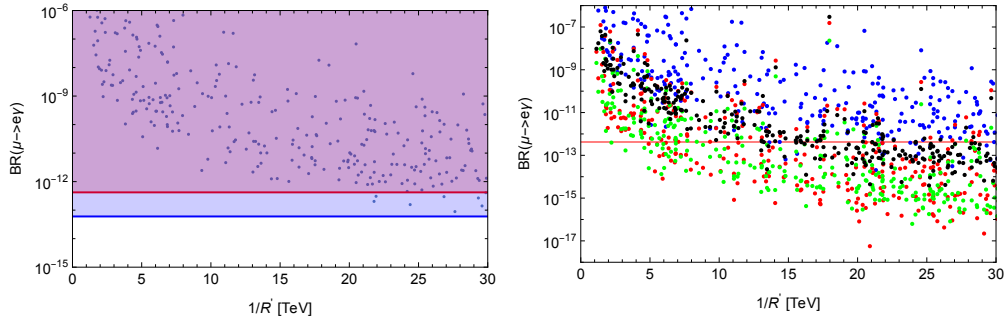


Figure 3.3: The current (red) and future (blue) constraints on the $\mu \rightarrow e\gamma$ decay, shown together with the results of our scan (left), and the relative size of the leptoquark (blue), Higgs (red), Z boson (green), and W boson (black) contributions (right), as a function of the IR scale $1/R'$.

colored scalars are generally absent in non-GUT gauge-Higgs unification. The results from the electron electric dipole moment are shown in Fig. 3.4 and are of similar strength as the future bound on the $\mu \rightarrow e\gamma$ measurement. Again, the leptoquark contributes the most.

The above results are an example of a broader issue in models that address the hierarchy problem. The flavor bounds for models that address the hierarchy problem will often be much larger than naturalness in the Higgs sector allows for. This has resulted in the use of flavor symmetries and the so-called minimal flavor violation (MFV) approach [249] in order to keep these bounds under control. When applying this approach to models with a warped extra dimension [229], it leads to less stringent flavor bounds, but one loses the ability to fully explain the SM mass and flavor hierarchies with order one parameters.

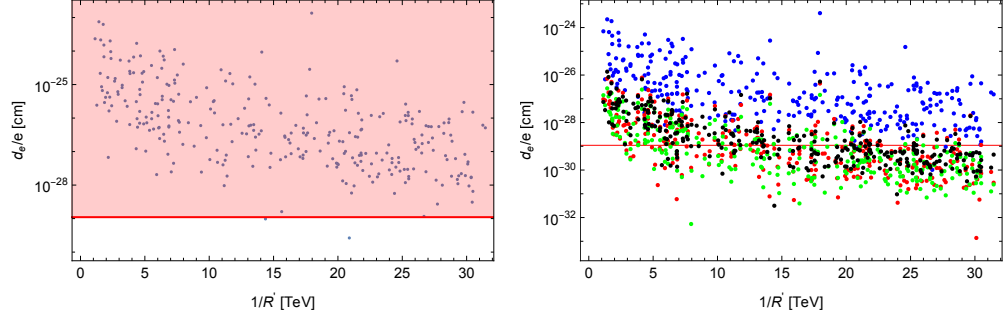


Figure 3.4: The current constraints on the electron electric dipole moment, shown together with the results of our scan (left), and relative size of the leptoquark (blue), Higgs (red), Z boson (green), and W boson (black) contributions (right), as a function of the IR scale $1/R'$.

3.5 The Scalar Potential

We now proceed with the calculation of the scalar potential. As discussed there are three scalars in the spectrum: the Higgs doublet, a leptoquark and a singlet. The scalar potential will therefore consist of three directions in field space. As seen in Sec. 3.1, in order to obtain a finite potential one needs to sum over the whole KK tower and apply the Coleman-Weinberg formula. Using dimensional regularization and techniques of complex analysis, this sum over KK modes can be neatly rewritten as the following integral (see for example [137, 250])

$$V(h, c, s) = \sum_r V_r(h, c, s) = \sum_r \frac{N_r}{(4\pi)^2} \int_0^\infty dp p^3 \log(\rho_r(-p^2, h, c, s)), \quad (3.104)$$

where $N_r = 3$ for gauge bosons, $N_r = -4N_c$ for quarks, and ρ_r denotes the corresponding spectral function, whose roots at $-p^2 = m_{n,r}^2$, $n \in \mathbb{N}$ encode the physical spectrum of the KK tower associated to particle r . ρ_r simply follows from solving the equations of motions in the presence of VEVs. In the holographic gauge the dependence can be completely gauged onto the IR boundary as discussed in Sec. 3.1 and the physical spectrum is encoded in the IR boundary conditions. The holographic gauge transformation on the IR brane for a warped extra dimension reads (see Eq (3.11)):

$$\Omega(z = R') = \exp\left(i v^{\hat{a}} T^{\hat{a}} / f\right), \quad f \equiv \frac{2\sqrt{R}}{g_5 R'}. \quad (3.105)$$

f is called the symmetry breaking scale and refers to the connection between models of gauge-Higgs unification with models of composite Higgs, a connection we will illustrate in Chapter 4. The largest contributions to the Higgs potential comes from the particles that couple in largest fashion to the Higgs: the top

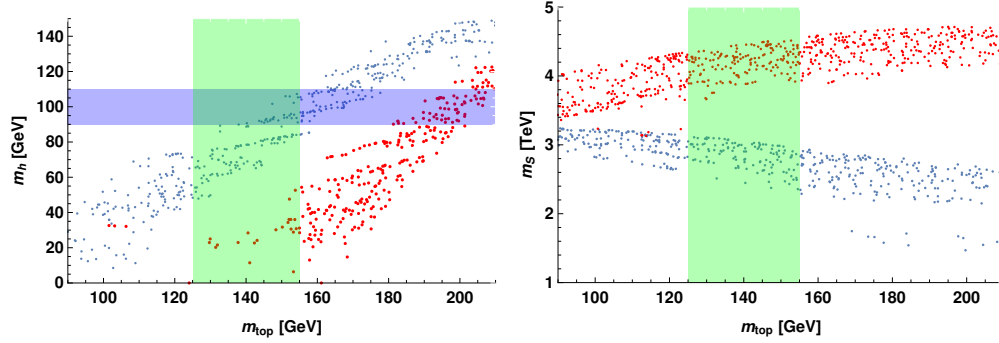


Figure 3.5: Left panel: The Higgs mass as a function of the top mass. Points in red feature $M_{\tilde{u}} > 0$ and predict the wrong Higgs mass while the points in blue belong to $M_{\tilde{u}} < 0$ and are compatible with the correct Higgs mass. Right panel: The mass of the leptoquark versus the top quark mass for the benchmark $1/R' = 10$ TeV. Points in red (blue) feature $M_{\tilde{u}} > 0$ ($M_{\tilde{u}} < 0$).

quark and the W/Z boson. Interestingly, due to the incomplete filling of the fermions into $SU(6)$ representations there is also the exotic up-type quark that is embedded in the same $\mathbf{20}$ as the top. Therefore it will couple with similar strength as the top, being also localized heavily in the IR. In general the potential in Eq. (3.104) can be expanded in the Higgs VEV resulting in the following functional form for the Higgs potential

$$V(h) \approx \alpha \sin^2(v/f) + \beta \sin^4(v/f), \quad (3.106)$$

where α, β consists of a momentum integral depending on the top, exotic and electroweak gauge bosons parameters. The resulting Higgs VEV from such a potential and the resulting Higgs mass can be found from minimizing the above potential:

$$\sin(v/f)^2 = \frac{-\alpha}{2\beta}, \quad m_h^2 = 8\beta/f^2 \sin^2(v/f). \quad (3.107)$$

In order to evade the discussed flavor bounds, especially coming from $\mu \rightarrow e\gamma$, a high symmetry breaking scale of $f \sim 10$ TeV is necessary. From the first condition one can see this will imply a level of fine-tuning in the Higgs sector at the promille level $\sim (v/f)^2$. However, once the Higgs potential is tuned to give the correct VEV, the Higgs mass is a non-trivial result. The numerical analysis from the author's paper in [III] shows that no additional tuning is necessary and one gets the correct Higgs mass after tuning for the correct Higgs VEV, as shown in Fig. 3.5. We also note the importance of the exotic sector with the sign of the UV brane mass, $M_{\tilde{u}}$, resulting in two branches with different predictions for the Higgs mass. Now that we have studied the Higgs potential, we turn to the analysis of the other directions in field space, namely the leptoquark VEV, c , and the singlet VEV, s .

3.5.1 Generation of the Leptoquark Mass

Since we do not need to fine tune for a small VEV in the case of the leptoquark or singlet (on the contrary we do not wish a leptoquark VEV, c , breaking color and charge), one can employ a more robust and analytical (but approximate) calculation that exploits the low-energy spectrum of the model. The result of this calculation will show that the leptoquark does not acquire a VEV and gets a mass of around $m_S = 0.3m_*$, with $m_* \sim 2/R'$, the generic scale at which the first KK states appear. This result follows from an analysis of the contributions to the potential along a small but non-zero VEV c . Such a VEV, implies the breaking of $S(3)_c \times U(1)_Y \rightarrow SU(2) \times U(1)$, giving rise to 5 Goldstone scalars that will be absorbed partly by the gluons and partly by the hypercharge boson. The spectrum thus consists of one massive gauge boson Z_c which is a mixture between the hypercharge boson and a gluon, and four massive W_c gauge bosons corresponding to the massive gluons. The mass relations follow straightforwardly

$$\begin{aligned} m_{Z_c} &= \frac{g_s c}{2 \cos \theta_{W,c}}, \\ m_{W_c} &= \frac{g_s c}{2}, \end{aligned} \quad (3.108)$$

with $\cos^2 \theta_{W,c} = 9g_s^2/(12g_s^2 + 4g'^2)$ the cosine of the *color* Weinberg angle squared. These massive gauge bosons will stabilize the potential along the color-broken direction in field space, preventing the formation of a VEV. One should also analyse the fermion content which can be important. Usually the top is the most important contribution to the Higgs potential, but in the color broken Universe, the right-handed top will mix with the electron singlet, forming the particle T_c . The Yukawa coupling of this particle to the leptoquark is (due to $SU(5)$ symmetry) equal to the usual top Yukawa, y_t resulting in the following mass:

$$m_{T_c} = \frac{y_t c}{\sqrt{2}}. \quad (3.109)$$

Now that we understand the low-energy spectrum in the color-broken Universe, one can estimate its contribution to the potential. For this we use an ansatz for the spectral functions of these particles [250]. We will use knowledge about its low-energy behavior, exhibiting a pole $f_{r;1} \rightarrow a/p^2$ as $p \rightarrow 0$ with a a constant determined by its coupling to the leptoquark, and its high-energy behavior, featuring exponential damping above the KK scale m_* , we then arrive at:

$$\begin{aligned} V(c) &= 4 \times \frac{3}{16\pi^2} \int_0^\infty dp p^3 \log \left(1 + (g_s f/m_*)^2 \frac{\sin^2(c/2f)}{\sinh^2(p/m_*)} \right) \\ &\quad + \frac{3}{16\pi^2} \int_0^\infty dp p^3 \log \left(1 + (g_s f/m_* \cos \theta_{W,c})^2 \frac{\sin^2(c/2f)}{\sinh^2(p/m_*)} \right) \\ &\quad - \frac{4}{16\pi^2} \int_0^\infty dp p^3 \log \left(1 + (y_t f/m_*)^2 \frac{\sin^2(c/\sqrt{2}f)}{\sinh^2(p/m_*)} \right). \end{aligned} \quad (3.110)$$

Approximating for simplicity $\cos^2 \theta_{W,c} \approx 1$, we find the mass squared of the leptoquark at the origin to be:

$$m_S^2 = \frac{\partial^2 V(c)}{\partial^2 c} \Big|_{c=0} = \frac{3\zeta(3)(15g_s^2 - 8y_t^2)}{64\pi^2} m_*^2 \approx (0.3m_*)^2. \quad (3.111)$$

Interestingly, we find the mass squared to be positive and therefore color remains unbroken. This is a general result and is due to the largeness of the strong coupling with respect to the top Yukawa (and the many more gauge boson degrees of freedom in comparison to fermionic degrees of freedom). This scalar leptoquark can be an interesting target for LHC searches, with the current bound being $m_S > 1.4$ TeV [251], as it will decay almost exclusively into $t\tau$. This is since the Yukawa couplings of the leptoquark are highly hierarchical in generation space with the more IR localized fermions, such as the top and tau, having large coupling. On the right panel of Fig. 3.5, we show the exact numerical results of evaluating the leptoquark mass. We notice unsurprisingly that the exotic sector also contributes to the mass generation of the leptoquark, an effect we neglected in our estimation. Instead, the numerical results point towards a lighter leptoquark of scale $m_S \approx (0.15 - 0.2m_*)$. Nevertheless, the leptoquark is unambiguously lighter than the other lightest KK bosons appearing at m_* and is thus the best collider target for these models.

3.5.2 Generation of the Singlet Mass

We now turn to the question of the singlet scalar s . The singlet scalar corresponds to the following generator of $SU(6)$

$$T_X = c \times \text{diag}(1, 1, 1, 1, 1 - 5), \quad (3.112)$$

with $c = 1/\sqrt{15}$ a normalization factor. This generator acts on the different $SU(5)$ representation as follows, where we omit for clarity the normalization factor:

$$\begin{aligned} \mathbf{6} &\rightarrow \mathbf{5}_1 \oplus \mathbf{1}_{-5} \\ \mathbf{15} &\rightarrow \mathbf{10}_2 \oplus \mathbf{5}_{-4} \\ \mathbf{20} &\rightarrow \mathbf{10}_{-3} \oplus \mathbf{10}^*_3. \end{aligned} \quad (3.113)$$

To understand its impact we go to the holographic basis, and thus perform the following gauge transformation

$$U = \exp(iT_X s/f), \quad (3.114)$$

which removes the singlet from the bulk but instead it acts on the IR brane. Therefore the IR brane mass from Eq.(3.50) in this gauge becomes:

$$\begin{aligned} S_{IR} = - \int d^4x \left(\frac{R'}{R}\right)^4 & (M_{q/e} e^{\frac{i5cs}{f}} \bar{\Psi}_{R,20,10} \Psi_{L,15,10} + M_{d/l} e^{\frac{-i5cs}{f}} \bar{\Psi}_{R,6,5} \Psi_{L,15,5} + \\ & M_\nu e^{\frac{-i5cs}{f}} \bar{\Psi}_{R,1,1} \Psi_{L,6,1} + \text{h.c.}) \Big|_{z=R'}. \end{aligned} \quad (3.115)$$

However, one can remove the s dependence above by appropriate vector-like transformation for the bulk fermions $\Psi_{L/R} \rightarrow e^{ins/f} \Psi_{L/R}$. These are vector-like transformation under $SU(6)$, however when restricted under the G_{SM} these are chiral and such transformation on the zero modes of a general $\Psi_{L/R}$ do not conserve the measure of the path integral which will induce the following terms

$$\begin{aligned} \mathcal{L}_{\text{WZW}} = & + \frac{1}{32\pi^2} \frac{1}{f} s (g_Y^2 n_B \varepsilon^{\mu\nu\alpha\beta} B_{\mu\nu} B_{\alpha\beta} + g^2 n_W \varepsilon^{\mu\nu\alpha\beta} \text{Tr}(W_{\mu\nu} W_{\alpha\beta}) \\ & + g_s^2 n_G \varepsilon^{\mu\nu\alpha\beta} \text{Tr}(G_{\mu\nu} G_{\alpha\beta})), \end{aligned} \quad (3.116)$$

with the n_i dependent on the specific incarnation of the model. The specific numbers will not matter but very interestingly, QCD instantons field configuration [252], originally found to solve the $U(1)_A$ problem of QCD [253] will then generate a potential for the singlet giving it a potential of the order of the QCD scale:

$$m_{\text{singlet}}^2 f^2 \sim m_\pi^2 f_\pi^2. \quad (3.117)$$

Our singlet scalar acts exactly as a bona fide axion with T_X the generator of the anomalous symmetry under QCD, solving the CP problem [254, 255]. However since the decay constant of the axion particle is tied to the electroweak scale f , if we wish to conserve a semi-natural Higgs potential, such heavy axions are ruled out. Current bounds require $f > 10^8$ GeV, resulting in a very light axion. It is an interesting model building feature of $SU(6)$ gauge-Higgs grand unification that it features the possibility to have a QCD axion and does not require any additional model building.

We will not pursue this option as it would imply a very large tuning in the Higgs potential, keeping the scale at $f \sim 10$ TeV instead, in line with flavor bounds. However we should then still find a way to generate a large mass for the singlet which would otherwise be too light. We omitted one crucial ingredient, the UV brane mass of Eq. (3.51) which connects the exotic fermions. Indeed the chiral rotations that removed s from the IR brane and the bulk, will reintroduce the singlet dependence on the UV brane through this UV brane mass. It becomes therefore impossible to remove the singlet from both branes and a potential for the singlet will be generated due to loops involving this exotic fermion. One can again estimate the size of the potential from an ansatz. Similar to the leptoquark, the high-energy behavior is exponentially damped for $p > m_*$, we will therefore use a $\cosh(p/m_*)^2$ for the KK damping behavior. In contrast to the leptoquark calculation, the exotic has a vector-like fermion mass m_E (see Eq. (3.65) for its value in terms of 5D parameters) which means the propagator will go like $m_E/(p^2 + m_E^2)$ (the overall potential is proportional the chirality-flipping part of the fermion propagator). Adding some more factors to recover a dimensionless expression and inserting an overall factor of y_t as the exotic couples to the KK modes with similar strength as the top quark, we find

the following leading singlet potential

$$V(s) = -\frac{4 \times 3}{16\pi^2} \int_0^\infty dp p^3 \log \left(1 + \frac{m_E y t}{p^2 + m_E^2} m_* \frac{f^2 \sin^2(s/\sqrt{2}f)}{m_*^2 \cosh^2(p/m_*)} \right), \quad (3.118)$$

which leads to the following singlet mass

$$m_{\text{singlet}}^2 = \frac{\partial^2 V(s)}{\partial s^2} \approx \begin{cases} -(0.3m_*)^2 (m_*/m_E), & m_* \ll m_E \\ -(0.3m_*)^2 (m_E/m_*), & m_E \ll m_* \end{cases}, \quad (3.119)$$

where we approximate the singlet potential for two different regimes. We notice that the sign of m_E becomes physical and determines whether the singlet gets a VEV. This is in agreement with the numerical results from our paper where $m_E < 0$ corresponded to a zero VEV for the singlet. We note that the exotics of the first two generations have an unsuppressed brane mass of $m_E \sim 1/R$, and thus these exotics contribute negligibly to the mass of the singlet scalar. For the third-generation exotic, interestingly the vector-like mass can become around the IR scale due to its IR localisation (see Eq. (3.65)). Both of the limiting cases $m_E \ll m_*$ and $m_E \gg m_*$ would result in a too light scalar. Interpolating the above results, we find a viable singlet scalar for $m_E \sim m_*$, resulting in a singlet mass of around $m_{\text{singlet}} \approx 0.3m_*$. We note that it would be, similar to the leptoquark, lighter than the other KK states and therefore be a promising target for collider searches. Indeed due to a non-zero coupling to the dual gluon field strength n_G , it could be produced at hadron colliders with subsequent decay into two photons.

3.6 Summary

We started this chapter with an introduction to the elegant mechanism of gauge-Higgs unification which protects the Higgs from radiative corrections due to the higher-dimensional gauge symmetry at small scales. After which we investigated different flavors of extra dimensions: a flat and a warped extra dimension. We saw that in order to have a model of gauge-Higgs unification which can reproduce the correct four-dimensional gravity without fine-tuning, a warped extra dimension is preferred.

We then constructed a model of gauge-Higgs *grand* unification based on the bulk symmetry $SU(6)$. Compared with models of electroweak gauge-Higgs unification, these models are motivated by a wish to unify the SM gauge forces and at the same time unify the SM fermions into simpler representation of the large gauge group. We constructed a minimal model based on four bulk representations of $SU(6)$ and used the power of the fifth dimension to explain the SM mass hierarchies, including neutrino masses, and the hierarchical CKM matrix. Due to the quark-lepton unification, the resulting PMNS matrix is anarchic which matches experimental observation. Nevertheless, since such a

setup allows for more flavor-breaking couplings compared with the mere three Yukawa matrices of the SM, and are necessary to explain the SM mass hierarchies, stringent constraints from flavor observables are expected. We evaluated a wide range of these observables and found a tension with obtaining a natural Higgs potential, implying a fine tuning at the promille level. Other signatures of the model include a leptoquark and singlet scalar whose mass generation we studied in detail and were shown to be below the rest of the KK states at $\sim 0.3m_*$ which could be targets for collider searches.

This chapter presented a change in spirit to the approach of the previous chapter (and the upcoming one) giving up on a fully natural Higgs potential but providing instead a model of unification with a compelling flavor structure from fully anarchic flavor mixings.

Chapter 4

A Natural Composite Higgs

In the previous chapter we entertained the idea that the Higgs is not a 4D *elementary* scalar, instead it is the scalar component of a five-dimensional gauge field. The five dimensional gauge symmetry is sufficient to forbid quadratically sensitive quantum corrections to the Higgs. In this chapter we entertain the closely related idea that the Higgs is a 4D *composite* scalar. The composite nature of the Higgs means the quadratically sensitive quantum corrections are naturally cut off at the scale of compositeness. Indeed the Higgs decomposes into its more fundamental constituents above such a scale and ceases to exist. However these models have come under pressure from null results at the LHC, since a composite Higgs means a composite sector with a whole host of other resonances. In particular, the SM fermions need to connect to the composite sector in order to gain a mass from the composite Higgs. The top, being the heaviest SM fermion, is in that regard the most promising candidate to look for signs of compositeness as its composite resonances are predicted to be light if one wishes to avoid excessive fine-tuning. These light *top partners* have been the target of many collider searches over the last years, their lower bounds now reaching 1500 GeV which means generic incarnations of the composite Higgs have reached levels of fine-tuning of 2%. The situation is even worsened as most composite Higgs models suffer from the awkward double-tuning problem: the quartic of the Higgs potential is generated at a subleading order with respect to the quadratic, worsening the naive tuning.

We end this thesis with a novel solution to the problem of double-tuning in models of composite Higgs through the introduction of *mirror fermions*. This mechanism goes beyond eliminating the problem of double fine-tuning by reducing the naive estimate of fine-tuning by a factor of four, thereby showing how a natural composite Higgs with tuning of 10% is still perfectly viable in the third run of the LHC.

This chapter begins in Sec. 4.1 with a motivation and introduction to models of composite Higgs. The necessary tools for a composite Higgs model builder are provided. We give a brief overview to the different incarnations of compos-

ite Higgs which will bring us to the interesting connection between models of composite Higgs and models of gauge-Higgs unification, which were the topic of the last chapter, bringing a close to the theoretical underpinnings of this thesis. In Sec. 4.2 we use the developed tools to give a brief introduction to the *minimal composite Higgs model* which will serve as an example of the double-tuning problem and the issue of the light top partners. Finally in Sec. 4.3 we present our solution to the double-tuning problem of composite Higgs using mirror fermions. We investigate the mechanism through a phenomenological model and discuss the resulting drastic reduction in fine-tuning. We end with a discussion of the unique experimental signatures of the mirror fermions.

4.1 Composite Higgs

The original models of composite Higgs [256–262] begin as an interpolation between the SM in which the Higgs is a fundamental scalar and models of technicolor [263, 264] (TC) which lack a scalar altogether. To understand the motivation behind this interpolation and thus models of composite Higgs, one has to understand the shortcomings of this latter theory first.

4.1.1 Technicolor

Technicolor is in essence a scaled up version of QCD in which electroweak symmetry is broken dynamically by the strong interactions of a new force: technicolor (see [82] for a review). Therefore those who wish to understand technicolor, QCD is a beautiful template with the definite advantage that it is realised in nature. QCD is a non-abelian gauge group based on $SU(3)_c$ whose coupling becomes strongly coupled in the infrared, eventually producing a whole host of composite particles/resonances with the curious property of color confinement. Although confinement is not proven, using the tools of anomaly matching [29] between the UV asymptotically free theory of quarks and gluons and the IR confined theory of baryons and mesons, one can prove that the flavor symmetry for the light quarks in the fermion sector of QCD, namely chiral symmetry, is spontaneously broken to its vector subgroup:

$$SU(2)_L \times SU(2)_R \rightarrow SU(2)_V. \quad (4.1)$$

This (approximate) flavor symmetry is only valid for the up and down quark (and to a lesser degree the strange quark) as the chiral symmetry is heavily broken by the heavy quark masses for the other flavors, indeed a Dirac mass constrains the left- and right-handed parts to transform equally. This pattern of symmetry breaking is also experimentally observed as the spectrum of QCD appears to be arranged by only one $SU(2)$ symmetry, namely the unbroken $SU(2)_V$. In contrast the axial generators are spontaneously broken by the following VEV

$$\langle \bar{\Psi}_i \Psi_j \rangle = \Lambda_{QCD}^3 \delta_{ij}, \quad (4.2)$$

where $i = 1, 2$ is a flavor index for the up and down quark. Indeed we see that a vector transformation preserves the vacuum while an axial transformation violates it. One can now describe the low-energy physics of the Goldstones purely on the basis of the above pattern of symmetry breaking, which by Goldstone's theorem produces three Goldstone bosons, the three QCD pions: π^0, π^\pm . However there is one element missing, namely that a part of the above global flavor symmetry is gauged, namely the electroweak gauge group which implies an interaction between the gauge bosons, W_μ^a and the weak current $J_{\mu,L}^a = (\bar{q}_L \gamma_\mu \tau^a q_L)^1$, which is nothing but the usual covariant derivative. Crucially, by Goldstone's theorem, the pions π^a are excited from the vacuum by generators that are not conserved by the vacuum, namely the axial generator $J_{A,\mu}^a = J_{R,\mu}^a - J_{L,\mu}^a$

$$\langle \Omega | J_{A,\mu}^a | \pi^b(p) \rangle = i p_\mu f_\pi \delta^{ab}, \quad (4.3)$$

with f_π setting the scale of chiral symmetry breaking. Such a matrix element implies the following Lagrangian interaction $J_{A,\mu}^a \partial^\mu \pi_a$, which results in pion exchange in the W^a boson 2-point function and a pole in the propagator of the W^a and leads to a mass for the W -boson. The resulting mass is however much below the correct electroweak scale, set instead by the scale of chiral symmetry breaking

$$m_W = \frac{g f_\pi}{2} \sim 29 \text{ MeV}, \quad (4.4)$$

many order of magnitude below its true mass. Moreover electromagnetism $Q = T_L^3 + Y$ remains intact as it is not broken by the vacuum (4.2). Therefore we see that all the qualitative features of EWSB are satisfied, only the scale is wrong. Moreover no fundamental scalar Higgs was necessary therefore no hierarchy problem was introduced. Instead the scale was set by the formation of a fermion condensate as in (4.2), triggered by the logarithmically growing coupling constant as it flows from the UV to the IR. This mechanism of creating large hierarchies in scales through a slowly running coupling constant is known as *dimensional transmutation* and is the backbone of non-SUSY solutions to the hierarchy problem.

Technicolor therefore comes out as a scaling up of QCD using a new strong gauge group, dubbed *technicolor*, with a new set of *technifermions* charged under the new force. A spontaneous breaking of a chiral symmetry amongst the technifermions as in (4.1), due to presumable confinement of the new force, will provide the necessary Goldstones that, after identifying parts of the chiral symmetry with the electroweak gauge group and gauging it, will give a mass to the electroweak gauge bosons. This time however the scale of chiral symmetry breaking is set by:

$$f_{TC} = 246 \text{ GeV}. \quad (4.5)$$

¹For simplicity we omit the $U(1)_Y$ gauge group which gauges the linear combination $Y = T_R^3 + B/2$

Although it furnishes a mass to the electroweak bosons, the SM fermions still remain massless since they do not couple to the condensate. This was addressed in models of Extended Technicolor (ETC) [265,266] where the technicolor gauge interactions, G_{TC} , are extended to a larger gauge group of extended technicolor, G_{ETC} , broken at a higher scale Λ_{ETC} to G_{TC} such that the SM fermions, $\psi_{L/R}$, and technicolor fermions, $Q_{L/R}$, can interact through the exchange of the heavy ETC bosons. Indeed such exchange will give rise to terms such as:

$$\mathcal{L}_{ETC} \supset \beta_{ab} \frac{\bar{Q}_L T^a Q_R \bar{\psi}_R T^b \psi_L}{\Lambda_{ETC}^2}. \quad (4.6)$$

Once the technifermions form a condensate (4.2) we find masses for the SM fermions on the order of:

$$m_\psi \sim \beta \frac{\Lambda_{TC}^3}{\Lambda_{ETC}^2}. \quad (4.7)$$

However the breaking of G_{ETC} will also induce other four fermions operators than the ones from Eq. 4.6, including operators with only SM fermions

$$\gamma_{ab} \frac{\bar{\psi}_L T^a \psi_R \bar{\psi}_R T^b \psi_L}{\Lambda_{ETC}^2}, \quad (4.8)$$

which will induce FCNCs. It becomes especially difficult to reconcile the heavy quarks while sufficiently suppressing FCNCs. We note that walking technicolor [267], in which the technicolor theory is not asymptotically free but instead exists at a conformal fixed point, meaning the coupling constant is approximately constant instead of going to zero like in QCD, these problems can be alleviated. Indeed in such a theory the condensate $\langle \bar{Q}Q \rangle$ is subject to large power-law renormalization effects and one can generate sufficiently large fermion masses despite a large Λ_{ETC} necessary to suppress FCNCs.

This ends our brief exploration of technicolor. Although a beautiful way to achieve EWSB without the need for an elementary scalar, it does not seem to be the way nature has chosen to break electroweak symmetry. Its final nail in the coffin is the discovery of a scalar particle at the LHC with seemingly all the properties of a Higgs particle. Nor in QCD nor in technicolor, is there a particle that can qualify as a Higgs boson. Of course there are 0^+ bosons in the spectrum of QCD but these are very broad and do not have the special relationship to the absorbed pion Goldstones that a Higgs would have, such as couplings proportional to mass.

Now that the main ideas behind technicolor have been illustrated, one can understand its progeny: composite Higgs models which do feature a light Higgs in its spectrum.

4.1.2 Composite Higgs

Models of composite Higgs can be understood as a modification of the flavor symmetry of a technicolor type theory, to include as a Goldstone not just a

triplet of pions but a full electroweak doublet that can function as a Higgs doublet. In the subsequent discussion we will consider these models in general terms: we consider a strongly coupled theory with a global flavor symmetry G . Moreover, we assume the strongly coupled theory condenses, at a scale f , such that the ground state of the theory doesn't exhibit the full flavor symmetry but instead a smaller subgroup H . In contrast to technicolor we do not want electroweak symmetry to be broken by the condensate. A crucial modification of the technicolor setup is therefore that one can embed the electroweak gauge group in H :

$$SU(2)_L \times U(1)_Y \subset H. \quad (4.9)$$

Instead, composite Higgs models wish to break electroweak symmetry in a second step by a Higgs doublet that is contained in the low-energy spectrum of the composite sector. The symmetry breaking scale f is therefore separated from the actual electroweak symmetry breaking scale, v , unlike in technicolor as in Eq. (4.5). This feature allows for a separation in scales between v and f , decoupling the effects of the strongly coupled sector as we take $v \ll f$. Again, using Goldstone's theorem one can choose an appropriate global symmetry G and the symmetry H of the ground state such that the Goldstones include an $SU(2)$ doublet:

$$G/H \supset (1, 2)_{1/2}. \quad (4.10)$$

Although the above characterisation might seem extremely vague, it is sufficient to construct a unique *phenomenological* Lagrangian of the resulting Goldstone bosons based on the symmetry breaking pattern $G \rightarrow H$. Indeed, this is the famous CCWZ construction by Callan, Coleman, Wess and Zumino [268, 269] who made the construction of such Lagrangians based on symmetry considerations, into a simple recipe one can follow. The starting point of the construction are the Goldstone fields, $\Pi^{\hat{a}}(x)$, that correspond to arbitrary local fluctuations in G around the vacuum \vec{V} of the theory:

$$\vec{\Phi}(x) = \exp\left(i\frac{2}{f}\Pi^{\hat{a}}(x)T^{\hat{a}}\right)\vec{V}. \quad (4.11)$$

Only the broken generators, $T^{\hat{a}}$, of the vacuum, namely $T^{\hat{a}}\vec{V} \neq 0$ correspond to physical Goldstones. Unbroken generators, denoted by T^a do not correspond to Goldstone degrees of freedom since they become annihilated by the vacuum, $T^a\vec{V} = 0$. If G is an exact global symmetry, the Goldstones are exactly massless and their VEVs are unobservable - indicating the absence of a potential for them. Indeed any $\langle \Pi^{\hat{a}} \rangle \neq 0$ can be removed by a redefinition of the $\Pi^{\hat{a}}$ fields using the global symmetry G .

The situation changes and becomes more interesting once we introduce explicit G -breaking interactions. The Goldstones get a potential from these interactions and are no longer massless: they become pseudo-Nambu-Goldstone bosons (pNGBs). Moreover, its VEV, $\langle \Pi^{\hat{a}} \rangle = v^{\hat{a}}$, becomes physical as we cannot use the explicitly broken G symmetry to redefine it away. The exact value

of v depends on the model and results from the minimization of the pNGB potential but generically we expect $v \sim f$. In that case electroweak symmetry is maximally broken at the scale of condensation and the model is technically no different from technicolor. The beauty of the composite Higgs models lies in the possibility, in principle, of having the vacuum point closely in the symmetry preserving direction \vec{V} and thus achieving a scale separation between the condensation scale and the electroweak symmetry breaking scale. This condition is expressed in the literature as the following ratio:

$$\xi \equiv \frac{v^2}{f^2} \ll 1. \quad (4.12)$$

In the limit of $\xi \rightarrow 0$ the strong sector decouples from electroweak physics and only the pNGB Higgs remains in the spectrum. Effectively we recover a SM Higgs as all the non-standard effects due to the composite sector decouple. However a small ξ as in Eq. (4.12) will usually only occur as a result of a lot of fine-tuning in the pNGB potential, indeed since the potential is generated at the scale f , a VEV of order v , will then require a fine-tuning of

$$\Delta_{\text{CH}} = \frac{f^2}{v^2}, \quad (4.13)$$

and one recovers the same quadratic sensitivity of the Higgs potential to higher scales as is well known from the SM. Therefore ideally the symmetry breaking scale f is not too high and experimental signatures of these models from the composite sector are expected. The absence of signals of new physics however, pushes composite Higgs models into fine-tuned areas. A solution to this persistent problem will be presented in Sec. 4.3.

4.1.3 CCWZ-construction

We now continue the general construction of the Lagrangian for the Goldstones following the CCWZ construction. We will largely follow the lecture notes by Panico and Wulzer [30]. Since the construction of our Lagrangian is merely constrained by symmetry requirements, it becomes of paramount importance to understand how the Goldstones, $\Pi^{\hat{a}}(x)$, transform under the symmetry group G . Instead of dealing directly with the Goldstones, it is more convenient to consider them in their exponentiated form, the Goldstone matrix

$$U[\Pi] = \exp\left(i\frac{2}{f}\Pi^{\hat{a}}T^{\hat{a}}\right), \quad (4.14)$$

which has the following convenient transformation properties under a generic element $g \in G$

$$U[\Pi] \rightarrow g \cdot U[\Pi] \cdot h^{-1}[\Pi; g], \quad (4.15)$$

with $h[\Pi; g] \in H$ in the unbroken group and depending on the element g . This transformation rule for the Goldstone matrix is comparatively easy (as

opposed to the transformation properties of the Goldstones themselves) and will serve to construct our effective Lagrangian for the Goldstone bosons. It is nevertheless illuminating to consider the transformation rules on the Goldstone bosons themselves. For a general transformation under the unbroken group $h = e^{i\alpha^a T^a}$, the Goldstones transform as

$$\Pi_{\hat{a}} \rightarrow (e^{i\alpha^a T_{\pi}^a})_{\hat{a}}^{\hat{b}} \Pi_{\hat{b}}, \quad (4.16)$$

with $T_{\pi}^{\hat{a}}$ the generators corresponding to the representation, \mathbf{r}_{π} of H under which the adjoint of G , $\mathbf{Ad}(G)$, decomposes under H :

$$\mathbf{Ad}(G) = \mathbf{Ad}(H) \oplus \mathbf{r}_{\pi}. \quad (4.17)$$

Unsurprisingly, the Goldstones transform linearly under the unbroken group. However, the full symmetry is G and the broken generators, $g = e^{i\alpha^a T^a}$, also correspond to symmetries of the theory, but their transformation rule can only be worked out at the infinitesimal level:

$$\Pi_{\hat{a}} \rightarrow \Pi_{\hat{a}} + \frac{f}{2} \alpha_{\hat{a}} + \mathcal{O}(\Pi^2). \quad (4.18)$$

Therefore due to the complicated non-linear transformation properties of the Goldstones, it becomes clear that the Goldstone matrix is a much more transparent object in the construction of a G -symmetric Lagrangian. Notice also that the above *shift* symmetry makes clear that our Lagrangian can only contain derivative interactions for the Goldstones or in other words no potential is allowed: the Goldstones are massless.

One can now start the construction of invariants which will serve as the basis for our Lagrangian. In order to respect the shift symmetry and to avoid trivial invariants such as $U^{\dagger}[\Pi]U[\Pi] = 1$, we have to include at least one derivative. The simplest example of which is the Maurer-Cartan form

$$iU[\Pi]^{-1} \partial_{\mu} U[\Pi] = d_{\mu, \hat{a}}[\Pi] T^{\hat{a}} + e_{\mu, a}[\Pi] T^a \equiv d_{\mu} + e_{\mu}, \quad (4.19)$$

which we decompose along the broken and unbroken generators. Through the transformation rule of the Goldstone matrix (4.15), one can deduce the following transformation properties of the d and e symbols:

$$\begin{aligned} d_{\mu}[\Pi] &\rightarrow h[\Pi, g] \cdot d_{\mu}[\Pi] \cdot h[\Pi, g]^{-1}, \\ e_{\mu}[\Pi] &\rightarrow h[\Pi, g] \cdot (e_{\mu}[\Pi] + i\partial_{\mu}) \cdot h[\Pi, g]^{-1}. \end{aligned} \quad (4.20)$$

Thus we see that d transforms linearly under the representation \mathbf{r}_{π} just as the Goldstones. This is a simple consequence of the following expansion:

$$d_{\mu, \hat{a}} = -\frac{\sqrt{2}}{f} \partial_{\mu} \Pi_{\hat{a}} + \mathcal{O}(\Pi^2). \quad (4.21)$$

However importantly, d keeps transforming under the full symmetry group G which is why it is the relevant object to construct invariants. The e symbol transforms as a gauge field associated with local H invariance. Therefore it can be used to construct covariant derivatives and field-strengths. The CCWZ prescription is now to construct invariants with the d and e symbols. The transformation rules of these symbols, although transforming under the full symmetry G , can be expressed concisely by elements $h \in H$. Therefore it suffices to construct H -invariant symbols, G -invariance will follow automatically. The leading term is the 2-derivative Lagrangian:

$$\mathcal{L}_{\partial^2} = \frac{f^2}{4} d_\mu^{\hat{a}} d^{\mu, \hat{a}} = \frac{1}{2} \partial_\mu \Pi^{\hat{a}} \partial^\mu \Pi^{\hat{a}} + \mathcal{O}((\partial\Pi)^2 (\Pi/f)^2). \quad (4.22)$$

It contains the kinetic terms for the Goldstones with an infinite set of 2-derivative interactions uniquely determined by the symmetry pattern of the Lagrangian $G \rightarrow H$ and the scale f . Any concrete model, such as for example a linear sigma model or a multi-site model as we will discuss later, based on that pattern of symmetry breaking will reproduce the exact same Lagrangian at the two-derivative level.

The CCWZ construction is easily generalized to the case when (parts of) the symmetries of G are gauged. The Lagrangian now has to be invariant under local transformations which means coupling the currents of the strong sector to the gauge fields:

$$\mathcal{L} \rightarrow \mathcal{L} + A_{\mu, A} J^{\mu, A}. \quad (4.23)$$

Therefore the partial derivative in the construction of the Maurer-Cartan form in Eq.(4.19) has to be promoted to the covariant derivative

$$iU[\Pi]^{-1} (A_\mu + \partial_\mu) U[\Pi] = d_{\mu, \hat{a}}[\Pi, A] T^{\hat{a}} + e_{\mu, a}[\Pi, A] T^a \equiv d_\mu + e_\mu, \quad (4.24)$$

with the d and e symbols now depending on the gauge fields A . The transformation properties are fully analogous except that they now transform under local transformations. The leading 2-derivative Lagrangian now also includes interactions with the gauge fields.

Although the 2-derivative Lagrangian is unique, fully determined by the symmetry breaking scale, higher order operators are not fixed. A complete UV description of the strong sector would allow the determination of the coefficients of these higher order operators. Later we will consider two possible UV completions of the composite sector namely, extra dimensions and multi-site models. For now, we want to develop a *power counting rule* to estimate these operators. Since higher order operators are the result of integrating out the resonances of the composite sector, we need to specify the typical mass m_* and the couplings g_* of the bosonic, σ and fermionic, Ψ resonances. Theories that can be fully specified with two such parameters are called *One Scale One Coupling* (1S1C) models. Using Naive Dimensional Analysis (NDA) [270, 271], the derived power counting rule is given by the following Lagrangian

$$\mathcal{L}_{\text{EFT}} = \frac{m_*^4}{g_*^2} \mathcal{L}_{\text{tree}} \left[\frac{\partial}{m_*}, \frac{g_* \Pi}{m_*}, \frac{g_* \sigma}{m_*}, \frac{g_* \Psi}{m_*^{3/2}}, \frac{g A_\mu}{m_*}, \frac{\lambda \psi}{m_*^{3/2}} \right], \quad (4.25)$$

where the last two entries represent higher dimensional operators involving elementary fermion fields, ψ , and gauge fields, A_μ , that communicate to the strong sector with coupling λ and g respectively. We introduce these couplings in the next section. It might occur that an operator cannot be generated at tree level and then becomes suppressed by additional loop factors $(1/16\pi^2)^n$. The requirement of the 2-derivative Lagrangian that insertions of the Goldstones are suppressed by f , results in the following relation between the two scales in the model:

$$m_* = g_* f. \quad (4.26)$$

This relation illustrates that indeed, by taking $1 < g_* < 4\pi$, one can separate the Goldstones, interacting with scale f , from the other composite resonances of scale m_* . Indeed to take QCD as an example, a genuine strongly coupled theory in which $g_* \approx 4\pi$, the pion decay constant, $f_\pi \sim 100$ MeV is an order of magnitude below the first genuine composite resonance such as the proton and neutron at ~ 1 GeV.

4.1.4 Generating the pNGB Potential

Until now, the Goldstones were massless as the G symmetry was kept intact. In this section we will develop the consequences of breaking the G symmetry explicitly which will mean a potential for the Goldstones, now pseudo-Nambu-Goldstone bosons (pNGBs), is generated at the loop-level. This potential will eventually lead to electroweak symmetry breaking if the Higgs pNGB gets a VEV.

There are two types of G -symmetry breaking interactions we consider. The first comes from gauging the currents of the strong sector, J_μ , that correspond to the electroweak symmetries:

$$\mathcal{L}_{\text{int}}^{\text{gauge}} = g A_\mu J^\mu. \quad (4.27)$$

The gauging naturally breaks the global symmetry G since we only gauge the $SU(2)_L \times U(1)_Y \subset H$ subset of the full G currents. The second source of G -symmetry breaking comes from the need to couple the SM fermions to the source of EWSB, which is the strong sector. A very elegant way of achieving this connection is through the hypothesis of partial compositeness [272] (PC) in which we couple the SM fermions, ψ , to fermionic operators of the strong sector $O^{\mathbf{R}}$ transforming in a certain representation \mathbf{R} of G :

$$\mathcal{L}_{\text{int}}^{\text{PC}} = \lambda \bar{\psi} O^{\mathbf{R}} + \text{h.c.} \quad (4.28)$$

Such couplings also break the global symmetry G as the SM fermions (usually) do not transform in full representations of G . The fermionic operator $O^{\mathbf{R}}$ is

expected to produce at least one resonance with a typical mass m_* once the strong sector condenses. The name partial compositeness refers to the fact that the SM fermions will mass mix with these composite resonances called *partners* thus gaining a mass. In the mass basis the SM fermions will therefore be partly composite. The heavier SM fermions will have to mass mix with greater strength and thus feature a larger coefficient λ in the equation above (4.28). In consequence, the heavy SM fermions will exhibit more composite-like behavior making them ideal targets for experimental signatures. We note that in 5D warped holographic UV completions, the PC hypothesis corresponds to the elegant embedding of SM fermions within a bulk 5D fermion of representation \mathbf{R} [165]. Whereas in fermionic UV completions of composite Higgs, it is a tough task to generate the necessary mixings [273–278].

To determine the consequences of these two G -breaking interactions, we denote both of these type of couplings as

$$\mathcal{L}_{\mathcal{G}^i} = g_E \Phi S^{\mathbf{R}}, \quad (4.29)$$

with $\Phi = \bar{\psi}, A_\mu$ denoting either a SM fermion or gauge field while $S^{\mathbf{R}}$ denotes a composite operator in a generic representation \mathbf{R} , representing either the conserved currents or fermionic operators. g_E parametrizes the strength of the coupling between the strong and elementary sector $g_E = g, g', g_s, \lambda_L, \lambda_R$. Furthermore we will promote the SM field Φ to a G representation, using the spurion method, thereby restoring (temporarily) G -invariance namely

$$\mathcal{L}_{\mathcal{G}^i} = g_E \Phi_\alpha \Lambda_I^\alpha (S^{\mathbf{R}})^I, \quad (4.30)$$

where I represents an index in the representation \mathbf{R} of the strong sector while α represents an index of a representation of the elementary sector, such as a weak or color index. At the end of the calculation, we set the spurions, Λ , back to their true G -breaking background value.

Now that the spurions transform in G representations, one can *dress* them by acting with the Goldstone matrix in the appropriate representation, $U^{\mathbf{R}}$, such that they transform under the full symmetry G merely with $h \in H$ elements:

$$\Lambda_D = U^{\mathbf{R}, \dagger} \Lambda. \quad (4.31)$$

The dressed spurion Λ_D will then decompose into H representations. One can then proceed with the construction, as the CCWZ prescribes, of H -invariant operators while G invariance will follow automatically. One can now construct the leading invariants that represent the one-particle-irreducible loops with zero external momentum, or in other words the effective potential. In order to obtain a sensible expansion, one expands the effective potential in insertions of spurions, or equivalently in powers of g_E . When the spurions are set to their G -breaking background values, we obtain the leading and subleading potentials for the pNGB, $V_2[\Pi/f]$ and $V_4[\Pi/f]$ for two, respectively four insertions of

g_E . The prefactors for the potential can be estimated using again dimensional analysis to be of the following order

$$\mathcal{L} = \frac{Nm_*^4}{64\pi^2} \left[\left(\frac{g_E}{g_*} \right)^2 V_2[H/f] + \left(\frac{g_E}{g_*} \right)^4 V_4[H/f] + \dots \right], \quad (4.32)$$

with N the degrees of freedom of the particle circulating in the loop. In order for the expansion in elementary couplings to make sense, one requires these couplings to be smaller than the composite couplings:

$$g_E < g_*. \quad (4.33)$$

In other words, the elementary sector should merely be a weak perturbation of the composite sector and G remains approximately a good symmetry.

4.1.5 UV Completions of Composite Higgs

The above formalism is very useful to parameterize the low-energy physics of a pNGB Higgs based on a general coset G/H , but by no means have we provided a realistic model of nature. We have discussed the composite Higgs in terms of its symmetries without asking the question of what is it made of? Although for most purposes such a symmetry based parametrization is enough, it is still worthwhile to ask what a possible UV completion could look like. It would be like investigating the theory of pions without asking what these pions could be made up of. It is the answering of this question that lead to the discovery of QCD, it is thus definitely a question worth asking.

The easiest possible answer for what the microscopic theory could be behind a general coset G/H , is simply a fundamental scalar transforming in some representation of G with a potential that gets a VEV resulting in a reduced symmetry H of the vacuum. This is not a satisfactory answer as it replaces one fundamental Higgs doublet with merely a new scalar, therefore reintroducing the hierarchy problem.

Since scalars shouldn't be used, one is naturally lead to using fermions to achieve the pattern of symmetry breaking $G \rightarrow H$. Taking inspiration from QCD/Technicolor, it is known that fermion bilinears that condense, can trigger the spontaneous breaking of a flavor symmetry without the use of scalars. However the possible patterns of symmetry breaking is limited. Indeed one can only have $SU(N)^2/SU(N)$, $SU(N)/SO(N)$ or $SU(2N)/Sp(2N)$ depending on whether the representations of the fermions charged under the new strong gauge group are complex, real or pseudo-real [279]. Notably even the minimal composite Higgs based on the coset $SO(5)/SO(4)$, which will be the subject of our next section, has no fermionic UV completion. It would be therefore very interesting whether different realizations of a composite Higgs exist that can accommodate more exotic cosets.

The answer to the above came as a result of trying to find phenomenological models of composite Higgs that allowed the Higgs potential to be calculated

and not merely estimated using NDA. Indeed, the Higgs potential of Eq. (4.32) simply arises as a quadratically divergent loop diagram that is simply cutoff at the scale, $\Lambda = m_* = g_* f$, where the physics becomes strongly coupled. If one can reduce the degree of divergence of such loops to the extent that it becomes logarithmically sensitive to the cutoff scale or even finite, the model becomes much more predictive. Furthermore, the role of the resonances of the strong sector remains unclear. It turns out the solution to both problems are intrinsically linked. Inspired by models of dimensional deconstruction [280,281], a mechanism called *collective symmetry breaking* [282,283] was found to lower the degree of divergence of the Higgs potential. It consists in enlarging the global symmetry, for example by simply extending the global symmetry G to $G \times G$ which is spontaneously broken to $H \times H$, while the full diagonal subgroup of $G \times G$ is gauged. Although such an extension doubles the amount of Goldstones, the additional Goldstones are absorbed by the additional gauging of the diagonal subgroup of $G \times G$. It turns out now that the leading contribution to the potential occurs from terms involving both sets of pNGBs lowering the quadratic divergence into a logarithmic divergence. Indeed the gauging of the diagonal subgroup of $G \times G$ implies also the existence of a global symmetry which requires the pNGBs to transform *collectively*. In terms of Feynman diagrams, what is happening is that the additional heavy gauge bosons due to the enlarging of the global symmetry are cancelling the quadratic sensitivity of the electroweak gauge bosons loop diagrams to the Higgs. Similar constructions exist for reducing the quadratic sensitivity of the fermion loops to the Higgs potential. An illustrative example of such a *little Higgs* comes from [284]. It is also possible to construct models exhibiting collective symmetry breaking not from a product group such as in the *littlest Higgs* [285] based on the coset $SU(5)/SO(5)$. Interestingly the latter also features a $\lambda \sim O(1)$ which naturally achieves $v^2/f^2 \ll 1$. This distinct feature from collective symmetry breaking is due to a tree level exchange of an additional triplet pNGB. The generation of such a large quartic is called *collective quartic*. These models are out of fashion due to their prediction of a, ironically, large Higgs mass.

However the lessons from collective symmetry breaking are certainly useful and have developed in a systematic method to obtain a fully finite and calculable Lagrangian based on an arbitrary symmetry breaking pattern by using multi-site models [286,287]. It is important to remember that these multi-site models are not meant to represent UV completions of a composite Higgs, merely to provide a simple phenomenological model providing a full calculable model through its use of the collective symmetry breaking mechanism.

Instead, it was realized that models of gauge-Higgs unification in a warped extra dimension provides a setting in which to realize a pNGB Higgs with collective symmetry breaking [165,210]. The inspiration behind this model is the celebrated AdS/CFT correspondence [288–290] which is a duality between a weakly coupled theory in the bulk of AdS_5 and a strongly coupled 4D conformal field theory. A heuristic argument illustrating why there should be such a

correspondence, comes from considering the metric of an AdS_5 space in an extra dimension:

$$ds^2 = \left(\frac{R}{z}\right)^2 (\eta_{\mu\nu} dx^\mu dx^\nu - dz^2). \quad (4.34)$$

We note that a transformation of the fifth dimension coordinate, $z \rightarrow e^\alpha z$, can be undone with a rescaling of the four-dimensional coordinates, $x \rightarrow e^\alpha x$. Therefore motion along the z axis is equivalent to increasing 4D length scale, which leads to the holographic interpretation in which motion along z corresponds to RG flow. Originally discovered as a correspondence between a string theory and a supersymmetric Yang-Mills theory, the implications of the correspondence to the 5D warped extra dimensional Randall-Sundrum model has been studied in [291, 292]. Indeed already in the conclusion of the original RS paper [153] the following was observed:

This is a potential resolution to the hierarchy problem akin in spirit to ideas of strongly coupled gauge theories which generate the low scale through an exponential times a fundamental high energy scale.

However in the original RS model, the Higgs corresponds to an ad hoc potential on the IR brane corresponding to the Higgs as a general bound state of the 4D CFT.

The eventual realization that a pNGB Higgs in a 4D CFT corresponds to the fifth component of a five dimensional bulk gauge field in a warped extra dimension, occurred in [165]. Later in [210], its application to the *minimal composite Higgs* came, based on the $SO(5)/SO(4)$ coset which we briefly review in the next section. The realization of partial compositeness with operators of certain scaling dimension also has an elegant realization in 5D as 5D bulk fermions with different localization along the extra dimension corresponding to different bulk mass [293].

The holographic realization of a pNGB Higgs is an exciting and realistic model of nature. We note that our topic of Chapter 3 could be interpreted as such a holographic realization of a Higgs pNGB (with an additional leptoquark and singlet) based on the coset $SU(6)/SU(5)$. We now turn to an analysis of the most cited composite Higgs model which will allow us to understand the issue of double-tuning and light top partners.

4.2 The Minimal Composite Higgs

The minimal composite Higgs model [210](MCHM), inspired by [165], is the minimal coset that provides a Higgs doublet and includes a *custodial* symmetry. In BSM model building, the inclusion of a custodial symmetry [294] to the new

physics sector has been an important ingredient since the advent of electroweak precision tests (EWPT) in the LEP area and parameterized by the S, T and U parameters [103, 104]. Especially the T parameter has become notorious in model building which measures deviations from the experimentally very well observed SM tree level relation:

$$\rho \equiv \frac{M_W^2}{M_Z^2 \cos^2 \theta_W} \approx 1. \quad (4.35)$$

Indeed the SM Higgs sector contains such a custodial symmetry that remains conserved even after the Higgs gets a VEV, namely $SU(2)_L \times SU(2)_R = SO(4) \rightarrow SO(3) = SU(2)_V$. This symmetry guarantees that the absorbed Goldstones transform as a triplet and, since the Goldstones provide a mass to the W/Z bosons through the Higgs mechanism, the relation in Eq. (4.35) can be proven to come out for such custodially endowed Higgs sectors. The Yukawa sector of the SM breaks this custodial symmetry since the RH top and bottom are not contained within a $SU(2)_R$ doublet and provides a small loop correction to Eq. (4.35).

More relevant to our discussion, large violations at tree-level of Eq. (4.35) are expected whenever considering a new Higgs sector unless it comes with a custodial symmetry as in the SM. In general the deviations from NP effects to ρ can be written in terms of the following dimension 6 operator O_T

$$\mathcal{L}_{d=6} \supset \frac{c_T}{2f^2} (H^\dagger \overleftrightarrow{D}_\mu H)^2, \quad (4.36)$$

which gives a contribution to ρ of \hat{T}

$$\Delta\rho = \hat{T} = c_T \frac{v^2}{f^2}, \quad (4.37)$$

with $\hat{T} = \alpha T$ related to the original definition of T . One can now immediately see that cosets without custodial protection must have a rather large symmetry breaking scale. For example for the coset $SU(6)/SU(5)$, the T operator is generated without any loop suppression: $c_T = 2/5$. From [295, 296] we get the 95% CL constraint $T < 0.25$ translating into

$$f > \sqrt{c_T} 5.5 \text{ TeV}, \quad (4.38)$$

or $f > 3.5$ TeV in the case of $SU(6)/SU(5)$. If one wishes to obtain an un-tuned composite Higgs, one is therefore quickly lead to custodial cosets that contain a $SO(4)$ in the unbroken group. The minimal option endowed with such a protection is the one that is now known as the minimal composite Higgs $SO(5)/SO(4)$ which has $c_T = 0$ at tree level. Indeed, applying the CCWZ formula and writing the 2-derivative Lagrangian (4.22) one finds no O_T operator. One does find other dimension six operators that provide a deviation in

$V = W, Z$ couplings to the Higgs namely:

$$k_V \equiv \frac{g_{hVV}^{CH}}{g_{hVV}^{SM}} = \sqrt{1 - \xi}, \quad \frac{g_{hhVV}^{CH}}{g_{hhVV}^{SM}} = 1 - 2\xi. \quad (4.39)$$

In fact these deviations from SM couplings provide the so-called IR contributions [297] to the electroweak parameters, S and T , on top of tree-level contributions from the strong sector vector resonances in the case of S (due to custodial symmetry there is no tree level contribution to T). Finally one also has radiative corrections from the strong sector fermionic resonances. A general analysis [298, 299] of all these contributions in the minimal composite Higgs sector points to

$$f \gtrsim 800 \text{ GeV}, \quad (4.40)$$

at the 95% CL (see [300] for an overview of the experimental constraints).

We now consider the fermionic sector in the minimal composite Higgs. Until now the discussion was common for all $SO(5)/SO(4)$ -type models. The fermion sector depends on the partial compositeness hypothesis:

$$\mathcal{L}_{PC} = \lambda_R \bar{t}_R O_L^{\mathbf{R}} + \lambda_L \bar{q}_L O_R^{\mathbf{R}'} + \text{h.c.} \quad (4.41)$$

The model dependence comes from the choice of representations \mathbf{R} and \mathbf{R}' under which the fermionic operators transform. The original MCHM used the spinorial $\mathbf{4}$ representation and is hence referred to as the MCHM₄, but was disregarded due to large correction to the $Zb\bar{b}$ vertex. Instead the choice of a fundamental $\mathbf{5}$ from [60] was more advantageous, but other representations such as the MCHM₁₀ and MCHM₁₄ have also been considered, see [66]. These distinct fermionic incarnations will lead to different deviation in Yukawa couplings from the SM prediction and can be used to constrain the breaking scale f . Global analysis [301] in Higgs physics is starting to become competitive with the ones from EWPT of $f \gtrsim 800$ GeV.

As an application of the introduced formalism in Sec. 4.1.4 we now estimate the Higgs potential for the MCHM₅. The $SO(5)$ breaking couplings from Eq. (4.41) can be made $SO(5)$ -invariant by the following spurion fields transforming as a $\mathbf{5}$ of $SO(5)$

$$\Delta_R = (0, 0, 0, 0, 1), \quad \Delta_L = \frac{1}{\sqrt{2}} \begin{pmatrix} 0 & 0 & -i & 1 & 0 \\ i & 1 & 0 & 0 & 0 \end{pmatrix}, \quad (4.42)$$

where we used the fact that a fundamental of $SO(5)$ decomposes into a bi-doublet and a singlet. After dressing both spurions with the Goldstone matrix, $U^{\mathbf{5}}$, we find objects transforming only under $SO(4)$ indices:

$$(\Delta_R^{D,4}, \Delta_R^{D,1}) \equiv U^{\mathbf{5},\dagger} \Delta_R, \quad (\Delta_L^{D,4}, \Delta_L^{D,1}) \equiv U^{\mathbf{5},\dagger} \Delta_L. \quad (4.43)$$

There are now two independent $SO(4)$ invariants that can be formed that correspond to the two Feynman diagrams of Fig. 4.1 with respectively a t_R and a doublet q_L in the loop.

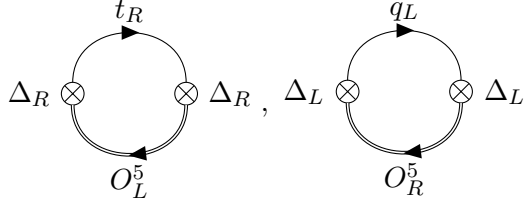


Figure 4.1: The leading contribution to the Higgs potential in the MCHM₅.

Using NDA from Eq. (4.32) for the prefactors, the leading potential is given by

$$V_2(h) = \frac{3m_*^4}{16\pi^2 g_*^2} \left(\frac{c_L}{2} \lambda_L^2 - c_R \lambda_R^2 \right) \sin^2(h/f), \quad (4.44)$$

with $c_{L/R} \sim 1$. This potential does not lead to a viable phenomenology as the only options for the minimum are $v = 0, f\frac{\pi}{2}$ whereas instead we want the option of $v < f$. The culprit is the absence of a quartic term in $\sin^4(h/f)$ at leading order in $\mathcal{O}(\lambda_{L/R}^2)$. Instead one has to expand the potential up to quartic order $\mathcal{O}(\lambda_{L/R}^4)$ in order to recover a viable functional form for the potential. Taking the contributions with four insertions of $\lambda_{L/R}$ into account we find approximately the following form for the potential

$$V(h) \approx \frac{3m_*^4}{16\pi^2 g_*^2} \left[a \lambda_t^2 \sin^2(h/f) + b \frac{\lambda_t^4}{g_*^2} \sin^4(h/f) \right], \quad (4.45)$$

with $\lambda_t = \max[\lambda_L, \lambda_R]$ and $a, b \sim 1$.

We are now in a position to understand the double-tuning problem. A viable VEV for the Higgs can now be generated from the above potential. Indeed minimization leads to the following VEV $\langle h \rangle = v$:

$$\sin^2(v/f) = \left(\frac{a}{2b} \right) \left(\frac{g_*}{\lambda_t} \right)^2. \quad (4.46)$$

In order to achieve $v \ll f$, there is unavoidable tuning between a, b known as *minimal tuning*, leading to tuning of the order of $(f/v)^2$ but there is a $(g_*/\lambda_t)^2$ enhancement of the minimal tuning due to the fact that the $\sin^4(h/f)$ term is only generated at subleading order. This tuning is known as *double-tuning*:

$$\Delta_5 \sim \left(\frac{f}{v} \right)^2 \left(\frac{g_*}{\lambda_t} \right)^2. \quad (4.47)$$

A different fermionic embedding such as the MCHM₁₄ solves this problem by generating the $\sin^4(h/f)$ term at leading order. Such a solution will eliminate the double tuning:

$$\Delta_{14} \sim \left(\frac{f}{v} \right)^2. \quad (4.48)$$

The resulting Higgs mass however will be too large due to the large quartic. Therefore a more appealing solution would be to generate the whole potential at subleading order. We will present such a solution in our next section.

We end our theoretical review on composite Higgs with the phenomenological problem of the light top partners. It comes from considering the resulting Higgs mass of the potential from Eq. (4.45):

$$m_{h,5}^2 = \frac{3}{2\pi^2} \lambda_t^4 v^2. \quad (4.49)$$

The problem of the light top partners comes from the fact that the $\lambda_{L/R}$ couplings generate the top mass and also control the mass of the lightest top resonance, the so-called *top partner* via the following relation (see for example [66]):

$$m_t \sim \frac{\lambda_L \lambda_R f}{\sqrt{2} m_{\text{partner}}} v. \quad (4.50)$$

One can substitute the λ_t dependence into Eq. (4.49), assuming $\lambda_L \sim \lambda_R$ and obtain the relation [63]:

$$m_{h,5} \sim \frac{\sqrt{3}}{\pi} \frac{m_{\text{partner}}}{f} m_t. \quad (4.51)$$

We see that a light Higgs boson requires light top partners to be found at the LHC. This connection was first noted in [60] and subsequently studied in [61–63, 65, 66, 302–305]. This should not come as a surprise as the top partner mass determines the strength with which the Higgs couples to the top through Eq.(4.50) and thus the size of the top loop contribution to the Higgs mass.

4.3 A Natural Composite Higgs

After this review on composite Higgs, we now come to a novel solution to the double-tuning problem. As we have seen, traditional incarnations of composite Higgs usually suffer from the issue of double-tuning meaning the quadratic contribution is generated at leading order, while the quartic of the Higgs is generated at subleading order. Symbolically one can write this using NDA as

$$V(h) \sim \lambda^2 h^2 + \lambda^2 (\lambda^2/g_*)^2 h^4, \quad (4.52)$$

with g_* the typical coupling of the strong sector and λ denotes here a generic G -breaking coupling between the elementary and strong sector. Since $\lambda < g_*$, we find the quadratic term to be much larger than the quartic, resulting in a badly tuned potential.

4.3.1 Mirror Fermions

Here we will investigate a solution to generate both the quadratic and quartic at subleading order $\mathcal{O}(\lambda^4)$. This can be done by using *mirror fermions*. The mechanism relies on the following property of some particular cosets G/H and particular representations \mathbf{R} of G

Mirror Fermions: *The quadratic contribution of a chiral fermion, ψ , to the pNGB potential of a coset G/H can be cancelled, at the price of a new massless conjugate fermion which we call the mirror fermion, ψ' , if the fermion ψ talks to a composite operator transforming under a representation \mathbf{R} of the group G*

$$\mathcal{L} = \lambda \bar{\psi} O^{\mathbf{R}} + h.c. \quad (4.53)$$

such that it decomposes in subrepresentations of H in the following way

$$\mathbf{R} = \mathbf{C} \oplus \bar{\mathbf{C}}, \quad (4.54)$$

with \mathbf{C} a representation of H and $\bar{\mathbf{C}}$ its complex conjugate. The cancellation occurs whenever the conjugate mirror fermion ψ' connects to the same fermionic operator $O^{\mathbf{R}}$

$$\mathcal{L} = \lambda \bar{\psi}' O^{\mathbf{R}} + h.c. \quad (4.55)$$

As the statement suggests, the cancellation is only exact when the mirror fermion becomes massless. In concrete models one will have to make the chiral mirror fermion massive by introducing its opposite chirality and giving a Dirac mass to the mirror fermion. Also note that the above Eq. (4.54) implies that \mathbf{R} is a real representation of G . The most minimal example of a representation satisfying the above is for the non-custodial coset $SU(6)/SU(5)$ and the fermion representation $\mathbf{20}$. Indeed the latter decomposes as

$$\mathbf{20} \rightarrow \mathbf{10} \oplus \bar{\mathbf{10}}, \quad (4.56)$$

under $SU(5)$. More interestingly, the statement also applies to the custodially symmetry coset $SO(11)/SO(10)$ and the fermion representation $\mathbf{32}$ which decomposes as:

$$\mathbf{32} \rightarrow \mathbf{16} \oplus \bar{\mathbf{16}}. \quad (4.57)$$

Before delving into the consequences of the statement, we prove it in full generality. We consider a strongly coupled sector with a spontaneously broken symmetry based on the coset G/H and a chiral fermion ψ , in a representation or subrepresentation of H , that talks to an strong sector operator $O^{\mathbf{R}}$, transforming under a representation \mathbf{R} of G

$$\mathcal{L}_{\text{PC}} \supset \lambda \bar{\psi} \Delta O^{\mathbf{R}} + h.c., \quad (4.58)$$

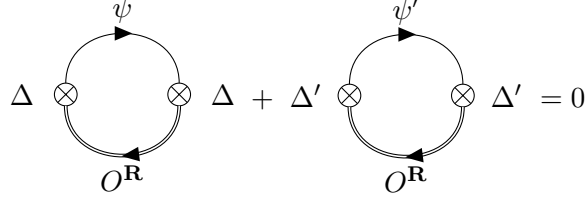


Figure 4.2: Cancellation mechanism of the leading contribution to the pNGB potential in terms of Feynman diagrams.

where we wrote the above in terms of a spurion Δ :

$$\Delta^i = \begin{cases} \Delta^{\{\alpha\}} = 1, \\ \Delta^{i \setminus \{\alpha\}} = 0, \end{cases} \quad (4.59)$$

where we indicate with i an index transforming according to the representation \mathbf{R} in G while $\alpha/\dot{\alpha}$ indicates an index transforming according to the rep $\mathbf{C}/\bar{\mathbf{C}}$ in H and $\{\alpha\}$ indicates the indices corresponding to the representation or subrepresentation in which ψ is embedded. In all cases we will consider ψ is strictly embedded within \mathbf{C} and thus $\{\alpha\} \subset \alpha$. The leading contribution in terms of a Feynman diagram can be read of on the left Fig. 4.2. Let us now see how we can cancel it by introducing a chiral exotic fermion ψ' of *opposite* quantum numbers within the complex conjugate representation of $\bar{\mathbf{C}}$ of H which we couple to the same operator $O^{\mathbf{R}}$. We thus extend the partial compositeness Lagrangian of Eq. (4.58) to the following:

$$\mathcal{L}_{\text{PC}} = \lambda \bar{\psi} \Delta O^{\mathbf{R}} + \lambda' \bar{\psi}' \Delta' O^{\mathbf{R}} + \text{h.c.} \quad (4.60)$$

We will assume that one can use the global symmetry G to impose $\lambda = \lambda'$. We now have a second spurion for the exotic reading

$$\Delta'^i = \begin{cases} \Delta'^{i \setminus \{\dot{\alpha}\}} = 0, \\ \Delta'^{\{\dot{\alpha}\}} = 1, \end{cases} \quad (4.61)$$

which will contribute to quadratic order in terms of the right Feynman diagram of Fig. 4.2.

We note that both fermions, ψ and ψ' couple to the exact same operator on the composite side, namely $O^{\mathbf{R}}$. However due to the particular embedding of ψ and ψ' within the representation respectively \mathbf{C} and $\bar{\mathbf{C}}$ of H they come with exact opposite sign and the quadratic contribution exactly cancels as shown diagrammatically in Fig. 4.2. In order to prove the statement we calculate the contributions to the potential. For this we need to act on the spurions, $\Delta^{(\prime)}$, with the inverse Goldstone matrix, here for convenience denoted with $U^{\mathbf{R}}$,

transforming in the suitable representation \mathbf{R} of G . The dressed spurions, $\Delta_D^{(\prime)}$, split into representations of H , in our case \mathbf{C} and $\bar{\mathbf{C}}$:

$$\begin{aligned}(\Delta_D^{\mathbf{C}}, \Delta_D^{\bar{\mathbf{C}}}) &\equiv (U^{\mathbf{R}})\Delta, \\(\Delta_D^{\prime\mathbf{C}}, \Delta_D^{\prime\bar{\mathbf{C}}}) &\equiv (U^{\mathbf{R}})\Delta'.\end{aligned}\tag{4.62}$$

We first calculate the contribution that flows through the \mathbf{C} component of the $O^{\mathbf{R}}$ composite operator (the $\bar{\mathbf{C}}$ case is fully analogous):

$$V_I = (\Delta_D^{\mathbf{C}})^\dagger \Delta_D^{\mathbf{C}} + (\Delta_D^{\prime\mathbf{C}})^\dagger \Delta_D^{\prime\mathbf{C}}.\tag{4.63}$$

One can simplify the above expression reverting back to indices. The above then becomes

$$V_I = \lambda^2 \psi_j (U^{\mathbf{R}, -1})_\alpha^j (U^{\mathbf{R}})_i^\alpha \psi^i + \lambda'^2 \psi'_j (U^{\mathbf{R}, -1})_\alpha^j (U^{\mathbf{R}})_i^\alpha \psi'^i,\tag{4.64}$$

exploiting the G symmetry $\lambda = \lambda'$, one finds:

$$V_I = \lambda^2 (\psi_j (U^{\mathbf{R}, -1})_\alpha^j (U^{\mathbf{R}})_i^\alpha \psi^i + \psi'_j (U^{\mathbf{R}, -1})_\alpha^j (U^{\mathbf{R}})_i^\alpha \psi'^i).\tag{4.65}$$

Together, both expression span a larger set of indices. Indeed one arrives at the following

$$V_I = \lambda^2 (\Psi_j (U^{\mathbf{R}, -1})_\alpha^j (U^{\mathbf{R}})_i^\alpha \Psi^i),\tag{4.66}$$

where Ψ is non-zero for both $\{\alpha\}$ and $\{\dot{\alpha}\}$:

$$\Psi^i = \begin{cases} \psi^{\{\alpha\}} = 1, \\ \psi^{\{\dot{\alpha}\}} = 1. \end{cases}\tag{4.67}$$

Consider now the closely related expression V_{II} with dotted α :

$$V_{II} = \lambda^2 (\Psi_j (U^{\mathbf{R}, -1})_\alpha^j (U^{\mathbf{R}})_i^{\dot{\alpha}} \Psi^i).\tag{4.68}$$

If we sum both expressions we can get rid of the Goldstone dependence finding

$$V_I + V_{II} = \lambda^2 (\Psi_j (U^{\mathbf{R}, -1})_\alpha^j (U^{\mathbf{R}})_i^k \Psi^i) = \lambda^2 (\Psi_j \delta_i^j \Psi^i) = \lambda^2 (2N),\tag{4.69}$$

with $N \equiv \#\{\alpha\}$, the dimensionality of the representation of ψ/ψ' . Moreover $V_I = V_{II}$, since the upper $\dot{\alpha}$ indices in V_{II} can be exchange for lower undotted α indices (remember that α denote indices in the \mathbf{C} representation while $\dot{\alpha}$ are indices in its conjugate representation $\bar{\mathbf{C}}$):

$$\begin{aligned}V_{II} &= \lambda^2 (\Psi_j (U^{\mathbf{R}, -1})_\alpha^j (U^{\mathbf{R}})_i^{\dot{\alpha}} \Psi^i) = \lambda^2 (\Psi_j (U^{\mathbf{R}, -1})^{j, \alpha} (U^{\mathbf{R}})_{\alpha, i} \Psi^i) \\ &= \lambda^2 (\Psi_j (U^{\mathbf{R}, -1})_\alpha^j (U^{\mathbf{R}})_i^\alpha \Psi^i) \\ &= V_I.\end{aligned}\tag{4.70}$$

$$\Delta + \Delta' = \mathcal{O}\left(\left(\frac{m_E}{m_*}\right)^2\right)$$

Figure 4.3: Cancellation mechanism of the leading pNGB potential in terms of Feynman diagrams in the presence of a Dirac mass for the exotic.

We therefore come to the conclusion that V_I is independent of the Goldstone and that its contribution consists only of the vacuum energy proportional to the number of fermionic degrees of freedom:

$$V_I = \lambda^2 N. \quad (4.71)$$

This ends to proof of the statement. Moreover the proof provides the recipe to generically cancel the quadratic contribution of any chiral fermion at the price of introducing a new exotic chiral fermion. Since this will in general introduce an unwanted massless fermion in the spectrum, an essential feature of this mechanism is the introduction of a chiral partner for the exotic and a Dirac mass, m_E :

$$\mathcal{L}_{\text{mass}} = m_E \bar{\psi}' \psi'. \quad (4.72)$$

In our envisaged setup the chiral partner of the exotic does not talk to the composite sector as it would spoil the mechanism² and the cancellation is on the order of $\mathcal{O}((m_E/m_*)^2)$. In terms of Feynman diagrams the cancellation of Fig. 4.2 is modified in realistic models into Fig. 4.3.

If one wishes to implement the above described cancellation mechanism in a realistic model one is directly lead to models in which the whole SM is part of a single simple group G , including color. This departs from usual composite Higgs model building where color is considered an external gauge group such as the minimal composite Higgs. Indeed, including color is not necessary as the coset G/H should minimally only include a Higgs pNGB and no other colored pNGB. Including color will result in additional (colored) pNGB besides the Higgs and is the area of composite GUT [306]. The smallest group of composite Higgs in which color is included is based on the coset $G/H = SU(6)/SU(5)$. Indeed as is well known and exploited by 4D grand unified theories, $G_{\text{SM}} \subset SU(5)$.

²If the chiral partner does talk to the composite sector there will be a new type of Feynman diagram connecting LH to RH spurions since the vector-like mass can provide a flipping of chirality whose overall contributions goes as m_E/m_* which could still be quite suppressed. However, there will be new quadratic contributions from the chiral partner of the exotic that remain uncancelled, defeating the whole mechanism.

Conveniently the $\mathbf{20}$, a pseudo-real representation of $SU(6)$, decomposes into the following under $SU(5)$:

$$\mathbf{20} = \mathbf{10} \oplus \bar{\mathbf{10}}. \quad (4.73)$$

Moving to a custodially symmetric case, we can choose the minimal coset $G/H = SO(11)/SO(10)$ for which the pseudo-real representation $\mathbf{32}$ decomposes into the following under $SO(10)$:

$$\mathbf{32} = \mathbf{16} \oplus \bar{\mathbf{16}}. \quad (4.74)$$

Also crucially, both of these cases permit the embedding of the right-handed top and the left-handed quark doublet which due to the large top mass are the most important contribution to the Higgs potential. Indeed, the $\mathbf{10}$ of $SU(5)$ decomposes under G_{SM} as follows

$$\mathbf{10} = (\mathbf{3}, \mathbf{2})_{1/6} \oplus (\mathbf{3}^*, \mathbf{1})_{-2/3} \oplus (\mathbf{1}, \mathbf{1})_1, \quad (4.75)$$

and the $\mathbf{16}$ contains a $\mathbf{10}$. In what follows, we will have in mind the custodial coset $SO(11)/SO(10)$ as it allows the model to have a low breaking scale f while still be allowed by EWPT. Moreover due to the identical fermion embedding in both of these cases, entirely dictated by the property of $\mathbf{R} = \mathbf{C} \oplus \bar{\mathbf{C}}$, the numerical results we will discuss in multi-site models are identical. The gauge sector will differ but its contribution to the Higgs potential is subleading and we will therefore not include it in our analysis.

Since we are considering extended cosets, there are other pNGBs included in the spectrum. Both $SU(6)/SU(5)$ and $SO(11)/SO(10)$ contain nearly identical pNGBs that decompose under G_{SM} as

$$G/H = (\mathbf{3}, \mathbf{1})_{-1/3} \oplus (\mathbf{1}, \mathbf{2})_{1/2}, \quad (4.76)$$

with the $SU(6)/SU(5)$ containing an additional singlet which remains massless since its generator corresponds to an unbroken global symmetry³. The scalar leptoquark, S , will get a large positive mass⁴ from the gauge sector estimated as

$$V(S) = m_*^4 \frac{3 \times 5 g_s^2}{64\pi^2 g_*^2} \sin^2(S/f), \quad (4.77)$$

where we include the 3×5 degrees of freedom coming from the 5 gluons that become heavy once the leptoquark gets a VEV, breaking color and charge to $SU(3)_c \times U(1)_Y \rightarrow SU(2) \times U(1)$. The resulting mass for the leptoquark is then $m_S = (15\alpha_s/8\pi)^{1/2} m_* \approx 0.25 m_*$. The fermion sector contribution to the leptoquark pNGB potential will be cancelled in exactly the same way due to the mirror fermion mechanism.

³The mass of the singlet for the non-custodial coset $SU(6)/SU(5)$ can be easily lifted by breaking this symmetry for example with a Majorana neutrino sector.

⁴Gauge bosons always tend to stabilize the potential [307].

4.3.2 A Model

We now come to the description of a model that implements the above mirror fermion cancellation mechanism. We will only be interested in cancelling the quadratic contributions to the Higgs potential from the q_L and the t_R as they are the largest due to the large top mass. The mirror fermion mechanism requires the introductions of mirror fermions which we call θ_L and ω_R . We note that these mirror fermions will end up mass mixing after EWSB. For the phenomenology of the model, we will be mainly interested in the lightest mass eigenstate mirror fermion, which we will call the *exotic*. In the following, we will use both the term mirror fermion and the term exotic, with the former emphasizing the cancellation mechanism and the latter emphasizing the phenomenology. Applying the results of the previous section we come to the following partial compositeness Lagrangian

$$\mathcal{L}_{\text{PC}} = \lambda_L(\bar{q}_L + \bar{\theta}_L)O_{\mathbf{R}}^{\mathbf{R}} + \lambda_R(\bar{t}_R + \bar{\omega}_R)O_{\mathbf{L}}^{\mathbf{R}} + \text{h.c.} + m_\theta\bar{\theta}\theta + m_\omega\bar{\omega}\omega, \quad (4.78)$$

where $O_{L/R}^{\mathbf{R}}$ is a left-/right-handed operator from the composite sector in the representation \mathbf{R} . As the cancellation between q_L and θ_L occurs separately from the cancellation between t_R and ω_R , it is not a requirement that the chiral operators $O_{L/R}^{\mathbf{R}}$ come from a Dirac operator (although we will later assume so). Since q_L and θ_L couple to the same operator $O_{\mathbf{R}}^{\mathbf{R}}$, it is natural for the coefficients of these interactions, λ_L , to be identical, controlled by the scaling dimension d_R of the operator $O_{\mathbf{R}}^{\mathbf{R}}$. Indeed we expect these coefficients in the IR to be

$$\lambda_L \sim \lambda_L(\Lambda_{\text{UV}}) \left(\frac{\Lambda_{\text{IR}}}{\Lambda_{\text{UV}}} \right)^{d_R - 5/2}, \quad (4.79)$$

with $\lambda_L(\Lambda_{\text{UV}})$ their value in the UV which is assumed to be equal by the global G symmetry. Fully analogously, the λ_R coefficient is determined by the scaling dimension d_L of the operator $O_{\mathbf{L}}^{\mathbf{R}}$ and is therefore identical for t_R and ω_R .

Up to now the discussion was fully general and would apply to any model implementing the mirror fermion mechanism. One can make an extra assumption on the strong sector of parity symmetry. In that case the two operators $O_{L/R}^{\mathbf{R}}$ do not have to be independent but can come from the same Dirac operator which would make the two scaling dimensions equal implying furthermore that $\lambda_L = \lambda_R$. In that case, all four partial compositeness interactions of Eq. (4.78) are determined by a single parameter λ .

In order to fully specify the third generation quark sector ⁵, we will also describe the connection of the right-handed bottom quark b_R to a representation \mathbf{R}' of G . In case of the $SU(6)/SU(5)$ the natural choice for \mathbf{R}' is the $\mathbf{15}$ of

⁵The first and second generation can be modelled in a similar fashion, however due to their small interaction strength with the composite sector, their contribution to the potential is less problematic.

$SU(6)$ as it includes a b_R , while for the $SO(11)/SO(10)$ coset the natural choice for \mathbf{R}' is a $\mathbf{32}$ of $SO(11)$:

$$\mathcal{L}_{\text{PC},b_R} = \lambda_b \bar{b}_R O_L^{\mathbf{R}'} + \text{h.c.} \quad (4.80)$$

Once G is spontaneously broken to H , the operator $O_L^{\mathbf{R}'}$ mixes with $O_R^{\mathbf{R}}$ and the bottom acquires a mass. This statement relies on the fact that the representation \mathbf{R}' to which b_R talks decomposes under H as follows

$$\mathbf{R}' = \mathbf{C} \oplus \dots, \quad (4.81)$$

and therefore the \mathbf{C} subrepresentation of $O_L^{\mathbf{R}'}$ and $O_R^{\mathbf{R}}$ can indeed connect. This is the case for both of our considered scenarios since $\mathbf{15} = \mathbf{10} \oplus \mathbf{5}$ and $\mathbf{32} = \mathbf{16} \oplus \bar{\mathbf{16}}$.

Having specified the partial compositeness hypothesis of the quarks, one can now analyse the model in a three-site model as described in [286] (see also [287]). Three sites is the minimal amount of *sites* in order for the Higgs potential to be fully calculable. These models are inspired by dimensional deconstruction of the fifth dimension in which the fifth dimension is discretized on different points [280, 281]. We provide in Appendix C the full three-site Lagrangian and the resulting mass matrix for the top $M_T(h)$ and exotic $M_E(h)$ and its associated strong sector resonances. Employing the CW formula [308] one can compute the resulting radiative potential

$$V_i(h) = -\frac{4N_c}{16\pi^2} \int_0^\infty dp p^3 \log \left(\det[M_i^\dagger(h)M_i(h) + p^2] \right), \quad (4.82)$$

with $i = T, E$. It is convenient to express the determinant as follows

$$\det[M_i^\dagger(h)M_i(h) + p^2] = 1 + a_i(p^2) \sin^2(h/f) + b_i(p^2) \sin^4(h/f), \quad (4.83)$$

where $a_i(p^2), b_i(p^2)$ depend on all the parameters of the model. Expanding the logarithm, one finds

$$V_i(h) \approx \alpha_i \sin^2(h/f) + \beta_i \sin^4(h/f), \quad (4.84)$$

with

$$\begin{aligned} \alpha_i &= -\frac{4N_c}{16\pi^2} \int_0^\infty dp p^3 a_i(p^2) \\ \beta_i &= -\frac{4N_c}{16\pi^2} \int_0^\infty dp p^3 (b_i(p^2) - a_i^2(p^2)/2). \end{aligned} \quad (4.85)$$

Summing up the contributions from the top and exotic sector as $\alpha = \alpha_T + \alpha_E$ and $\beta = \beta_T + \beta_E$, the resulting VEV $\langle h \rangle = v$ and Higgs mass m_h then follows:

$$\sin(v/f)^2 = \frac{-\alpha}{2\beta}, \quad m_h^2 = 8\beta/f^2 \sin^2(v/f). \quad (4.86)$$

One can explicitly check that the mirror fermion mechanism is at work in the three-site model. Indeed, α is now generated at fourth order in $\lambda_{L/R}$ in the limit of small exotic Dirac masses

$$\frac{\partial^2 \alpha}{\partial^2 \lambda_{L/R}} \Big|_{m_\omega, m_\theta \rightarrow 0} = \frac{\partial^2 \alpha_E}{\partial^2 \lambda_{L/R}} \Big|_{m_\omega, m_\theta \rightarrow 0} + \frac{\partial^2 \alpha_T}{\partial^2 \lambda_{L/R}} = 0, \quad (4.87)$$

as one has an exact cancellation between the leading contribution to the Higgs potential of top and the exotic for both λ_L and λ_R .

4.3.3 Naive Dimensional Analysis

Before giving quantitative results from the three-site model, we give a naive dimensional analysis [270,271] (NDA) of the model. By modeling the composite sector with a single fermionic mass scale $m_* = g_* f$ with a strong coupling $1 < g_* < 4\pi$ one gets the following estimate for both α, β , using the results from Sec. 4.1.4:

$$\alpha, \beta \sim \frac{N_c}{16\pi^2} \lambda_{L/R}^4 f^4. \quad (4.88)$$

Since both are generated at the same order we find a minimal tuning of:

$$\Delta_{\text{mirror}} = \frac{1}{\xi}. \quad (4.89)$$

The resulting Higgs mass estimate reads

$$m_{h, \text{mirror}}^2 \sim \frac{N_c}{2\pi^2} \lambda_{L/R}^4 v^2 \sim \frac{N_c}{2\pi^2} g_*^2 v^2 \sim \left((500(g_*/5) \text{ GeV})^2 \right), \quad (4.90)$$

where in the second step we use that $(\lambda_L \lambda_R)/g_* \sim y_t$ in order to obtain the correct top mass. We now compare this to the other known minimally tuned model, the MCHM₁₄ where both the quadratic and quartic of the Higgs potential are generated at the quadratic level. The prediction for the Higgs mass is [303]

$$m_{h, 14+14}^2 \sim \frac{N_c}{2\pi^2} \lambda_{L/R}^2 g_*^2 v^2 \sim \frac{N_c}{2\pi^2} g_*^3 v^2 \sim \left(1000(g_*/5)^{3/2} \text{ GeV} \right)^2, \quad (4.91)$$

where we use the same approximation in the second step. The resulting Higgs mass in the mirror fermion scenario is much more advantageous since the potential is fully generated at the subleading level. This results in the Higgs mass being only linearly sensitive to the strong coupling g_* in contrast to the $g_*^{3/2}$ in the case of the MCHM₁₄. Furthermore, the Higgs mass is also predicted to be lighter in (4.90). There is a caveat though, which is that for the MCHM₁₄ one can make the RH top completely composite $\lambda_R \sim g_*$ meaning it is part of the strong sector and doesn't contribute to the Higgs potential. In that case one

can take in the above equation $\lambda_{L/R} = \lambda_L \sim y_t$ and the resulting Higgs mass estimate becomes identical to the mirror fermion case:

$$m_{h,14+1}^2 = m_{h,\text{mirror}}^2. \quad (4.92)$$

Therefore, even though the potential is generated at the subleading order, the resulting Higgs mass prediction is of same order as the in the MCHM₁₄₊₁ with a composite t_R .

From the above analysis in the mirror fermion model, one expects indeed a model with minimal tuning. Furthermore, a light Higgs $m_h = 125$ GeV generally requires a small g_* which also implies the presence of light top partners. Lastly, for the cancellation of the quadratic to occur, one expects $m_{\theta,\omega}$ to be small and therefore light exotics. We will now investigate whether these naive estimates are in agreement with the results of the three-site model.

4.3.4 Numerical Results

For the numerical results we scan all the mass parameters in the three-site model (see Appendix C) over $m \in [-5f, +5f]$ for a symmetry breaking scale $f = 1600$ GeV. Moreover we take $\lambda \equiv \lambda_L = \lambda_R$ under the assumption of a parity symmetric strong sector. The results for a general $\lambda_L \neq \lambda_R$ are similar. We fix the partial compositeness λ to reproduce the correct top mass m_t and filter out the points that do not give a correct electroweak scale of $v = 246$ GeV.

The spectrum of resonances in the model is shown in Fig. 4.4 where the mass of the lightest top partner, m_T^{min} , and the lightest exotic, m_E^{min} , as a function of the Higgs mass is shown. From various LHC searches [40–44], the bound on the top partners has reached an impressive $\gtrsim 1500$ GeV which we denote by the red coloring. While a generous region for the correct Higgs mass, $90 \text{ GeV} < m_h < 130 \text{ GeV}$, is shaded blue. Unsurprisingly, the issue of the light top partners is therefore not solved in this setup. Indeed we take $f = 1600$ GeV in order to have the top partner sufficiently heavy for a light Higgs mass. As we discuss in the next section, due to the unconventional decay signature of the exotic, we do not place a bound on its mass.

Having studied the spectrum of the resonances as a function of the Higgs mass, we now select the points with the correct Higgs mass and turn to the study of the tuning. We use the Barbieri-Guidice measure [309, 310], $\Delta_{\text{BG}}(O)$ which measures the dependence of an observable $O(p_i)$, with respect to the parameters, p_i of the theory:

$$\Delta_{\text{BG}}(O) = \max \left| \frac{\partial \log O(p_i)}{\partial \log p_i} \right|. \quad (4.93)$$

The study of tuning in the Higgs potential usually uses the Z -boson mass, or equivalently, the Higgs VEV as an observable which is a combination of the quadratic and the quartic of the potential. In order to have a conservative

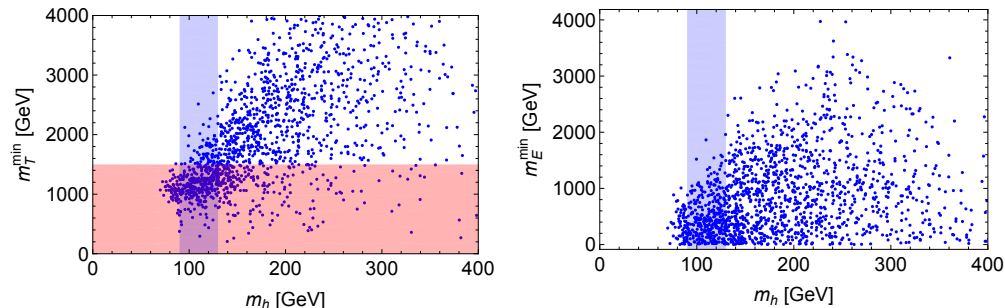


Figure 4.4: The mass of the lightest top partner (left) and the mass of the lightest exotic (right) as a function of the Higgs mass, m_h in the three-site model for $f = 1600$ GeV. The approximate bound on top partners is indicated in red $m > 1500$ GeV, while the correct Higgs mass is indicated in blue $90 \text{ GeV} < m_h < 130 \text{ GeV}$.

estimate of the tuning, we will also study the tuning in the quadratic alone, or equivalently the Higgs mass, and take the maximum of both tunings:

$$\Delta_{\text{BG}} = \max(\Delta_{\text{BG}}(v^2), \Delta_{\text{BG}}(m_H^2)). \quad (4.94)$$

As discussed, in models of composite Higgs the naive minimal fine-tuning, assuming no double-fine tuning is present, is expected to be $\Delta \sim 1/\xi$. For our benchmark of $f = 1600$ GeV we expect therefore $\Delta \sim 42$. The results are shown in Fig. 4.5. On the left side we plot the lightest top partner as a function of the tuning Δ and we note that the tuning is independent of the top partner spectrum. However most points are clustered decidedly under the minimal tuning around $\Delta_{\text{BG}} \sim 20$ and some points even lower around $\Delta_{\text{BG}} \sim 10$. Therefore not only is there no issue of double-fine tuning, the cancellation of the quadratic due to the mirror fermions has softened the tuning seemingly more and one finds viable points with heavy top partners and a correct Higgs for very little tuning of $\Delta_{\text{BG}} \sim 10$ while having a large symmetry breaking scale of $f = 1600$ GeV. The *cost* of this drastic reduction is of course the additional exotic that is quite light. On the right side of Fig. 4.5 we plot the correlation between the top partner and the exotic and we observe that the following bound, colored in red, is obeyed:

$$m_E^{\text{min}} \lesssim m_T^{\text{min}}. \quad (4.95)$$

Therefore the exotics become a very attractive target for collider searches as they are quite a bit lighter than the top partners. However no current searches exist for resonances with these decay channels as we discuss in the next section.

4.3.5 Phenomenology of the Exotic

We now come to a discussion of the exotic, a crucial aspect in the cancellation mechanism. Indeed, the obtained drastic reduction in fine-tuning comes at the

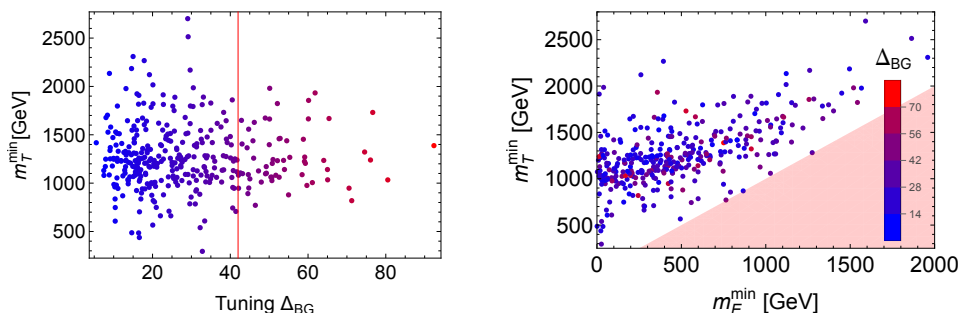


Figure 4.5: Top partner mass as a function of the fine-tuning (left) and as a function of the exotic mass (right). The minimal expected tuning, $\Delta \sim 1/\xi \sim 42$ is indicated on the left panel by the red line.

price of these light mirror fermions or exotics. It becomes important to determine possible bounds on their mass. In both considered incarnations of the model, the coset $SO(11)/SO(10)$ and the coset $SU(6)/SU(5)$, there is a global symmetry that corresponds to baryon number for the SM fermions, while the exotic fermions get unconventional baryon numbers charge of $B = 2/3$ (see [2,3] for example for the $SU(6)/SU(5)$ case). It is a very convenient feature of composite GUTs (and equally of models of gauge-Higgs grand unification) that they have a global baryon number and therefore the proton, being the lightest charged particle under baryon number, remains absolutely stable.⁶ The presence of a conserved baryon number in these composite GUT type models is a consequence of the imperfect unification of SM fermions in complete GUT representations. Indeed, the incomplete filling of SM fermions into representations of G of the strong sector, is what allows baryon number to be conserved. In contrast in 4D GUTs, a generation of fermions fits perfectly into a $\mathbf{16}(\mathbf{10} \oplus \mathbf{5} \oplus \mathbf{1})$ of $SO(10)(SU(5))$ which is too constraining for defining a global baryon number.

In order to discuss the decay channel of the exotic, one should also discuss the other pNGB besides the Higgs, which is the leptoquark with quantum numbers $(\mathbf{3}, \mathbf{1})_{-1/3}$ with baryon number $1/3$. Since the bounds on such a leptoquark, with decays into $t\tau$, are quite high at $m_E^{\min} > 1.4$ TeV [251] it is safe to assume for this analysis that $m_{\text{exotic}} < m_S$. The allowed decay of the exotic therefore proceeds through on off-shell S namely, $E \rightarrow Sb$ or through an off-shell $X^{-4/3}/Y^{-1/3}$ vector resonance of the composite sector, $E \rightarrow X^{-4/3}t, Y^{-1/3}b$. While the decays of $X^{-4/3}$ and $Y^{-1/3}$ proceed through third generation quarks and leptons, namely $X^{-4/3} \rightarrow b\tau$ and $Y^{-1/3} \rightarrow t\tau/b\nu$. In total this results in two different final states for the exotic fermion namely $E \rightarrow tb\tau$ and $E \rightarrow bb\nu$. The latter decay is suppressed by the bottom mass with respect to the first decay. QCD double production of the exotic will

⁶However such a global baryon number is not protected from higher dimensional operators suppressed by merely the compositeness scale m_* . It therefore becomes necessary to gauge the baryon number, see [166,311].

therefore result in the following spectacular final state $E\bar{E} \rightarrow tb\tau\bar{t}\bar{b}\bar{\tau}$ which has no dedicated search at the LHC. However due to the very unique signatures, we expect the bounds on such exotics to be very strong when such an analysis is done.

4.3.6 The Holographic 5D Dual

The possible UV completions we envisage are necessarily holographic as the cosets $SU(6)/SU(5)$ and $SO(11)/SO(10)$ are not realizable as fermion flavor symmetries that are spontaneously broken by the formation of a fermion condensate. As we discussed in section 4.1.5, the holographic dual of models of composite Higgs is formulated on a slice of a five-dimensional warped space with a UV brane at $z = R$, presumably at the Planck scale, and an IR brane at $z = R'$ around the scale of symmetry breaking f . The warped metric corresponds to the following ansatz:

$$ds^2 = \left(\frac{R}{z}\right)^2 (\eta_{\mu\nu} dx^\mu dx^\nu - dz^2). \quad (4.96)$$

The pNGB Higgs corresponds to the fifth component of the higher dimensional bulk gauge field of G , which is broken by boundary conditions on the IR brane to the group H . As also discussed, the partial compositeness hypothesis corresponds to embedding the SM fermions into 5D bulk fermions of representation \mathbf{R} with a certain 5D mass.

In the case that $\lambda_L \neq \lambda_R$ and thus the couplings represent two different parameters, the corresponding holographic implementations would be to embed q_L, θ_L and t_R, ω_R in two different 5D bulk fermions of representation \mathbf{R} with different 5D masses representing the different scalings and thus resulting in different λ_L, λ_R . In the case that $\lambda_L = \lambda_R$, one would ideally want to embed all fermions into the same 5D bulk fermion with a unique 5D mass. This is however not possible since one cannot embed all four chiral fermions within a single bulk fermion of representation \mathbf{R} as the necessary boundary conditions would break the H symmetry on the IR brane. Instead one would still have to use two bulk fermions with presumably a discrete symmetry between them such that they have the same bulk mass.

Another intriguing aspect of the holographic dual concerns the Dirac masses $m_{\theta,\omega}$ necessary to give a mass to the otherwise massless exotics. In the 4D formulation, the origin of these Dirac masses remains unclear. Indeed, one wishes to have $m_{\theta,\omega} \lesssim m_*$ in order for the cancellation of the quadratic to occur, but since these Dirac masses are in the elementary sector and thus not connected to the composite sector, there is no reason for this inequality to be obeyed. Although such a small Dirac mass does not introduce a hierarchy problem as a small Higgs mass does⁷, it does introduce a so-called *coincidence*

⁷Radiative corrections to Dirac masses are proportional to its tree level value due to chiral symmetry and thus technically natural.

problem. In the holographic dual these light Dirac mass have a very elegant origin. Indeed in the holographic dual, the Dirac mass, m_ω , (the m_θ case is analogous) corresponds to a brane mass on the UV brane that mixes the bulk 5D fermion containing the $\omega_R(x, z)$ and its chiral partner $\omega_L(x)$ that is localized on the UV brane

$$\mathcal{L}_{UV} = \int d^4x \frac{M_{UV}}{\sqrt{R}} \bar{\omega}_L(x) \omega_R(x, z = R) + \text{h.c.}, \quad (4.97)$$

with $M_{UV} \sim \mathcal{O}(1)$. This provides indeed the required 4D mass, m_ω , but to estimate its size we require the value of $\omega_R(x, z = R)$ on the UV brane which depends on the 5D mass of the bulk fermion, $m \equiv c/R$, where we use the dimensionless c . There are two regimes depending on whether the $\omega_R(x, z)$ is UV ($c > 0.5$) or IR localized ($c < 0.5$):

$$m_\omega \sim \begin{cases} M_{UV}/R & (c > 0.5) \\ M_{UV}/\sqrt{RR'} (R'/R)^c (-c + 1) & (c < 0.5) \end{cases}. \quad (4.98)$$

Unsurprisingly, for a UV localized fermion the Dirac mass is naturally of the order of the UV scale, but for a IR localized fermion its mass is exponentially suppressed and can become easily at or below the composite scale. Furthermore, since these exotics have equal localizations as the top (indeed the cancellation mechanism requires this), they will be naturally IR localized just as the top.

4.4 Summary

After an overview of the different aspects involved in composite Higgs model building in Sec. 4.1, we provided an illustration of these aspects by working out the minimal composite Higgs based on the coset $SO(5)/SO(4)$ in Sec. 4.2. Although an extremely appealing and minimal model, null results from searches at the LHC for the light top partners have driven these models into more fine-tuned regions. The problem of double-tuning that these models suffer from worsens the required fine-tuning.

In Sec. 4.3 we have proposed a novel solution to these problems by cancelling the leading contribution to the Higgs potential in the fermion sector with the use of mirror fermions. Although such a cancellation seems similar to the mechanism of twin Higgs, and also its application to composite Higgs (see [47–49]), no discrete symmetry is required or doubling of the whole SM content. Instead, the mechanism relies on the particular properties of some real representations \mathbf{R} that decompose into a complex representation \mathbf{C} and its complex conjugate $\bar{\mathbf{C}}$ according to

$$\mathbf{R} = \mathbf{C} \oplus \bar{\mathbf{C}}. \quad (4.99)$$

The leading order contribution of the mirror fermion to the potential comes with exactly opposite sign and the total leading order potential is therefore cancelled.

We then studied possible incarnations of this mechanism based on the cosets $SU(6)/SU(5)$ and $SO(11)/SO(10)$. Especially the latter is a promising coset as it contains a custodial symmetry which allows the symmetry breaking scale to be low and still agree with EWPT. We then analysed the model in a three-site model studying the spectrum, the Higgs mass and the resulting tuning. The results are quite remarkable, for a large symmetry breaking scale $f = 1600$ GeV, we achieve to have a correct Higgs mass with minimal tuning $\Delta \sim 10 - 20$ and sufficiently heavy top partners, whereas generic composite Higgs models predict $\Delta > 40$.

Our model is to be compared with other recent proposals aimed at addressing the mentioned ubiquitous problems of composite Higgs. For example the idea of breaking the Goldstone symmetry *softly* [312] (see [313] for the holographic 5D implementation) works by augmenting the elementary fermions into complete representations of the group G , such that partial compositeness interactions do not violate the G -symmetry. Instead the explicit breaking of G comes from the Dirac masses necessary to make the additional elementary fermions heavy. Such sequestering of the breaking of the Goldstone symmetry has the exciting consequence of making the top partners heavier in comparison to standard composite Higgs scenarios although the issue of double fine-tuning remains unsolved. Another proposal is the idea of maximal symmetry breaking [314,315] which supposes an accidental symmetry in the mass spectrum of the fermion composite sector larger than H . Such a symmetry also forbids the generation of the leading order potential in the fermion sector. Instead the full potential is generated at subleading order, although it predicts the phenomenologically unviable $\xi = v^2/f^2 = 0.5$. Most interestingly, the combination of these two ideas can result in drastic reductions in fine-tuning of composite Higgs models as shown in [316].

Our proposed mechanism of cancellation with the introduction of mirror fermions is thus more alike to the maximal symmetry breaking case since the potential is fully generated at subleading order in both cases, although the mechanisms are completely different. The mirror fermion mechanism does not impose the constraint of $v^2/f^2 = 1/2$. Furthermore, the mirror fermion mechanism has strikingly different signatures, predicting light exotic fermions with spectacular decays that have no current LHC searches.

Chapter 5

Conclusion

The completion of the Standard Model with the discovery of the Higgs boson in 2012 represented a milestone for the scientific understanding of mankind and a testament to the tremendous predictive power of quantum field theory. It represented a century long journey of combining the theory of special relativity with quantum mechanics along with ingenious experiments increasing our understanding of the smallest scales. However particle physics has not played its role just yet and our increased understanding of the cosmological evolution of our Universe has highlighted deep shortcomings in our understanding of fundamental physics: the nature of dark matter and dark energy remain mysterious while the generation of a baryon asymmetry is lacking within the SM. Together with the internal inconsistency of the appearance of a Landau pole and the search to find a quantum theory of gravity, these puzzles have strengthened the belief that the SM is only an EFT valid at least up to the TeV scale.

It is however when embedding the SM into a more UV complete theory that could address some of these problems that we encounter the hierarchy problem: a sensitivity of four-dimensional fundamental scalars to the highest scale in the theory, leaving a light Higgs seemingly as a huge accident of nature. There are two viable approaches to this conundrum. The first is to do nothing, and instead tackle directly the other open problems of nature. Indeed, the hierarchy problem is not an inconsistency and could simply be due to anthropic principles, physics that cannot be captured by EFT considerations or sheer coincidence. The other approach is to take this puzzle as a hint and look for theories in which this sensitivity of the Higgs to higher scales vanishes. This means departing from the Higgs as a four-dimensional fundamental scalar. These frameworks involve either the addition of a new symmetry such as SUSY or going to composite Higgs models. By looking for the open problems of the SM from within these frameworks, the innumerable ways in which to address these open problems gets narrowed down and signatures at the TeV scale are expected.

However, the absence of such signals at the LHC has put the latter approach

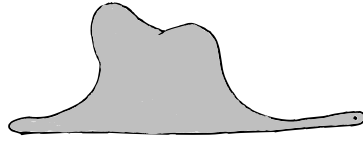
under pressure and has increased the generic fine-tuning of these models. Ironically this is exactly what these models were supposed to avoid. Although there is still a large difference between a 1% level tuning necessary to hide signatures of compositeness or SUSY at the LHC or the intangible $10^{-32}\%$ level tuning for a Planck scale UV completion, it still remains an awkward feature of these models. Much of this thesis has been preoccupied with this question. In particular, we have attempted to ask whether the absence of signals at the LHC could still be reconciled with minimally tuned models. This question is definitely positive as twin Higgs models already suggested a long time ago, but in this thesis we have expanded on that question and suggested new surprising observables to look for naturalness at the LHC.

In Chapter 2 we tackled the question of the large top Yukawa. Due to its largeness, it is by far the main contributor in the SM EFT to the radiative mass of the Higgs, increasing the generic fine-tuning within a SUSY and compositeness framework. We asked whether the actual top Yukawa contribution to the Higgs mass could be smaller than what the IR point of view seems to imply. Indeed the uncertainties on top Yukawa are at the 20% level and are only measured at the electroweak scale. It still remains very plausible that the top Yukawa behaves fundamentally different at the TeV scale. We identified two scenarios. The first consists of a strong running of the top Yukawa due to a new force which decreases the top Yukawa in the UV. While the second scenario consists in generating the top Yukawa at the loop level. Both of these scenarios radically change the nature of the top Yukawa in the UV and in particular its contribution to the Higgs mass can be dramatically reduced. If such a mechanism would be at play in nature, it could mean that our expectation for the scale at which the SM EFT must be completed for a natural Higgs, might be an underestimate and actually the W boson contribution may be the driving force of the hierarchy problem. This would imply an increase by a factor three of the scale at which the hierarchy problem should be addressed. The question of naturalness may in that case be only addressed at a more powerful collider such as a 100 TeV hadronic collider. However such large effects on the top Yukawa require additional degrees of freedom with unique signatures already at the TeV scale. At the hand of a simplified model we investigated the mechanism and pointed out the novel signatures in which naturalness may be hiding at the TeV scale such as a running top mass, deviations in 4-top measurements and new broad resonances.

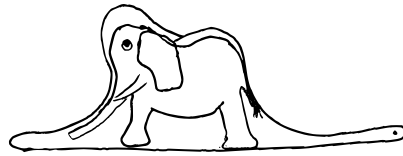
In Chapter 3 we departed from this paradigm of naturalness and instead looked for a theory with a compelling flavor structure. We took the old idea of gauge-Higgs unification, which solves the hierarchy problem by embedding the Higgs within a five-dimensional gauge field and thus protected by a higher dimensional gauge symmetry, and investigated it with a $SU(6)$ bulk gauge symmetry in a warped extra dimension. The $SU(6)$ gauge symmetry is the minimal gauge symmetry that unifies the SM gauge group in such a setup. We identified a minimal model using four bulk fermions and illustrated the

interesting connection that exists in such a model between the mass hierarchies, the CKM and the PMNS matrix. The model also allowed us to show the flip side of the hierarchy problem: flavor constraints already push the generic scale of the SM EFT cutoff far beyond which can be considered natural. A UV completion that provides a natural Higgs must therefore also have a peculiar flavor structure in order to escape these bounds. One can use flavor symmetries in order to engineer this protection, however a warped extra dimension provides already a built-in protection. We investigated the flavor constraints in our model without the use of additional flavor constraints and find that the bounds from the electron electric dipole moment and the decay $\mu \rightarrow e\gamma$ push the model to higher scales implying a certain tuning in the Higgs potential. Although the Kaluza-Klein excitations are out of reach of the LHC, the extended scalar spectrum provides an accessible window to the high-energy structure the model with not only a Higgs, but also a scalar leptoquark and singlet whose mass generation we studied in detail and could be accessible at TeV colliders.

Finally we ended this thesis in Chapter 4 with a novel model of composite Higgs. Seeking to generate the composite Higgs potential fully at the subleading order in the fermion sector, we found a way to cancel the leading fermion contributions to the Higgs potential with the use of mirror fermions. Instead of imposing a Z_2 symmetry which twin Higgs models rely upon, we identified a unique property of some fermion representations that allows for such a cancellation naturally. We found models based on the cosets $SU(6)/SU(5)$ and $SO(11)/SO(10)$ that contained such a representation and performed a numerical analysis of the model. We found that such a mechanism featured a considerable reduction in fine-tuning in models of composite Higgs and allows for a fully natural Higgs with as little as 10% tuning with sufficiently heavy top partners. Since the mentioned cosets do not allow for a four-dimensional fermionic UV completion, we analysed the implications of the five-dimensional holographic incarnation for such models. Moreover we identified the unique decays of the mirror fermions which due to their exotic baryon charge may have escaped detection so far. Only a dedicated collider search will provide the answer and test whether naturalness at the LHC remains hidden in these light exotics.



Mon dessin ne représentait pas un chapeau. Il représentait un serpent boa qui digérait un éléphant.



J'ai alors dessiné l'intérieur du serpent boa, afin que les grandes personnes puissent comprendre.

Le Petit Prince
Antoine de Saint-Exupéry

Acknowledgments

My foremost thanks goes to my supervisor Florian Goertz. Your encouragements combined with your willingness to always take time and discuss all the physics on my mind have made this thesis possible. The care and kindness you emanate are the backbone of the great atmosphere in your group of which I had the pleasure of being a member over the last years. Your guidance but at the same time your trust in letting me pursue my own ideas, often failing but also succeeding, have contributed to my formation as a scientist. I can only be grateful.

I would also like to thank Tilman Plehn for agreeing to be the second referee of this thesis and Loredana Gastaldo and Matthias Bartelmann for being part of my examination committee.

I owe my main collaborators many thanks for their deep knowledge and their unquestioning willingness to share it with me: Simone Blasi for showing me how all the 5D warped stuff works, Andrei Angelescu for teaching me the mysteries of flavor and its anomalies, and Yi Chung for showing me non-perturbative physics does not need to be so scary (as long as you can find a suitable NJL model). I also thank Sascha Weber for his work on the gauge-Higgs grand unification project and Maya Hager for her work on the composite Higgs model and sharing the burden of the scans with me. I must also thank Sudip Jana and Andreas Trautner for our short but fruitful collaboration (ESPRL!).

Although I did not have the opportunity to work in a scientific manner with the other not aforementioned postdocs, doctoral and master students at the MPIK, I want to thank them for their kindness in various ways over the last years: Aqeel Ahmed, Cristina Benso, Thede de Boer, Ting Cheng, Oleg Chkvorets, Salva Centelles Chulia, Frederik Depta, Sven Fabian, Matteo Guida, Tim Hebermann, Johannes Herms, Carlos Jaramillo, Sophie Klett, Thomas Rink, Philipp Saake, Manibrata Sen, Aika Tada, Valentin Tenorth, Nele Volmer. In particular, I have to thank Maya Hager for being such a nice office mate and our many interesting conversations and Álvaro Pastor-Gutiérrez for his friendship and our passionate discussions on mid-18th century architectural nomenclature.

Thank you to Manfred Lindner, Anja Berneiser and Britta Schwarz for giving this division every chance and opportunity to make great and stimulating research possible.

The completion of this thesis would have been far from certain without the close friends I made along the way. Jeff Kuntz and Jonas Rezacek, moving to a new place is a daunting experience, but when I got to know you, I knew it was going to be all right. Whether in the confines of the institute or asymptotically free from it, the many good memories we share will stay with me. That also includes Lukrécia Mertová more often than not and the HITS crew who I enjoyed the company of on many good occasions.

I am especially grateful to the precious few friends I had the luck to encounter over the course of my physics education whether in Luxembourg, Leuven or Zürich: your long-lasting friendship means a lot to me.

A special thanks goes to Gergana Borisova, making your acquaintance has not only proven to be highly helpful in the writing of this thesis – providing the German translation of the abstract and the illustrations of this thesis – it has also been a unique source of happiness to me.

Finally, I owe my sisters, parents and grandparents for their love and support which I carry close to my heart. In particular my mother for her unwavering love at every crossroads in my life.

Appendix A

A NJL UV completion

As discussed in Chapter 2, large couplings are required in the simplified scalar model to generate the large top Yukawa which implies a strongly coupled UV-completion. In this Appendix, we propose a possible UV theory for the simplified model, which provides a validation of the idea.

A.1 A New Global Symmetry

Before discussing the strongly coupled UV theory, let us explore the required ingredients and in particular the symmetry structure of such a theory. In Eq. (2.32), that the minimal couplings for generating the top Yukawa coupling is given. Among them, the trilinear coupling

$$\mathcal{L}_{\text{trilinear}} = -V S_R S_L^\dagger H + \text{h.c.} , \quad (\text{A.1})$$

appears the most complicated. To generate it, we extend the SM with a $SU(3)_L \times SU(2)_R$ global symmetry¹. By introducing a scalar Φ under a representation $(3, 2)$ of the global symmetry, we it contains the scalars H , S_L , S_R together with a singlet S_V as

$$\Phi = (3, 2) \xrightarrow{\text{under SM}} \begin{pmatrix} 1_0 & 1_{Q_F - \frac{2}{3}} \\ 2_{\frac{1}{6} - Q_F} & 2_{-\frac{1}{2}} \end{pmatrix} = \begin{pmatrix} S_V^* & S_R^* \\ S_L & H \end{pmatrix}, \quad (\text{A.2})$$

where the hypercharge corresponds to the desired value from Eq. (2.33). This origin of this assignment will be explained in the next section.

The global symmetry allows for the following $SU(3)_L \times SU(2)_R$ -symmetric potential given by

$$V(\Phi) = -\mu^2 |\Phi^\dagger \Phi| + \lambda |\Phi^\dagger \Phi|^2 . \quad (\text{A.3})$$

¹The same symmetry has been studied in the CHM with top seesaw mechanism [317, 318] for a different purpose.

If the singlet S_V gets a nontrivial VEV, $\langle S_V \rangle = \sqrt{\mu^2/\lambda}$, one obtains the desired trilinear coupling

$$V(\Phi) \supset V(S_R S_L^\dagger H) + \text{h.c.} , \quad (\text{A.4})$$

with as coefficient $V = 2\lambda\langle S_V \rangle$. However this such a breaking of the global symmetry will result in S_L and S_R as massless Nambu-Goldstone bosons. The full potential should therefore include symmetry breaking terms, for example the SM gauge interactions. By including such terms, the following two things happen: First, the loop potential generated by the gauge interactions will preserve $\langle \Phi \rangle = \langle S_V \rangle = \sqrt{\mu^2/\lambda}$ as S_V is a SM singlet. Second, both S_L and S_R will obtain a mass from the loop potential.²

Concerning the fermion sector, we extend the SM content by the following vector-like fermions F , according to the following representations of the global symmetry

$$Q_L = \begin{pmatrix} F_L \\ t_L \\ b_L \end{pmatrix}, \quad Q_R = \begin{pmatrix} F_R \\ t_R \end{pmatrix}, \quad (\text{A.5})$$

where Q_L is a triplet under $SU(3)_L$ and Q_R is a doublet under $SU(2)_R$. One can then write down a Yukawa coupling between Q and Φ as

$$\begin{aligned} \mathcal{L}_{\text{Yukawa}} &= -y \bar{Q}_L \Phi Q_R \\ &\supset -y_L \bar{q}_L S_L F_R - y_R \bar{t}_R S_R F_L + \text{h.c.} , \end{aligned} \quad (\text{A.6})$$

which indeed includes the two Yukawa couplings one needs for the simplified model with relation $y = y_L = y_R^*$. The Lagrangian also includes a Dirac mass for the vector-like fermion $y \bar{F}_R S_V F_L$. However, there is an unwanted tree-level Yukawa coupling $y \bar{q}_L H t_R$. The value of y is unviable and we need to modify the above setup to get a realistic model.

A.2 An NJL Model

In order to obtain a viable model, we separate the fields into two sectors, a strong sector and a weak sector. The strong sector will feature the large couplings and while the weak sector includes the SM matter. Starting with the strong sector, we introduce the following fermions:

$$Q'_L = \begin{pmatrix} F'_L \\ t'_L \\ b'_L \end{pmatrix}, \quad Q'_R = \begin{pmatrix} F'_R \\ t'_R \end{pmatrix}. \quad (\text{A.7})$$

²If the charge $Q_F = 2/3$, then S_R will become a singlet and the argument fails. However, by assuming another $U(1)'$ gauge symmetry with the similar charge but $Q_F \neq 2/3$, a mass will still be generated

A non-perturbative origin is expected in order to get large couplings. We consider a strong interaction among these fermions mediated by massive gauge bosons with mass M' , which arises from a gauge symmetry. At scales below M' , one integrates out the massive gauge bosons to arrive at the following effective four-fermion vertex term

$$\begin{aligned}\mathcal{L}_{\text{eff}} &= -\frac{g'^2}{M'^2} \left(\bar{Q}'_{L,i} \gamma^\mu T_{ij}^a Q'_{L,j} \right) \left(\bar{Q}'_{R,i} \gamma_\mu T_{ij}^a Q'_{R,j} \right) \\ &\supset \frac{g'^2}{M'^2} \left(\bar{Q}'_L Q'_{R,i} \right) \left(\bar{Q}'_R Q'_{L,j} \right),\end{aligned}\quad (\text{A.8})$$

with g' is the coupling between the gauge bosons and Q' . For large enough coupling, a fermion condensate will be formed and can be described by the following bound state

$$\bar{Q}'_R Q'_L = \begin{pmatrix} \bar{F}'_R F'_L & \bar{t}'_R F'_L \\ \bar{F}'_R q'_L & \bar{t}'_R q'_L \end{pmatrix} = \begin{pmatrix} S_V^* & S_R^* \\ S_L & S_H \end{pmatrix}, \quad (\text{A.9})$$

which carries identical symmetries as the scalar field Φ from the previous section. Indeed, the scalar field Φ is a bound state formed by Q'_L and Q'_R , which is a natural origin for scalars in a strongly coupled theory.

With the help of the fermion bubble approximation, one obtains an effective Lagrangian at a scale $\mu < M'$. The effective Lagrangian at the new scale μ is then be given by

$$\begin{aligned}\mathcal{L}_{\Phi,\mu} &= |\partial\Phi|^2 - \tilde{M}(\mu)^2 |\Phi|^2 - \tilde{\lambda}(\mu) |\Phi|^4 \\ &\quad - \tilde{y}(\mu) \bar{Q}'_L \Phi Q'_R + \text{h.c.},\end{aligned}\quad (\text{A.10})$$

where the coefficients read (defining $\ln(M'^2/\mu^2) = C$):

$$\begin{aligned}\tilde{M}(\mu)^2 &= \left(\frac{4\pi}{\sqrt{NC}} \frac{M'}{g'} \right)^2 \left(1 - \frac{g'^2}{g_c^2} + \frac{g'^2 \mu^2}{g_c^2 M'^2} \right), \\ \tilde{\lambda}(\mu) &= \frac{16\pi^2}{NC}, \quad \tilde{y}(\mu) = \frac{4\pi}{\sqrt{NC}}.\end{aligned}\quad (\text{A.11})$$

To get the desired potential, we need a condensate to be formed, i.e. $g' > g_c$. In junction with the loop potential induced by the SM gauge interaction (or some new $U(1)'$ gauge interaction), we get a VEV for S_V

$$\langle S_V \rangle = \langle \Phi \rangle \sim \sqrt{\frac{-\tilde{M}^2}{2\tilde{\lambda}}} \sim f' \sqrt{\frac{g'^2}{g_c^2} - 1}, \quad (\text{A.12})$$

with $f' \equiv M'/g'$ the symmetry breaking scale of the strong sector. The couplings in the strong sector now read

$$\begin{aligned}\mathcal{L}_\Phi &\supset 2\tilde{\lambda} \langle S_V \rangle (S_R S_L^\dagger S_H) \\ &\quad - \tilde{y} \bar{q}'_L S_L F'_R - \tilde{y} \bar{t}'_R S_R F'_L + \text{h.c.},\end{aligned}\quad (\text{A.13})$$

which is identical to the desired terms we need for the simplified scalar model. However the terms are generated from a bona fide strongly coupled theory, where the couplings are naturally large. Moreover, the masses of the scalars S_L and S_R are generated from a loop-induced potential, but they can be much lighter in comparison to M' due to the nature of pNGBs.

A.3 Connecting Elementary with Strong Sector

Finally, one needs to connect the strong sector with the elementary sector containing the fermions and the Higgs. Starting with the fermion sector, besides SM fermions, one still need a vector-like fermion F with a mass M_F as shown in (A.5). To achieve the required couplings with the NJL model described in the previous section, we need two new extended $SU(2)$ gauge symmetries, $SU(2)_{L'}$ for the left-handed top quark and $SU(2)_{R'}$ for the right-handed top quark. The gauge symmetries are broken at the scales $f_{L/R}$. Introducing two new $SU(2)_{L'}$ doublets (the $SU(2)_{R'}$ case is analogous)

$$\psi_{q_L} = \begin{pmatrix} q'_L \\ q_L \end{pmatrix}, \quad \psi_{F_R} = \begin{pmatrix} F_R \\ F'_R \end{pmatrix}, \quad (\text{A.14})$$

the $SU(2)_{L'}$ gauge interaction will give rise to the following effective term

$$\begin{aligned} \mathcal{L}_{\text{eff}} &= -\frac{1}{f_L^2} \left(\bar{\psi}_{q_L} \gamma^\mu T^a \psi_{q_L} \right) \left(\bar{\psi}_{F_R} \gamma_\mu T^a \psi_{F_R} \right) \\ &\supset \frac{1}{f_L^2} \left(\bar{F}'_R q'_L \right) (\bar{q}_L F_R) \rightarrow y_L \bar{q}_L S_L F_R, \end{aligned} \quad (\text{A.15})$$

where the desired Yukawa coupling from the simplified model is generated once the fermions in the strong sector form the bound states. The generic estimation for the size of the Yukawa coupling is

$$y_L \sim \frac{4\pi}{\sqrt{NC}} f'^2 \times \frac{1}{f_L^2} = \frac{4\pi}{\sqrt{NC}} \frac{f'^2}{f_L^2} \quad (\text{A.16})$$

with f' is the VEV of the bound state. Switching to $SU(2)_{R'}$, we get

$$y_R \sim \frac{4\pi}{\sqrt{NC}} f'^2 \times \frac{1}{f_R^2} = \frac{4\pi}{\sqrt{NC}} \frac{f'^2}{f_R^2}. \quad (\text{A.17})$$

For $f' \sim f_L \sim f_R$, then generically we obtain a large Yukawa coupling

$$y_L \sim y_R \sim \frac{4\pi}{\sqrt{NC}}. \quad (\text{A.18})$$

As a consequence, even though the top quarks and the vector-like fermion F are not part of the strong sector directly, we still get the desired large Yukawa couplings.

Concerning the Higgs sector, there is already a Higgs-like scalar bound state S_H in the strong sector and all we need is a mixing term between it and SM Higgs $H^\dagger S_H$. Due to its bound state nature $S_H = \bar{t}'_R q'_L$, the mixing can be obtained by a coupling between the SM Higgs and the constituent fermion fields. As discussed in Chapter 2, the mechanism is used to assist a model like SUSY or composite Higgs. We thus consider these two possibilities.

First, if the SM Higgs is elementary as in SUSY, the mixing can be obtained by a Yukawa coupling between Higgs and the fermions in the strong sector as

$$\mathcal{L} = -y' \bar{q}'_L H t'_R \rightarrow y' f'^2 H^\dagger S_H. \quad (\text{A.19})$$

After integrating out the heavy S_H , we obtain

$$\mathcal{L}_{\text{trilinear}} = V(S_R S_L^\dagger H) + \text{h.c.}, \quad (\text{A.20})$$

with

$$V \sim 2 \tilde{\lambda} \langle S_V \rangle y' \frac{f'^2}{M_H^2}, \quad (\text{A.21})$$

with M_H the mass of S_H . The trilinear coupling is controlled by the new Yukawa coupling y' which can be small and can therefore suppress the top Yukawa coupling from a generic large coupling to the desired top Yukawa of $\mathcal{O}(1)$.

In composite Higgs models, the SM Higgs is itself composite, composed of ψ_L and ψ_R . Mixing it with the bound state S_L , requires a similar construction as for the extended gauge symmetry such that the following four-fermion interactions are produced

$$\begin{aligned} \mathcal{L}_{\text{eff}} &= -\frac{1}{f_E^2} \left(\bar{\psi}_L \gamma^\mu T^a q'_L \right) \left(\bar{\psi}_R \gamma_\mu T^a t'_R \right) \\ &\supset \frac{1}{f_E^2} \left(\bar{\psi}_R \psi_L \right) \left(\bar{q}'_L t'_R \right) \rightarrow \frac{f^2 f'^2}{f_E^2} H^\dagger S_H, \end{aligned} \quad (\text{A.22})$$

with f_E the scale of the extended gauge symmetry while f is the breaking scale of the composite Higgs model. Again, integrating out the heavy S_H , we obtain the trilinear coupling with coefficient

$$V \sim 2 \tilde{\lambda} \langle S_V \rangle \frac{f^2 f'^2}{f_E^2 M_H^2}. \quad (\text{A.23})$$

The overall construction of the top Yukawa vertex in the UV strongly coupled theory is shown in Fig. A.1, with the scalars now replaced by the bound states of fermions. The red line represents the gauge bosons of the extended gauge symmetry and the blue point represents the mechanism to connect the Higgs to the strong sector.

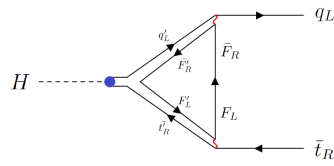


Figure A.1: Feynman diagram of the loop-generated top Yukawa coupling from a strongly coupled UV theory.

Appendix B

Warped Gauge and Fermion Fields

B.1 Gauge Fields

The 5D Yang-Mills lagrangian for a generic gauge group is the starting point

$$\begin{aligned} S_{\text{YM}} &= \int_R^{R'} d^4x dz \sqrt{G} \left(-\frac{1}{2} G^{MN} G^{AB} \text{Tr}(F_{MA} F_{NB}) \right) \\ &= \int_R^{R'} d^4x dz \left(\frac{R}{z} \right) \left(-\frac{1}{4} F_{AB}^a F^{AB,a} \right), \end{aligned} \quad (\text{B.1})$$

where G^{MN} denotes the 5D warped metric (3.43) and G its determinant. We will only be interested in the solution of the free lagrangian and therefore neglect the self-interactions contained in the above term that can be treated perturbatively. More problematic in the above action are the quadratic mixing terms between A_μ and A_5 . However those can be cancelled by taking a convenient form for the gauge-fixing term:

$$S_{\text{GF}} = \int d^4x dz \left(\frac{R}{z} \right) \left(-\frac{1}{2\xi} \left(\partial_\mu A^\mu - \xi \frac{z}{R} \partial_5 \left(\frac{R}{z} A_5 \right) \right)^2 \right). \quad (\text{B.2})$$

We now proceed to vary the action $S_{\text{YM}} + S_{\text{GF}}$ under δA_μ and δA_5 . Requiring, by the action principle, that the action vanishes we obtain the equations of motions

$$\begin{aligned} \left[\eta^{\mu\nu} \partial^2 - \left(1 - \frac{1}{\xi} \right) \partial^\mu \partial^\nu \right] A_\nu - z \partial_5 \left(\frac{1}{z} \partial_5 A^\mu \right) &= 0, \\ \partial^2 A_5 - \xi \partial_5 \left(z \partial_5 \left(\frac{1}{z} A_5 \right) \right) &= 0. \end{aligned} \quad (\text{B.3})$$

In contrast to 4D equations of motions where fields are taken to vanish at infinity, integration by parts along the fifth dimension will lead to boundary

conditions for the fields

$$\begin{aligned} \int d^4x \left[\frac{R}{z} \left(\partial_\mu A_5 - \partial_5 A_\mu \right) \delta A^\mu \right]_{z=R}^{z=R'} &= 0, \\ \int d^4x \left[\frac{R}{z} \left(\partial_\mu A^\mu - \xi z \left(\partial_5 \left(\frac{1}{z} A_5 \right) \right) \right) \delta A_5 \right]_{z=R}^{z=R'} &= 0. \end{aligned} \quad (\text{B.4})$$

In the following we will consider two possible boundary conditions that fulfill the above, namely

$$\begin{aligned} (+) : A_5|_{z=R,R'} &= 0, \partial_5 A_\mu|_{z=R,R'} = 0, \\ (-) : A_\mu|_{z=R,R'} &= 0, \partial_5 \left(\frac{1}{z} A_5 \right)|_{z=R,R'} = 0. \end{aligned} \quad (\text{B.5})$$

where (+)/(-) refers to a Neumann/Dirichlet BC for the A_μ field which will imply the opposite for the A_5 field. Unsurprisingly for a zero mode gauge boson to occur, one must choose (+, +) boundary conditions at both UV/IR brane, while a zero mode scalar field, relevant for gauge-Higgs unification, will occur for (-, -) boundary conditions. The mixed boundary conditions (+, -)/(-, +) give rise to massive gauge fields.

One can now solve the above differential equations by a simple separation of variables between the compact parameter, z , and the usual 4D space-time variable x^μ . In the context of extra dimensions this is called a Kaluza-Klein (KK) decomposition

$$A_\mu(x, z) = \sum_n f_{n,A}(z) A_{\mu,n}(x), \quad A_5(x, z) = \sum_n f_{n,5}(z) A_{5,n}(x), \quad (\text{B.6})$$

in which the 5D field is expanded in an infinite sum of 4D fields, $A_{\mu/5,n}(x)$ with a specific localization, or wavefunction, along the extra dimension $f_{n,A/5}(z)$ and a mass m_n . The 4D fields obey the usual 4D equations of motions:

$$\left[\eta^{\mu\nu} \partial^2 - \left(1 - \frac{1}{\xi} \right) \partial^\mu \partial^\nu \right] A_{\nu,n} + m_n^2 A_n^\mu = 0, \quad \partial^2 A_{5,n} + m_{5,n}^2 A_{5,n} = 0, \quad (\text{B.7})$$

which leads to the following equations for the bulk profiles:

$$-m_n^2 f_{n,A} = z \partial_5 \left(\frac{1}{z} \partial_5 f_{n,A} \right), \quad -m_{5,n}^2 f_{n,5} = \xi \partial_5 \left(z \partial_5 \left(\frac{1}{z} f_{n,5} \right) \right). \quad (\text{B.8})$$

From the first equation one gets that a massless gauge boson has a constant bulk profile implying indeed (+, +) boundary conditions for such a mode. The second equation implies that a massless scalar has a linear bulk profile $f_{0,5} \sim z$ with indeed (-, -) boundary conditions. Interestingly for a general massive vector boson $m_m > 0$ with profile $f_{n,A}$, one finds a scalar mode with profile $f_{n,5} = \frac{1}{m_n} \partial_5 f_{n,A}$ with mass $m_{5,n} = \sqrt{\xi} m_n$. The gauge dependence already indicates that the corresponding scalar cannot be a physical spectrum. Instead, we are reminded

of the same ξ dependence for Goldstone bosons that provide the longitudinal component of a massive gauge boson (see for example [136]). Indeed, the whole tower of scalar modes (with the possible exception of a physical massless scalar), are Goldstones and absorbed by the massive gauge bosons.

The normalization of the gauge boson follows from requiring canonical kinetic terms in the lagrangian and leads to

$$\int_R^{R'} dz \frac{R}{z} f_{n,A} f_{m,A} = \delta_{n,m}. \quad (\text{B.9})$$

The profile of the zero mode gauge boson then follows

$$f_{0,A}(z) = \sqrt{\frac{1}{R \log\left(\frac{R'}{R}\right)}}. \quad (\text{B.10})$$

The normalization of the Goldstones is automatically satisfied by virtue of the equations of motions if the massive gauge fields satisfy (B.9).

We now briefly discuss the different type of massive gauge bosons. The profiles $f_{n,(+,\pm)}(z)$ of $(+, \pm)$ are given in terms of the following Bessel functions

$$f_{n,(+,\pm)}(z) = N_{n,(+,\pm)} z \left(J_1(m_{n,(+,\pm)} z) - \frac{J_0(m_{n,(+,\pm)} R) Y_1(m_{n,(+,\pm)} z)}{Y_0(m_{n,(+,\pm)} R)} \right), \quad (\text{B.11})$$

with $N_{n,(+,\pm)}$ the normalization constants. The masses of the KK tower, $m_{n,(+,\pm)}$, are determined by applying the IR boundary conditions. The $(+, +)$ boundary conditions will feature a zero mode with a flat profile while the first KK mode is at $m_{1,(+,+)} \sim 2.45/R'$. $(+, -)$ boundary conditions do not have a zero mode as the gauge symmetry is broken on the IR but instead feature a rather light first KK mode at $m_{1,(+,-)} \sim 0.25/R'$.

The $(-, \pm)$ gauge bosons feature a different UV boundary condition, their profile is therefore a different linear combination of Bessel functions:

$$f_{n,(-,\pm)}(z) = N_{n,(-,\pm)} z \left(J_1(m_{n,(-,\pm)} z) - \frac{J_1(m_{n,(-,\pm)} R) Y_1(m_{n,(-,\pm)} z)}{Y_1(m_{n,(-,\pm)} R)} \right). \quad (\text{B.12})$$

The lightest KK masses of these boundary conditions are $m_{1,(-,+)} \sim 2.40/R'$ and $m_{1,(-,-)} \sim 3.83/R'$.

Recall that for the $(-, -)$ boundary condition there is a massless scalar in the physical spectrum, $A_5^{\hat{a}}(x)$, with normalized bulk profile $f_5(z)$

$$A_5(x, z) \supset f_5(z) A_5^{\hat{a}}(x) T^{\hat{a}} = \sqrt{\frac{2}{R}} \frac{z}{R'} A_5^{\hat{a}}(x) T^{\hat{a}}, \quad (\text{B.13})$$

where we denote $T^{\hat{a}}$ as the generators of the bulk gauge group with $(-, -)$ boundary conditions and thus a massless scalar. As discussed, gauge-Higgs unification relies on embedding the Higgs field in such a zero mode. Moreover a potential for $A_5^{\hat{a}}(x)$ is forbidden by 5D gauge symmetry, but due to finite-volume effects a finite potential is generated at loop-level inducing a VEV $\langle A_5^{\hat{a}}(x) \rangle = v^{\hat{a}}$ and inducing possibly spontaneous symmetry breaking.

B.2 Fermion Fields

Having discussed 5D warped gauge fields, we now turn to the discussion of fermionic fields, starting with its action:

$$S_{\text{Fermion}} = \int d^4x \int_R^{R'} dz \sqrt{G} \left(\frac{i}{2} (\bar{\Psi} e_a^M \gamma^a D_M \Psi - \overline{D_M \Psi} e_a^M \gamma^a \Psi) - m \bar{\Psi} \Psi \right). \quad (\text{B.14})$$

The Dirac algebra now has to be generalized to 5D which implies the inclusion of γ^5 as the fifth gamma matrix in the Dirac algebra $\{\gamma^a, \gamma^b\} = 2\eta^{ab}$, making 5D fermions non-chiral. For warped space, the fünfbein e_a^M is given by $e_a^M = (R/z)\delta_a^M$. In the absence of gauge interactions the covariant derivative in warped space is given by $D_\mu \Psi = (\partial_\mu + \gamma_\mu \gamma_5 / (4z)) \Psi$, and $D_5 \Psi = \partial_5 \Psi$. Inserting these terms into the above action and simplifying we find

$$S_{\text{Fermion}} = \int d^4x \int_R^{R'} dz \left(\frac{R}{z} \right)^4 \left(\frac{i}{2} (\bar{\Psi} \gamma^\mu \overleftrightarrow{\partial}_\mu \Psi + \bar{\Psi} \gamma^5 \overleftrightarrow{\partial}_5 \Psi) - \frac{mR}{z} \bar{\Psi} \Psi \right), \quad (\text{B.15})$$

with $\overleftrightarrow{\partial} = \overrightarrow{\partial} - \overleftarrow{\partial}$. After integration by parts, which results in boundary terms along the fifth compact dimension, we obtain

$$S_{\text{Fermion}} = \int d^4x \int_R^{R'} dz \left(\frac{R}{z} \right)^4 \bar{\Psi} \left(i\gamma^\mu \partial_\mu + i\gamma^5 \partial_5 - \frac{2i}{z} \gamma_5 - \frac{c}{z} \right) \Psi - \frac{i}{2} \int d^4x \left(\frac{R}{z} \right)^4 [\bar{\Psi} \gamma^5 \Psi]_{z=R}^{z=R'}, \quad (\text{B.16})$$

where we define the dimensionless mass parameter $c \equiv mR$. Decomposing the 5D fermions into their chiral components, $\Psi = (\chi, \bar{\psi})^T$, we are lead to the following bulk action with boundary terms

$$S_{\text{Fermion}} = \int d^4x \int_R^{R'} dz \left(\frac{R}{z} \right)^4 \left(i\bar{\chi} \bar{\sigma}^\mu \partial_\mu \chi + i\psi \sigma^\mu \partial_\mu \bar{\psi} - \psi \partial_5 \chi + \bar{\chi} \partial_5 \bar{\psi} + \frac{2-c}{z} \psi \chi - \frac{2+c}{z} \bar{\chi} \bar{\psi} \right) + \frac{1}{2} \int d^4x \left(\frac{R}{z} \right)^4 [\psi \chi - \bar{\chi} \bar{\psi}]_{z=R}^{z=R'}. \quad (\text{B.17})$$

After varying the action for $\bar{\chi}$ and ψ , we obtain a set of coupled bulk equations of motions

$$i\bar{\sigma}^\mu \partial_\mu \chi + \partial_5 \bar{\psi} - \frac{c+2}{z} \bar{\psi} = 0, \quad i\sigma^\mu \partial_\mu \bar{\psi} - \partial_5 \chi + \frac{2-c}{z} \chi = 0, \quad (\text{B.18})$$

as well as a boundary term

$$\frac{1}{2} \int d^4x \left[\left(\frac{R}{z} \right)^4 (\psi \delta \chi + \delta \psi \chi - \bar{\chi} \delta \bar{\psi} - \delta \bar{\chi} \bar{\psi}) \right]_{z=R}^{z=R'} = 0. \quad (\text{B.19})$$

In the following we will denote with (+)/(-) a Dirichlet boundary condition for the right handed/left handed field, implying a Neumann-like BC for the

opposing chirality by virtue of the equations of motion, namely

$$\begin{aligned}\Psi(-) : \chi(x, z) = 0 &\implies \partial_5 \psi(x, z) = \frac{2+c}{z} \psi(x, z), \\ \Psi(+) : \psi(x, z) = 0 &\implies \partial_5 \chi(x, z) = \frac{2-c}{z} \chi(x, z).\end{aligned}\quad (\text{B.20})$$

Once again the solutions are found by a separation of variables, writing the 5D bulk fermion field as a sum over 4D fermion $\chi_n(x)/\psi_n(x)$ fields with a wavefunction, $f_{L/R}(z)$

$$\chi(x, z) = \sum_n f_{n,L}(z) \chi_n(x), \quad \bar{\psi}(x, z) = \sum_n f_{n,R}(z) \bar{\psi}_n(x), \quad (\text{B.21})$$

and each 4D spinor obeys the 4D Dirac equation with mass m_n :

$$i\bar{\sigma}^\mu \partial_\mu \chi_n - m_n \bar{\psi}_n = 0, \quad i\sigma^\mu \partial_\mu \bar{\psi}_n - m_n \chi_n = 0. \quad (\text{B.22})$$

After inserting the KK decomposition into the equations of motions we find a first order differential equation for the bulk profiles

$$f'_{n,R} + m_n f_{n,L} - \frac{c+2}{z} f_{n,R} = 0, \quad f'_{n,L} - m_n f_{n,R} + \frac{c-2}{z} f_{n,L} = 0. \quad (\text{B.23})$$

The profiles themselves are orthonormalized, such that the kinetic terms for the 4D fields are canonically normalized and do not mix, resulting in the conditions

$$\int_R^{R'} dz \left(\frac{R}{z}\right)^4 f_{n,L}(z) f_{m,L}(z) = \int_R^{R'} dz \left(\frac{R}{z}\right)^4 f_{n,R}(z) f_{m,R}(z) = \delta_{n,m}. \quad (\text{B.24})$$

In the case of a zero mode, $m_n = 0$, the left and right handed profiles decouple and we are left with

$$f_{0,L} = \frac{1}{\sqrt{R'}} \left(\frac{z}{R}\right)^2 \left(\frac{z}{R'}\right)^{-c} f(c), \quad f_{0,R} = \frac{1}{\sqrt{R'}} \left(\frac{z}{R}\right)^2 \left(\frac{z}{R'}\right)^c f(-c), \quad (\text{B.25})$$

with the *flavor function*

$$f(c) = \frac{\sqrt{1-2c}}{\sqrt{1-(R'/R)^{2c-1}}}, \quad (\text{B.26})$$

indicating the overlap of the fermion bulk profile with the IR brane which for phenomenological studies is a very useful quantity. Such zero modes are a feature of interval-like theories (such as an orbifold) in which one has localized branes on which boundary conditions can be specified: $(+, +)/(-, -)$ boundary condition will give rise to a massless left/right handed fermion $\chi_0(x)/\psi_0(x)$.

The more general case of a $m_n \neq 0$ fermion can be solved by separating the coupled Eqs. (B.23) into two independent but second order differential equations

$$\begin{aligned} f''_{n,L} - \frac{4}{z} f'_{n,L} + \left(m_n^2 - \frac{c^2 + c - 6}{z^2}\right) f_{n,L} &= 0, \\ f''_{n,R} - \frac{4}{z} f'_{n,R} + \left(m_n^2 - \frac{c^2 - c - 6}{z^2}\right) f_{n,R} &= 0, \end{aligned} \quad (\text{B.27})$$

which is solved by Bessel functions. The warped sine and cosine functions [250]

$$\begin{aligned} S(z, m, c) &= \frac{\pi}{2} m R \left(\frac{z}{R}\right)^{1/2+c} \left(J_{1/2+c}(mR) Y_{1/2+c}(mz) \right. \\ &\quad \left. - J_{1/2+c}(mz) Y_{1/2+c}(mR) \right), \\ C(z, m, c) &= \frac{\pi m R}{2 \cos(c\pi)} \left(\frac{z}{R}\right)^{1/2+c} \left(J_{-1/2+c}(mR) J_{-1/2-c}(mz) \right. \\ &\quad \left. + J_{1/2+c}(mz) J_{1/2-c}(mR) \right), \end{aligned} \quad (\text{B.28})$$

provide a useful parametrization of Bessel functions such that the general solutions to Eq. (B.27) can be constructed as

$$\begin{aligned} f_{n,L}(z) &= \left(\frac{R}{z}\right)^{c-2} (b_n S(z, m_n, c) - a_n C(z, m_n, c)), \\ f_{n,R}(z) &= \left(\frac{R}{z}\right)^{-c-2} (a_n S(z, m_n, -c) + b_n C(z, m_n, -c)). \end{aligned} \quad (\text{B.29})$$

with a_n, b_n determined by the UV boundary conditions and the overall normalization while m_n follows from applying the IR boundary condition.

B.3 Zero Mode Approximation

In this appendix we provide the solutions of the SU(6) gauge-Higgs grand unification model from section 3.3 for the wave functions and mass matrices of the fermions in the Zero Mode Approximation (ZMA) in which we do not take into account fermion-mass mixing with the KK modes.

In the quark sector, we find the following profiles

$$\begin{aligned} f_{u_R}(z) &= \frac{1}{\sqrt{R'}} \left(\frac{z}{R}\right)^2 \left(\frac{z}{R'}\right)^{c_{20}} f_{-c_{20}}, \\ f_{d_R}(z) &= \frac{1}{\sqrt{R'}} \left(\frac{z}{R}\right)^2 \left(\frac{z}{R'}\right)^{c_6} f_{-c_6}, \\ f_{d'_R}(z) &= -\frac{1}{\sqrt{R'}} \left(\frac{z}{R}\right)^2 \left(\frac{z}{R'}\right)^{c_{15}} M_{d/l}^\dagger f_{-c_6}, \end{aligned} \quad (\text{B.30})$$

with the latter profile due to the IR brane mass term $M_{d/l}$ which implies the IR BC $f_{d'_R}(R') = -M_{d/l}^\dagger f_{d_R}(R')$. For the quark doublet we find the following profiles

$$\begin{aligned} f_{q_L}(z) &= \frac{1}{\sqrt{R'}} \left(\frac{z}{R}\right)^2 \left(\frac{z}{R'}\right)^{-c_{15}} f_{c_{15}}, \\ f_{q'_L}(z) &= \frac{1}{\sqrt{R'}} \left(\frac{z}{R}\right)^2 \left(\frac{z}{R'}\right)^{-c_{20}} M_{q/e} f_{c_{15}}, \end{aligned} \quad (\text{B.31})$$

where the latter profile results from the IR brane mass term $M_{q/e}$ which implies the IR BC $f_{q'_L}(R') = M_{q/e} f_{q_L}(R')$. The above fermion profiles result in the following non-canonical kinetic terms

$$\begin{aligned} K_{u_R} &= 1, \\ K_{d_R} &= 1 + f_{-c_6} M_{d/l} f_{-c_{15}}^{-2} M_{d/l}^\dagger f_{-c_6}, \\ K_{q_L} &= 1 + f_{c_{15}} M_{q/e}^\dagger f_{c_{20}}^{-2} M_{q/e} f_{c_{15}}, \end{aligned} \quad (\text{B.32})$$

which implies the need for an additional normalization of $\psi \rightarrow K^{-1/2} \psi$. The overlap of the left and right handed modes with the Higgs boson, results in the following mass matrices in the flavor basis:

$$\begin{aligned} \mathcal{M}_u &= \frac{g_* v}{2\sqrt{2}} f_{c_{15}} M_{q/e}^\dagger f_{-c_{20}}, \\ \mathcal{M}_d &= -\frac{g_* v}{2\sqrt{2}} f_{c_{15}} M_{d/l}^\dagger f_{-c_6}. \end{aligned} \quad (\text{B.33})$$

We proceed similarly for the lepton sector, resulting in the following profiles for the SM zero modes

$$\begin{aligned} f_{l_R^c}(z) &= \frac{1}{\sqrt{R'}} \left(\frac{z}{R}\right)^2 \left(\frac{z}{R'}\right)^{c_6} f_{-c_6}, \\ f_{l'_R}(z) &= -\frac{1}{\sqrt{R'}} \left(\frac{z}{R}\right)^2 \left(\frac{z}{R'}\right)^{c_{15}} M_{d/l}^\dagger f_{-c_6}, \\ f_{e_L^c}(z) &= \frac{1}{\sqrt{R'}} \left(\frac{z}{R}\right)^2 \left(\frac{z}{R'}\right)^{-c_{15}} f_{c_{15}}, \\ f_{e'_L}(z) &= \frac{1}{\sqrt{R'}} \left(\frac{z}{R}\right)^2 \left(\frac{z}{R'}\right)^{-c_{20}} M_{q/e} f_{c_{15}}, \\ f_{\nu_L^c}(z) &= \frac{1}{\sqrt{R'}} \left(\frac{z}{R}\right)^2 \left(\frac{z}{R'}\right)^{-c_6} f_{c_6}, \\ f_{\nu'_L}(z) &= \frac{1}{\sqrt{R'}} \left(\frac{z}{R}\right)^2 \left(\frac{z}{R'}\right)^{-c_1} M_\nu f_{c_6}, \end{aligned} \quad (\text{B.34})$$

The lepton kinetic mixing matrices are given by

$$\begin{aligned} K_{l_R^c} &= 1 + f_{-c_6} M_{d/l} f_{-c_{15}}^{-2} M_{d/l}^\dagger f_{-c_6}, \\ K_{e_L^c} &= 1 + f_{c_{15}} M_{q/e}^\dagger f_{c_{20}}^{-2} M_{q/e} f_{c_{15}}, \\ K_{\nu_L^c} &= 1 + f_{c_6} M_\nu^\dagger f_{c_1}^{-2} M_\nu f_{c_6}, \end{aligned} \quad (\text{B.35})$$

and the mass matrices in the flavor basis are

$$\begin{aligned}\mathcal{M}_{ec} &= -\frac{g_*v}{2\sqrt{2}}f_{-c_6}M_{d/l}f_{c_{15}}, \\ \mathcal{M}_{\nu^c} &= \frac{g_*v}{2\sqrt{2}}f_{-c_6}f_{c_6}.\end{aligned}\tag{B.36}$$

Appendix C

A Three-Site Model

In this appendix we describe the three-site model that provides a phenomenological incarnation of the mirror fermion cancellation mechanism.

The first site is identified with the elementary sector in which all the SM fermions and the mirror fermions (with their Dirac mass reside), while the second and third site form the strongly coupled sector. The corresponding Lagrangian describing the link between the elementary sector and the second site, describing the partial compositeness of the quarks from Eq. (4.78), reads

$$\mathcal{L}_{\text{PC}} = \lambda_L f (\bar{Q}_L + \bar{\Theta}_L) U^{\mathbf{R}} \psi^{\mathbf{R}} + \lambda_R f (\bar{T}_R + \bar{\Omega}_R) U^{\mathbf{R}} \psi^{\mathbf{R}} + \text{h.c.} , \quad (\text{C.1})$$

where Q_L, Θ_L, T_R and Ω_R describe the spurion embedding of the quark doublet and top singlet and their mirror fermions into the representation \mathbf{R} of G . $\psi^{\mathbf{R}}$ is a strong sector fermion on the second site in the representation \mathbf{R} , while $U^{\mathbf{R}}$ is the Goldstone matrix transforming in the representation \mathbf{R}

$$U^{\mathbf{R}} = \exp \left(2i \Pi_{\hat{\alpha}} T_{\hat{\alpha}}^{\mathbf{R}} / f \right), \quad (\text{C.2})$$

with $T_{\hat{\alpha}}^{\mathbf{R}}$ the broken generators of G/H in the representation \mathbf{R} normalised such that $\text{Tr}(T_i T_j) = \delta_{ij}/2$.

In order to make the chiral mirror fermions heavy, we introduce their opposite chirality and give them a Dirac mass on the first site as indicated by the second line of Eq. (4.78):

$$\mathcal{L}_{\text{Dirac}} = m_{\omega} \bar{\omega} \omega + m_{\theta} \bar{\theta} \theta. \quad (\text{C.3})$$

We also include a partial compositeness hypothesis for the b_R as illustrated by Eq.(4.80):

$$\mathcal{L}_{\text{PC}} = \lambda_b f \bar{B}_R U^{\mathbf{R}'} \psi^{\mathbf{R}'} + \text{h.c.} . \quad (\text{C.4})$$

Although the impact of the bottom sector on the potential is negligible, some of the strong sector resonances contained in $\psi^{\mathbf{R}'}$ will mix with the top and exotic resonances impacting the phenomenology. It is therefore important to incorporate their effect.

We now describe the second and third site, or the strong sector, omitting the kinetic terms:

$$\begin{aligned}
\mathcal{L}_{\text{strong}} = & m_{\mathbf{R}} \bar{\psi}^{\mathbf{R}} \psi^{\mathbf{R}} + m_{\mathbf{R}'} \bar{\psi}^{\mathbf{R}'} \psi^{\mathbf{R}'} \\
& + \Delta_{\mathbf{R}} \bar{\psi}^{\mathbf{R}} \tilde{\psi}^{\mathbf{R}} + \Delta_{\mathbf{R}'} \bar{\psi}^{\mathbf{R}'} \tilde{\psi}^{\mathbf{R}'} + \text{h.c.} \\
& + \tilde{m}_{\mathbf{C}} \bar{\psi}^{\mathbf{C}} \tilde{\psi}^{\mathbf{C}} + \tilde{m}_{\bar{\mathbf{C}}} \bar{\psi}^{\bar{\mathbf{C}}} \tilde{\psi}^{\bar{\mathbf{C}}} + \tilde{m}'_{\mathbf{C}} \bar{\psi}'^{\mathbf{C}} \tilde{\psi}'^{\mathbf{C}} \\
& + \tilde{m}_{L,\mathbf{C}} \bar{\psi}^{\mathbf{C}} P_L \tilde{\psi}'^{\mathbf{C}} + \tilde{m}_{R,\mathbf{C}} \bar{\psi}^{\mathbf{C}} P_R \tilde{\psi}'^{\mathbf{C}} + \text{h.c.}, \tag{C.5}
\end{aligned}$$

with $\tilde{\psi}^{\mathbf{R}} = (\tilde{\psi}^{\mathbf{C}}, \tilde{\psi}^{\bar{\mathbf{C}}})$ and $\tilde{\psi}^{\mathbf{R}'} = (\tilde{\psi}'^{\mathbf{C}}, \dots)$ the strong sector fermions living on the third site. The first line contains the Dirac mass for the two second site fermions, $\psi^{\mathbf{R}}$ and $\psi^{\mathbf{R}'}$, while the second line connect the second site fermions to the third site fermions, $\tilde{\psi}^{\mathbf{R}}$ and $\tilde{\psi}^{\mathbf{R}'}$. Notice that these masses respect the global symmetry G . The breaking of G happens only on the third site where all the masses consistent with the symmetry H are written down. These correspond to the last two lines of Eq. (C.5) with the third line corresponding to the H invariant masses of the second site fermions while the last line corresponds to the H -invariant masses between the third site fermions $\tilde{\psi}^{\mathbf{R}}$ and $\tilde{\psi}^{\mathbf{R}'}$. The fact that such H -invariant masses exist relies on embedding the b_R in a \mathbf{R}' such that it decomposes in H as

$$\mathbf{R}' = \mathbf{C} \oplus \dots, \tag{C.6}$$

without which the right-handed bottom wouldn't connect to the left-handed bottom and remain massless (see main text for more details).

The above fully describes the fermion sector of the three-site model and allows to extract the mass matrices $M_T(h)$ and $M_E(h)$ for the top and exotic respectively and associated strong sector resonances which determines the radiative Higgs potential of the model.

Bibliography

- [1] A. Bally, Y. Chung and F. Goertz, *Hierarchy problem and the top Yukawa coupling: An alternative to top partner solutions*, *Phys. Rev. D* **108** (2023) 055008 [2211.17254].
- [2] A. Angelescu, A. Bally, S. Blasi and F. Goertz, *Minimal $SU(6)$ gauge-Higgs grand unification*, *Phys. Rev. D* **105** (2022) 035026 [2104.07366].
- [3] A. Angelescu, A. Bally, F. Goertz and S. Weber, *$SU(6)$ gauge-Higgs grand unification: minimal viable models and flavor*, *JHEP* **04** (2023) 012 [2208.13782].
- [4] A. Angelescu, A. Bally, F. Goertz and M. Hager, *Restoring Naturalness via Conjugate Fermions*, 2309.05698.
- [5] A. Bally, S. Jana and A. Trautner, *Neutrino self-interactions and XENON1T electron recoil excess*, *Phys. Rev. Lett.* **125** (2020) 161802 [2006.11919].
- [6] G. Arcadi, A. Bally, F. Goertz, K. Tame-Narvaez, V. Tenorth and S. Vogl, *EFT interpretation of XENON1T electron recoil excess: Neutrinos and dark matter*, *Phys. Rev. D* **103** (2021) 023024 [2007.08500].
- [7] A. Bally, Y. Chung and F. Goertz, *The Hierarchy Problem and the Top Yukawa*, in *57th Rencontres de Moriond on QCD and High Energy Interactions*, 4, 2023 [2304.11891].
- [8] F. Goertz, A. Angelescu, A. Bally and S. Blasi, *Unification of Gauge Symmetries ... including their breaking*, *PoS EPS-HEP2021* (2022) 698 [2109.14538].
- [9] C.D. Anderson, *The positive electron*, *Phys. Rev.* **43** (1933) 491.
- [10] J. Schwinger, *On quantum-electrodynamics and the magnetic moment of the electron*, *Phys. Rev.* **73** (1948) 416.

- [11] Y. Nambu, *Quasi-particles and gauge invariance in the theory of superconductivity*, *Phys. Rev.* **117** (1960) 648.
- [12] J. Goldstone, *Field Theories with Superconductor Solutions*, *Nuovo Cim.* **19** (1961) 154.
- [13] J. Goldstone, A. Salam and S. Weinberg, *Broken symmetries*, *Phys. Rev.* **127** (1962) 965.
- [14] F. Englert and R. Brout, *Broken symmetry and the mass of gauge vector mesons*, *Phys. Rev. Lett.* **13** (1964) 321.
- [15] P.W. Higgs, *Broken symmetries and the masses of gauge bosons*, *Phys. Rev. Lett.* **13** (1964) 508.
- [16] G.S. Guralnik, C.R. Hagen and T.W.B. Kibble, *Global conservation laws and massless particles*, *Phys. Rev. Lett.* **13** (1964) 585.
- [17] S. Weinberg, *A model of leptons*, *Phys. Rev. Lett.* **19** (1967) 1264.
- [18] A. Salam, *Weak and Electromagnetic Interactions*, *Conf. Proc. C* **680519** (1968) 367.
- [19] D.J. Gross and F. Wilczek, *Ultraviolet behavior of non-abelian gauge theories*, *Phys. Rev. Lett.* **30** (1973) 1343.
- [20] H.D. Politzer, *Reliable perturbative results for strong interactions?*, *Phys. Rev. Lett.* **30** (1973) 1346.
- [21] CMS collaboration, *Observation of a New Boson at a Mass of 125 GeV with the CMS Experiment at the LHC*, *Phys. Lett. B* **716** (2012) 30 [1207.7235].
- [22] ATLAS collaboration, *Observation of a new particle in the search for the Standard Model Higgs boson with the ATLAS detector at the LHC*, *Phys. Lett. B* **716** (2012) 1 [1207.7214].
- [23] PLANCK collaboration, *Planck 2018 results. I. Overview and the cosmological legacy of Planck*, *Astron. Astrophys.* **641** (2020) A1 [1807.06205].
- [24] G. Bertone, D. Hooper and J. Silk, *Particle dark matter: Evidence, candidates and constraints*, *Phys. Rept.* **405** (2005) 279 [hep-ph/0404175].
- [25] H. Georgi and S.L. Glashow, *Unity of All Elementary Particle Forces*, *Phys. Rev. Lett.* **32** (1974) 438.
- [26] J.C. Pati and A. Salam, *Unified Lepton-Hadron Symmetry and a Gauge Theory of the Basic Interactions*, *Phys. Rev. D* **8** (1973) 1240.

- [27] H. Fritzsch and P. Minkowski, *Unified Interactions of Leptons and Hadrons*, *Annals Phys.* **93** (1975) 193.
- [28] P.A.M. Dirac, *New basis for cosmology*, *Proc. Roy. Soc. Lond. A* **165** (1938) 199.
- [29] G. 't Hooft, *Naturalness, chiral symmetry, and spontaneous chiral symmetry breaking*, *NATO Sci. Ser. B* **59** (1980) 135.
- [30] G. Panico and A. Wulzer, *The Composite Nambu-Goldstone Higgs*, vol. 913, Springer (2016), 10.1007/978-3-319-22617-0, [1506.01961].
- [31] R. Haag, J.T. Lopuszanski and M. Sohnius, *All Possible Generators of Supersymmetries of the s Matrix*, *Nucl. Phys. B* **88** (1975) 257.
- [32] S. Dimopoulos and H. Georgi, *Softly Broken Supersymmetry and $SU(5)$* , *Nucl. Phys. B* **193** (1981) 150.
- [33] S. Dimopoulos, S. Raby and F. Wilczek, *Supersymmetry and the scale of unification*, *Phys. Rev. D* **24** (1981) 1681.
- [34] L.E. Ibanez and G.G. Ross, *Low-Energy Predictions in Supersymmetric Grand Unified Theories*, *Phys. Lett. B* **105** (1981) 439.
- [35] R. Barbieri and A. Strumia, *The 'LEP paradox'*, in *4th Rencontres du Vietnam: Physics at Extreme Energies (Particle Physics and Astrophysics)*, 7, 2000 [hep-ph/0007265].
- [36] S. Weinberg, *Anthropic Bound on the Cosmological Constant*, *Phys. Rev. Lett.* **59** (1987) 2607.
- [37] P.W. Graham, D.E. Kaplan and S. Rajendran, *Cosmological Relaxation of the Electroweak Scale*, *Phys. Rev. Lett.* **115** (2015) 221801 [1504.07551].
- [38] CMS collaboration, *Search for top squark pair production using dilepton final states in pp collision data collected at $\sqrt{s} = 13$ TeV*, *Eur. Phys. J. C* **81** (2021) 3 [2008.05936].
- [39] ATLAS collaboration, *Search for top squarks in events with a Higgs or Z boson using 139 fb^{-1} of pp collision data at $\sqrt{s} = 13$ TeV with the ATLAS detector*, *Eur. Phys. J. C* **80** (2020) 1080 [2006.05880].
- [40] CMS collaboration, *Search for pair production of vectorlike quarks in the fully hadronic final state*, *Phys. Rev. D* **100** (2019) 072001 [1906.11903].
- [41] ATLAS collaboration, *Combination of the searches for pair-produced vector-like partners of the third-generation quarks at $\sqrt{s} = 13$ TeV with the ATLAS detector*, *Phys. Rev. Lett.* **121** (2018) 211801 [1808.02343].

- [42] ATLAS collaboration, *Search for pair-production of vector-like quarks in pp collision events at $\sqrt{s} = 13$ TeV with at least one leptonically decaying Z boson and a third-generation quark with the ATLAS detector*, 2210.15413.
- [43] CMS collaboration, *Search for pair production of vector-like quarks in leptonic final states in proton-proton collisions at $\sqrt{s} = 13$ TeV*, 2209.07327.
- [44] ATLAS collaboration, *Search for single production of a vectorlike T quark decaying into a Higgs boson and top quark with fully hadronic final states using the ATLAS detector*, *Phys. Rev. D* **105** (2022) 092012 [2201.07045].
- [45] A. Arvanitaki, N. Craig, S. Dimopoulos and G. Villadoro, *Mini-Split*, *JHEP* **02** (2013) 126 [1210.0555].
- [46] Z. Chacko, H.-S. Goh and R. Harnik, *The Twin Higgs: Natural electroweak breaking from mirror symmetry*, *Phys. Rev. Lett.* **96** (2006) 231802 [hep-ph/0506256].
- [47] M. Geller and O. Telem, *Holographic Twin Higgs Model*, *Phys. Rev. Lett.* **114** (2015) 191801 [1411.2974].
- [48] R. Barbieri, D. Greco, R. Rattazzi and A. Wulzer, *The Composite Twin Higgs scenario*, *JHEP* **08** (2015) 161 [1501.07803].
- [49] M. Low, A. Tesi and L.-T. Wang, *Twin Higgs mechanism and a composite Higgs boson*, *Phys. Rev. D* **91** (2015) 095012 [1501.07890].
- [50] G. Burdman, Z. Chacko, H.-S. Goh and R. Harnik, *Folded supersymmetry and the LEP paradox*, *JHEP* **02** (2007) 009 [hep-ph/0609152].
- [51] B. Batell, M. Low, E.T. Neil and C.B. Verhaaren, *Review of Neutral Naturalness*, in *Snowmass 2021*, 3, 2022 [2203.05531].
- [52] ATLAS collaboration, *Combined measurements of Higgs boson production and decay using up to 139 fb^{-1} of proton-proton collision data at $\sqrt{s} = 13$ TeV collected with the ATLAS experiment*, .
- [53] CMS collaboration, *Combined Higgs boson production and decay measurements with up to 137 fb^{-1} of proton-proton collision data at $\sqrt{s} = 13$ TeV*, .
- [54] CMS collaboration, *Measurement of the Higgs boson production rate in association with top quarks in final states with electrons, muons, and hadronically decaying tau leptons at $\sqrt{s} = 13$ TeV*, *Eur. Phys. J. C* **81** (2021) 378 [2011.03652].

- [55] D. Gonçalves, T. Han and S. Mukhopadhyay, *Higgs Couplings at High Scales*, *Phys. Rev. D* **98** (2018) 015023 [1803.09751].
- [56] D. Gonçalves, T. Han, S. Ching Iris Leung and H. Qin, *Off-shell Higgs couplings in $H^* \rightarrow ZZ \rightarrow \ell\nu\nu$* , *Phys. Lett. B* **817** (2021) 136329 [2012.05272].
- [57] R. Mammen Abraham, D. Gonçalves, T. Han, S.C.I. Leung and H. Qin, *Directly probing the Higgs-top coupling at high scales*, *Phys. Lett. B* **825** (2022) 136839 [2106.00018].
- [58] P. Bittar and G. Burdman, *Form factors in Higgs couplings from physics beyond the standard model*, *JHEP* **10** (2022) 004 [2204.07094].
- [59] CMS collaboration, *Running of the top quark mass from proton-proton collisions at $\sqrt{s} = 13\text{TeV}$* , *Phys. Lett. B* **803** (2020) 135263 [1909.09193].
- [60] R. Contino, L. Da Rold and A. Pomarol, *Light custodians in natural composite Higgs models*, *Phys. Rev. D* **75** (2007) 055014 [hep-ph/0612048].
- [61] C. Csaki, A. Falkowski and A. Weiler, *The Flavor of the Composite Pseudo-Goldstone Higgs*, *JHEP* **09** (2008) 008 [0804.1954].
- [62] S. De Curtis, M. Redi and A. Tesi, *The 4D Composite Higgs*, *JHEP* **04** (2012) 042 [1110.1613].
- [63] O. Matsedonskyi, G. Panico and A. Wulzer, *Light Top Partners for a Light Composite Higgs*, *JHEP* **01** (2013) 164 [1204.6333].
- [64] D. Marzocca, M. Serone and J. Shu, *General Composite Higgs Models*, *JHEP* **08** (2012) 013 [1205.0770].
- [65] A. Pomarol and F. Riva, *The Composite Higgs and Light Resonance Connection*, *JHEP* **08** (2012) 135 [1205.6434].
- [66] A. Carmona and F. Goertz, *A naturally light Higgs without light Top Partners*, *JHEP* **05** (2015) 002 [1410.8555].
- [67] K.G. Chetyrkin and M.F. Zoller, *Three-loop β -functions for top-Yukawa and the Higgs self-interaction in the Standard Model*, *JHEP* **06** (2012) 033 [1205.2892].
- [68] A.V. Bednyakov, A.F. Pikelner and V.N. Velizhanin, *Yukawa coupling beta-functions in the Standard Model at three loops*, *Phys. Lett. B* **722** (2013) 336 [1212.6829].

- [69] T.P. Cheng, E. Eichten and L.-F. Li, *Higgs phenomena in asymptotically free gauge theories*, *Phys. Rev. D* **9** (1974) 2259.
- [70] M.T. Vaughn, *Renormalization Group Constraints on Unified Gauge Theories. 2. Yukawa and Scalar Quartic Couplings*, *Z. Phys. C* **13** (1982) 139.
- [71] M.E. Machacek and M.T. Vaughn, *Two Loop Renormalization Group Equations in a General Quantum Field Theory. 3. Scalar Quartic Couplings*, *Nucl. Phys. B* **249** (1985) 70.
- [72] B.C. Allanach, J. Davighi and S. Melville, *An Anomaly-free Atlas: charting the space of flavour-dependent gauged $U(1)$ extensions of the Standard Model*, *JHEP* **02** (2019) 082 [[1812.04602](#)].
- [73] K.S. Babu, A. Friedland, P.A.N. Machado and I. Mocioiu, *Flavor Gauge Models Below the Fermi Scale*, *JHEP* **12** (2017) 096 [[1705.01822](#)].
- [74] M. Carena, A. Daleo, B.A. Dobrescu and T.M.P. Tait, *Z' gauge bosons at the Tevatron*, *Phys. Rev. D* **70** (2004) 093009 [[hep-ph/0408098](#)].
- [75] A. Hayreter, X.-G. He and G. Valencia, *LHC constraints on W' , Z' that couple mainly to third generation fermions*, *Eur. Phys. J. C* **80** (2020) 912 [[1912.06344](#)].
- [76] C.T. Hill, *Topcolor: Top quark condensation in a gauge extension of the standard model*, *Phys. Lett. B* **266** (1991) 419.
- [77] R.S. Chivukula, E.H. Simmons, B. Coleppa, H.E. Logan and A. Martin, *Top-Higgs and Top-Pion Phenomenology in the Top Triangle Moose Model*, *Phys. Rev. D* **83** (2011) 055013 [[1101.6023](#)].
- [78] R.S. Chivukula, E.H. Simmons, B. Coleppa, H.E. Logan and A. Martin, *LHC Limits on the Top-Higgs in Models with Strong Top-Quark Dynamics*, *Phys. Rev. D* **84** (2011) 095022 [[1108.4000](#)].
- [79] Y. Nambu and G. Jona-Lasinio, *Dynamical model of elementary particles based on an analogy with superconductivity. i*, *Phys. Rev.* **122** (1961) 345.
- [80] Y. Nambu and G. Jona-Lasinio, *Dynamical model of elementary particles based on an analogy with superconductivity. ii*, *Phys. Rev.* **124** (1961) 246.
- [81] W.A. Bardeen, C.T. Hill and M. Lindner, *Minimal Dynamical Symmetry Breaking of the Standard Model*, *Phys. Rev. D* **41** (1990) 1647.
- [82] C.T. Hill and E.H. Simmons, *Strong Dynamics and Electroweak Symmetry Breaking*, *Phys. Rept.* **381** (2003) 235 [[hep-ph/0203079](#)].

- [83] V.A. Miransky, M. Tanabashi and K. Yamawaki, *Dynamical Electroweak Symmetry Breaking with Large Anomalous Dimension and t Quark Condensate*, *Phys. Lett. B* **221** (1989) 177.
- [84] V.A. Miransky, M. Tanabashi and K. Yamawaki, *Is the t Quark Responsible for the Mass of W and Z Bosons?*, *Mod. Phys. Lett. A* **4** (1989) 1043.
- [85] C.T. Hill, *Topcolor assisted technicolor*, *Phys. Lett. B* **345** (1995) 483 [[hep-ph/9411426](#)].
- [86] K.R. Dienes, E. Dudas and T. Gherghetta, *Extra space-time dimensions and unification*, *Phys. Lett. B* **436** (1998) 55 [[hep-ph/9803466](#)].
- [87] K.R. Dienes, E. Dudas and T. Gherghetta, *Grand unification at intermediate mass scales through extra dimensions*, *Nucl. Phys. B* **537** (1999) 47 [[hep-ph/9806292](#)].
- [88] G. Bhattacharyya, A. Datta, S.K. Majee and A. Raychaudhuri, *Power law blitzkrieg in universal extra dimension scenarios*, *Nucl. Phys. B* **760** (2007) 117 [[hep-ph/0608208](#)].
- [89] S.J. Brodsky and G.P. Lepage, *Exclusive Processes in Quantum Chromodynamics*, *Adv. Ser. Direct. High Energy Phys.* **5** (1989) 93.
- [90] M.M. Defranchis, J. Kieseler, K. Lipka and J. Mazzitelli, *Running of the top quark mass at NNLO in QCD*, 2208.11399.
- [91] R. Frederix, D. Pagani and M. Zaro, *Large NLO corrections in $t\bar{t}W^\pm$ and $t\bar{t}t$ hadroproduction from supposedly subleading EW contributions*, *JHEP* **02** (2018) 031 [[1711.02116](#)].
- [92] ATLAS collaboration, *Evidence for $t\bar{t}t$ production in the multilepton final state in proton-proton collisions at $\sqrt{s} = 13$ TeV with the ATLAS detector*, *Eur. Phys. J. C* **80** (2020) 1085 [[2007.14858](#)].
- [93] ATLAS collaboration, *Measurement of the $t\bar{t}t$ production cross section in pp collisions at $\sqrt{s} = 13$ TeV with the ATLAS detector*, *JHEP* **11** (2021) 118 [[2106.11683](#)].
- [94] CMS collaboration, *Search for production of four top quarks in final states with same-sign or multiple leptons in proton-proton collisions at $\sqrt{s} = 13$ TeV*, *Eur. Phys. J. C* **80** (2020) 75 [[1908.06463](#)].
- [95] CMS collaboration, *Evidence for four-top quark production in proton-proton collisions at $\sqrt{s} = 13$ TeV*, 2303.03864.
- [96] CMS collaboration, *Observation of four top quark production in proton-proton collisions at $\sqrt{s} = 13$ TeV*, 2305.13439.

- [97] L. Darmé, B. Fuks and F. Maltoni, *Top-philic heavy resonances in four-top final states and their EFT interpretation*, *JHEP* **09** (2021) 143 [2104.09512].
- [98] G. Banelli, E. Salvioni, J. Serra, T. Theil and A. Weiler, *The Present and Future of Four Top Operators*, *JHEP* **02** (2021) 043 [2010.05915].
- [99] F. Blekman, F. Déliot, V. Dutta and E. Usai, *Four-top quark physics at the LHC*, *Universe* **8** (2022) 638 [2208.04085].
- [100] L. Di Luzio, M. Kirk and A. Lenz, *Updated B_s -mixing constraints on new physics models for $b \rightarrow s\ell^+\ell^-$ anomalies*, *Phys. Rev. D* **97** (2018) 095035 [1712.06572].
- [101] D. King, A. Lenz and T. Rauh, *B_s mixing observables and $|V_{td}/V_{ts}|$ from sum rules*, *JHEP* **05** (2019) 034 [1904.00940].
- [102] HFLAV collaboration, *Averages of b -hadron, c -hadron, and τ -lepton properties as of 2018*, *Eur. Phys. J. C* **81** (2021) 226 [1909.12524].
- [103] M.E. Peskin and T. Takeuchi, *A New constraint on a strongly interacting Higgs sector*, *Phys. Rev. Lett.* **65** (1990) 964.
- [104] M.E. Peskin and T. Takeuchi, *Estimation of oblique electroweak corrections*, *Phys. Rev. D* **46** (1992) 381.
- [105] C.-T. Lu, L. Wu, Y. Wu and B. Zhu, *Electroweak precision fit and new physics in light of the W boson mass*, *Phys. Rev. D* **106** (2022) 035034 [2204.03796].
- [106] A. Strumia, *Interpreting electroweak precision data including the W -mass CDF anomaly*, *JHEP* **08** (2022) 248 [2204.04191].
- [107] J. de Blas, M. Pierini, L. Reina and L. Silvestrini, *Impact of the Recent Measurements of the Top-Quark and W -Boson Masses on Electroweak Precision Fits*, *Phys. Rev. Lett.* **129** (2022) 271801 [2204.04204].
- [108] E. Bagnaschi, J. Ellis, M. Madigan, K. Mimasu, V. Sanz and T. You, *SMEFT analysis of m_W* , *JHEP* **08** (2022) 308 [2204.05260].
- [109] P. Asadi, C. Cesarotti, K. Fraser, S. Homiller and A. Parikh, *Oblique Lessons from the W Mass Measurement at CDF II*, 2204.05283.
- [110] CDF collaboration, *High-precision measurement of the W boson mass with the CDF II detector*, *Science* **376** (2022) 170.
- [111] B. Batell, S. Gori and L.-T. Wang, *Higgs Couplings and Precision Electroweak Data*, *JHEP* **01** (2013) 139 [1209.6382].

- [112] D. Guadagnoli and G. Isidori, *B*($B_s \rightarrow \mu^+ \mu^-$) as an electroweak precision test, *Phys. Lett. B* **724** (2013) 63 [1302.3909].
- [113] ATLAS collaboration, *Search for a scalar partner of the top quark in the all-hadronic $t\bar{t}$ plus missing transverse momentum final state at $\sqrt{s} = 13$ TeV with the ATLAS detector*, *Eur. Phys. J. C* **80** (2020) 737 [2004.14060].
- [114] ATLAS collaboration, *Search for new phenomena in events with two opposite-charge leptons, jets and missing transverse momentum in pp collisions at $\sqrt{s} = 13$ TeV with the ATLAS detector*, *JHEP* **04** (2021) 165 [2102.01444].
- [115] ATLAS collaboration, *Search for new phenomena with top quark pairs in final states with one lepton, jets, and missing transverse momentum in pp collisions at $\sqrt{s} = 13$ TeV with the ATLAS detector*, *JHEP* **04** (2021) 174 [2012.03799].
- [116] CMS collaboration, *Search for direct top squark pair production in events with one lepton, jets, and missing transverse momentum at 13 TeV with the CMS experiment*, *JHEP* **05** (2020) 032 [1912.08887].
- [117] CMS collaboration, *Combined searches for the production of supersymmetric top quark partners in proton–proton collisions at $\sqrt{s} = 13$ TeV*, *Eur. Phys. J. C* **81** (2021) 970 [2107.10892].
- [118] CMS collaboration, *Search for top squark production in fully-hadronic final states in proton-proton collisions at $\sqrt{s} = 13$ TeV*, *Phys. Rev. D* **104** (2021) 052001 [2103.01290].
- [119] CMS collaboration, *Search for top squarks in final states with two top quarks and several light-flavor jets in proton-proton collisions at $\sqrt{s} = 13$ TeV*, *Phys. Rev. D* **104** (2021) 032006 [2102.06976].
- [120] N.S. Manton, *A New Six-Dimensional Approach to the Weinberg-Salam Model*, *Nucl. Phys. B* **158** (1979) 141.
- [121] D.B. Fairlie, *Higgs' Fields and the Determination of the Weinberg Angle*, *Phys. Lett. B* **82** (1979) 97.
- [122] Y. Hosotani, *Dynamical Mass Generation by Compact Extra Dimensions*, *Phys. Lett. B* **126** (1983) 309.
- [123] Y. Hosotani, *Dynamical Gauge Symmetry Breaking as the Casimir Effect*, *Phys. Lett. B* **129** (1983) 193.
- [124] Y. Hosotani, *Dynamics of Nonintegrable Phases and Gauge Symmetry Breaking*, *Annals Phys.* **190** (1989) 233.

- [125] P. Candelas, G.T. Horowitz, A. Strominger and E. Witten, *Vacuum configurations for superstrings*, *Nucl. Phys. B* **258** (1985) 46.
- [126] E. Witten, *Symmetry breaking patterns in superstring models*, *Nucl. Phys. B* **258** (1985) 75.
- [127] L.J. Dixon, J.A. Harvey, C. Vafa and E. Witten, *Strings on Orbifolds*, *Nucl. Phys. B* **261** (1985) 678.
- [128] A. Hebecker and J. March-Russell, *A Minimal $S^{*}1 / (Z(2) \times Z\text{-prime}(2))$ orbifold GUT*, *Nucl. Phys. B* **613** (2001) 3 [[hep-ph/0106166](#)].
- [129] Y. Kawamura, *Triplet doublet splitting, proton stability and extra dimension*, *Prog. Theor. Phys.* **105** (2001) 999 [[hep-ph/0012125](#)].
- [130] G. Altarelli and F. Feruglio, *$SU(5)$ grand unification in extra dimensions and proton decay*, *Phys. Lett. B* **511** (2001) 257 [[hep-ph/0102301](#)].
- [131] L.J. Hall and Y. Nomura, *Gauge unification in higher dimensions*, *Phys. Rev. D* **64** (2001) 055003 [[hep-ph/0103125](#)].
- [132] M. Quiros, *New ideas in symmetry breaking*, in *Theoretical Advanced Study Institute in Elementary Particle Physics (TASI 2002): Particle Physics and Cosmology: The Quest for Physics Beyond the Standard Model(s)*, pp. 549–601, 2, 2003 [[hep-ph/0302189](#)].
- [133] A. Hebecker and J. March-Russell, *The structure of GUT breaking by orbifolding*, *Nucl. Phys. B* **625** (2002) 128 [[hep-ph/0107039](#)].
- [134] C. Csaki, C. Grojean, H. Murayama, L. Pilo and J. Terning, *Gauge theories on an interval: Unitarity without a Higgs*, *Phys. Rev. D* **69** (2004) 055006 [[hep-ph/0305237](#)].
- [135] M.B. Green, J.H. Schwarz and E. Witten, *SUPERSTRING THEORY. VOL. 1: INTRODUCTION*, Cambridge Monographs on Mathematical Physics, Cambridge Monographs on Mathematical Physics (7, 1988).
- [136] M.E. Peskin and D.V. Schroeder, *An Introduction to quantum field theory*, Addison-Wesley, Reading, USA (1995).
- [137] K.-y. Oda and A. Weiler, *Wilson lines in warped space: Dynamical symmetry breaking and restoration*, *Phys. Lett. B* **606** (2005) 408 [[hep-ph/0410061](#)].
- [138] Y. Hosotani and M. Mabe, *Higgs boson mass and electroweak-gravity hierarchy from dynamical gauge-Higgs unification in the warped spacetime*, *Phys. Lett. B* **615** (2005) 257 [[hep-ph/0503020](#)].

- [139] G. von Gersdorff, N. Irges and M. Quiros, *Radiative brane mass terms in D greater than 5 orbifold gauge theories*, *Phys. Lett. B* **551** (2003) 351 [[hep-ph/0210134](#)].
- [140] G. von Gersdorff, N. Irges and M. Quiros, *Finite mass corrections in orbifold gauge theories*, in *37th Rencontres de Moriond on Electroweak Interactions and Unified Theories*, pp. 169–176, 6, 2002 [[hep-ph/0206029](#)].
- [141] R. Contino, *The Higgs as a Composite Nambu-Goldstone Boson*, in *Theoretical Advanced Study Institute in Elementary Particle Physics: Physics of the Large and the Small*, pp. 235–306, 2011, DOI [[1005.4269](#)].
- [142] M. Serone, *Holographic Methods and Gauge-Higgs Unification in Flat Extra Dimensions*, *New J. Phys.* **12** (2010) 075013 [[0909.5619](#)].
- [143] C.A. Scrucca, M. Serone and L. Silvestrini, *Electroweak symmetry breaking and fermion masses from extra dimensions*, *Nucl. Phys. B* **669** (2003) 128 [[hep-ph/0304220](#)].
- [144] M. Carena, T.M.P. Tait and C.E.M. Wagner, *Branes and Orbifolds are Opaque*, *Acta Phys. Polon. B* **33** (2002) 2355 [[hep-ph/0207056](#)].
- [145] I. Antoniadis, K. Benakli and M. Quiros, *Finite Higgs mass without supersymmetry*, *New J. Phys.* **3** (2001) 20 [[hep-th/0108005](#)].
- [146] M. Kubo, C.S. Lim and H. Yamashita, *The Hosotani mechanism in bulk gauge theories with an orbifold extra space $S^{*1} / Z(2)$* , *Mod. Phys. Lett. A* **17** (2002) 2249 [[hep-ph/0111327](#)].
- [147] G. Cacciapaglia, C. Csaki and S.C. Park, *Fully radiative electroweak symmetry breaking*, *JHEP* **03** (2006) 099 [[hep-ph/0510366](#)].
- [148] G. Burdman and Y. Nomura, *Unification of Higgs and Gauge Fields in Five Dimensions*, *Nucl. Phys. B* **656** (2003) 3 [[hep-ph/0210257](#)].
- [149] N. Arkani-Hamed, S. Dimopoulos and G.R. Dvali, *The Hierarchy problem and new dimensions at a millimeter*, *Phys. Lett. B* **429** (1998) 263 [[hep-ph/9803315](#)].
- [150] I. Antoniadis, N. Arkani-Hamed, S. Dimopoulos and G.R. Dvali, *New dimensions at a millimeter to a Fermi and superstrings at a TeV*, *Phys. Lett. B* **436** (1998) 257 [[hep-ph/9804398](#)].
- [151] N. Arkani-Hamed, S. Dimopoulos and G.R. Dvali, *Phenomenology, astrophysics and cosmology of theories with submillimeter dimensions and TeV scale quantum gravity*, *Phys. Rev. D* **59** (1999) 086004 [[hep-ph/9807344](#)].

- [152] W.-H. Tan, S.-Q. Yang, C.-G. Shao, J. Li, A.-B. Du, B.-F. Zhan et al., *New test of the gravitational inverse-square law at the submillimeter range with dual modulation and compensation*, *Phys. Rev. Lett.* **116** (2016) 131101.
- [153] L. Randall and R. Sundrum, *A Large mass hierarchy from a small extra dimension*, *Phys. Rev. Lett.* **83** (1999) 3370 [[hep-ph/9905221](#)].
- [154] L. Randall and R. Sundrum, *An Alternative to compactification*, *Phys. Rev. Lett.* **83** (1999) 4690 [[hep-th/9906064](#)].
- [155] T. Taylor and G. Veneziano, *Dilaton couplings at large distances*, *Physics Letters B* **213** (1988) 450.
- [156] W.D. Goldberger and M.B. Wise, *Phenomenology of a stabilized modulus*, *Phys. Lett. B* **475** (2000) 275 [[hep-ph/9911457](#)].
- [157] W.D. Goldberger and M.B. Wise, *Modulus stabilization with bulk fields*, *Phys. Rev. Lett.* **83** (1999) 4922 [[hep-ph/9907447](#)].
- [158] C. Csaki, M. Graesser, L. Randall and J. Terning, *Cosmology of brane models with radion stabilization*, *Phys. Rev. D* **62** (2000) 045015 [[hep-ph/9911406](#)].
- [159] C. Csaki, M.L. Graesser and G.D. Kribs, *Radion dynamics and electroweak physics*, *Phys. Rev. D* **63** (2001) 065002 [[hep-th/0008151](#)].
- [160] H. Davoudiasl, J.L. Hewett and T.G. Rizzo, *Phenomenology of the Randall-Sundrum Gauge Hierarchy Model*, *Phys. Rev. Lett.* **84** (2000) 2080 [[hep-ph/9909255](#)].
- [161] H. Davoudiasl, J.L. Hewett and T.G. Rizzo, *Bulk gauge fields in the Randall-Sundrum model*, *Phys. Lett. B* **473** (2000) 43 [[hep-ph/9911262](#)].
- [162] A. Pomarol, *Gauge bosons in a five-dimensional theory with localized gravity*, *Phys. Lett. B* **486** (2000) 153 [[hep-ph/9911294](#)].
- [163] Y. Grossman and M. Neubert, *Neutrino masses and mixings in nonfactorizable geometry*, *Phys. Lett. B* **474** (2000) 361 [[hep-ph/9912408](#)].
- [164] T. Gherghetta and A. Pomarol, *Bulk fields and supersymmetry in a slice of AdS*, *Nucl. Phys. B* **586** (2000) 141 [[hep-ph/0003129](#)].
- [165] R. Contino, Y. Nomura and A. Pomarol, *Higgs as a holographic pseudoGoldstone boson*, *Nucl. Phys. B* **671** (2003) 148 [[hep-ph/0306259](#)].

- [166] K. Agashe and G. Servant, *Baryon number in warped GUTs: Model building and (dark matter related) phenomenology*, *JCAP* **02** (2005) 002 [[hep-ph/0411254](#)].
- [167] K. Agashe, R. Contino and R. Sundrum, *Top compositeness and precision unification*, *Phys. Rev. Lett.* **95** (2005) 171804 [[hep-ph/0502222](#)].
- [168] Y. Hosotani and N. Yamatsu, *Gauge-Higgs grand unification*, *PTEP* **2015** (2015) 111B01 [[1504.03817](#)].
- [169] A. Furui, Y. Hosotani and N. Yamatsu, *Toward Realistic Gauge-Higgs Grand Unification*, *PTEP* **2016** (2016) 093B01 [[1606.07222](#)].
- [170] Y. Hosotani and N. Yamatsu, *Electroweak symmetry breaking and mass spectra in six-dimensional gauge-Higgs grand unification*, *PTEP* **2018** (2018) 023B05 [[1710.04811](#)].
- [171] Y. Hosotani and N. Yamatsu, *Gauge-Higgs seesaw mechanism in 6-dimensional grand unification*, *PTEP* **2017** (2017) 091B01 [[1706.03503](#)].
- [172] S. Funatsu, H. Hatanaka, Y. Hosotani, Y. Orikasa and N. Yamatsu, *GUT inspired $SO(5) \times U(1) \times SU(3)$ gauge-Higgs unification*, *Phys. Rev. D* **99** (2019) 095010 [[1902.01603](#)].
- [173] S. Funatsu, H. Hatanaka, Y. Hosotani, Y. Orikasa and N. Yamatsu, *CKM matrix and FCNC suppression in $SO(5) \times U(1) \times SU(3)$ gauge-Higgs unification*, *Phys. Rev. D* **101** (2020) 055016 [[1909.00190](#)].
- [174] S. Funatsu, H. Hatanaka, Y. Hosotani, Y. Orikasa and N. Yamatsu, *Effective potential and universality in GUT-inspired gauge-Higgs unification*, *Phys. Rev. D* **102** (2020) 015005 [[2002.09262](#)].
- [175] S. Funatsu, H. Hatanaka, Y. Hosotani, Y. Orikasa and N. Yamatsu, *Fermion pair production at e^-e^+ linear collider experiments in GUT inspired gauge-Higgs unification*, *Phys. Rev. D* **102** (2020) 015029 [[2006.02157](#)].
- [176] S. Funatsu, H. Hatanaka, Y. Hosotani, Y. Orikasa and N. Yamatsu, *Linear Collider Signals of Z' Bosons in GUT Inspired Gauge-Higgs Unification*, in *International Workshop on Future Linear Colliders*, **3**, 2021 [[2103.16320](#)].
- [177] S. Funatsu, H. Hatanaka, Y. Hosotani, Y. Orikasa and N. Yamatsu, *Electroweak and left-right phase transitions in $SO(5) \times U(1) \times SU(3)$ gauge-Higgs unification*, *Phys. Rev. D* **104** (2021) 115018 [[2104.02870](#)].

- [178] S. Funatsu, H. Hatanaka, Y. Hosotani, Y. Orikasa and N. Yamatsu, *Signals of W' and Z' bosons at the LHC in the $SU(3) \times SO(5) \times U(1)$ gauge-Higgs unification*, 2111.05624.
- [179] N. Maru, H. Takahashi and Y. Yatagai, *Gauge Coupling Unification in simplified Grand Gauge-Higgs Unification*, 2207.10253.
- [180] L.J. Hall, Y. Nomura and D. Tucker-Smith, *Gauge Higgs unification in higher dimensions*, *Nucl. Phys. B* **639** (2002) 307 [hep-ph/0107331].
- [181] N. Haba, Y. Hosotani, Y. Kawamura and T. Yamashita, *Dynamical symmetry breaking in gauge Higgs unification on orbifold*, *Phys. Rev. D* **70** (2004) 015010 [hep-ph/0401183].
- [182] C.S. Lim and N. Maru, *Towards a realistic grand gauge-Higgs unification*, *Phys. Lett. B* **653** (2007) 320 [0706.1397].
- [183] N. Maru and Y. Yatagai, *Improving fermion mass hierarchy in grand gauge-Higgs unification with localized gauge kinetic terms*, *Eur. Phys. J. C* **80** (2020) 933 [1911.03465].
- [184] N. Maru and Y. Yatagai, *Fermion Mass Hierarchy in Grand Gauge-Higgs Unification*, *PTEP* **2019** (2019) 083B03 [1903.08359].
- [185] N. Maru, H. Takahashi and Y. Yatagai, *Fermion Mass Hierarchy and Mixing in simplified Grand Gauge-Higgs Unification*, 2205.05824.
- [186] S.J. Huber and Q. Shafi, *Fermion masses, mixings and proton decay in a Randall-Sundrum model*, *Phys. Lett. B* **498** (2001) 256 [hep-ph/0010195].
- [187] S.J. Huber, *Flavor violation and warped geometry*, *Nucl. Phys. B* **666** (2003) 269 [hep-ph/0303183].
- [188] N. Arkani-Hamed and M. Schmaltz, *Hierarchies without symmetries from extra dimensions*, *Phys. Rev. D* **61** (2000) 033005 [hep-ph/9903417].
- [189] S. Casagrande, F. Goertz, U. Haisch, M. Neubert and T. Pfoh, *Flavor Physics in the Randall-Sundrum Model: I. Theoretical Setup and Electroweak Precision Tests*, *JHEP* **10** (2008) 094 [0807.4937].
- [190] PARTICLE DATA GROUP collaboration, *Review of Particle Physics*, *PTEP* **2020** (2020) 083C01.
- [191] I. Esteban, M.C. Gonzalez-Garcia, M. Maltoni, T. Schwetz and A. Zhou, *The fate of hints: updated global analysis of three-flavor neutrino oscillations*, *JHEP* **09** (2020) 178 [2007.14792].

- [192] J. Santiago, *Minimal Flavor Protection: A New Flavor Paradigm in Warped Models*, *JHEP* **12** (2008) 046 [0806.1230].
- [193] K. Agashe, G. Perez and A. Soni, *B-factory signals for a warped extra dimension*, *Phys. Rev. Lett.* **93** (2004) 201804 [hep-ph/0406101].
- [194] K. Agashe, G. Perez and A. Soni, *Flavor structure of warped extra dimension models*, *Phys. Rev. D* **71** (2005) 016002 [hep-ph/0408134].
- [195] M. Blanke, A.J. Buras, B. Duling, K. Gemmler and S. Gori, *Rare K and B Decays in a Warped Extra Dimension with Custodial Protection*, *JHEP* **03** (2009) 108 [0812.3803].
- [196] K. Agashe, A. Azatov and L. Zhu, *Flavor Violation Tests of Warped/Composite SM in the Two-Site Approach*, *Phys. Rev. D* **79** (2009) 056006 [0810.1016].
- [197] M. Blanke, A.J. Buras, B. Duling, S. Gori and A. Weiler, $\Delta F=2$ *Observables and Fine-Tuning in a Warped Extra Dimension with Custodial Protection*, *JHEP* **03** (2009) 001 [0809.1073].
- [198] M. Bauer, S. Casagrande, U. Haisch and M. Neubert, *Flavor Physics in the Randall-Sundrum Model: II. Tree-Level Weak-Interaction Processes*, *JHEP* **09** (2010) 017 [0912.1625].
- [199] M.E. Albrecht, M. Blanke, A.J. Buras, B. Duling and K. Gemmler, *Electroweak and Flavour Structure of a Warped Extra Dimension with Custodial Protection*, *JHEP* **09** (2009) 064 [0903.2415].
- [200] B. Keren-Zur, P. Lodone, M. Nardecchia, D. Pappadopulo, R. Rattazzi and L. Vecchi, *On Partial Compositeness and the CP asymmetry in charm decays*, *Nucl. Phys. B* **867** (2013) 394 [1205.5803].
- [201] K. Agashe, A.E. Blechman and F. Petriello, *Probing the Randall-Sundrum geometric origin of flavor with lepton flavor violation*, *Phys. Rev. D* **74** (2006) 053011 [hep-ph/0606021].
- [202] O. Gedalia, G. Isidori and G. Perez, *Combining Direct & Indirect Kaon CP Violation to Constrain the Warped KK Scale*, *Phys. Lett. B* **682** (2009) 200 [0905.3264].
- [203] C. Csaki, Y. Grossman, P. Tanedo and Y. Tsai, *Warped penguin diagrams*, *Phys. Rev. D* **83** (2011) 073002 [1004.2037].
- [204] M. Blanke, B. Shakya, P. Tanedo and Y. Tsai, *The Birds and the Bs in RS: The $b\to s\gamma$ penguin in a warped extra dimension*, *JHEP* **08** (2012) 038 [1203.6650].

- [205] M. Beneke, P. Dey and J. Rohrwild, *The muon anomalous magnetic moment in the Randall-Sundrum model*, *JHEP* **08** (2013) 010 [1209.5897].
- [206] M. König, M. Neubert and D.M. Straub, *Dipole operator constraints on composite Higgs models*, *Eur. Phys. J. C* **74** (2014) 2945 [1403.2756].
- [207] M. Beneke, P. Moch and J. Rohrwild, *Lepton flavour violation in RS models with a brane- or nearly brane-localized Higgs*, *Nucl. Phys. B* **906** (2016) 561 [1508.01705].
- [208] P. Moch and J. Rohrwild, $\bar{B} \rightarrow X_s \gamma$ *with a warped bulk Higgs*, *Nucl. Phys. B* **902** (2016) 142 [1509.04643].
- [209] K. Agashe, A. Delgado, M.J. May and R. Sundrum, *RS1, custodial isospin and precision tests*, *JHEP* **08** (2003) 050 [hep-ph/0308036].
- [210] K. Agashe, R. Contino and A. Pomarol, *The Minimal composite Higgs model*, *Nucl. Phys. B* **719** (2005) 165 [hep-ph/0412089].
- [211] S.L. Glashow, J. Iliopoulos and L. Maiani, *Weak Interactions with Lepton-Hadron Symmetry*, *Phys. Rev. D* **2** (1970) 1285.
- [212] C. Csaki, C. Delaunay, C. Grojean and Y. Grossman, *A Model of Lepton Masses from a Warped Extra Dimension*, *JHEP* **10** (2008) 055 [0806.0356].
- [213] G. Perez and L. Randall, *Natural Neutrino Masses and Mixings from Warped Geometry*, *JHEP* **01** (2009) 077 [0805.4652].
- [214] M.-C. Chen and H.-B. Yu, *Minimal Flavor Violation in the Lepton Sector of the Randall-Sundrum Model*, *Phys. Lett. B* **672** (2009) 253 [0804.2503].
- [215] M.-C. Chen, K.T. Mahanthappa and F. Yu, *A Viable Randall-Sundrum Model for Quarks and Leptons with T-prime Family Symmetry*, *Phys. Rev. D* **81** (2010) 036004 [0907.3963].
- [216] A. Kadosh and E. Pallante, *An $A(4)$ flavor model for quarks and leptons in warped geometry*, *JHEP* **08** (2010) 115 [1004.0321].
- [217] F. del Aguila, A. Carmona and J. Santiago, *Neutrino Masses from an A_4 Symmetry in Holographic Composite Higgs Models*, *JHEP* **08** (2010) 127 [1001.5151].
- [218] C. Hagedorn and M. Serone, *General Lepton Mixing in Holographic Composite Higgs Models*, *JHEP* **02** (2012) 077 [1110.4612].

- [219] C. Hagedorn and M. Serone, *Leptons in Holographic Composite Higgs Models with Non-Abelian Discrete Symmetries*, *JHEP* **10** (2011) 083 [1106.4021].
- [220] G. von Gersdorff, M. Quiros and M. Wiechers, *Neutrino Mixing from Wilson Lines in Warped Space*, *JHEP* **02** (2013) 079 [1208.4300].
- [221] A. Kadosh, Θ_13 and charged Lepton Flavor Violation in "warped" A_4 models, *JHEP* **06** (2013) 114 [1303.2645].
- [222] G.-J. Ding and Y.-L. Zhou, *Dirac Neutrinos with S_4 Flavor Symmetry in Warped Extra Dimensions*, *Nucl. Phys. B* **876** (2013) 418 [1304.2645].
- [223] M. Frank, C. Hamzaoui, N. Pourtolami and M. Toharia, *Unified Flavor Symmetry from warped dimensions*, *Phys. Lett. B* **742** (2015) 178 [1406.2331].
- [224] P. Chen, G.-J. Ding, A.D. Rojas, C.A. Vaquera-Araujo and J.W.F. Valle, *Warped flavor symmetry predictions for neutrino physics*, *JHEP* **01** (2016) 007 [1509.06683].
- [225] M. Frigerio, M. Nardecchia, J. Serra and L. Vecchi, *The Bearable Compositeness of Leptons*, *JHEP* **10** (2018) 017 [1807.04279].
- [226] F. Goertz, *Flavour observables and composite dynamics: leptons*, *Eur. Phys. J. ST* **231** (2022) 1287.
- [227] F. Goertz, *Lepton Flavor in Composite Higgs Models*, *PoS PANIC2021* (2022) 149 [2112.01450].
- [228] G. Cacciapaglia, C. Csaki, J. Galloway, G. Marandella, J. Terning and A. Weiler, *A GIM Mechanism from Extra Dimensions*, *JHEP* **04** (2008) 006 [0709.1714].
- [229] A.L. Fitzpatrick, G. Perez and L. Randall, *Flavor anarchy in a Randall-Sundrum model with 5D minimal flavor violation and a low Kaluza-Klein scale*, *Phys. Rev. Lett.* **100** (2008) 171604 [0710.1869].
- [230] C. Csaki and D. Curtin, *A Flavor Protection for Warped Higgsless Models*, *Phys. Rev. D* **80** (2009) 015027 [0904.2137].
- [231] C. Csaki, G. Perez, Z. Surujon and A. Weiler, *Flavor Alignment via Shining in RS*, *Phys. Rev. D* **81** (2010) 075025 [0907.0474].
- [232] G.N. Wojcik and T.G. Rizzo, *Local $SU(2) \times U(1)$ quark flavor symmetry in the RS bulk*, *JHEP* **02** (2020) 179 [1909.13153].
- [233] J. Barnard, T. Gherghetta, T.S. Ray and A. Spray, *The Unnatural Composite Higgs*, *JHEP* **01** (2015) 067 [1409.7391].

- [234] UTFIT collaboration, *Model-independent constraints on $\Delta F = 2$ operators and the scale of new physics*, *JHEP* **03** (2008) 049 [0707.0636].
- [235] Y. Kuno and Y. Okada, *Muon decay and physics beyond the standard model*, *Rev. Mod. Phys.* **73** (2001) 151 [hep-ph/9909265].
- [236] W.-F. Chang and J.N. Ng, *Lepton flavor violation in extra dimension models*, *Phys. Rev. D* **71** (2005) 053003 [hep-ph/0501161].
- [237] U. Bellgardt, G. Otter, R. Eichler, L. Felawka, C. Niebuhr, H. Walter et al., *Search for the decay*, *Nuclear Physics B* **299** (1988) 1.
- [238] Mu3E collaboration, *Searching for Lepton Flavour Violation with the Mu3e Experiment*, *PoS NuFact2017* (2017) 105 [1802.09851].
- [239] H.C. Chiang, E. Oset, T.S. Kosmas, A. Faessler and J.D. Vergados, *Coherent and incoherent (μ^- , e^-) conversion in nuclei*, *Nucl. Phys. A* **559** (1993) 526.
- [240] R. Kitano, M. Koike and Y. Okada, *Detailed calculation of lepton flavor violating muon electron conversion rate for various nuclei*, *Phys. Rev. D* **66** (2002) 096002 [hep-ph/0203110].
- [241] H.V. Klapdor-Kleingrothaus and I.V. Krivosheina, eds., *Lepton and baryon number violation in particle physics, astrophysics and cosmology. Proceedings, 1st International Symposium, Lepton-baryon'98, Trento, Italy, April 20-25, 1998*, 1999.
- [242] SINDRUM II collaboration, *A Search for muon to electron conversion in muonic gold*, *Eur. Phys. J. C* **47** (2006) 337.
- [243] E. Diociaiuti, *$\mu \rightarrow e$ conversion and the Mu2e experiment at Fermilab*, *PoS EPS-HEP2019* (2020) 232.
- [244] L. Lavoura, *General formulae for $f(1) \rightarrow f(2)$ gamma*, *Eur. Phys. J. C* **29** (2003) 191 [hep-ph/0302221].
- [245] MEG collaboration, *Search for the lepton flavour violating decay $\mu^+ \rightarrow e^+ \gamma$ with the full dataset of the MEG experiment*, *Eur. Phys. J. C* **76** (2016) 434 [1605.05081].
- [246] MEG II collaboration, *The design of the MEG II experiment*, *Eur. Phys. J. C* **78** (2018) 380 [1801.04688].
- [247] PARTICLE DATA GROUP collaboration, *Review of Particle Physics*, *PTEP* **2022** (2022) 083C01.

- [248] K. Agashe, M. Bauer, F. Goertz, S.J. Lee, L. Vecchi, L.-T. Wang et al., *Constraining RS Models by Future Flavor and Collider Measurements: A Snowmass Whitepaper*, 1310.1070.
- [249] G. D'Ambrosio, G.F. Giudice, G. Isidori and A. Strumia, *Minimal flavor violation: An Effective field theory approach*, *Nucl. Phys. B* **645** (2002) 155 [[hep-ph/0207036](#)].
- [250] A. Falkowski, *About the holographic pseudo-Goldstone boson*, *Phys. Rev. D* **75** (2007) 025017 [[hep-ph/0610336](#)].
- [251] ATLAS collaboration, *Search for pair production of third-generation scalar leptoquarks decaying into a top quark and a τ -lepton in pp collisions at $\sqrt{s} = 13$ TeV with the ATLAS detector*, *JHEP* **06** (2021) 179 [[2101.11582](#)].
- [252] G. 't Hooft, *Symmetry Breaking Through Bell-Jackiw Anomalies*, *Phys. Rev. Lett.* **37** (1976) 8.
- [253] S. Weinberg, *The U(1) Problem*, *Phys. Rev. D* **11** (1975) 3583.
- [254] R.D. Peccei and H.R. Quinn, *CP Conservation in the Presence of Instantons*, *Phys. Rev. Lett.* **38** (1977) 1440.
- [255] S. Weinberg, *A New Light Boson?*, *Phys. Rev. Lett.* **40** (1978) 223.
- [256] D.B. Kaplan and H. Georgi, *SU(2) x U(1) Breaking by Vacuum Misalignment*, *Phys. Lett. B* **136** (1984) 183.
- [257] D.B. Kaplan, H. Georgi and S. Dimopoulos, *Composite Higgs Scalars*, *Phys. Lett. B* **136** (1984) 187.
- [258] H. Georgi, D.B. Kaplan and P. Galison, *Calculation of the Composite Higgs Mass*, *Phys. Lett. B* **143** (1984) 152.
- [259] T. Banks, *CONSTRAINTS ON SU(2) x U(1) BREAKING BY VACUUM MISALIGNMENT*, *Nucl. Phys. B* **243** (1984) 125.
- [260] H. Georgi and D.B. Kaplan, *Composite Higgs and Custodial SU(2)*, *Phys. Lett. B* **145** (1984) 216.
- [261] M.J. Dugan, H. Georgi and D.B. Kaplan, *Anatomy of a Composite Higgs Model*, *Nucl. Phys. B* **254** (1985) 299.
- [262] H. Georgi, *A Tool Kit for Builders of Composite Models*, *Nucl. Phys. B* **266** (1986) 274.
- [263] S. Weinberg, *Implications of dynamical symmetry breaking*, *Phys. Rev. D* **13** (1976) 974.

- [264] L. Susskind, *Dynamics of spontaneous symmetry breaking in the weinberg-salam theory*, *Phys. Rev. D* **20** (1979) 2619.
- [265] E. Eichten and K.D. Lane, *Dynamical Breaking of Weak Interaction Symmetries*, *Phys. Lett. B* **90** (1980) 125.
- [266] S. Dimopoulos and L. Susskind, *Mass Without Scalars*, *Nucl. Phys. B* **155** (1979) 237.
- [267] B. Holdom, *Raising the Sideways Scale*, *Phys. Rev. D* **24** (1981) 1441.
- [268] S.R. Coleman, J. Wess and B. Zumino, *Structure of phenomenological Lagrangians. 1.*, *Phys. Rev.* **177** (1969) 2239.
- [269] C.G. Callan, Jr., S.R. Coleman, J. Wess and B. Zumino, *Structure of phenomenological Lagrangians. 2.*, *Phys. Rev.* **177** (1969) 2247.
- [270] A. Manohar and H. Georgi, *Chiral Quarks and the Nonrelativistic Quark Model*, *Nucl. Phys. B* **234** (1984) 189.
- [271] G.F. Giudice, C. Grojean, A. Pomarol and R. Rattazzi, *The Strongly-Interacting Light Higgs*, *JHEP* **06** (2007) 045 [hep-ph/0703164].
- [272] D.B. Kaplan, *Flavor at SSC energies: A New mechanism for dynamically generated fermion masses*, *Nucl. Phys. B* **365** (1991) 259.
- [273] F. Caracciolo, A. Parolini and M. Serone, *UV Completions of Composite Higgs Models with Partial Compositeness*, *JHEP* **02** (2013) 066 [1211.7290].
- [274] D. Marzocca, A. Parolini and M. Serone, *Supersymmetry with a pNGB Higgs and Partial Compositeness*, *JHEP* **03** (2014) 099 [1312.5664].
- [275] J. Barnard, T. Gherghetta and T.S. Ray, *UV descriptions of composite Higgs models without elementary scalars*, *JHEP* **02** (2014) 002 [1311.6562].
- [276] G. Ferretti and D. Karateev, *Fermionic UV completions of Composite Higgs models*, *JHEP* **03** (2014) 077 [1312.5330].
- [277] G. Ferretti, *UV Completions of Partial Compositeness: The Case for a $SU(4)$ Gauge Group*, *JHEP* **06** (2014) 142 [1404.7137].
- [278] G. Cacciapaglia and F. Sannino, *Fundamental Composite (Goldstone) Higgs Dynamics*, *JHEP* **04** (2014) 111 [1402.0233].
- [279] E. Witten, *Current Algebra, Baryons, and Quark Confinement*, *Nucl. Phys. B* **223** (1983) 433.

- [280] N. Arkani-Hamed, A.G. Cohen and H. Georgi, *(De)constructing dimensions*, *Phys. Rev. Lett.* **86** (2001) 4757 [[hep-th/0104005](#)].
- [281] C.T. Hill, S. Pokorski and J. Wang, *Gauge Invariant Effective Lagrangian for Kaluza-Klein Modes*, *Phys. Rev. D* **64** (2001) 105005 [[hep-th/0104035](#)].
- [282] N. Arkani-Hamed, A.G. Cohen and H. Georgi, *Electroweak symmetry breaking from dimensional deconstruction*, *Phys. Lett. B* **513** (2001) 232 [[hep-ph/0105239](#)].
- [283] N. Arkani-Hamed, A.G. Cohen, E. Katz, A.E. Nelson, T. Gregoire and J.G. Wacker, *The Minimal moose for a little Higgs*, *JHEP* **08** (2002) 021 [[hep-ph/0206020](#)].
- [284] M. Schmaltz, *The Simplest little Higgs*, *JHEP* **08** (2004) 056 [[hep-ph/0407143](#)].
- [285] N. Arkani-Hamed, A.G. Cohen, E. Katz and A.E. Nelson, *The Littlest Higgs*, *JHEP* **07** (2002) 034 [[hep-ph/0206021](#)].
- [286] G. Panico and A. Wulzer, *The Discrete Composite Higgs Model*, *JHEP* **09** (2011) 135 [[1106.2719](#)].
- [287] R. Contino, T. Kramer, M. Son and R. Sundrum, *Warped/composite phenomenology simplified*, *JHEP* **05** (2007) 074 [[hep-ph/0612180](#)].
- [288] J.M. Maldacena, *The Large N limit of superconformal field theories and supergravity*, *Adv. Theor. Math. Phys.* **2** (1998) 231 [[hep-th/9711200](#)].
- [289] S.S. Gubser, I.R. Klebanov and A.M. Polyakov, *Gauge theory correlators from noncritical string theory*, *Phys. Lett. B* **428** (1998) 105 [[hep-th/9802109](#)].
- [290] E. Witten, *Anti-de Sitter space and holography*, *Adv. Theor. Math. Phys.* **2** (1998) 253 [[hep-th/9802150](#)].
- [291] N. Arkani-Hamed, M. Porrati and L. Randall, *Holography and phenomenology*, *JHEP* **08** (2001) 017 [[hep-th/0012148](#)].
- [292] R. Rattazzi and A. Zaffaroni, *Comments on the holographic picture of the Randall-Sundrum model*, *JHEP* **04** (2001) 021 [[hep-th/0012248](#)].
- [293] R. Contino and A. Pomarol, *Holography for fermions*, *JHEP* **11** (2004) 058 [[hep-th/0406257](#)].
- [294] P. Sikivie, L. Susskind, M.B. Voloshin and V.I. Zakharov, *Isospin Breaking in Technicolor Models*, *Nucl. Phys. B* **173** (1980) 189.

- [295] GFITTER GROUP collaboration, *The global electroweak fit at NNLO and prospects for the LHC and ILC*, *Eur. Phys. J. C* **74** (2014) 3046 [1407.3792].
- [296] J. Haller, A. Hoecker, R. Kogler, K. Mönig, T. Peiffer and J. Stelzer, *Update of the global electroweak fit and constraints on two-Higgs-doublet models*, *Eur. Phys. J. C* **78** (2018) 675 [1803.01853].
- [297] R. Barbieri, B. Bellazzini, V.S. Rychkov and A. Varagnolo, *The Higgs boson from an extended symmetry*, *Phys. Rev. D* **76** (2007) 115008 [0706.0432].
- [298] A. Thamm, R. Torre and A. Wulzer, *Future tests of Higgs compositeness: direct vs indirect*, *JHEP* **07** (2015) 100 [1502.01701].
- [299] D. Ghosh, M. Salvarezza and F. Senia, *Extending the Analysis of Electroweak Precision Constraints in Composite Higgs Models*, *Nucl. Phys. B* **914** (2017) 346 [1511.08235].
- [300] F. Goertz, *Composite Higgs theory*, *PoS ALPS2018* (2018) 012 [1812.07362].
- [301] J. de Blas, O. Eberhardt and C. Krause, *Current and Future Constraints on Higgs Couplings in the Nonlinear Effective Theory*, *JHEP* **07** (2018) 048 [1803.00939].
- [302] M. Redi and A. Tesi, *Implications of a Light Higgs in Composite Models*, *JHEP* **10** (2012) 166 [1205.0232].
- [303] G. Panico, M. Redi, A. Tesi and A. Wulzer, *On the Tuning and the Mass of the Composite Higgs*, *JHEP* **03** (2013) 051 [1210.7114].
- [304] D. Pappadopulo, A. Thamm and R. Torre, *A minimally tuned composite Higgs model from an extra dimension*, *JHEP* **07** (2013) 058 [1303.3062].
- [305] B. Bellazzini, C. Csáki and J. Serra, *Composite Higgses*, *Eur. Phys. J. C* **74** (2014) 2766 [1401.2457].
- [306] M. Frigerio, J. Serra and A. Varagnolo, *Composite GUTs: models and expectations at the LHC*, *JHEP* **06** (2011) 029 [1103.2997].
- [307] E. Witten, *Some Inequalities Among Hadron Masses*, *Phys. Rev. Lett.* **51** (1983) 2351.
- [308] S.R. Coleman and E.J. Weinberg, *Radiative Corrections as the Origin of Spontaneous Symmetry Breaking*, *Phys. Rev. D* **7** (1973) 1888.
- [309] J.R. Ellis, K. Enqvist, D.V. Nanopoulos and F. Zwirner, *Observables in Low-Energy Superstring Models*, *Mod. Phys. Lett. A* **1** (1986) 57.

- [310] R. Barbieri and G.F. Giudice, *Upper Bounds on Supersymmetric Particle Masses*, *Nucl. Phys. B* **306** (1988) 63.
- [311] K. Agashe and G. Servant, *Warped unification, proton stability and dark matter*, *Phys. Rev. Lett.* **93** (2004) 231805 [[hep-ph/0403143](#)].
- [312] S. Blasi and F. Goertz, *Softened Symmetry Breaking in Composite Higgs Models*, *Phys. Rev. Lett.* **123** (2019) 221801 [[1903.06146](#)].
- [313] S. Blasi, J. Bollig and F. Goertz, *Holographic composite Higgs model building: soft breaking, maximal symmetry, and the Higgs mass*, *JHEP* **07** (2023) 048 [[2212.11007](#)].
- [314] C. Csaki, T. Ma and J. Shu, *Maximally Symmetric Composite Higgs Models*, *Phys. Rev. Lett.* **119** (2017) 131803 [[1702.00405](#)].
- [315] C. Csáki, T. Ma, J. Shu and J.-H. Yu, *Emergence of Maximal Symmetry*, *Phys. Rev. Lett.* **124** (2020) 241801 [[1810.07704](#)].
- [316] S. Blasi, C. Csaki and F. Goertz, *A natural composite Higgs via universal boundary conditions*, *SciPost Phys.* **10** (2021) 121 [[2004.06120](#)].
- [317] H.-C. Cheng, B.A. Dobrescu and J. Gu, *Higgs Mass from Compositeness at a Multi-TeV Scale*, *JHEP* **08** (2014) 095 [[1311.5928](#)].
- [318] Y. Chung, *Explaining the $R_{K^{(*)}}$ anomalies and the CDF M_W in Flavorful Top Seesaw Models with Gauged $U(1)_{L(-R)}$* , [2210.13402](#).